

The importance of MpsAB for bacterial growth under atmospheric CO₂ levels

Dissertation

der Mathematisch-Naturwissenschaftlichen Fakultät
der Eberhard Karls Universität Tübingen
zur Erlangung des Grades eines
Doktors der Naturwissenschaften
(Dr. rer. nat.)

vorgelegt von
Sook-Ha Fan
aus Perak
Malaysia

Tübingen
2019

Gedruckt mit Genehmigung der Mathematisch-Naturwissenschaftlichen Fakultät der
Eberhard Karls Universität Tübingen.

Tag der mündlichen Qualifikation:

03.12.2019

Dekan:

Prof. Dr. Wolfgang Rosenstiel

1. Berichterstatter:

Prof. Dr. Friedrich Götz

2. Berichterstatter:

Prof. Dr. Andreas Peschel

Für meine Familie

The copyright of this thesis belongs to Sook-Ha Fan and unauthorized production is prohibited. The copyrights of some parts of this thesis are held by third parties and are indicated in the respective sections. In particular, the attached publications are copyrighted and reproduction remains with the respective publisher if not stated otherwise.

Table of contents

Table of contents	I
Abbreviations and symbols	III
Preamble	V
Summary	1
Zusammenfassung	2
List of publications and personal contributions	4
Accepted, peer reviewed publications.....	4
Unpublished manuscript.....	5
Chapter 1:	6
The importance of MpsAB for growth under atmospheric CO₂ levels	6
1.1 Introduction	7
1.1.1 <i>Staphylococcus aureus</i>	7
1.1.2 Small colony variants.....	8
1.1.3 <i>S. aureus</i> metabolism.....	12
1.1.4 Glycolysis.....	12
1.1.5 Pentose phosphate pathway.....	13
1.1.6 TCA cycle.....	13
1.1.7 Electron transport chain.....	15
1.1.8 Membrane potential-generating system operon in <i>S. aureus</i>	17
1.2 Objectives	21
1.3 Results	22
1.3.1 Growth defect of $\Delta mpsABC$ in atmospheric air can be rescued by elevated CO ₂ and bicarbonate.....	22
1.3.2 MpsABC increase the uptake of bicarbonate.....	28
1.3.3 Impaired membrane potential in $\Delta mpsABC$ is rescued by elevated CO ₂	30
1.3.4 <i>mpsA</i> expression was downregulated under 5% CO ₂	31
1.3.5 <i>mpsAB</i> complements an <i>E. coli</i> CA mutant and vice versa.....	32
1.3.6 Oleic acid supplementation.....	33
1.3.7 $\Delta mpsA$ in atmospheric conditions produces fewer hemolytic toxins and is less pathogenic.....	35

1.3.8	Phylogenetic distribution of <i>mpsAB</i> homologs.....	37
1.4	Discussion.....	43
1.4.1	Growth impairment of <i>mps</i> deletion mutants and its rescue by elevated CO ₂ /bicarbonate.....	43
1.4.2	Role of MpsAB in bicarbonate uptake.....	43
1.4.3	Carbonic anhydrase (CA) and MpsAB.....	44
1.4.4	MpsAB as a bicarbonate transporter.....	45
1.4.5	Distribution of MpsAB.....	46
1.4.6	Carbon concentrating mechanism.....	47
1.4.7	Bicarbonate transporters.....	47
1.4.8	MpsAB as a bicarbonate transporter in <i>S. aureus</i>	48
1.4.9	Importance of bicarbonate.....	49
1.4.10	Carboxylation enzymes and biotin-dependent enzymes.....	50
1.4.11	MpsAB is indirectly linked to UFA biosynthesis.....	52
1.4.12	Virulence attenuation by MpsAB.....	53
1.4.13	MpsAB and the link to fitness and pathogenicity.....	54
1.4.14	The link between metabolism and pathogenicity and virulence.....	54
1.5	Concluding remarks.....	55
Chapter 2	Human host cell invasion is triggered by <i>Staphylococcus aureus</i> Lpl protein via activation of Hsp90 receptor.....	57
2.1	Introduction.....	58
2.2	Objectives.....	59
2.3	Results and discussion.....	60
References		65
Acknowledgements		76
Appendix		77
	Written permission for the use of Table 1 from ASM Press.....	77
	Accepted publications.....	79
	Publication in preparation.....	108

Abbreviations and symbols

Abbreviations

ABC transporter	ATP-binding cassette transporters
ATP	Adenosine Triphosphate
CA	Carbonic anhydrase
CBB	Calvin-Benson-Bassham
CCCP	Carbonyl cyanide m-chlorophenyl hydrazine
CCS	Carbon concentrating system
C _i	Inorganic carbon species
CO ₂	Carbon dioxide
cyt	Cytochrome
DIC	Dissolved inorganic carbon
DNA	Deoxyribonucleic acid
EMP	Embden-Meyerhof-Parnas
F-actin	Filamentous-actin
FADH ₂	Flavin adenine dinucleotide
FnBP	Fibronectin binding protein
G	Gonidial
g	Gram
h	Hour
HPLC	High Performance Liquid Chromatography
Hsp90	Heat shock protein 90
kDa	Kilo Dalton
Lpls	Lipoprotein-like lipoproteins
Lqo	L-lactate oxidoreductase (Lqo)
MHA	Mueller Hinton Agar
MIC	Minimum inhibitory concentration
min	Minute
mM	Mili Molar
Mps	Membrane potential-generating system
MQ	Menaquinone
Mqo	Malate quinone oxidoreductase
MRSA	Methicillin resistant <i>Staphylococcus aureus</i>
MS	Mass spectrometry
MSCRAMM	Microbial surface components recognizing adhesive matrix molecules
NADH	Nicotinamide adenine dinucleotide
NBC	Sodium bicarbonate cotransporter
Ndh1	NADH:quinone oxidoreductase typeV1, bacterial!complex I

Ndh2	Alternative NADH:quinone oxidoreductase typeV2
Ni-NTA	Nickel-nitrilotriacetic acid Ni-NTA
NPPC	Non-professional phagocytes
OD	Optical density
PEP	Phosphoenolpyruvate
Pta-AckA	Phosphotransacetylase-acetate kinase
Rubisco	Ribulose-1,5-Bisphosphate Carboxylase/Oxygenase
SCV	Small colony variant
Sdh	Succinate dehydrogenase
SDS-PAGE	Sodium dodecyl sulfate polyacrylamide gel electrophoresis
sec	Second
SEM	Standard error mean
SFA	Saturated fatty acid
siRNA	Small interfering Ribonucleic Acid
sp	Signal peptide
SraP	Serine-rich adhesin for platelets
SulP	Sulfate permease
TCA	Tricarboxylic acid cycle
TSB	Tryptic soy broth
UFA	Unsaturated fatty acid
VRSA	Vancomycin-resistant <i>Staphylococcus aureus</i>
μM	Micro Molar

Symbols

Δ	Genetic deletion
ΔΨ	Membrane potential
°C	Degree Celsius
%	Percentage
μ	Micro

Preamble

This thesis represents a cumulative doctoral thesis. Therefore, sections from this thesis may have been published before or are intended to be submitted to peer-reviewed journals. This thesis may contain identical passages and/or figures adopted from these manuscripts without separately marking their origin, as the attached manuscripts are an essential part of this thesis. The concerned manuscripts have been authored or co-authored by me and were the result of my doctoral work and are listed on page 4-5, where the contributions to each project can be found.

Summary

Almost 50 years ago, carbon dioxide (CO₂) dependent variants were described in non-autotrophic bacteria. However, the underlying mechanism of CO₂-dependency are not clear. In this study, we demonstrate that the *Staphylococcus aureus* *mpsAB* operon does not only contribute to the production of membrane potential but is also vital for growth under atmospheric CO₂ concentration. Deletion mutants of *mpsA*, *mpsB*, and *mpsABC* hardly grew under atmospheric air conditions but could be restored to near wild-type levels under elevated CO₂ or bicarbonate concentrations. Uptake studies with radiolabeled sodium bicarbonate (NaH¹⁴CO₃) revealed that MpsAB represents a bicarbonate/dissolved inorganic carbon (DIC) transporter. Additionally, an *Escherichia coli* carbonic anhydrase (CA) *can* mutant which is unable to grow under atmospheric air but can grow when elevated CO₂ is present, can be complemented by *S. aureus* *mpsAB* and vice versa. This mutual complementation experiments indicate that both the DIC transporter and CA represent a DIC concentrating system that can functionally substitute each other. Compared to the wild type, production of hemolytic toxins are less in *S. aureus* *mps* mutants and they also display less virulence in mouse model of infection. Phylogenetic analysis reveals that MpsAB homologs are ubiquitous in bacteria and frequently occur side-by-side on the genome. Interestingly, the majority of bacteria possess homologs of either MpsAB or CA, while both are present in some highly pathogenic species. Taken together, MpsAB is proposed to act as a DIC transporter or bicarbonate concentrating system, potentially operating as a sodium bicarbonate cotransporter.

In a separate work, the mechanisms behind the host cell internalization triggered by Lpl proteins was elucidated. Lipoprotein-like lipoproteins (Lpls) is encoded by the *S. aureus* *lpl* cluster on a pathogenicity island named *vSa* island which consists of 10 *lpl* paralogue genes. By using recombinant Lpl1 protein as a model of Lpls, the host receptor for Lpl-induced *S. aureus* USA300 invasion of human keratinocytes was identified as human heat shock protein Hsp90 via pull-down assay. Synthetic peptides which covers the Lpl1 sequence resulted in double to five-fold higher rate of *S. aureus* invasion in HaCaT cells and in primary human keratinocytes. Lpl-Hsp90 interaction stimulates F-actin formation, leading to an endocytosis-like engulfment of *S. aureus*.

Zusammenfassung

Vor fast 50 Jahren wurden kohlendioxidabhängige Varianten bei nicht autotrophen Bakterien beschrieben. Der zugrunde liegende Mechanismus der CO₂-Abhängigkeit war jedoch nicht klar. In dieser Arbeit zeigen wir, dass das *mpsAB*-Operon *Staphylococcus aureus* nicht nur zur Bildung von Membranpotenzial beiträgt, sondern auch für das Wachstum unter atmosphärischer CO₂-Konzentration von entscheidender Bedeutung ist. Deletionsmutanten von *mpsA*, *mpsB* und *mpsABC* wuchsen unter atmosphärischen Luftbedingungen kaum, konnten jedoch durch erhöhte CO₂- oder Bicarbonatkonzentration auf nahezu Wildtyp-Niveaus wiederhergestellt werden. Aufnahmestudien mit radioaktiv markiertem Natriumbicarbonat (NaH¹⁴CO₃) zeigten, dass MpsAB ein Transporter für Bicarbonat bzw. gelöstem anorganischen Kohlenstoff ist (auch DIC genannt für ‚dissolved inorganic carbon‘). Zusätzlich kann eine *Escherichia coli*-Carboanhydrase (CA) -*can* Mutante, die in atmosphärischer Luft nicht, aber bei Vorhandensein von erhöhtem CO₂ wachsen kann, durch *S. aureus mpsAB* komplementiert werden, und umgekehrt eine *S. aureus mpsAB* Mutante kann durch *can* aus *E. coli* komplementiert werden. Diese gegenseitigen Komplementationsexperimente zeigen, dass sowohl der DIC-Transporter als auch die CA ein DIC-Konzentrierungssystem darstellen, das sich funktionell ersetzen kann. Verglichen mit dem Wildtyp ist die Produktion von hämolytischen Toxinen in *S. aureus mps*-Mutanten geringer und sie zeigen auch eine geringere Virulenz im Maus-Infektionsmodell. Die phylogenetische Analyse zeigt, dass MpsAB-Homologe in Bakterien weit verbreitet sind und häufig nebeneinander im Genom auftreten. Interessanterweise besitzt die Mehrheit der Bakterien Homologe von entweder MpsAB oder CA, während in hoch pathogenen Arten sogar beide vorhanden sind. Wir postulieren, dass MpsAB HCO₃⁻ in Symport mit Na⁺ transportiert (Natriumbikarbonat-Cotransporter); entsprechende Tranporter sind auch bei Säugern weit verbreitet.

In einer weiteren Arbeit leistete ich einen Beitrag zur Aufklärung des Lpl-induzierten Invasionsmechanismus in Wirtszellen. Die Gene für die Lipoprotein-ähnlichen Lipoproteine (Lpls) sind bei *S. aureus* in einer Pathogenitätsinsel namens vSaα-Insel kodiert, die aus 10 lpl paralogen Geenen besteht. Mit Hilfe des rekombinanten Lpl1-Proteins, das als Lpl-Modellprotein fungierte, wurde der Wirtsrezeptor für die Lpl-

induzierte Invasion von humanen Keratinozyten durch *S. aureus* USA300 identifiziert. Es handelt sich um das humane Hitzeschockprotein Hsp90, das mittels Pull-Down-Assay identifiziert wurde. Synthetische Peptide, die die Lpl1-Sequenz abdecken, führten zu einer 3-5-fach höheren Invasion von *S. aureus* in HaCaT-Zellen und in primären menschlichen Keratinozyten. Die Lpl-Hsp90-Wechselwirkung stimuliert die Bildung von F-Aktin, was zu einer endozytoseartigen Umhüllung von *S. aureus* führt.

List of publications and personal contributions

Accepted, peer reviewed publications

This thesis is based on the following publications:

Publication 1:

Sook-Ha Fan, Patrick Ebner, Sebastian Reichert, Tobias Hertlein, Susanne Zabel, Aditya Kumar Lankapalli, Kay Nieselt, Knut Ohlsen & Friedrich Götz (2019). **MpsAB is important for *Staphylococcus aureus* virulence and growth at atmospheric CO₂ levels**, *Nat Commun.* 2019 Aug 9;10(1):3627. doi: 0.1038/s41467-019-11547-5.

Personal contributions:

Study design, experimental design, construction of all plasmids and strains, growth studies on solid and liquid media, complementation studies with bicarbonate and CO₂, most of the uptake studies with radiolabeled bicarbonate, complementation experiments of $\Delta mpsABC$ and EDCM636, membrane potential measurement, qRT-PCR, *Galleria mellonella* infection model, *mpsAB* homologs distribution analysis, CA assays.

Publication 2:

Paula M. Tribelli, Arif Luqman, Minh-Thu Nguyen, Johannes Madlung, **Sook-Ha Fan**, Boris Macek, Peter Sass, Katharina Bitschar, Birgit Schitteck, Dorothee Kretschmer & Friedrich Götz (2019). ***Staphylococcus aureus* Lpl protein triggers human host cell invasion via activation of Hsp90 receptor**. *Cellular Microbiology*, 2019;e13111. doi: 10.1111/cmi.13111.

Personal contributions:

Expression and purification of Lpl1 protein, SDS-PAGE of the purified protein, Bradford assay, writing a part of Methods section, supported the writing and corrections of the article, critical proofreading of the manuscript.

Unpublished manuscript :

Manuscript not discussed in the current thesis:

Stefan Raue, **Sook-Ha Fan**, Ralf Rosenstein, Susanne Zabel, Arif Luqman, Kay Nieselt & Friedrich Götz. **The genome of *Staphylococcus epidermidis* O47**. In preparation.

Personal contributions:

Biofilm assay, MIC determinations, resequencing of certain genes and verifications, coordinating and compilation of results, supported the writing and corrections of the manuscript, critical proofreading of the manuscript.

Chapter 1:

The importance of MpsAB for *Staphylococcus aureus* virulence and growth under atmospheric CO₂ levels

Fan SH, Ebner P, Reichert S, Hertlein T, Zabel S, Lankapalli AK, Nieselt K, Ohlsen K, Götz F., “MpsAB is important for ***Staphylococcus aureus* virulence and growth at atmospheric CO₂ levels**”, *Nat Commun.* 2019 Aug 9;10(1):3627. doi: 0.1038/s41467-019-11547-5.

1.1 Introduction

1.1.1 *Staphylococcus aureus*

Staphylococci were first described in 1880 when Scottish surgeon Alexander Ogston reported on the its isolation from a surgical abscess (Ogston, 1880, Licitra, 2013). He named the bacterial genus as *Staphylococcus* two years later (Ogston, 1882). *Staphylococcus* originates from the Greek word *staphyle*, which means 'a bunch of grapes' and *kokkos* means 'berry' (Licitra, 2013). Later in 1884, German physician Rosenbach divided the genus by the colonies' pigmentation; *S. aureus* from the Latin word *aurum*, which means 'gold' and *S. albus* (now known as *S. epidermidis*) from the word *albus* for 'white' (Rosenbach, 1884).

Taxonomically, Staphylococci are a member of the phylum *Firmicutes*, class *Bacilli*, order *Bacillales* and family *Staphylococcaceae*. *Staphylococcus* are Gram-positive cocci that forms irregular grape-like clusters and are non-motile and non-pore forming. They have low DNA G+C content of 33-40% mol and most species are facultative anaerobes (Götz *et al.*, 2006). Facultative anaerobes are defined as organisms that can respire in the presence of oxygen, organics, nitrate or nitrite as an electron acceptor and switch to carbohydrates fermentation in the absence of such electron acceptors. Bacteria described as facultative anaerobes usually possess high adaptability to different environments (Somerville, 2016).

Out of all the *Staphylococcus* species, *S. aureus* is the most important pathogen in terms of human infections. It is a notorious bacterium that exists as a harmless commensal in the nose, with about 20% and 60% of the healthy people are persistent and intermittent carriers *S. aureus* respectively (Kluytmans *et al.*, 1997). Nevertheless, it is also an opportunistic pathogen that is capable of causing a variety of diseases, including life-threatening infections such as endocarditis, osteomyelitis and bacteremia/sepsis (Gordon & Lowy, 2008). The ability of *S. aureus* to evade our immune system and to develop resistance to antibiotics have become an endless research interest over the years. Of particular concern are the emergence of Methicillin-resistant *S. aureus* (MRSA), and recently Vancomycin-resistant *S. aureus* (VRSA) strains (Chambers & Deleo, 2009).

1.1.2 Small colony variants

In addition to the worrying trend of these antibiotics resistant strains, *S. aureus* infections are often complicated by its persistent and recurrent nature even with appropriate antibiotic treatment (Proctor *et al.*, 1994). Over the past 20 years, the underlying mechanisms for such persistence in bacteria have been gradually elucidated and most of the pathways involve changes in metabolism (Proctor *et al.*, 2014). One of the prominent phenotypes linked to these chronic and recurrent infections are the small colony variants (SCVs). Numerous studies on SCVs have contributed greatly to the understanding of bacteria persistence (Proctor *et al.*, 2006, Proctor *et al.*, 2014).

Early reports on a variant subpopulation of staphylococci, the so-called “Zwergkolonien” which means “dwarf colonies” in old German spelling could be traced back to almost a hundred years ago (Kolle & Hetsch, 1906). In the following years, most studies designated these SCVs as dwarf or gonidial (G) colonies (Hale, 1947, Goudie & Goudie, 1955). However, researchers at that time showed little interest in SCVs due to its occasional case reports and limited techniques to analyze its auxotrophy (Goudie & Goudie, 1955, Melter & Radojevic, 2010). Renewed interest in these SCVs emerged in the 1990’s when the phenotypic characteristics of *S. aureus* SCVs isolated from patients were studied and detailed analysis on molecular level was performed (Proctor *et al.*, 1995).

SCVs are defined as a slow-growing bacterial subpopulation with distinctive phenotypic and pathogenic traits (Proctor *et al.*, 2006). Phenotypically, its slow growth leads to the development of micro or pinpoint colonies, characterized by being one-tenth of the size of normal wild-type colonies (1-3 mm in diameter) on solid media after 24-72 h of incubation (Proctor *et al.*, 2006, von Eiff, 2006). In contrast to the normal staphylococcal phenotype, SCVs have no or strongly reduced pigmentation and hemolysis as well as atypical colony morphology (Proctor *et al.*, 2006). For example, thymidine-dependent SCVs frequently display an unusual “fried egg” -like colonies, with translucent edges surrounding a smaller, elevated pigmented center (Kahl *et al.*, 2003). Low electrical potential across membrane and increased resistance towards aminoglycosides are reported as one of the phenotypic characteristics of *S. aureus* SCVs (Baumert *et al.*, 2002, Koo *et al.*, 1996, Proctor *et al.*, 1995, Proctor *et al.*, 1994). In addition, SCVs also have unusual biochemical

characteristics such as mannitol-salt-agar-negative and thus posing a challenge to clinical microbiologists with regard to its identification (Proctor *et al.*, 2006).

Although *S. aureus* SCVs are the most extensively studied species, a wide range of SCVs from bacterial genera and species have been reported, including staphylococcal species such as *S. capitis*, *S. epidermidis*, *S. lugdunensis*, *S. pseudintermedius* and *S. warneri* (von Eiff *et al.*, 1999, Baddour *et al.*, 1990, Adler *et al.*, 2003, Seifert *et al.*, 2005, Savini *et al.*, 2014, Bogut *et al.*, 2014). Examples of SCVs described for Gram-positive bacteria are *Bacillus licheniformis*, *Enterococcus faecalis*, *Enterococcus faecium* and *Streptococcus tigurinus* (Idelevich *et al.*, 2013, Kubota *et al.*, 2013, Grobner *et al.*, 2012, Zbinden *et al.*, 2014). The occurrence of SCVs in Gram-negative bacteria were reported for *Brucella melitensis*, *Burkholderia cepacia*, *Burkholderia pseudomallei*, *Enterobacter aerogenes*, *Escherichia coli*, *Neisseria gonorrhoeae*, *Pseudomonas aeruginosa* and *Salmonella serovars* (Hall & Spink, 1947, Haussler *et al.*, 2003, Haussler *et al.*, 1999a, Coman *et al.*, 2008, Colwell, 1946, Borderon & Horodniceanu, 1978, Roggenkamp *et al.*, 1998, Morton & Shoemaker, 1945, Haussler *et al.*, 1999b, Jacobsen, 1910, Morris *et al.*, 1943).

Even though the slow growth rate in bacteria can be caused by many changes in their metabolism, SCVs recovered from clinical samples revealed only a limited number of defects. Two groups of SCVs that are being consistently recovered showed deficiency in electron transport and thymidine synthesis, in which their auxotrophic phenotypes can be reversed by supplementation (Proctor *et al.*, 2006). Electron transport-defective SCV phenotype can be due to several genetic mutations. For example, a mutation in *menD* blocks the biosynthesis of menadione, which is isoprenylated to menaquinone and in turn accepts electron from NADH/FADH₂ in the electron transport chain (Proctor *et al.*, 2006, Bates *et al.*, 2003). Another mutation, *hemB* blocks the biosynthesis of haem whereas *ctaA* blocks the biosynthesis of haemA, and both are involved in the cytochrome synthesis (von Eiff *et al.*, 1997, Bates *et al.*, 2003, Clements *et al.*, 1999). Additionally, mutations in encoded by *thyA* (thymidylate synthase, which converts thymidine from uracil) results in a thymidine-auxotrophic strain with typical SCV formation (Besier *et al.*, 2007a, Besier *et al.*, 2007b, Chatterjee *et al.*, 2008).

Besides, defects in unsaturated fatty acids biosynthesis can also lead to SCV phenotype. The membrane-anchoring isoprenoid tail, synthesized from unsaturated

fatty acids is added to menadione to form menaquinone (Collins & Jones, 1981, Goldenbaum & White, 1974, Kaplan & Dye, 1976). As a result, the absence of this lipid would impair the electron transport chain formation (McNamara & Proctor, 2000). Proctor (Proctor, 2019) summarized all mutations found in SCVs to date, with regard to reduced ATP and the metabolic pathways involved, as shown in Table 1.

With regard to these auxotrophic SCVs, many researchers characterized the molecular basis of its virulence and regulation and some common features are reported irrespective of the underlying auxotrophism (Kahl, 2014). In comparison to the normal *S. aureus* phenotypes, the tricarboxylic acid cycle (TCA) cycle and the global regulator *agr* of these SCVs are found to be down-regulated and virulence factors such as adhesins are up-regulated and expression of α -hemolysin is decreased (von Eiff *et al.*, 2006, Kohler *et al.*, 2003, Seggewiss *et al.*, 2006, Kriegeskorte *et al.*, 2011, Moisan *et al.*, 2006). An additional feature that is common among the hemin and menadione-dependent SCVs is the increased biofilm formation (Mitchell *et al.*, 2008, Mitchell *et al.*, 2010a, Mitchell *et al.*, 2010b, Singh *et al.*, 2009, Singh *et al.*, 2010).

In addition to these well-studied auxotrophism, SCVs with CO₂ dependency have occasionally been isolated (Goudie & Goudie, 1955, Sherris, 1952, Hale, 1951, Thomas, 1955, Slifkin *et al.*, 1971). In earlier times, these CO₂-dependent SCVs were recovered from patients with soft tissue and skin infections (Goudie & Goudie, 1955, Sherris, 1952, Hale, 1951, Thomas, 1955, Slifkin *et al.*, 1971). More recently, SCVs isolated from patients with various infections including respiratory and wound infections were found to be CO₂-dependent (Gomez-Gonzalez *et al.*, 2010). To date, however, none of the underlying mechanism of CO₂ dependence have been elucidated.

Table 1: Metabolic pathways and mutations found in SCVs with reduced ATP

Stage in electron transport	Biochemical reaction	Genes involved in electron transport pathways	Mutated genes that produce SCVs	Mutations discovered in clinical SCVs
Dinucleotide oxidation	NADH oxidation	<i>ndh2</i> (major pathway)	<i>ndh2</i>	No
			<i>nasED</i>	No
			<i>lqo, mqo, glpD</i>	No
	FADH oxidation	<i>sdh, fadD</i>	<i>sdhCAB</i>	No
Membrane translocation of protons	Makes a proton gradient	<i>mpsABC</i>	<i>mpsA</i>	No
		<i>qoxABCD</i> (Cyt <i>aa₃</i> oxidase)		
		<i>cydAB</i> (Cyt <i>bd</i> oxidase)	<i>cydAB</i>	No
Transfer of electrons to cytochromes	Menaquinone transfers electrons to cytochromes	Menadione biosynthesis	<i>menB, menC, menE, menF</i>	Yes, yes, yes, yes
			<i>menG, aroD</i>	Yes, no
			<i>menA, menD</i>	Yes, no
Oxidation of cytochromes	Electrons move from cytochrome to oxygen (nitrate)	Isoprenoid tail	<i>ispA, mvaS</i>	No, no
			Heme biosynthesis	<i>hemB, hemG</i>
		Cytochrome protein biosynthesis	<i>hemC, hemD, hemE, hemH, hemQ</i>	No, no, no, no, no
			<i>ctaA, ctaB</i>	No, no
ATP production	Proton reentry	<i>atpCDGAHFEBI</i>	<i>qoxB + cydAB</i>	No, no
Production of NADH	Tricarboxylic acid cycle is major producer of NADH	<i>citB</i> (reduced aconitase activity turns off TCA)	No	No
		<i>odhAB</i> (α -ketoglutarate dehydrogenase complex)	<i>thyA</i> mutation suppresses <i>citB</i> activation	Yes
			<i>odhA, odhB</i>	No, no

Table reproduced from (Proctor, 2019), with written permission from ASM Press.

1.1.3 *S. aureus* metabolism

In general, metabolism can be divided into two main parts; catabolism or 'breaking down' which generates energy and anabolism or 'building up' which requires energy. Metabolism can as well be separated into central, intermediary and additionally in eukaryotes, peripheral metabolism (Somerville, 2016). Central metabolism comprising of glycolytic (also known as Embden-Meyerhof-Parnas or EMP), pentose phosphate and TCA cycle pathways is both anabolic and catabolic. In this respect, all three pathways are complete for *S. aureus* except for TCA cycle where a glyoxylate shunt is lacking (Somerville & Proctor, 2009). These pathways provide *S. aureus* with the 13 biosynthetic intermediates needed to make all biosynthetic precursors (Somerville & Proctor, 2009, Somerville, 2016). Catabolism of carbohydrates are mainly through the glycolytic and pentose phosphate pathways; however when the culture medium is rich with nutrients, the TCA cycle is mostly repressed (Collins & Lascelles, 1962, Strasters & Winkler, 1963).

1.1.4 Glycolysis

In *S. aureus*, the majority of the sugars and sugar alcohols will enter into glycolysis following conversion into fructose-6-phosphate (Somerville, 2016). The process of glycolysis is illustrated in the upper half of Figure 1. For every molecule of glucose consumed, glycolysis produces two molecules of pyruvate and reduces two molecules of NAD^+ to NADH (Somerville & Proctor, 2009). The catabolic fate of pyruvate depends considerably on the availability of oxygen whereas glycolysis is independent of oxygen (Somerville, 2016).

During aerobic growth, pyruvate is oxidized to acetyl coenzyme A (acetyl-CoA) and CO_2 , driven by pyruvate dehydrogenase complex (Gardner & Lascelles, 1962). When certain TCA cycle intermediates are present in the culture medium, acetyl-CoA can be further oxidized by the TCA cycle (Goldschmidt & Powelson, 1953). During nutrient-rich growth, however, only a small number of acetyl-CoA enters into the TCA cycle (Collins & Lascelles, 1962, Strasters & Winkler, 1963, Somerville *et al.*, 2003a). During exponential growth phase, acetyl-CoA is converted into acetyl-phosphate, which can be used as a substrate for acetate kinase in substrate-level phosphorylation for the generation of ATP and acetate (Somerville *et al.*, 2003b,

Somerville & Proctor, 2009). If oxygen is absent, anaerobic growth occurs where pyruvate is mainly metabolized to lactic acid, with the concurrent re-oxidation of NADH so that glycolysis can continue (Kendall A.I. *et al.*, 1930, Krebs, 1937). Irrespective of the organic acids produced, accumulation of both lactic acid or acetic acid in the culture medium will cause to its acidification. However, if the growth conditions are favorable, both acids can be utilized as carbon sources provided that electron acceptor is available to facilitate oxidation of reduced dinucleotides (Somerville, 2016).

1.1.5 Pentose phosphate pathway

Besides glycolysis, catabolism of carbohydrates in *S. aureus* also occurs through pentose phosphate pathway. Three of the 13 biosynthetic intermediates (ribose-5-phosphate, sedoheptulose-7-phosphate and erythrose-4-phosphate) are produced when activated carbohydrates are shunted into the pentose phosphate pathway (Warburg *et al.*, 1935, Dickens, 1938, Somerville, 2016). At the same time, pentose phosphate pathway also reduces NADP⁺ to NADPH/H⁺ (Figure 1) which can function as an electron donor in biosynthesis (Somerville, 2016).

1.1.6 TCA cycle

Apart from supplying biosynthetic intermediates, the TCA cycle also play a role in the generation of reduced NADPH, NADH, FADH₂ and menaquinol which act as electron donors in the electron transport chain and also generates a small amount of energy in the form of ATP (Somerville, 2016). Acetyl-CoA, which condensates with oxaloacetate, marks the entry of carbon into the TCA cycle. Due to the catabolite repression during exponential growth phase, low amount of carbon flows into the TCA cycle. Consequently, acetyl-CoA is shunted into the phosphotransacetylase/acetate kinase (Pta/AckA) pathway, leading to the accumulation of acetate in the culture medium. (Somerville, 2016). In this respect, *S. aureus* has plenty of acetate to fuel the TCA cycle during the post-exponential growth phase (Somerville, 2016).

The TCA cycle starts with aldol condensation that adds two carbons from acetyl-CoA to oxaloacetate to generate citrate, losing two carbons as CO₂ along the process and

regenerates oxaloacetate to keep the TCA cycle going (Figure 1). The TCA cycle utilized the highest amount of NAD^+ to release NADH . Subsequently, these NADH must be re-oxidized due to the NAD(P)^+ requirement for the activity of multiple reactions in the cell, for example, dehydrogenases (Proctor, 2019).

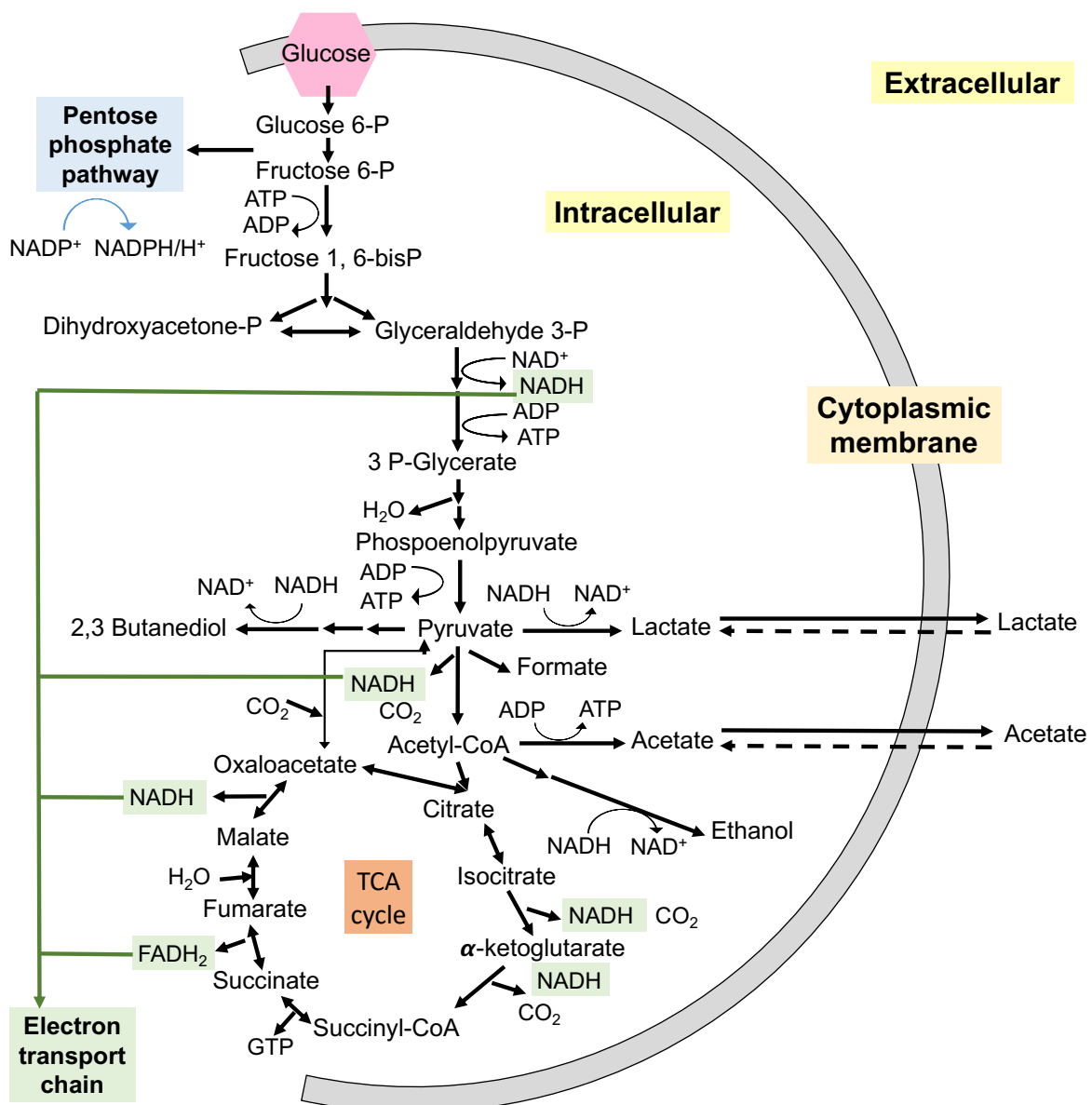


Figure 1: Central carbon metabolism in *S. aureus*. Glycolysis and TCA cycle pathways are illustrated in detailed while pentose phosphate pathway and electron transport chain are shown briefly. Dashed arrows indicate the flow of fermentation products (lactate and acetate) back into the cell for reutilization after the depletion of glucose.

1.1.7 Electron transport chain

While the oxidation of NADH and FADH₂ can occur through many reactions, the largest number of oxidation is achieved through the electron transport chain (Proctor, 2019). *S. aureus* synthesizes only one quinone, menaquinone, that is formed from menadione (Proctor, 2019). In aerobic growth, electrons from NADH enter the electron transfer chain which are then transferred to menaquinone by NADH dehydrogenase complex (Bayer *et al.*, 2006). In the case of *S. aureus*, this is accomplished by an alternative non-electrogenic type 2 NADH: quinone oxidoreductase (Ndh2), as shown in Figure 2 (Mayer *et al.*, 2015). Additionally, electrons also enter the respiratory chain via alternative entry points such as respiratory complexes which do not coupled their substrate oxidation with cation translocation. Succinate dehydrogenase (Sdh), a representative of a typical complex II, L-lactate oxidoreductase (Lqo) and malate quinone oxidoreductase (Mqo) also feed the menaquinone pool (Collins & Jones, 1981, Gaupp *et al.*, 2010, Fuller *et al.*, 2011, Stockland & San Clemente, 1969). Menaquinone then transfer the electrons to cytochromes and finally the electrons are transfer to oxygen, generating water.

S. aureus has two terminal menaquinol oxidase for the reduction of terminal electron acceptor oxygen instead of cytochrome *c* oxidase (Faller & Schleifer, 1981, Faller *et al.*, 1980, Thöny-Meyer, 1997). Cytochrome *aa*₃ oxidase (QoxABCD) which translocate protons is most active when oxygen supply is abundant while cytochrome *bd* oxidase (CydAB) is active under reduced oxygen conditions and does not translocate cations (Thöny-Meyer, 1997, Clements *et al.*, 1999, Hammer *et al.*, 2013, Voggu *et al.*, 2006, Cotter *et al.*, 1997, Winstedt *et al.*, 1998). The presence of a third terminal oxidase, cytochrome *bo* oxidase is still not clear as there is no gene annotation for it to date (Götz & Mayer, 2013).

In the absence of oxygen, *S. aureus* can grow well anaerobically using nitrate or nitrite as alternative electron acceptors in the electron transfer chains (Somerville & Proctor, 2009). Anaerobic respiration is also linked to nitrate reductase complex and its activation involves an oxygen-sensitive two-component regulator, NreBC. Genes involved in the nitrate reduction to ammonia are activated by NreBC, coupled with NADH oxidation (Niemann *et al.*, 2014).

Taken together, Ndh2 (NADH dehydrogenase), cytochromes and the nitrate reductase complex are the major complexes involved in oxidation of dinucleotides and transportation of protons across the membrane in *S. aureus* (Proctor, 2019). This produce a pH and electrochemical gradient (membrane potential, $\Delta\Psi$) across the membrane. The protons re-enter the cytoplasm through a large transmembrane protein complex, F₀F₁ ATP synthase (ATPase), with the production of ATP (Fillingame, 1997). The proton gradient is utilized by F₀F₁ ATP synthase to release ATP into the cytoplasm.

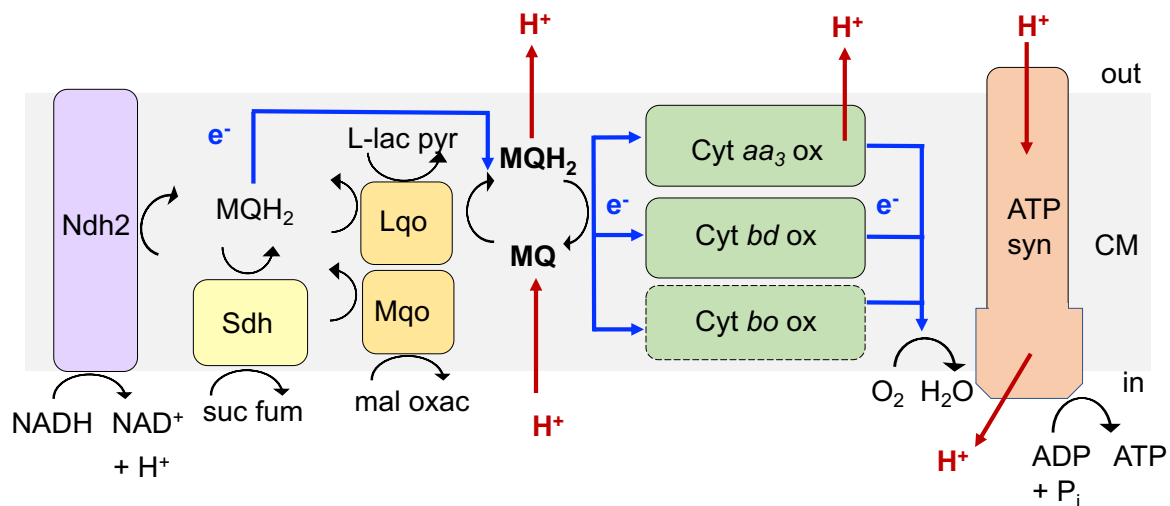


Figure 2: Schematic of the *S. aureus* aerobic respiratory chain. The non-electrogenic Ndh2 constitutes the main NADH:quinone oxidoreductase in *S. aureus*. Electrons enter the electron transport chain from NADH reduce menaquinone (MQ) to menaquinol (MQH₂). In addition, the respiratory complexes succinate dehydrogenase (Sdh), L-lactate:quinone oxidoreductase (Lqo) and malate:quinone oxidoreductase (Mqo) also transfer electrons to menaquinone with oxidation of their respective substrates. Oxidation of the menaquinol by terminal oxidases cytochrome *aa*₃ oxidase (Cyt *aa*₃ ox), cytochrome *bd* oxidase (Cyt *bd* ox) and cytochrome *bo* oxidase (Cyt *bo* ox) eventually reduce oxygen and generating water and moving the protons across the membrane. Protons reenter the cytoplasm through ATP synthase complex and generate ATP. Dash lines means the Cyt *bo* ox is not identified conclusively. suc: succinate; fum: fumarate; L-lac: L-lactate; pyr: pyruvate; mal: malate; oxac: oxaloacetate; H⁺: proton; out: outside; in: inside; CM: cytoplasmic membrane. Figure adapted from (Mayer *et al.*, 2015) and edited.

1.1.8 Membrane potential-generating system (*mps*) operon in *S. aureus*

Previous work by (Mayer *et al.*, 2015) investigated whether *S. aureus* have a type 1 NADH: quinone oxidoreductase (Ndh1) which is an electrogenic proton pump that translocates cations such as H⁺ or Na⁺. Bioinformatics analyses showed that the typical *nuo* operon encoding Ndh1 (complex I) is absent in *S. aureus* but rather the putative Ndh2 which is non-electrogenic is present. This Ndh2 consists of 402 amino acids, with 28% sequence identity and 46% similarity to the *E. coli* Ndh2, and was demonstrated to be the major NADH-oxidizing enzyme in *S. aureus*.

In addition, a hypothetical protein exhibiting sequence similarity to the proton-translocating subunit NuoL of *E. coli* complex I was identified. This *nuoL*-like gene in *S. aureus* was named *mpsA*, in which Mps stands for membrane potential-generating system and is embedded in an operon of previously of unknown function. *mpsA* is co-transcribed with *mpsB* and is further separated from the downstream *mpsC* by a weak transcription terminator while a second stronger rho-independent terminator is found downstream of *mpsC* (Figure 3). MpsA is a membrane protein consisting of 494 amino acids with predicted 14 transmembrane helices (TMHs), similar to that of NuoL (Efremov & Sazanov, 2011). MpsB and MpsC, comprising of 901 and 120 amino acids respectively, show no significant homologies to proteins of known function. Despite that, a conserved metal binding motif which is predicted to be zinc was identified in cytoplasmic protein MpsB. The *mpsABC* operon is highly conserved within the genus *Staphylococcus*, with MpsA, MpsB and MpsC showing 98-99% amino acid sequence identity in *S. aureus* strains and at least 50%, 46% and 71% identity respectively, in other *Staphylococcus* species (Mayer *et al.*, 2015).

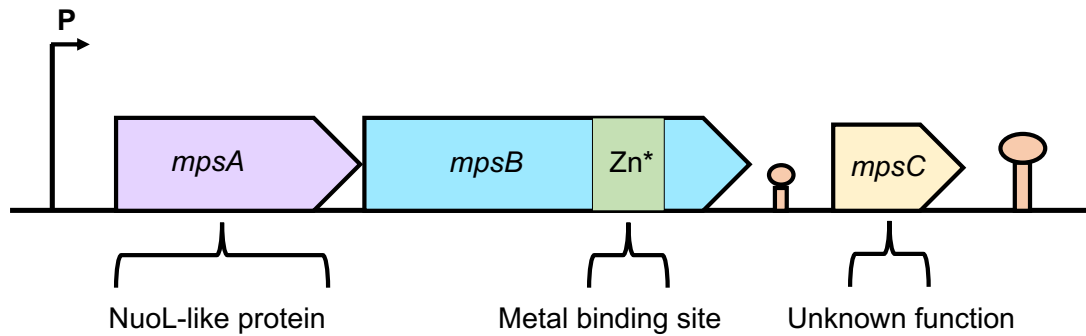


Figure 3: Homologue of the ion-translocating subunit NuoL of bacterial NADH:ubiquinone reoxidoreductase (complex I) in the genome of *S. aureus*, embedded in an operon of unknown function. The size of corresponding protein MpsA, MpsB and MpsC are 494, 901 and 120 amino acids respectively. MpsA (area in purple) shows homology with NuoL-like protein of bacterial complex I. Area shaded in green represent region with homology to a metal binding site, *predicted to be zinc (Zn). P: potential promoter region. Figure adapted from (Mayer *et al.*, 2015) and edited.

Deletion mutant of *mpsA* ($\Delta mpsA$) and the whole operon ($\Delta mpsABC$) caused a typical small colony variant (SCV)-like growth phenotype, with slow-growing and reduced or non-pigmented colonies on solid agar. The same observation was also seen in liquid medium where the growth of $\Delta mpsA$ in aerobic conditions was delayed in the first 24 h before reaching a similar OD₅₇₈ of the wild-type SA113 (WT) at 72 h (Figure 4a) (Mayer *et al.*, 2015). Such phenotype is typically seen in *S. aureus* SCVs because the colony size is limited by reduced availability of energy (Gaupp *et al.*, 2010, von Eiff *et al.*, 1997, McNamara & Proctor, 2000). In both cases, $\Delta mpsABC$ was more severely affected than $\Delta mpsA$, suggesting that all the three or at least *mpsA* and *mpsB* act together. The overlapping of the stop codon of *mpsA* with Shine-Dalgarno sequence of *mpsB* indicates the possibility of translational coupling of both genes (Mayer *et al.*, 2015).

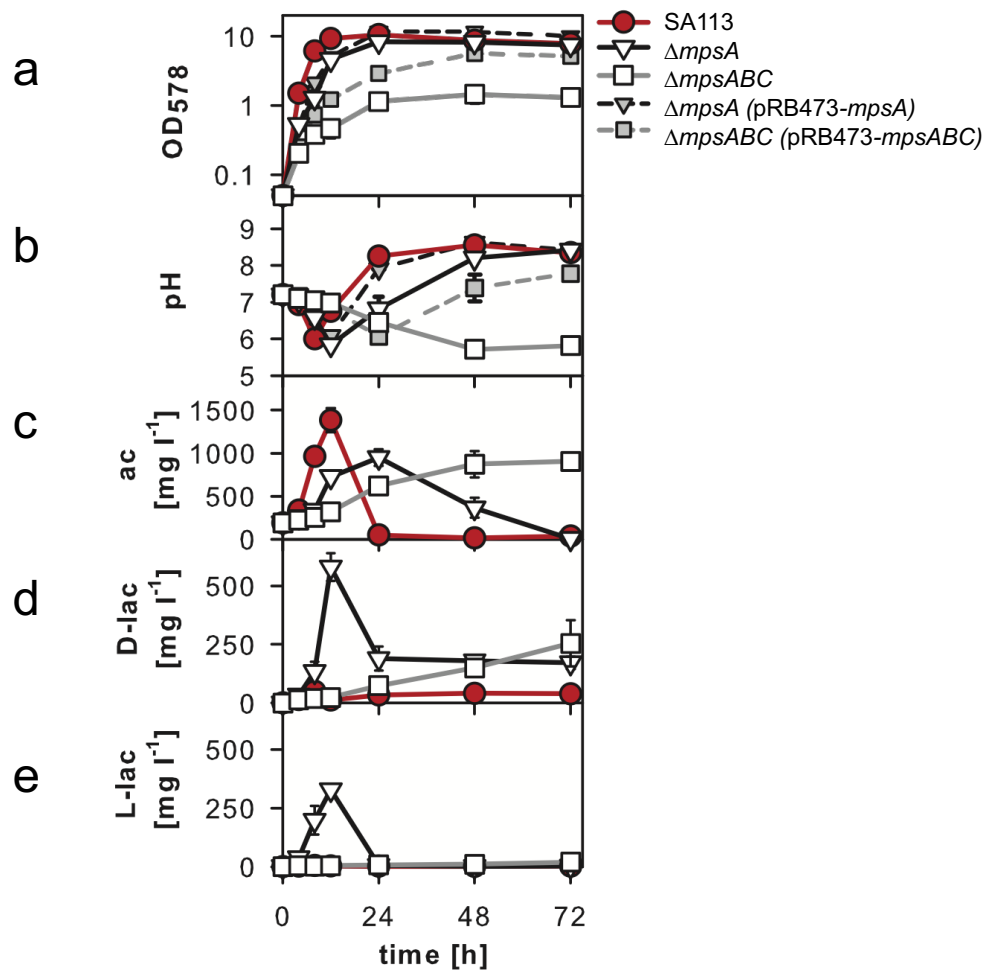


Figure 4: The growth, pH profile and extracellular metabolites in *S. aureus* wild-type SA113, $\Delta mpsA$, $\Delta mpsABC$ and its complemented mutants in aerobic conditions. a) Growth as indicated as indicated as cell density at OD₅₇₈; b) extracellular pH; concentrations of extracellular c) acetic acid; d) D-lactic acid; e) L-lactic acid. Red line with circle indicates SA113. Figure adapted from (Mayer *et al.*, 2015) and edited.

The pH profile of the supernatant of the deletion mutants was also consistent with the growth profile, showing delayed acidification and re-alkalization compared to the wild-type (Figure 4b). In WT, the characteristic drop in pH during the exponential growth phase was caused by excessive production and excretion of fermentation products (Mayer *et al.*, 2015) (Figure 4c to e), in agreement with earlier report (Somerville *et al.*, 2002). After the depletion of glucose, the pH subsequently rose because fermentation products were re-utilized and amino acids derived from the medium were also utilized, releasing pH-increasing ammonia (Somerville *et al.*, 2002, Brückner & Titgemeyer, 2002, Egeter & Brückner, 1996, Jankovic & Brückner, 2002, Mayer *et al.*, 2014, Somerville *et al.*, 2003b). In both the mutants, the delayed

production of acetate reflects its growth retardation while the increased extracellular lactate concentrations displayed similarities seen in those with respiratory impairment (Mayer *et al.*, 2015). Lactate production has been shown to be elevated under oxygen-depleted conditions (Kendall A.I. *et al.*, 1930, Krebs, 1937).

Given that *E. coli* NuoL participates in cation translocation and therefore, the $\Delta\Psi$ -generating unit of complex I, the $\Delta\Psi$ of $\Delta mpsA$ and $\Delta mpsABC$ were assayed to evaluate its effect in *S. aureus*. Indeed, the $\Delta\Psi$ generation was significantly decreased in the both mutants, with a more severe effect seen in $\Delta mpsABC$. Mps was thus named because of this membrane potential phenotype (Mayer *et al.*, 2015). As decreased $\Delta\Psi$ is associated with tolerance towards aminoglycoside antibiotics for instance, gentamicin, susceptibility of the mutants to gentamicin was also tested (Mates *et al.*, 1982, Mates *et al.*, 1983). The minimum inhibitory concentration (MIC) for the both mutants were increased in comparison to the WT (Mayer *et al.*, 2015), consistent with reports that the uptake of gentamicin is dependent on $\Delta\Psi$ (Mates *et al.*, 1982, Bryan & Kwan, 1983, Eisenberg *et al.*, 1984).

Furthermore, the role of MpsABC in aerobic respiration was supported by the observation that both $\Delta mpsA$ and $\Delta mpsABC$ showed decreased oxygen consumption rates after induction with glucose and succinate. MpsABC are implied to be a membrane potential-generating system which can substitute the function of the ion translocation role of complex I in *S. aureus*. Such a suggestion is plausible since there is no classical complex I that can catalyze both NADH oxidation and cation translocation detected in *S. aureus* and Ndh2 is present and demonstrated to be active. Therefore, MpsABC are suggested to be involved in aerobic respiration and perhaps connected to Ndh2, either directly or indirectly (Mayer *et al.*, 2015).

Additionally, MpsABC was shown to possess a cation-translocating system, with Na^+ transport capability by employing an *E. coli* strain with Na^+/H^+ antiporter deficiency, *E. coli* EP432,. Growth of *E. coli* EP432 expressing *mpsA* and *mpsABC* in 100 mM NaCl resulted in an OD_{578} of 0.1 and 0.18 respectively, while the control strain carrying the empty vector reached an OD_{578} of 0.14. This observation suggests that the presence of transmembrane protein MpsA alone creates a pore within the membrane of EP432, resulting in the leakage of Na^+ into the cell and subsequently inhibits growth. Similar observation is expected for strain carrying MpsABC if such

outcome were caused by membrane perturbation. On the contrary, Na⁺ extrusion was achieved when all the three proteins are present, as seen with the increased NaCl tolerance (Mayer *et al.*, 2015).

Taken together, the results show that the importance of MpsABC for the growth of *S. aureus* and its absence is highly deleterious for this bacteria. MpsABC constitute a significant part of the respiratory chain in *S. aureus*, playing a role as an electrogenic unit responsible for membrane potential generation (Mayer *et al.*, 2015).

1.2 Objectives

The present study continued the work of (Mayer *et al.*, 2015). The major aim of this study was to analyze the function of MpsABC in greater detail, especially MpsB. This protein is of particular interest because MpsB contains a predicted metal binding site, which is reminiscent of a carbonic anhydrase (CA) motif. The importance of this enzyme has been shown in other pathogens such as *E. coli* and *Streptococcus pneumoniae* where CA is essential for its growth in CO₂-poor environmental ambient air. Numerous metabolic process and biosynthetic needs require either bicarbonate (HCO₃⁻) or CO₂. The only known pathway for supplying bicarbonate is through the hydration of CO₂, a role traditionally played by CA.

Therefore, the first aim of this study was to perform deletion mutant of *mpsB*, as well as other deletion mutants of the *mps* operon to assess its contribution to the bacteria growth. Since CA deletion mutants of *E. coli* and *S. pneumoniae* can only grow in the presence of high CO₂, growth studies with the *mps* deletion mutants were conducted in the atmospheric air as well as in high CO₂ (5%) and bicarbonate supplementation. To this end, elevated CO₂ and bicarbonate restored the growth delay of the mutants to almost WT level. To further evaluate the direct role of MpsABC in bicarbonate transport, the bicarbonate activity between the WT and $\Delta mpsABC$ were compared using radiolabeled NaH¹⁴CO₃.

In view of the potential CA motif in MpsB, the protein was expressed and isolated from *S. aureus* for the detection of CA activity. However, since there was no CA activity detected, complementation of a CO₂-dependent *E. coli* mutant, EDCM636 with *mpsA*, *mpsB*, *mpsAB* and *mpsABC* and vice versa were carried out.

Since MpsABC was first demonstrated to be involved in membrane potential, the effect of 5% CO₂ on the $\Delta\Psi$ generation between the WT and $\Delta mpsABC$ were also addressed. In addition, the expression of *mpsA* under 5% CO₂ conditions were also evaluated. Considering the significant effect of *mps* in major pathogen like *S. aureus*, the role of *mps* in virulence was characterized in terms of hemolytic toxins production and survival rate of *Galleria mellonella* larvae in an invertebrate infection model as well as an intranasal mouse infection model.

Finally, the phylogenetic distribution of *mpsAB* homologs was examined in the genomes of Staphylococcal bacteria, *Firmicutes* and also multiple phyla of prokaryotes.

1.3 Results

1.3.1 Growth defect of $\Delta mpsABC$ in atmospheric air can be rescued by elevated CO₂ and bicarbonate

Previous study have reported that the deletion of the *mpsABC* operon in *S. aureus* strain SA113 caused a pronounced growth defect, showing the typical SCV-like growth phenotype (Mayer *et al.*, 2015). In this study, single deletion mutants of $\Delta mpsA$, $\Delta mpsB$, $\Delta mpsC$ as well as a deletion of the entire operon, $\Delta mpsABC$ was constructed in in the *agr*-positive *S. aureus* strain HG001 (Herbert *et al.*, 2010). The growth of the mutants in liquid medium under atmospheric growth conditions were analyzed. Figure 5 displays the slow growth of $\Delta mpsA$, $\Delta mpsB$, and $\Delta mpsABC$, which did not reach the final cell density of the WT HG001 even after 72 h. On the contrary, $\Delta mpsC$ was not affected in its growth, suggesting that *mpsC* has no contribution to the activity of *mpsAB*.

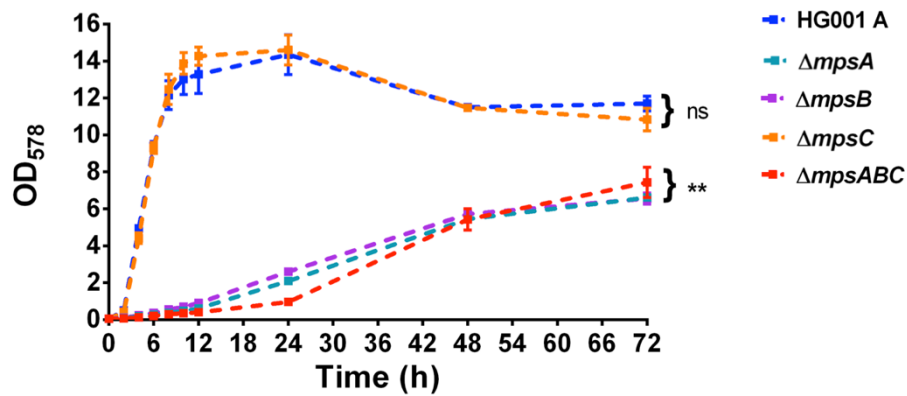


Figure 5: Growth of HG001 *mps* deletion mutants under atmospheric air. Growth of wild type HG001, $\Delta mpsA$, $\Delta mpsB$, $\Delta mpsC$ and $\Delta mpsABC$ in atmospheric (A) conditions. The growth of all mutants was significantly lower compared to HG001, (** $p < 0.01$ by unpaired two-sided *t*-test), except for $\Delta mpsC$. No significant (ns) difference in growth between $\Delta mpsC$ and HG001 was found. Each point shown in the graph represents the mean value \pm standard error mean (SEM) from three independent experiments. Figure adapted from (Fan *et al.*, 2019) and edited.

It is interesting to note that the growth of the mutants could be restored to almost WT levels when cultivated in liquid medium, Tryptic soy broth (TSB) under high (5%) CO_2 levels when cultivated in liquid medium, Tryptic soy broth (TSB) under high (5%) CO_2 concentrations (Figure 6). By comparing the growth in the absence or presence of 5% CO_2 conditions, the latter significantly improved the growth of the $\Delta mpsABC$ (Figure 6a). The growth trend is comparable to that of the complemented mutant $\Delta mpsABC(pRB473-mpsABC)$ under atmospheric conditions. The growth-promoting effect of CO_2 was also observed in $\Delta mpsA$ and $\Delta mpsB$ (Figure 6b,c). The growth enhancing-effect of CO_2 was also reflected in the colony size. In comparison between both growth conditions, the colonies of all the mutants in 5% CO_2 were significantly bigger than those cultivated under atmospheric air (Figure 7). The colony size of the WT was generally not affected by CO_2 , although there was a slight increase in size.

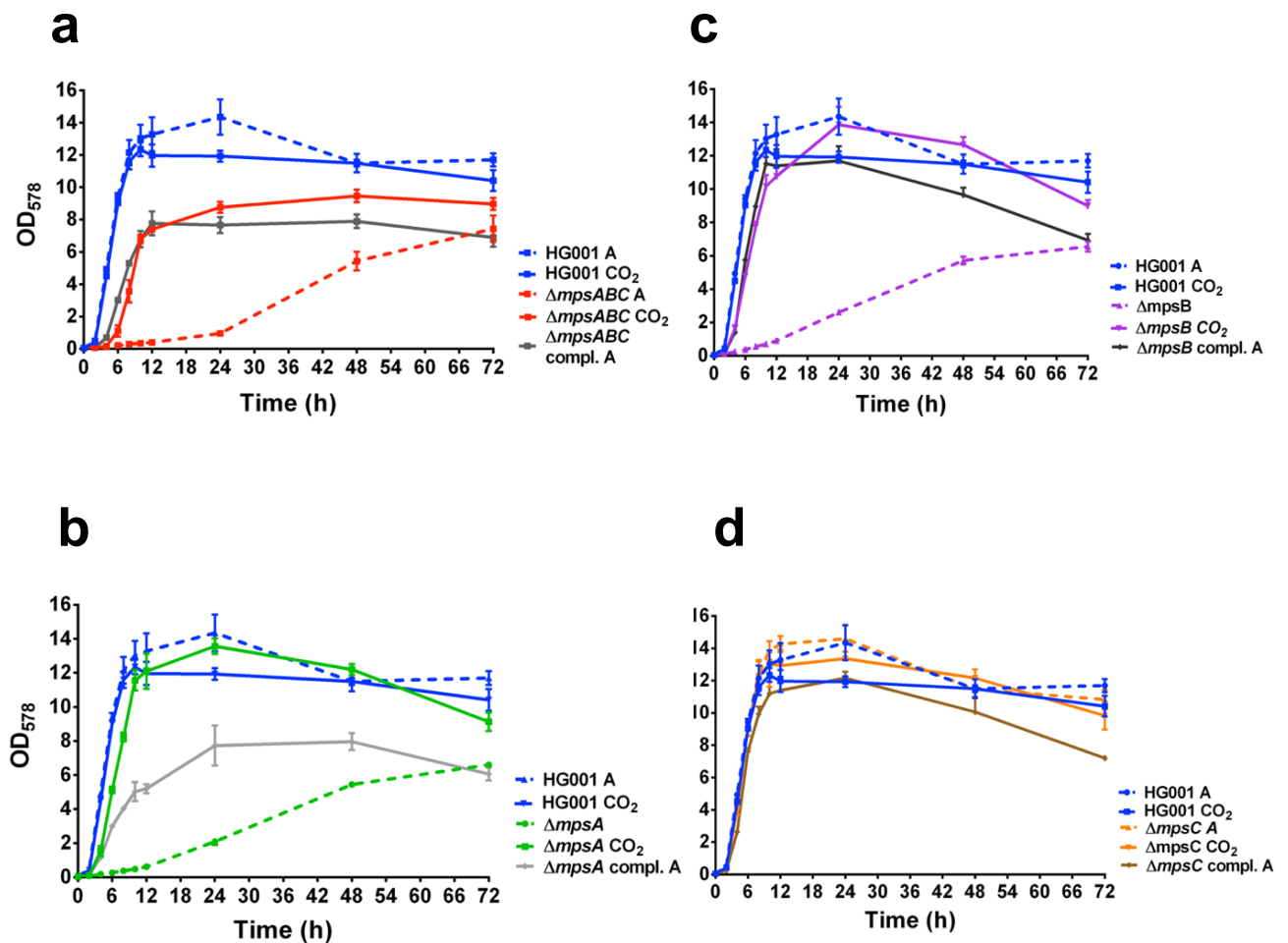


Figure 6: Growth of HG001 *mps* deletion mutants. Growth of HG001, (a) $\Delta mpsABC$, (b) $\Delta mpsA$, (c) $\Delta mpsB$ and (d) $\Delta mpsC$ and their corresponding complemented mutants in atmospheric conditions (A) and 5% CO₂. The growth of the $\Delta mpsA$ and $\Delta mpsC$ can also be complemented by plasmid pRB473 carrying *mpsA* and *mpsC* respectively. The growth of $\Delta mpsB$ was complemented by plasmid pctuf carrying *mpsB*. Each point shown in the graph represents the mean value \pm standard error mean (SEM) from three independent experiments. Figure adapted from (Fan *et al.*, 2019) and edited.

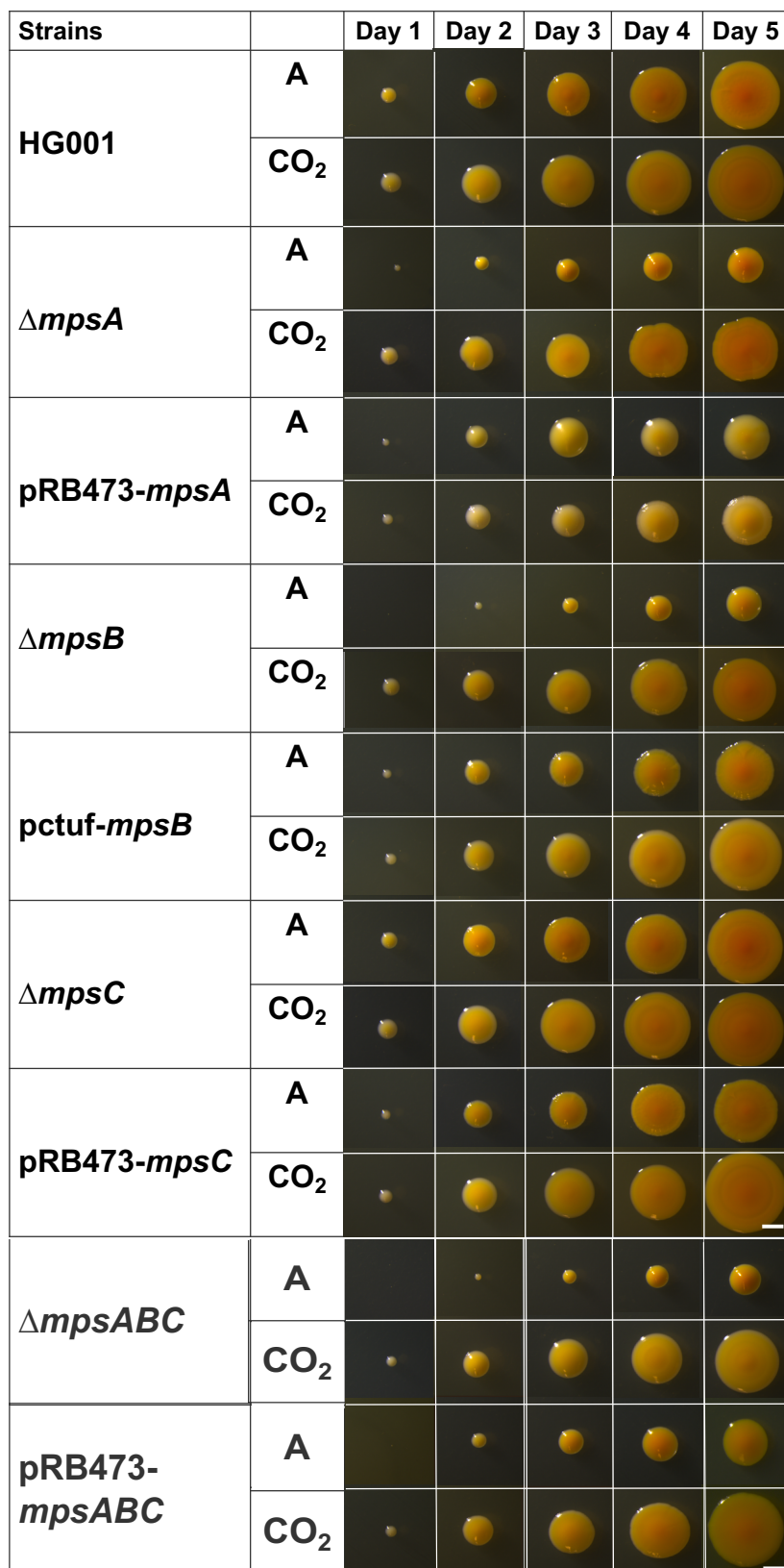


Figure 7: Colony appearances of HG001 deletion mutants. Colony appearance of wild type HG001, $\Delta mpsA$, $\Delta mpsB$ and $\Delta mpsC$ and its corresponding complemented mutant during five days of incubation in atmospheric conditions and 5% CO₂. White bar represents a scale of 1 mm. Figure adapted from (Fan *et al.*, 2019) and edited.

Considering that CO₂ and bicarbonate are interconvertible in aqueous solution, complementation of $\Delta mpsABC$ using sodium bicarbonate (NaHCO₃) was also attempted. For $\Delta mpsABC$, growth medium was supplemented with 1-50 mM of NaHCO₃ and growth was monitored for 24 h. There was no difference observed in the growth at low concentration of 1 mM NaHCO₃ (Figure 8a). With increasing NaHCO₃ concentrations of up to 50 mM, however, the growth increased gradually before achieving the final OD values similar to that of 5% CO₂. Similarly, additions of NaHCO₃ improved the growth of $\Delta mpsB$ in a concentration dependent manner up to 70 mM during the course of 72 h (Figure 8b). For better clarity, the growth curves of $\Delta mpsB$ is illustrated using OD as a function of bicarbonate concentration at 8 h and 24 h (Figure 8c). The growth studies suggest that the growth deficiency of *mps* mutants can be principally compensated, by supplementation of 5% CO₂ and high concentrations of NaHCO₃.

Of note, the pH of the medium (TSB) increased with NaHCO₃ supplementation, even though the pH effect did not play a vital role on the growth of the mutants. For the generation of Figure 6a, the pH levels were determined prior to the experiment. As shown in Table 2, the pH of the medium increased with the increased concentration of NaHCO₃. Additionally, the effect of pH was evaluated on the growth of $\Delta mpsABC$ using 20 mM NaHCO₃ which recorded an initial pH of 7.582.

The growth of the $\Delta mpsABC$ in CO₂ and NaHCO₃ were similar (Figure 9a), although the extracellular pH of the medium with NaHCO₃ was higher (Figure 9b), indicating that pH of the medium does not play a crucial role in promoting the growth.

Table 2: pH of medium with addition of NaHCO₃

Supplementation	pH of medium (TSB) at the beginning
Aerobic (TSB only)	7.173
1 mM NaHCO ₃	7.199
5 mM NaHCO ₃	7.306
10 mM NaHCO ₃	7.380
50 mM NaHCO ₃	7.782
CO ₂ (TSB only)	7.156

Table adapted from supplementary information of (Fan *et al.*, 2019) and edited.

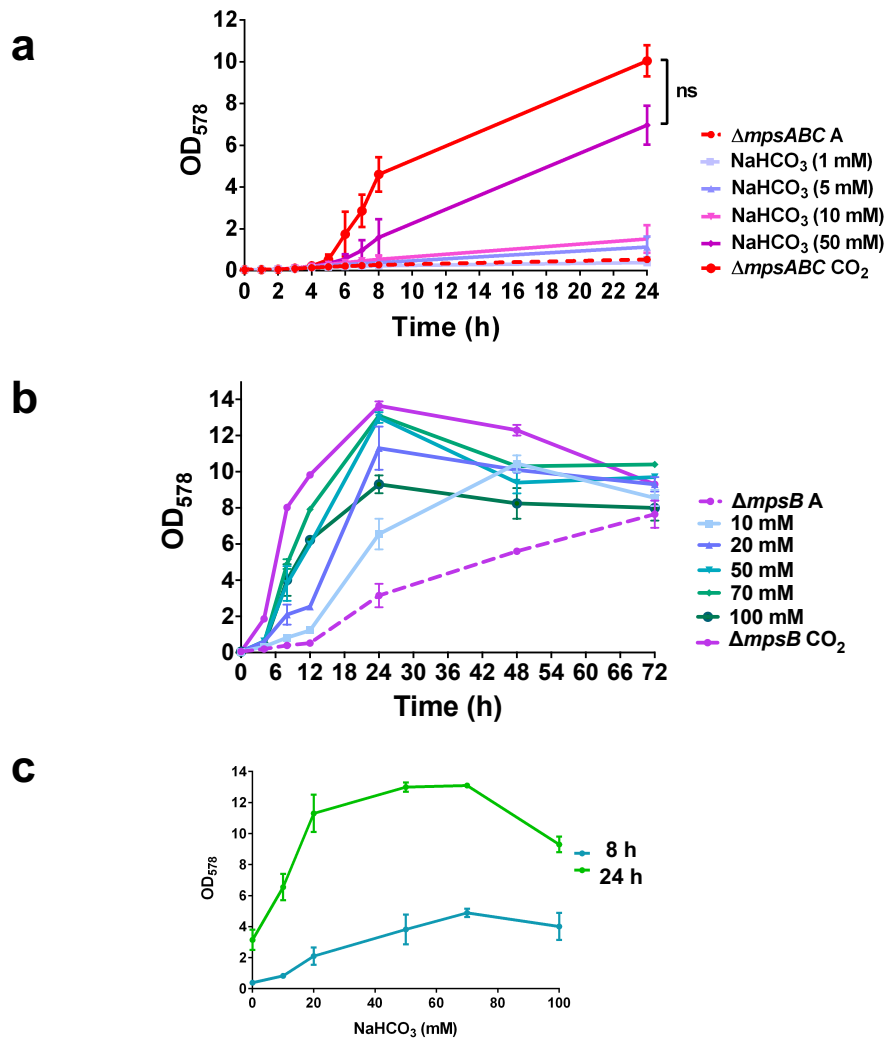


Figure 8: Growth of HG001 *mps* deletion mutants can be complemented with NaHCO₃.

(a) Growth of $\Delta mpsABC$ in atmospheric (A) and with additions of NaHCO₃ ranging from concentrations of 1 mM to 50 mM, and 5% CO₂. The growth of $\Delta mpsABC$ with addition of 50 mM NaHCO₃ was similar to that under 5% CO₂, as there was no significance difference (ns) between the two conditions ($p > 0.05$) by unpaired two-sided *t*-test (b) Growth of $\Delta mpsB$ in atmospheric (A) and with additions of NaHCO₃ and also 5% CO₂. Each concentration of NaHCO₃ is indicated in the graph, ranging from 10 mM to 100 mM. Additions of NaHCO₃ improved the growth of $\Delta mpsB$ in a concentration dependent manner up to 70 mM. (c) The same graph as in (b) but illustrated with OD as a function of bicarbonate concentration at 8 h and 24 h. Each point shown in the graph represents the mean value \pm standard error mean (SEM) from two independent experiments. Figure adapted from (Fan *et al.*, 2019) and edited.

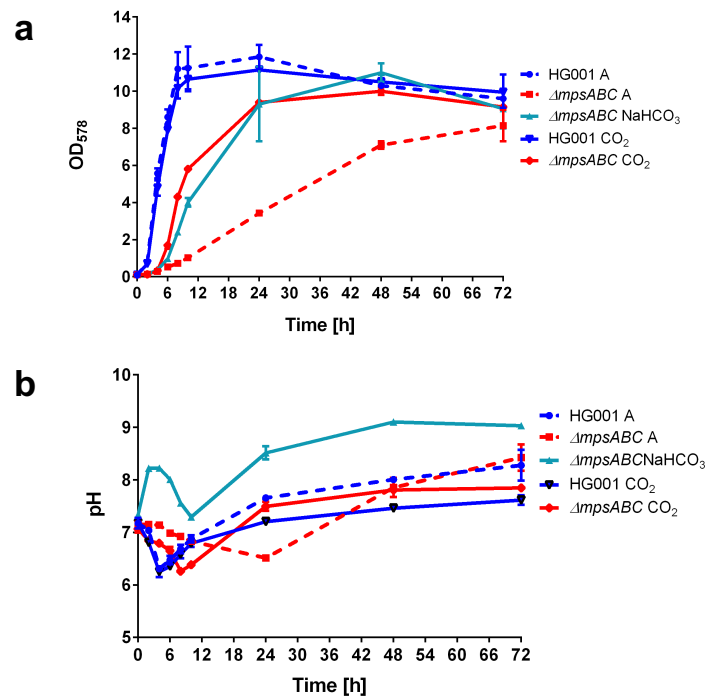


Figure 9: The (a) growth and (b) extracellular pH of WT HG001 and $\Delta mpsABC$ in atmospheric conditions (A) and 5% CO₂ and 20 mM NaHCO₃. Each point shown in the graph represents the mean value \pm standard error mean (SEM) from two independent experiments. Figure adapted from supplementary information of (Fan *et al.*, 2019) and edited.

1.3.2 MpsABC increase the uptake of bicarbonate

The rescue of the severe growth defect of $\Delta mpsABC$ by CO₂ and bicarbonate pointed to the suggestion that MpsAB may have a role in CO₂ and/or bicarbonate transport. Due to the difficulty in the determination of CO₂ transport, the bicarbonate uptake activity using radiolabeled NaH¹⁴CO₃ was employed instead. Both the WT and $\Delta mpsABC$ were grown aerobically until the respective exponential growth phase was reached and then washed to remove the growth media before resuspended to the same OD₅₇₈ in Tris buffer. A trial of using a mixture of “cold” NaHCO₃ and “hot” NaH¹⁴CO₃ resulted the very low detection of ¹⁴C uptake due to the rapid evaporation of CO₂, especially in the WT (Figure 10a). Therefore an aconitase inhibitor, fluorocitrate, was used to block the TCA cycle to ensure that the intracellular accumulation of NaH¹⁴CO₃ can occur and not expired quickly by decarboxylation reactions of the TCA cycle. For this reason, the cell suspensions were pre-incubated with fluorocitrate and glucose as an energy source since the cells were resuspended in only Tris buffer. After adding NaH¹⁴CO₃ (“hot” only), samples were promptly

harvested at specified time points and measurement of ^{14}C uptake was performed using liquid scintillation counting. Within 120 sec, an immediate uptake occurred before reaching a steady state level (Figure 10b). In comparison to the WT HG001, $\Delta mpsABC$ exhibited a significant decline in ^{14}C uptake in the first 120 sec. Subsequently, $\Delta mpsABC$ revealed a 6.6-fold lower radioactivity than the WT strain after 15 min, implying that the bicarbonate uptake was defective in the mutant.

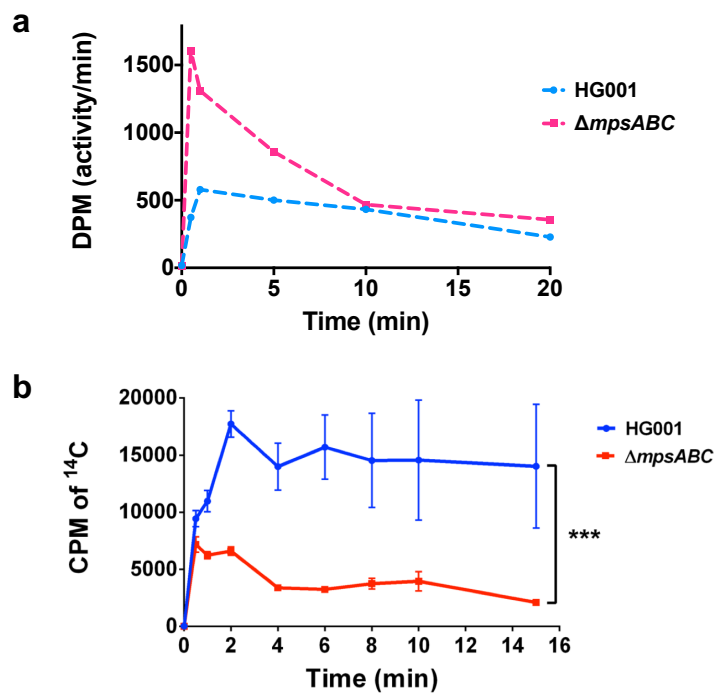


Figure 10: Uptake of $\text{NaH}^{14}\text{CO}_3$ by HG001 and $\Delta mpsABC$ in the (a) absence and (b) presence of fluorocitrate. (a) Trial results of the $\text{NaH}^{14}\text{CO}_3$ uptake without pre-incubation of fluorocitrate. 0.1 mM of NaHCO_3 (“cold”) and 50 μCi $\text{NaH}^{14}\text{CO}_3$ (“hot”) were added at time 0 to the each bacterial sample and 1 ml of cell samples collected at times indicated. Graph represent one replicate. (DPM=disintegrations per minute) (b) Cells were pre-incubated with fluorocitrate for 30 mins prior to the addition of $\text{NaH}^{14}\text{CO}_3$ (50 μCi). $\text{NaH}^{14}\text{CO}_3$ was added at time 0 and 1 ml of cell samples collected at times indicated. Determination of H^{14}CO_3 uptake in terms of ^{14}C accumulation in cells measured by liquid scintillation counting. The $\text{NaH}^{14}\text{CO}_3$ uptake in $\Delta mpsABC$ was significantly lower than WT HG001; *** $p < 0.001$ by paired two-sided t -test. Each point shown in the graph represents the mean value \pm standard error mean (SEM) from three independent experiments. (CPM=counts per minute). Figure adapted from (Fan *et al.*, 2019) and edited.

1.3.3 Impaired membrane potential in $\Delta mpsABC$ is rescued by elevated CO_2

MpsABC was previously described to represent a membrane potential-generating and cation-translocating system in *S. aureus* and $\Delta mpsABC$ is severely affected in $\Delta\Psi$ generation (Mayer *et al.*, 2015). Since elevated CO_2 rescues the growth of $\Delta mpsABC$, the restoration of $\Delta\Psi$ in the mutant grown under 5% CO_2 was also examined. The $\Delta\Psi$ of WT HG001 cultivated under atmospheric air was set equal to 100% and used as a basis for comparison with other strains. In atmospheric air, the $\Delta\Psi$ of $\Delta mpsABC$ was dropped to only 18% of the WT but increased to 134% in the presence of 5% CO_2 while it was 164% for the WT (Figure 11). The H^+ ionophore CCCP was used as a negative control, causing a collapse of $\Delta\Psi$ in all strains tested in both conditions. On the basis of these findings, both growth and $\Delta\Psi$ generation could be restored by elevated levels of CO_2 .

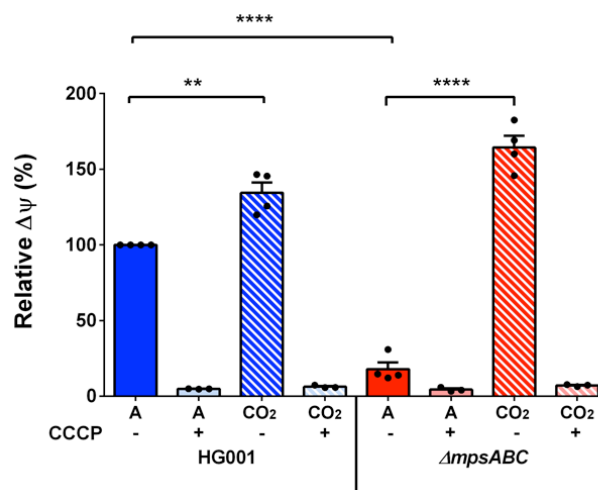


Figure 11: $\Delta mpsABC$ cultivated in 5% CO_2 displayed increase membrane potential ($\Delta\Psi$) in comparison to those cultivated in atmospheric conditions. BacLight bacterial $\Delta\Psi$ kit was used to determine the $\Delta\Psi$ by measuring the fluorescence intensity. The values for WT HG001 in atmospheric were set equal to 100%. Cells were cultivated until exponential phase in atmospheric (A) and 5% CO_2 (CO_2). The H^+ ionophore CCCP was used as a negative control, causing a collapse of $\Delta\Psi$ in all strains tested in both conditions. Cultivation under 5% CO_2 conditions resulted in a significantly higher relative membrane potential in HG001 and $\Delta mpsABC$, (** $p < 0.01$ and *** $p < 0.001$ respectively), as determined by unpaired two-sided *t*-test) in comparison to their corresponding strains in atmospheric conditions. Every bar shown in the graph represents the mean value \pm standard error mean (SEM) from four independent experiments (three independent experiments for CCCP), each with three technical replicates. Figure adapted from (Fan *et al.*, 2019) and edited.

1.3.4 *mpsA* expression was downregulated under 5% CO₂ conditions

In view of the responsiveness of the *mps* mutants with the exception of $\Delta mpsC$ to 5% CO₂, the influence of high CO₂ levels on *mps* transcription was investigated. Thus, qRT-PCR was carried out to assess the *mpsA* transcription in atmospheric and 5% CO₂ conditions. Three different *S. aureus* WT strains were used for the purpose of excluding strain-specific effects, namely HG001, USA300 LAC and MW2 (USA400). RNA was isolated from exponential growth phase cells, cultivated under atmospheric air and in 5% CO₂ and comparison of mRNA from both conditions were evaluated. Transcript abundance for every strain grown under 5% CO₂ was normalized to its corresponding strain cultivated in atmospheric conditions. *mpsA* in HG001 cultivated in elevated CO₂ was the most downregulated, at 2.5-fold, followed by USA300 2-fold and MW2 1.7-fold, relative to their growth in atmospheric air (Figure 12). Although the expression of *mpsA* under 5% CO₂ was generally lower in all the three strains evaluated, only the downregulation in HG001 reached statistical significance ($p < 0.05$). Additionally, Aureowiki also reported a downregulation of *mpsA* (SAOUHSC_00412) by CO₂ under cell culture conditions (Fuchs *et al.*, 2018).

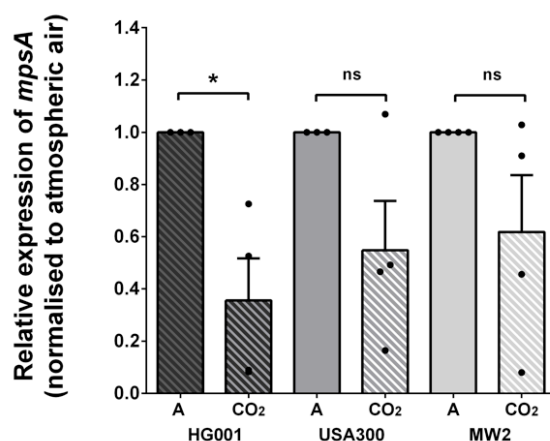


Figure 12: *mpsA* expression in three WT *S. aureus* strains HG001, USA300 and MW2 under atmospheric and 5% CO₂ conditions. *mpsA* expression under 5% CO₂ conditions was normalized to its corresponding strains grown in atmospheric (A) conditions. Only the expression of *mpsA* in HG001 was significantly reduced under 5% CO₂ in comparison to atmospheric conditions; * $p < 0.05$ by unpaired two-sided *t*-test. (ns = not significant). Every bar shown in the graph represents the mean value \pm standard error mean (SEM) from four independent experiments, each with three technical replicates. Figure adapted from (Fan *et al.*, 2019) and edited.

1.3.5 *mpsAB* complements an *E. coli* CA mutant and vice versa

MpsB has been previously described to contain a metal binding motif consisting of His607, Cys622, and Cys625, resembling CA motif (Mayer *et al.*, 2015). Hence, detection of CA activity was attempted with purified MpsB protein and cell extracts expressing MpsABC; however it was unsuccessful even with various methods. Owing to a lack of any detectable CA activity, complementation of a CO₂-dependent *E. coli* mutant, EDCM636 with *mpsAB* was carried out. EDCM636 is an *E. coli* K-12 mutant in which the CA gene, *can*, was deleted (Merlin *et al.*, 2003). As a consequence, this strain can grow in the presence of high CO₂ but not under atmospheric air, a phenotype similar to that of HG001 Δ *mpsABC*. Therefore, *S. aureus mpsA*, *mpsB*, *mpsAB* and *mpsABC* genes were inserted into EDCM636 while the vector alone, (pRB473) served as control. It is interesting to note that the growth of EDCM636 under atmospheric air could not be restored by neither *mpsA* nor *mpsB*. On the hand, plasmids carrying *mpsAB* and *mpsABC* were able to restore the growth equally well, demonstrating that *mpsC* is dispensable. Under 5% CO₂ conditions, all six strains were able to grow, as expected (Figure 13a).

Following the successful complementation of EDCM636 by *mpsAB*, the next question to be addressed was whether the CA gene (*can*) from *E. coli* could complement the *S. aureus* Δ *mpsABC*. For this approach, the *E. coli* K-12 *can* was expressed in Δ *mpsABC*(pTX30-*can*) under a xylose inducible promoter. In the absence of xylose, Δ *mpsABC*(pTX30-*can*) could barely grow under atmospheric air. However, growth was restored when the presence of xylose induced the expression of *can* (Figure 13b) whereas all clones grew under 5% CO₂ conditions. This observation indicates that both bicarbonate transporter *mpsAB* and CA enable growth under CO₂-poor atmospheric air and are interchangeable. While both the proteins differ in their activities, they constitute a CO₂/bicarbonate concentrating system (CCS) that can functionally substitute each other.

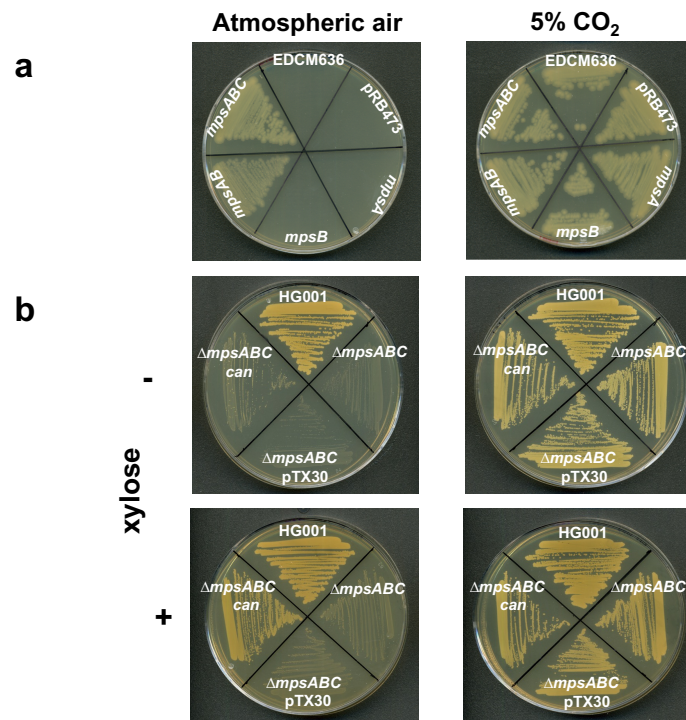


Figure 13: *mpsAB(C)* complements an *E. coli* carbonic anhydrase mutant and vice versa.

(a) Complementation of *E. coli* CA mutant (EDCM636) with plasmid pRB473 carrying *mpsAB* and *mpsABC* using its native promoter in atmospheric (left) and 5% CO₂ (right). Clockwise from the top; EDCM636, EDCM636 pRB473 (empty plasmid), EDCM636 pRB473 *mpsA*, EDCM636 pRB473 *mpsB*, EDCM636 pRB473 *mpsAB* and EDCM636 pRB473 *mpsABC* (b) complementation of $\Delta mpsABC$ with pTX30, a xylose-inducible promoter plasmid carrying *can*, a CA from *E. coli* MG1655. Clockwise from the top; wild-type HG001, $\Delta mpsABC$, $\Delta mpsABC$ pTX30 (empty plasmid) and $\Delta mpsABC$ pTX30 *can*. Plates were supplemented with xylose (+) or without xylose (-). Figure adapted from (Fan *et al.*, 2019).

1.3.6 Oleic acid supplementation

Fatty acids is one of the biosynthetic pathways involving a bicarbonate-dependent carboxylation step, and therefore could possibly attributed to the growth defect seen in $\Delta mpsABC$ (Aguilera *et al.*, 2005). In order to examine whether this step is accountable for the growth impairment of the mutant in atmospheric CO₂, the growth medium of $\Delta mpsABC$ and WT HG001 was supplemented with oleic acid using disk diffusion assay. No visible growth-promoting effect was seen in HG001 as the there was no difference in growth between the control and with 30 mM oleic acid dissolved in Tween 80 or NaOH (Figure 14). After 24 h incubation, HG001 grew equally well on the whole Mueller-Hinton agar (MHA) under all conditions tested.

In contrast, $\Delta mpsABC$ on MHA grew extremely slow, even with the addition of glucose. Figure 14 shows the agar plates of $\Delta mpsABC$ after 72 h of incubation under atmospheric air. Supplementation with oleic acid partially restored the SCV growth phenotype to a certain extent, although not as good as the wild type. Bacterial lawn can be seen surrounding the disks impregnated with oleic acid, with more confluent growth on disk with oleic acid diluted Tween 80 than in NaOH. The same trend was observed on MHA plates with addition of glucose, although the growth was not as confluent as on MHA alone. The observation of oleic acid which is an unsaturated fatty acid (UFA) could partially reverse the poor growth of $\Delta mpsABC$ under atmospheric conditions suggests that MspAB is linked to UFA biosynthesis, either directly or indirectly.

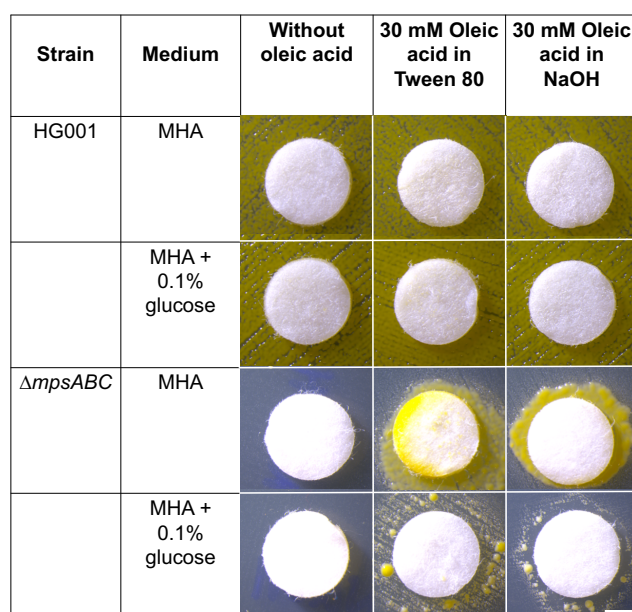


Figure 14: Supplementation of oleic acid improved the growth of $\Delta mpsABC$ under atmospheric air. The growth phenotype of HG001 and $\Delta mpsABC$ on MHA (with and without 0.1% glucose) after 24 h and 72 h of incubation respectively using disk diffusion assay. Stocks of oleic acid were dissolved in ethanol and diluted with 0.1% Tween 80 and another dissolved and diluted in 50 mM NaOH, both at a final concentration of 30mM. Disks were impregnated with 10 μ l of each of these oleic acid solutions and were laid on top of the MHA which was spread with bacterial suspension at an OD₅₇₈ of 0.1. Disks impregnated with only the diluents (0.1% Tween and 50 mM NaOH respectively) were used as controls. Experiments were performed in three independent replicates. Scale bar indicates 2 mm.

1.3.7 *ΔmpsA* in atmospheric conditions produces fewer hemolytic toxins and is less pathogenic

The impact of the of MpsAB observed on growth and $\Delta\Psi$ raise the possibility that toxin production and virulence could also be affected. To address this point, *ΔmpsA* and HG001 grown under atmospheric and 5% CO₂ was tested for hemolytic activity using sheep blood agar followed by cold shock treatment. The WT HG001 produced a hemolysis zone irrespective of the presence of 5% CO₂. Under atmospheric air, no visible hemolytic zone was observed for *ΔmpsA* whereas toxin production was restored in the presence of 5% CO₂, as seen from the clear halo on blood agar (Figure 15a). *ΔmpsB* and *ΔmpsABC* showed the same results (Figure 15b).

In view of the decreased toxin production, the relevance of this effect *in vivo* was also investigated using *G. mellonella* larvae as an invertebrate infection model. During the course of five days, the survival rate of larvae injected with WT HG001, *ΔmpsA* and PBS as control were monitored. At the end of the period, 95% of the larvae in the PBS control group were alive. On the contrary, the survival rate of larvae infected with HG001 and *ΔmpsA* were 13% and 53% respectively (Figure 15c), indicating that the deletion of *mpsA* causing *S. aureus* to become less virulent

The involvement of *mpsAB* to the pathogenesis of *S. aureus* was evaluated via an intranasal mouse infection model (pneumonia model) using female Balb/c mice. They were intranasally infected with HG001 and *ΔmpsA* and were sacrificed after 48 h. The lungs, kidneys and livers were recovered for the determination of bacterial burden. In comparison to the WT, significant lower bacterial load of *ΔmpsA* was only found in the lung although all the three organs generally showed a lower bacterial burden (Figure 15d). This mouse infection model demonstrated the attenuation of pathogenicity in *ΔmpsA* in comparison to the WT strain. Collectively, these findings indicate that *mps* as a functional bicarbonate transport system is important for fitness and pathogenicity *in vivo*.

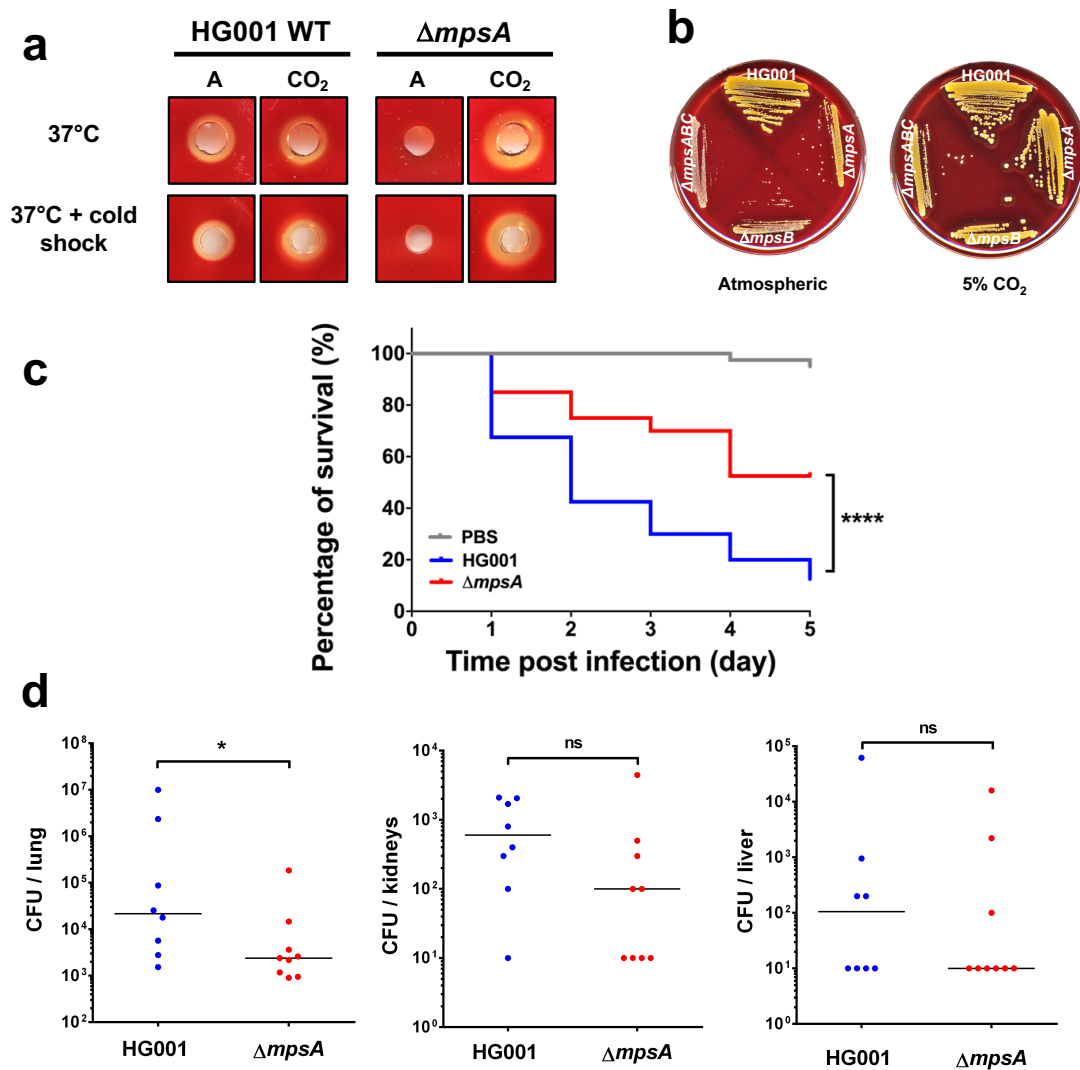


Figure 15: $\Delta mpsA$ produces less hemolytic toxin in atmospheric conditions and is less virulent in animal infection models. (a) The production of hemolytic toxin WT HG001 and $\Delta mpsA$ cultivated at 37°C under atmospheric (left) and 5% CO₂ (right), after overnight incubation (above) and cold shock treatment (below) (b) The production of hemolytic toxin in HG001 and its three *mps* mutant strains ($\Delta mpsA$, $\Delta mpsB$ and $\Delta mpsABC$) grown under atmospheric and 5% CO₂ conditions (c) Kaplan-Meier plot of the survival of *Galleria mellonella* larvae infected with HG001 and $\Delta mpsA$. The survival rate of larvae infected with $\Delta mpsA$ was significantly better in comparison to the larvae infected with wild-type HG001; ****p < 0.0001 as determined by Log-rank (Mantel-Cox) test (d) Comparison of bacterial burden in WT HG001 and $\Delta mpsA$ in the lung, kidneys and liver using a 48 h intranasal mouse infection model (pneumonia model). In comparison to WT, significantly lower bacterial burden of $\Delta mpsA$ in the lung was found (*p=0.036) while no significant difference (ns) was found in bacterial burden in the kidney and liver between the two strains. The number of bacteria per organ based on determination of CFU in WT (n=8 mice) and $\Delta mpsA$ (n=9 mice) is shown. The vertical line denotes the median. The detection limit was 10 CFU per organ. Data were analyzed using two-tailed Mann Whitney test. Figure adapted from (Fan *et al.*, 2019) and edited.

1.3.8 Phylogenetic distribution of *mpsAB* homologs

Finally, the phylogenetic distribution of *mpsAB* was examined considering its major implications in *S. aureus*. Queries of the RefSeq database showed that genes homologous to *mpsA* and *mpsB* were detected in almost all staphylococci as well as in several species within the *Firmicutes* phylum (Figure 16 and 17). Many of these bacteria from *Firmicutes* are mostly from *Bacillus* and a few from *Alicyclobacillus*, *Geobacillus*, *Parageobacillus*, *Sulfobacillus* and *Thermaerobacter*. Moreover, *mpsAB* homologs are also found extensively in the genomes of numerous prokaryotes phyla including *Proteobacteria*, *Actinobacteria*, and *Bacteroidetes* (Figure 18). High conservation of MpsAB is seen in the genus *Staphylococcus* while a lesser degree is observed in *Bacillus* and other *Firmicutes* (Figure 16 and 19). In most genomes, homologs of *mpsA* and *mpsB* are mostly adjacent, except for a few in *Actinobacteria* and *Proteobacteria*. In one of the ferrous-iron-oxidizing bacteria, *Acidimicrobium ferrooxidans*, a single fused gene of *mpsAB* homologs is found (Figure 19).

In addition, *S. aureus* *mpsAB* homologs were identified in other human pathogens, namely *Bacillus anthracis*, *Legionella pneumophila* and *Vibrio cholerae* (Table 3), where all three of them also contain genes encoding CA-like domain. *Macrococcus caseolyticus* JCSC5402, *Staphylococcus carnosus* TM300 and *Staphylococcus pseudintermedius* ED99 are the only members of the family *Staphylococcaceae* where *mpsAB* homologs are absent but CA homologs are present instead. Several other human pathogens also share this surprising feature; Gram-positive bacteria such as *Listeria monocytogenes*, *Streptococcus pyogenes*, *Enterococcus faecalis*, *Enterococcus faecium*, *Mycobacterium tuberculosis*, and Gram-negative bacteria like *Helicobacter pylori*, *Escherichia coli* and *Pseudomonas aeruginosa* (Table 3). The finding that these medically important bacteria have either CA or *mpsAB* homologs highlights the significance of bicarbonate/CO₂ supply in microorganisms.

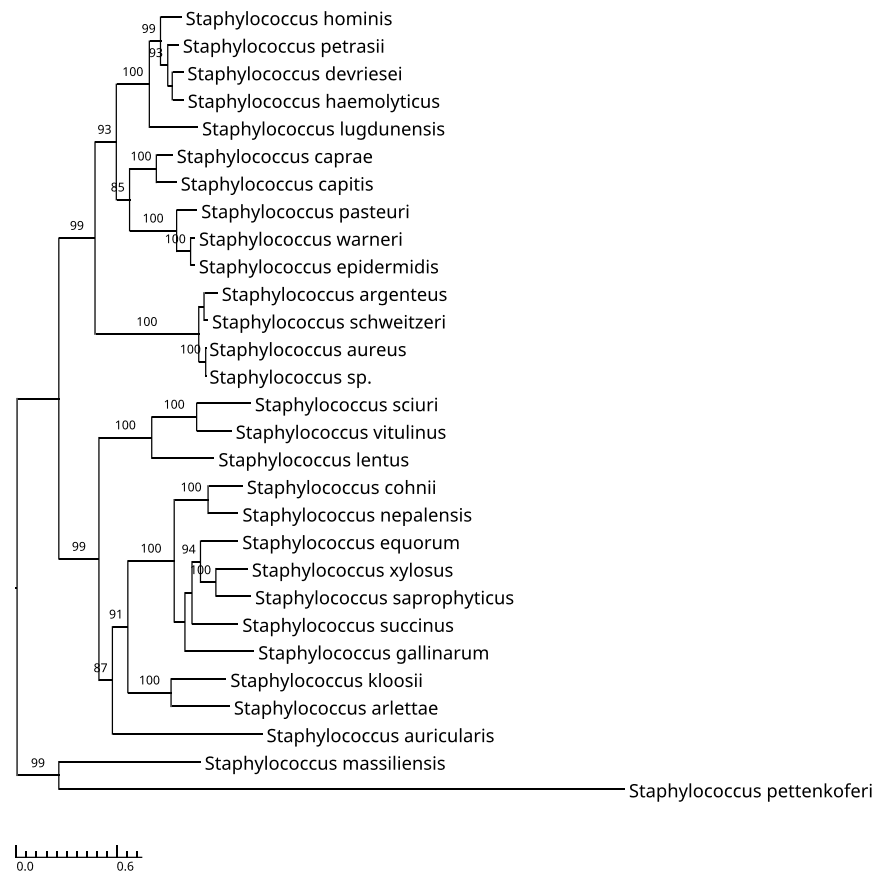


Figure 16: Homologs of *mpsAB* are highly conserved in *Staphylococci*. Maximum likelihood phylogenetic analysis of concatenated alignments of *mpsA* and *mpsB* homologs amongst the genus *Staphylococcus*. Node support is depicted by bootstrap values from 100 resamplings of the alignment when they exceeded 70%. Figure taken from supplementary information of (Fan *et al.*, 2019).

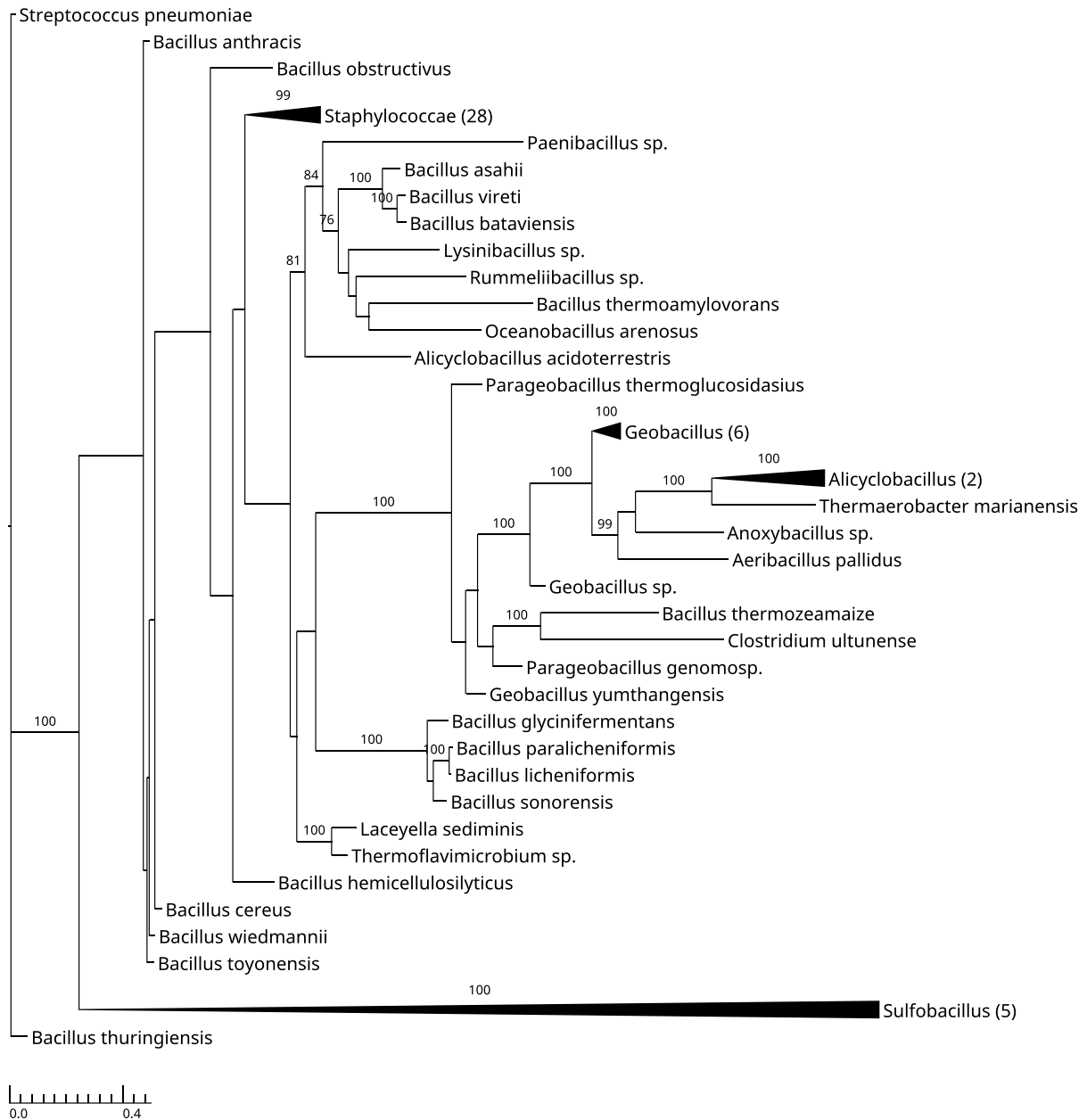


Figure 17: *mpsAB* homologs are widely found in the *Firmicutes* phylum. Maximum likelihood phylogenetic analysis of concatenated alignments of *mpsA* and *mpsB* homologs amongst the phylum *Firmicutes*. Node support is depicted by bootstrap values from 100 resamplings of the alignment when they exceeded 70%. Collapsed clades are labeled by the genus of associated taxa. The number of taxa belonging to the respective clade is indicated in brackets. Figure taken from (Fan *et al.*, 2019).

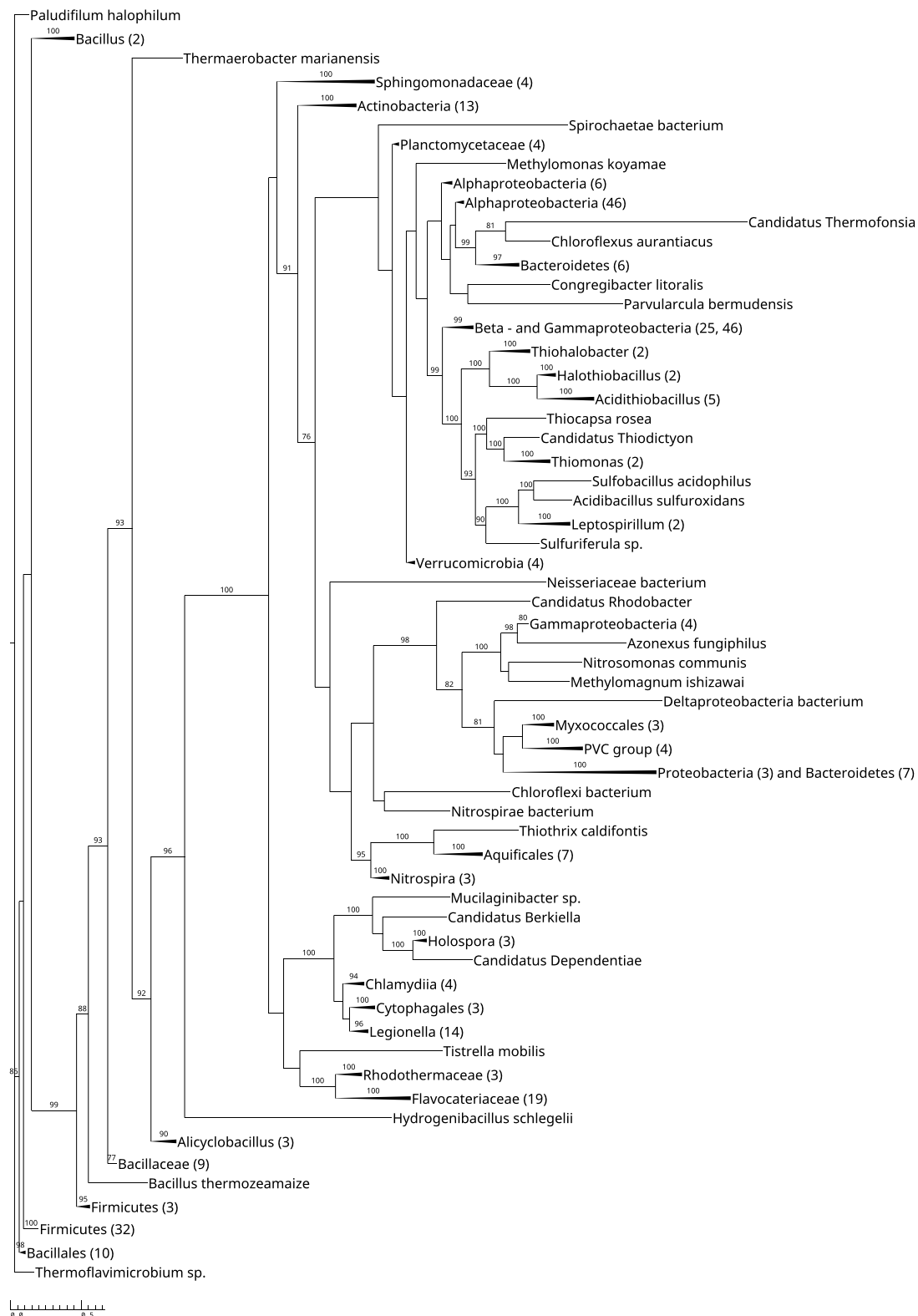


Figure 18: MpsABs homologs are widespread in multiple bacterial phyla. Maximum likelihood phylogenetic analysis of concatenated alignments of *mpsA* and *mpsB* homologs amongst the bacterial domain. Node support is depicted by bootstrap values from 100 resamplings of the alignment when they exceeded 70%. Collapsed clades are labeled by the shared taxonomic rank of associated taxa. The number of taxa belonging to the respective clade is indicated in brackets. Figure taken from supplementary information of (Fan *et al.*, 2019).

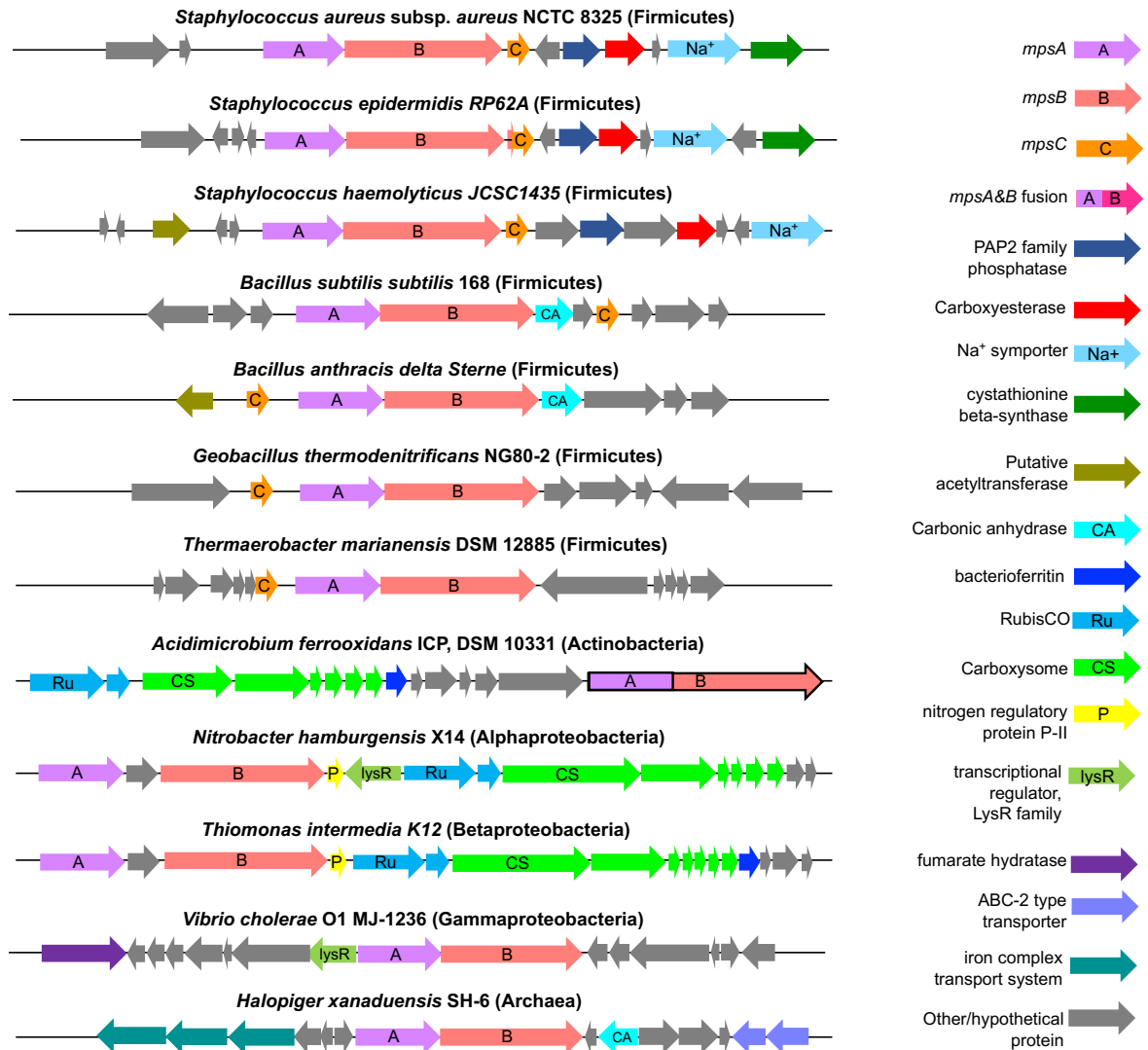


Figure 19: Gene synteny displaying the genome organization around *mpsAB* in *S. aureus* and its homologs in selected genomes. Homologs of *mpsAB* are almost always collocated. *mpsAB* homolog exists as a single fused gene in *Acidimicrobium ferrooxidans*, depicted in bold arrow outline. The *mpsAB* gene always points to the right, even if it is located on the complementary strand. Figure taken from supplementary information of (Fan *et al.*, 2019).

Table 3: Distribution of homologs of MpsAB and carbonic anhydrase (CA) in numerous species

Species	MpsAB homolog	CA homolog
<i>Staphylococcus aureus aureus</i> NCTC 8325	+	-
<i>Staphylococcus carnosus carnosus</i> TM300	-	+(a)
<i>Staphylococcus pseudintermedius</i> ED99	-	+(a)
<i>Macrococcus caseolyticus</i> JCSC5402	-	+(a)
<i>Bacillus anthracis</i> delta Sterne	+	+(a)
<i>Bacillus subtilis subtilis</i> 168	+	++(a)
<i>Listeria monocytogenes</i> R479a	-	+(b)
<i>Streptococcus pneumoniae</i> R6	-	+(a)
<i>Streptococcus pyogenes</i> A20	-	+(a)
<i>Enterococcus faecalis</i> V583	-	+(b)
<i>Enterococcus faecium</i> DO	-	+(b)
<i>Mycobacterium tuberculosis</i> H37Rv	-	+++ (a)*
<i>Helicobacter pylori</i> J99	-	+(a) +(b)
<i>Escherichia coli</i> O157:H7 Sakai (EHEC)	-	++(a)
<i>Legionella pneumophila pneumophila</i> Philadelphia-1	+	+++ (a)*
<i>Pseudomonas aeruginosa</i> PAO1	-	+++ (a)
<i>Vibrio cholerae</i> sv. O1 bv. El Tor N16961	+	+(a) +(b)

Homologies were deduced based on PFM domains search from finished bacterial genomes in Integrated Microbial Genomes & Microbiomes (IGM/G) database. MpsA, MpsB, prokaryotic type-CA and eukaryotic-type CA belongs to PFM00361, PFM10070, PFM00484 and PFM00194 respectively. +/- indicates the presence or absence of homolog while (a) and (b) denotes prokaryotic and eukaryotic-CA respectively. *One of the three CAs listed is a gene fusion and has a probable transmembrane domain where the N-terminal part has PFM00916 (sulfate transporter family) and PFM00484 in the C-terminal part. Table taken from (Fan *et al.*, 2019).

1.4 Discussion

1.4.1 Growth impairment of *mps* deletion mutants and its rescue by elevated CO₂/bicarbonate

Although more than half a century has passed since the first CO₂-dependent SCVs in *S. aureus* was documented, not much is known the genetic basis of such dependency and how *S. aureus* responds to changes in the availability of CO₂. In this study, elevated CO₂ levels (5%) or ≥ 50 mM bicarbonate could mainly rescued the severe growth impairment of the $\Delta mpsABC$ under CO₂-poor atmospheric levels (Figure 6-8). Of note, the atmospheric CO₂ levels is 0.04% and thus 5% CO₂ used in this study represents a 125 times increase in CO₂ availability. In addition to growth, elevated CO₂ also restored the defect in membrane potential and influenced gene expression as evident by the downregulation of *mpsA* in strain HG001.

However, no growth impairment or phenotypic alteration seen when *mpsC* was deleted, indicating that it is not a functioning part of the *mpsAB* operon. Support for this hypothesis can be seen from the complementation of *E. coli* CA mutant by *mpsAB* alone and gene synteny showing that *mpsC* is not collated with homologs of *mpsAB* in other bacteria except for staphylococci. Overall, these findings argue for MpsAB as a bicarbonate or DIC transporter, capable of intracellular DIC accumulation.

1.4.2 Role of MpsAB in bicarbonate uptake

The role of MpsABC in bicarbonate uptake was further supported by uptake studies using radiolabeled NaH¹⁴CO₃, where significant amount of H¹⁴CO₃⁻ accumulated in the cytoplasm of the WT in comparison to $\Delta mpsABC$. The first trial of the uptake experiment without fluorocitrate preincubation has led to an extremely low amount of ¹⁴C uptake in both the strains, particularly in the WT (Figure 10a). In fact, the initial results almost looked opposite of what is expected, where the mutant had a higher uptake than the WT. This is due to the fact that *S. aureus* lacks a glyoxylate shunt which bypasses the decarboxylation steps of the TCA cycle. For each two carbons that enters the cycle as acetyl-CoA, two carbons escape in the form of CO₂ (Somerville, 2016). Therefore, cell suspensions were preincubated with fluorocitrate,

an aconitase inhibitor to block the catalyzation of stereospecific isomerization of citrate to isocitrate, thus preventing the loss of $\text{H}^{14}\text{CO}_3^-$ from the cells in the form of CO_2 . As a result, a six fold higher ^{14}C uptake in the WT was seen and further confirming the role of MpsAB.

This experiment was tricky as CO_2 evaporation has to be avoided as much as possible and this is most probably the reason for the increased deviations seen after 5 mins. One consideration for substrate uptake is that the first 2 min are critical and in this experiment, the standard error means (SEM) were low within the given duration. The addition of fluorocitrate was unlikely to completely inhibit the TCA cycle; however the higher concentration could not be used because of the possible side effects that might occur. In this uptake study, 10 mM fluorocitrate was used while the concentration used in aconitase enzyme assay is usually 100 μM .

1.4.3 Carbonic anhydrase (CA) and MpsAB

CA, also known as carbonate dehydratase is a zinc-containing metalloenzyme that catalyze the inter-conversion of CO_2 and water to bicarbonate and hydrogen ions ($\text{CO}_2 + \text{H}_2\text{O} \leftrightarrow \text{HCO}_3^- + \text{H}^+$). Therefore, it was postulated *mpsAB* could complement an *E.coli* CA deletion mutant in (EDCM636). The *E. coli* CA, encoded by the *can* gene belongs to the β -class CA family, is reported to be essential for growth under atmospheric air but not under elevated CO_2 conditions (Merlin *et al.*, 2003). Indeed, *E. coli can* mutant could be complemented by *mpsAB* and the other way around; *S. aureus mpsABC* mutant could be complemented by *E. coli* specific *can*. Because of the mutual complementation, it is presumed that MpsAB or MpsAB might have CA activity. However, there was no detectable enzyme activity was found in the purified protein or whole cell extracts. Despite the lack of CA activity, the successful complementation experiments suggest that both MpsAB and CA differ in their enzymatic mechanisms, yet they give rise to the same functional output; specifically to prevent CO_2 expiration by trapping it in the form of bicarbonate for anaplerotic metabolism. Even though a functional TCA cycle produces a substantial amount of CO_2 , this CO_2 would be lost because it not sufficiently concentrated for anaplerotic reactions. To avoid this, CA acts to convert CO_2 to bicarbonate, significantly delaying the release of intracellular CO_2 and supplying sufficient bicarbonate to meet the requirement of carboxylation reactions (Burghout *et al.*, 2010).

1.4.4 MpsAB as a bicarbonate transporter

The complementation of EDCM636 was only successful with both *mpsA* and *mpsB*, indicating that they work together as a transporter. The collocation of MpsAB homologs on chromosomes in numerous bacteria spanning many phyla further supports this concept (Figure 18 and 19). Moreover, the protein encoded by *mpsA* belongs to PFam00361, which comprised of a diverse family of membrane-spanning proton-conducting transporters, including NADH:quinone oxidoreductase subunits (complex I) (El-Gebali *et al.*, 2019, Walker, 1992). In this connection, MpsABC have been previously shown to represent a cation-translocating system, capable of Na⁺ transport, bearing similarity to NuoL (Mayer *et al.*, 2015). MpsB is a member of PFam10070, which consists of a family of conserved proteins in bacteria that have no characterized function.

On the basis of these findings, a model is proposed for MpsAB as a sodium bicarbonate cotransporter (NBC) as depicted in Figure 20. These transporters are common in mammals, which play an important role in intracellular and whole body pH maintenance and also in trans-epithelial transport processes (Boron *et al.*, 2009). Such bicarbonate cotransporters consist of 13 transmembrane domains, while MpsA likewise has 14 (Felder *et al.*, 2016). It remains unclear whether mammals also need a MpsB homolog; though the NBC stoichiometry in *Xenopus* oocytes is 1 Na⁺: 2 HCO₃⁻, suggesting a potential accessory protein interaction (Romero, 2001). Since CO₂ is volatile, transporting it in the form of bicarbonate or DIC allows carboxylation reactions of anaplerotic metabolisms to proceed by trapping it in dissolved forms within the cytoplasm. Examples of such reactions in *Firmicutes* are pyruvate carboxylase feeding the TCA cycle, acetyl-CoA-carboxylase as the first enzyme of fatty acid synthesis, or phosphoribosylaminoimidazole carboxylase involved in purine biosynthesis.

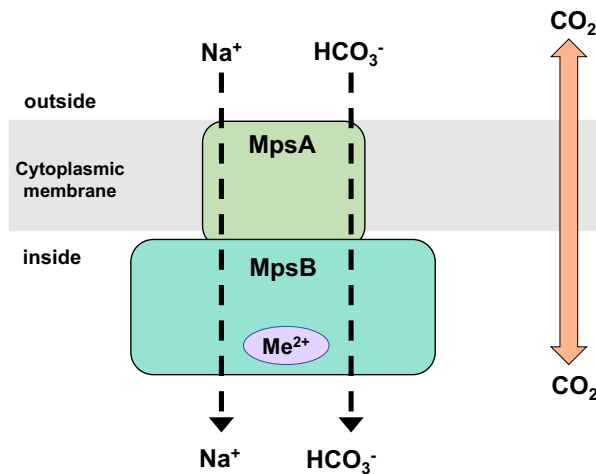


Figure 20: Proposed model of MpsAB. MpsAB is proposed to represent a sodium bicarbonate cotransporter (NBC). Such transporters are common in mammals and are expressed throughout the body. In contrast to CO_2 which can diffuse passively in and out of the cells, bicarbonate (HCO_3^-) requires a transporter to be transferred into the cells. In *S. aureus*, MpsAB most likely act together as cotransporter to transport Na^+ and HCO_3^- . Me^{2+} depicts a predicted metal binding site in MpsB, possibly Zn. Figure adapted from (Fan *et al.*, 2019) and edited.

1.4.5 Distribution of MpsAB

Phylogenetic analysis indicated that *mpsAB* are extensively distributed among *Firmicutes* as well as throughout many phyla (Figure 16-18). Microorganisms with homologs of MpsAB adopt a broad range of different lifestyles, including CO_2 -fixing bacteria (e.g., *Chloroflexus aurantiacus*), nitrogen-fixing bacteria (e.g., *Bradyrhizobium oligotrophicum* and *Frankia sp*), hyperthermophilic (e.g., *Aquifex aeolicus*) as well as thermophilic and acidophilic (e.g., *Acidimicrobium ferrooxidans* and *Acidithiobacillus caldus*).

Besides, MpsAB homologs were also identified in the gammaproteobacterial chemolithoautotroph *Thiomicrospira crunogena* (Mangiapia *et al.*, 2017). As with *S. aureus*, co-transcription of *T. crunogena* genes *Tcr_0853* and *Tcr_0854* (*mpsA* and *mpsB* homologs respectively) and high- CO_2 -requiring mutant phenotype were reported, thereby representing a potential DIC transporter (Mangiapia *et al.*, 2017). *T. crunogena* has CO_2 concentrating mechanism (CCM), though the DIC uptake process is not clear, as cyanobacterial transporter homologs are absent. Nevertheless, it is believed that a DIC concentrating system in autotrophic bacteria is essential to ensure that Ribulose-1,5-Bisphosphate Carboxylase/Oxygenase

(Rubisco) is saturated with CO₂, thus allowing carboxylation to proceed at its maximum rate.

1.4.6 Carbon concentrating mechanism

The major carbon fixation cycle in nature, Calvin-Benson-Bassham (CBB) cycle uses one of the most ubiquitous, yet one of the least efficient enzymes known, Rubisco to fix CO₂ (Liang *et al.*, 2018). Despite its central role, problem with Rubisco arises because of its non-specific reaction with oxygen (Raven & Beardall, 2016). In this regard, the atmospheric air content in ancient times was relatively O₂-low and CO₂-high. Given the CO₂-rich atmosphere levels, CO₂-fixing enzymes in autotrophic bacteria, for example Rubisco could function properly even with low affinity and limited specificity between CO₂ and O₂. However, over the subsequent 2.5 billion years, the atmosphere became O₂-rich and CO₂-poor due to oxygenic photosynthesis (Raven *et al.*, 2017). As a result, the CO₂ levels in the cytoplasm became too low for CO₂ fixation and assimilation to work properly (Tabita *et al.*, 2008, Shih *et al.*, 2016). Thus it is presumed that autotrophic bacteria growing in atmosphere seem to uniformly have CCMs (Raven *et al.*, 2017).

Bacterial CCMs involve two main components. Firstly, inorganic carbon species (Ci; HCO₃⁻ and CO₂) are actively transported resulting in conditional accumulation of HCO₃ in the cytosol. Secondly, the concentrated HCO₃ is then employed to supply elevated CO₂ concentrations around Rubisco, which is encapsulated in carboxysomes together with CA (Price, 2011). Because HCO₃⁻ escapes less readily across the cell membrane, accumulation of charged HCO₃⁻ is preferred to CO₂. Active HCO₃⁻ transport and facilitated uptake of CO₂ produce a cytosolic HCO₃ concentration of more than 10 mM, which is approximately 30 times the equilibrium concentration of HCO₃ in water at neutral pH at 25°C (Mangan *et al.*, 2016).

1.4.7 Bicarbonate transporters

DIC transporters from four evolutionary distinct families were recently described in a number of sulfur-oxidizing chemolithoautotrophs (Scott *et al.*, 2019). Two of such DIC transporters displayed DIC uptake activity despite sharing low protein identity with the well-studied cyanobacterial transporters, SbtA and SuIP-family bicarbonate

transporters (Scott *et al.*, 2019). SbtA is an inducible, high affinity Na⁺-dependent HCO₃⁻ transporter whereas BicA is a low-affinity, high-flux Na⁺-dependent HCO₃⁻ transporter which belongs to the widespread SuIP/SLC26 family (Shibata *et al.*, 2002, Price *et al.*, 2004). Both transporters are also acting as a probable Na⁺/HCO₃⁻ symporter (Price, 2011). In addition, heterologous expression of chromate ion transporter (Chr) from *Hydrogenovibrio thermophilus* in *E. coli* also demonstrated DIC uptake capability (Scott *et al.*, 2019). The last family of transporters reported by the same study is a two component DIC transporter encoded by the genes *Tcr_0853* and *Tcr_0854* in *Hydrogenovibrio crunogenus* (previously known as *T. crunogena*), as previously discussed earlier (Mangiapia *et al.*, 2017, Scott *et al.*, 2019).

Another well-documented DIC transporter found in cyanobacteria is BCTI, an inducible, high-affinity HCO₃⁻ transporter encoded by the *cmpABCD* operon and is a member of the ATP binding cassette (ABC) transporter family (Omata *et al.*, 1999). It is likely that these transporters vary in terms of affinities for DIC or transport mechanisms (as cation symporter or anion antiporter) and forms of DIC (CO₂, HCO₃⁻, CO₃²⁻), thus providing advantages under certain growth conditions (Scott *et al.*, 2019). Among all these transporters families, MpsAB belong to the same family whose protein encoded by *Tcr_0853* and *Tcr_0854* from *H. crunogenus* with respect to function and homology. Both protein have 29-30% sequence identity. In *Firmicutes*, this transporter and its function have not been reported so far.

1.4.8 MpsAB as bicarbonate transporter in *S. aureus*

Like many other *Firmicutes*, staphylococci are neither autotrophic nor have common carboxysome structures or Rubisco. This surprising finding leads to a thought-provoking question: why do they require DIC concentrating system such as MpsAB? The most logical explanation would be that under atmospheric CO₂ levels, insufficient HCO₃⁻ is being supplied to the enzymes involved in substrate carboxylation. As a result, higher concentration of HCO₃⁻ is needed for proper activity. Biotin-dependent pyruvate carboxylase, for instance, play a key role in fueling the TCA cycle with oxaloacetate (discussed in detail in later section). Impairment of this reaction would result in impairment not only of TCA cycle but also of respiration and membrane potential. Such characteristics are precisely the observed phenotype of *mpsABC* mutant, which displayed the common features of SCV under atmospheric CO₂ and

comparable with the *S. aureus hemB* mutant (von Eiff *et al.*, 1997, Mayer *et al.*, 2015).

It is also tempting to suggest that MpsAB may be fulfilling a role generally played by CA or other known bicarbonate transporter from cyanobacteria, which function to prevent the depletion of cellular DIC. The absence of such enzyme or transporter in *S. aureus* means a DIC concentrating mechanism is likely to be significant for its growth and survival because CO₂ or HCO₃⁻ is essential for many cellular processes. *S. aureus* needs to adapt to a diverse environmental conditions, as reflected by the different niches it occupies; from commensal inhabitant on environmentally exposed skin and mucous membranes to colonizer and pathogen inside the mammalian host. During this process, one of the apparent environmental conditions would be encountered by *S. aureus* is the differences in CO₂ levels. Sufficient intracellular HCO₃⁻/CO₂ supply would be assured by having a DIC concentrating mechanism. Taken together, these hypotheses could explain the role of MpsAB outside of known carbon-fixing bacteria.

1.4.9 Importance of bicarbonate

The importance of bicarbonate can be attributed to its demand considering its requirement in three classes of pathways (Merlin *et al.*, 2003). Bicarbonate and/or CO₂ is incorporated into the cell mass from biosynthesis of amino acids such as arginine and aspartic acid and nucleic acids uracil and adenine (Merlin *et al.*, 2003, Langereis *et al.*, 2013). When grown on simple substrate, 1 g atom per mole of arginine or nucleotide base is derived from bicarbonate ion and they are incorporated by carboxylase-catalyzed reactions (Merlin *et al.*, 2003).

Bicarbonate is also required for fatty acid biosynthesis, through incorporation into malonyl-CoA via acetyl-CoA carboxylase which is the first committed step of this process (Fujita *et al.*, 2007). In a subsequent condensation step, CO₂ is released. For every two-carbon unit incorporated into lipid, one molecule of bicarbonate is required (Merlin *et al.*, 2003).

Another crucial role of bicarbonate is in central metabolism, considering that it is the substrate for biotin carboxylase to generate carboxybiotin (discussed below), which in turn serves as substrate for other carboxylases like PEP-, or pyruvate carboxylase.

This enzyme catalyzed the formation of oxaloacetate from pyruvate to replenish the TCA cycle and biosynthetic reactions. The *E. coli* biotin carboxylase, for instance, has a relatively high K_m value for bicarbonate at 16 mM, suggesting that the enzyme has a very poor affinity for bicarbonate (Chou *et al.*, 2009). This scenario implies that a high concentration of bicarbonate within the cell is required to feed the TCA cycle and fatty acids synthesis and also indirectly affects respiration and membrane potential. In this context, reduced TCA cycle activity means fewer reducing equivalents NADH and FADH₂ are being produced, leading to decreased electrons delivery to the electron transport chain. As a result, the lower electron flux translates to diminished membrane potential which is required to generate ATP and consequently an impaired respiration. Support for this hypothesis can be observed from the severe decline in membrane potential generation in $\Delta mpsABC$ in this study and also decreased oxygen consumption in previous study (Mayer *et al.*, 2015).

1.4.10 Carboxylation enzymes and biotin-dependent enzymes

The significance of bicarbonate emphasizes the roles of enzyme like CA or bicarbonate transporter MpsAB that are far more extensive than previously recognized. From a chemical reactivity point of view, CO₂ would seem to be a more suitable substrate than bicarbonate for carboxylation reactions considering it would be more prone to nucleophilic attack. On the other hand, the equilibrium between dissolved CO₂ and bicarbonate at physiological pH implicates that the concentration of bicarbonate is 20-fold greater in aqueous medium. Because bicarbonate is a more polar molecule compared to CO₂, it is likely to have stronger potential for binding to enzyme. Even though the decarboxylation reactions in catabolic processes produce CO₂, a number of carboxylation enzymes have evolved to use bicarbonate as substrate rather than CO₂ (Chegwidden *et al.*, 2000).

A broad number of carboxylation enzymes catalyze reactions for which CA or MpsAB could be expected to supply HCO₃⁻/CO₂ for biosynthesis and metabolism. Some of these enzymes are known to bind bicarbonate as substrate but typically convert it to CO₂ or its activated form (Chegwidden *et al.*, 2000). Such carboxylating enzymes require biotin as co-factor, therefore are called biotin-dependent carboxylases. Table

4 shows the selected prokaryotic carboxylases and its corresponding carboxylation reactions.

Figure 20 shows biotin structure and examples of the major carboxylation reactions involving the transfer of CO_2 to the respective substrate using biotin as a co-factor. Biotin is covalently bound to the carboxylase or transcarboxylase it serves as a co-factor. A peptidyl linkage is formed between the carboxylic acid moiety of biotin and the ϵ -amino group of peptidyl lysine of the enzyme. This biotin-lysine adduct is termed biocytin and it is released after biotin-containing carboxylases is degraded by biocytinase (Rucker R. B. *et al.*, 2008).

Table 4: Prokaryotic carboxylation enzymes using $\text{HCO}_3^- / \text{CO}_2$ as substrate

Substrate	EC number	Enzyme	Reaction	Co-factor
HCO_3^-	4.1.1.31	phosphoenolpyruvate carboxylase	phosphoenolpyruvate + HCO_3^- + ATP \rightleftharpoons oxaloacetate + ADP + P_i	
	6.3.4.16	carbamoyl-phosphate synthase	ammonia + ATP + HCO_3^- + H_2O \rightleftharpoons carbamoyl-phosphate + ADP + P_i	
	6.4.1.1	pyruvate carboxylase	pyruvate + ATP + HCO_3^- \rightleftharpoons oxaloacetate + ADP + P_i	biotin
	6.4.1.2	acetyl-CoA carboxylase	acetyl-CoA + ATP + HCO_3^- \rightleftharpoons malonyl-CoA + ADP + P_i	biotin
	6.4.1.3	propionyl-CoA carboxylase	propanoyl-CoA + ATP + HCO_3^- \rightleftharpoons methylmalonyl-CoA + ADP + P_i	biotin
	6.4.1.4	methylcrotonoyl-CoA carboxylase	3-methylcrotonoyl-CoA + ATP + HCO_3^- \rightleftharpoons 3-methylglutaconyl-CoA + ADP + P_i	biotin
	6.4.1.5	geranyl-CoA carboxylase	geranyl-CoA + ATP + HCO_3^- \rightleftharpoons 3(4-methylpent-3-en-1-yl)-pent-2-enedioyl-CoA + ADP + P_i	biotin
CO_2	4.1.1.39	Rubisco	D-ribulose-1,5-biphosphate + CO_2 \rightleftharpoons 2 D-3-phosphoglycerate	
	6.3.4.14	biotin carboxylase	biotin-carboxyl-carrier protein + ATP + CO_2 \rightleftharpoons carboxylbiotin-carboxyl-carrier protein + ADP + P_i	biotin

Table adapted from (Smith & Ferry, 2000) and edited.

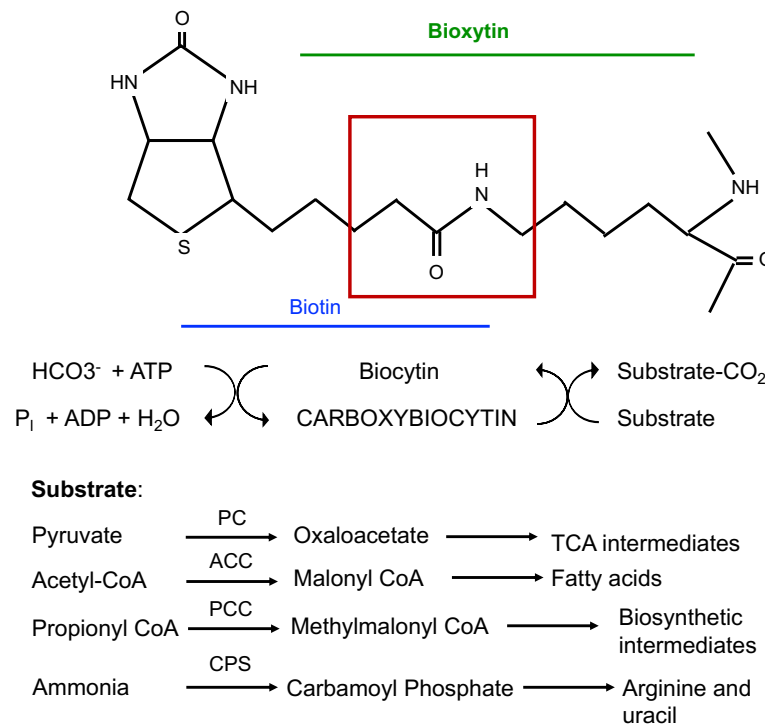


Figure 20: Biotin structure and examples of biotin-dependent carboxylations. Biotin is covalently bound to the enzymes by a peptide bond between carboxylic acid moiety and the ϵ -amino group of peptidyl lysine of the enzyme. Biocytin, the biotin-lysine adduct is released after biotin-containing carboxylases is degraded by biocytinase. Examples of major biotin-dependent carboxylation reactions involving the transfer of CO_2 to its corresponding substrate. Carboxylase involved are depicted above the arrow. PC: pyruvate carboxylase; ACC: acetyl-CoA carboxylase, PCC: propionyl-CoA carboxylase, CPS: carbamoyl-phosphate synthase. Figure adapted from (Rucker R. B. *et al.*, 2008) and edited.

1.4.11 MpsAB is indirectly linked to UFA biosynthesis

As discussed in the previous section, the biosynthetic pathways for nucleic acids, fatty acids and a few amino acids comprise a biotin-dependent carboxylation step which require bicarbonate. This requirement could be responsible for the observed growth defect of $\Delta mpsABC$ under atmospheric CO_2 conditions. Indeed, supplementation of UFA oleic acid at 30 mM could partially restore the growth of the mutant, although not to the same extent as the wild type. This observation implies that one of the potential functions of bicarbonate is related, at least indirectly to fatty acids biosynthesis. MpsAB is probably supplying bicarbonate needed for the carboxylation step for acetyl-CoA to be incorporated into malonyl-CoA as the first step of fatty acid biosynthesis (Fujita *et al.*, 2007).

Consistent with this observation, a *S. pneumoniae* (TIGR4) CA deletion mutant supplemented with sodium hydrogen carbonate and several metabolic intermediates (adenine, arginine, uracil, aspartic acid) as well as saturated fatty acid (SFA) palmitic acid and oleic acid only showed growth restoration with sodium hydrogen carbonate, as expected (Burghout *et al.*, 2010). This *S. pneumoniae* CA deletion mutant also exhibited the same poor growth phenotype as *S. aureus* $\Delta mpsABC$ under atmospheric CO₂ conditions. While the other metabolites could not reverse the CO₂ dependence of the *S. pneumoniae* CA deletion mutant, only oleic acid could in part rescue its growth. This indicates that UFAs are more easily depleted under CO₂ poor conditions although the synthesis of SFAs and UFAs basically take place through the same pathway (Marrakchi *et al.*, 2002, Burghout *et al.*, 2010). In contrast, supplementation with similar metabolic intermediates did not complement the growth defect of a nontypeable *Haemophilus influenzae* (strain Rd) CA deletion mutant, except for sodium bicarbonate (Langereis *et al.*, 2013).

1.4.12 Virulence attenuation by MpsAB

Apart from the less hemolytic toxins being produced, the virulence attenuation of the $\Delta mpsA$ can also be observed *in vivo*. The killing rate of those infected by the mutant was significantly lower in the *G. mellonella* larvae survival model. Likewise, significant reduction in the $\Delta mpsA$ bacteria burden of the lung in the intranasal mouse infection was also seen. A lung infection model (pneumonia model) was chosen in this study due to the higher CO₂ concentrations and therefore the $\Delta mpsA$ was expected to have a greater opportunity to grow. Within this context, the CO₂ formed during respiration is transported by blood through the venous system to the lungs, where the CO₂ concentration in exhaled air is approximately 3.8% of the tidal air or 450 liters per day (Cherniack & Longobardo, 1970).

Nevertheless, no statistically significant difference was found in bacteria burden of the kidney and liver of HG001 versus $\Delta mpsA$. One explanation for this is that the primary organ infected by *S. aureus* was lung and from there, spreads to other organs throughout the course of infection. The spread of bacteria is a complex process in which the bacteria have to pass several barriers from the lung epithelium, followed by blood vessels endothelium and again afterwards the blood vessels

endothelium to establish infections in other organs. Hence, the kidney and liver have a lower infection burden than in the lung, consistent with observation by (Lee *et al.*, 2010).

1.4.13 MpsAB and the link to fitness and pathogenicity

Given the somewhat interchangeable role of MpsAB and CA, their existence and distribution in *Firmicutes* were compared. Either one of the genes tend to be present in this phyla; in some instances the presence of both genes are found in the same strain or species, such as in *B. anthracis* and *B. subtilis* (Table 3). Similarly, this finding also applies to some pathogenic Gram-positive and Gram-negative bacterial species. Remarkably, the occurrences of *mpsAB* homologs and at least two CA homologs are found in some highly pathogenic species for instance *Legionella pneumophila* and *Vibrio cholera*, whereas two or three CA homologs are identified in *Mycobacterium tuberculosis*, *Helicobacter pylori*, *E. coli* O157:H7 and *Pseudomonas aeruginosa*. The relevance of the distribution of *mpsAB* and CA in these bacterial species or strain is still unclear. The occurrence of several CA genes homologs and/or *mpsAB* and the combined results in this study establish that there is an important linkage between DIC concentrating mechanism and both fitness and pathogenicity in these microorganisms. The reduced virulence of $\Delta mpsA$ is assumed to be due to very low levels of bicarbonate in the cells. In this respect, membrane potential and ATP which are important for toxin secretion, are subsequently affected.

1.4.14 The link between metabolism and pathogenicity and virulence

Bacteria, like any other organisms need carbon and energy for vital processes such as growth and replication. These requirements are fulfilled with a process called catabolism where complex organic molecules like carbohydrates, lipids and proteins are being broken down enzymatically. Carbon and energy can be derived from the environment by non-pathogenic bacteria by means of host symbiosis or as freely-living microorganism and in pathogenic bacteria, at least on a temporary basis by acting as a parasite or in a destructive manner from the host organism. The latter is achieved to some extent via synthesis of a wide variety of virulence determinants capable of causing the death of host cells and then catabolizing macromolecules.

Thus, it is no surprise that nutrient availability controls the regulation of various virulence determinants (Somerville & Proctor, 2009). In fact, one of the earliest physiological findings described was the link between the synthesis of virulence determinants (erepsin/protease) and nutrient availability (Berman & Rettger, 1916, Berman & Rettger, 1918, Kendall *et al.*, 1913).

In this regard, the connection between metabolism and its effects on the virulence and antibiotic resistance have only recently been investigated in detail. A large number of studies involving TCA cycle in the regulation or influence of staphylococcal virulence and/or virulence factor biosynthesis have been reported. One of the early example is that inactivation of the TCA cycle resulted in a glutamate auxotrophy and caused the metabolic inhibition of delta-toxin (*hld*) biosynthesis. Due to the absence of glutamate, the message of delta-toxin in the form of RNAIII is present but its translation does not occur. This metabolic inhibition of delta-toxin translation could be reversed by supplementing the growth medium with excess glutamate (Somerville *et al.*, 2003a). Unpublished observations from C.Y. Lee and G.A. Somerville also mentioned that inactivation of TCA cycle hinders the biosynthesis of oxaloacetate for conversion to phosphoenolpyruvate (PEP) and utilization in gluconeogenesis. As a result, the bacteria is not able to synthesize the biosynthetic precursors of capsule (Somerville & Proctor, 2009). A more recent study reported that pyruvate causes changes in the entire metabolic flux and increase the pathogenicity in *S. aureus*. Pyruvate was demonstrated to induce the generation of virulence factors like pore-forming leucocidins, resulting in the increased virulence of MRSA clone USA300 (Harper *et al.*, 2018). Altogether, these reports add to growing evidence of a consistent relationship between metabolism and pathogenicity as well as virulence.

1.5 Concluding remarks

Integrating all of the insights derived from this study, MpsAB is proposed to represent a DIC transporter that is crucial for the growth of *S. aureus* under CO₂-poor atmospheric air. The functionality of MpsAB in this regard may help shed some light on previous findings on CO₂-dependent variants. This transporter system underlies the significance of CO₂/bicarbonate in the fitness, pathogenicity and virulence of *S. aureus*. Moreover, homologs of *mpsAB* are ubiquitously found in a wide range of microorganisms which adopt various lifestyles and inhabit a diverse array of niches.

Defying the conventional views of DIC transporters, MpsA has a pivotal role even in non-autotrophic bacteria via concentration of bicarbonate for anaplerotic pathways that are applicable across diverse microorganisms. A noteworthy observation in this work was that MpsAB and CA could functionally substitute each other in the mutual complementation experiments, further corroborating the importance of bicarbonate. In this connection, many pathogenic species possess either MpsAB or CA while both are found in some of them, indicating their crucial function in growth and virulence.

However, there are many questions that remain to be elucidated. The presence of a predicted metal binding site reminiscent of a CA-like domain in MpsB hinted at the enzymatic activity of MpsB. As CA was not detectable in this study, it remains a puzzling question whether the CA activity is extremely low or that MpsA and MpsB must function together in an intact cell that require a cation gradient. The former can be tested by reconstituting the purified protein into proteoliposomes and then recover its CA activity while the latter can be investigated, perhaps using a series of CA inhibitors. In addition, the precise mechanisms of how this transporter function could be explored through in vitro reconstitution and structure determination. Since the tendency for either MpsAB or CA is fully evident in staphylococcal species, it would be interesting to express staphylococcal CA, for example *S. carnosus* CA in MpsAB-containing *S. aureus* or vice versa. If fitness in terms of growth is the key benefit of having a DIC concentrating system, having both CA and MpsAB would therefore result in a much higher growth in comparison with the wild-type.

Chapter 2

Human host cell invasion is triggered by *Staphylococcus aureus* Lpl protein via activation of Hsp90 receptor

Tribelli PM, Luqman A, Nguyen MT, Madlung J, **Fan SH**, Macek B, Sass P, Bitschar K, Schittek B, Kretschmer D and Götz F., “***Staphylococcus aureus* Lpl protein triggers human host cell invasion via activation of Hsp90 receptor**”. *Cellular Microbiology*, 2019;e13111. <https://doi.org/10.1111/cmi.13111>

2.1 Introduction

Although initially classified as an extracellular pathogen, *S. aureus* is now considered as a facultative intracellular pathogen (Sendi & Proctor, 2009). Many cell types can ingest *S. aureus*, where the bacteria can survive within these host cells for various periods of time (Fraunholz & Sinha, 2012). Some strains of *S. aureus* are reported to be able to trigger internalization by non-professional phagocytes (NPPCs) such as endothelial, epithelial, fibroblast and osteoblast (Peacock *et al.*, 1999, Almeida *et al.*, 1996, Usui *et al.*, 1992, Ellington *et al.*, 1999). This bacterial internalization is a strategy that enable them to evade the host immune response and survive inside the host cells as well as confer protection against the antibiotics administered.

Adhesion to the host cells is a prerequisite for any internalization into NPPCs. In this regard, this process mostly involves fibronectin (Fn)-bridging between Fn-binding proteins (FnBPs) on the bacteria and $\alpha 5\beta 1$ integrin on the host cell surface (Tran Van Nhieu & Isberg, 1993, Sinha *et al.*, 1999, Fowler *et al.*, 2000, Grundmeier *et al.*, 2004). Although this pathway is mainly recognized as the major internalization process, many other so-called secondary mechanisms also exist.

Generally, such mechanisms involve proteins called microbial surface components recognizing adhesive matrix molecules (MSCRAMMs). Examples of these proteins are bacterial major autolysin (Atl), clumping factor A (ClfA), serine aspartate repeat-containing protein D (SdrD) and serine-rich adhesin for platelets (SraP) (Josse *et al.*, 2017, Zapotoczna *et al.*, 2013). With the exception of Atl, these MSCRAMMs have a cell-wall anchoring sequence found in their C-terminal part while a signal peptide and subsequently ligand binding region are found in the N-terminal region (Josse *et al.*, 2017). These alternative mechanisms are postulated to be an adaptation of bacterial internalization strategies in response to various environmental conditions. Therefore, in the absence or lack of Fn for example, invasion can be triggered by using alternative binding partners and/or upregulating either side of adhesion machinery (Josse *et al.*, 2017).

2.2 Objectives

Recent work has shown host cell internalization can be induced by a certain class of lipoproteins (Nguyen *et al.*, 2015). The so-called “lipoprotein-like” (*lpl*) genes are located in a cluster of pathogenicity island called vSα, which are non-phage and non-staphylococcal cassette chromosome genomic islands. This genomic island is found in all *S. aureus* genomes sequenced to date (Diep *et al.*, 2006, Shahmirzadi *et al.*, 2016). There are ten paralogous genes (*lpl* 0410-0419) within the vSα island, encoding *lpl* protein with high sequence similarity and another two accessory genes (Nguyen *et al.*, 2015).

To assess the role of *lpl* gene cluster particular in virulence, the whole gene cluster was deleted in *S. aureus* USA300. The deletion mutant displayed a significant decrease in *S. aureus* invasion into human keratinocytes and mouse skin, as well as lower pathogenicity in a murine kidney abscess model (Nguyen *et al.*, 2015). In addition, the Lpl lipoproteins also delay the G2/M phase transition in HeLa cells (Nguyen *et al.*, 2016). However, the mechanisms underlying the host cell internalization triggered by Lpl proteins remained unknown. Therefore, the aim of this study was to identify the host cell receptor for Lpl-induced *S. aureus* invasion in human keratinocytes and to unravel this mechanism.

By performing pull-down assay using recombinant Lpl1 protein as a model of Lpls, the host receptor for Lpl-induced *S. aureus* USA300 invasion of human keratinocytes was identified as human heat shock protein Hsp90. Further experiments were performed to confirm its role in triggering the host cell invasion. First, the host cell receptor, Hsp90 was blocked using specific antibodies and geldanamycin, a Hsp90 activity inhibitor. This is further confirmed by silencing the expression of Hsp90α mRNA by an antisense RNA (siRNA). Next, the mechanism of which causes the internalization of the bacteria into the host cell was determined by checking actin polymerization. Finally, the Lpl epitopes that trigger the internalization of *S. aureus* was also identified.

2.3 Results and discussion

The Lpl used in this study is termed Lpl1-his and was obtained from purified C-terminal his-tagged Lpl protein lacking the lipid signal (-sp). It was isolated from the cytoplasmic fraction of *S. aureus* SA113 carrying pTX30::lpl-his (-sp) as described earlier (Nguyen *et al.*, 2015). The purification of Lpl1-his was visualized by SDS-PAGE (Figure 21) which showed a band size of approximately 35 kDa. The total amount of protein was determined by Bradford assay. The purified Lpl1-his was then used to perform the pull-down experiments and Lpl1-Hsp90 α/β interaction studies such as F-actin formation, ATPase activity and also far-western blot experiments.

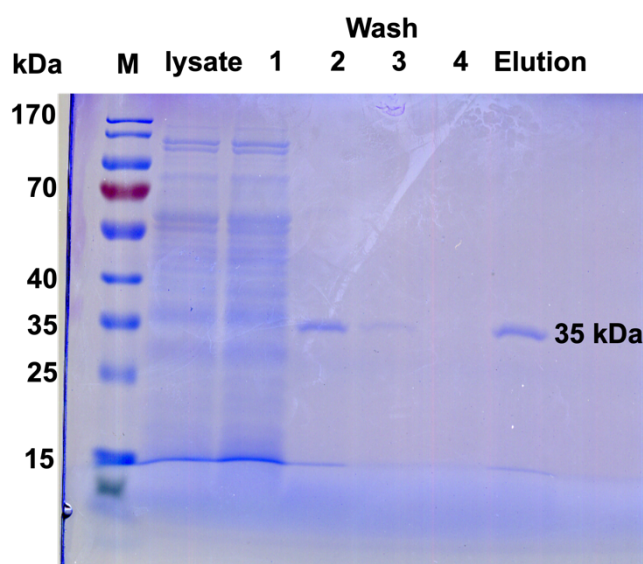


Figure 21: SDS-PAGE gel stained with Coomassie blue showing purified Lpl1-his. M: prestained protein leader (Fermentas); lysate: cell lysate from the cytoplasmic fraction of *S. aureus* SA113 carrying pTX30::lpl1-his (-sp); wash: wash fractions during Ni-NTA purification 1-4; Elution: elution fraction after purification.

It was previously reported that the internalization into a human keratinocytes cell line, HaCat cells and human primary cells were increased by the Lpl lipoproteins from *S. aureus* (Nguyen *et al.*, 2015). It is postulated that the protein part of the Lpl interacts with the potential host receptor since the lipid moiety is anchored to the cytoplasmic membrane. Pull-down experiment was employed to identify the potential host cell receptor, with purified Lpl1-his as a 'bait' and bound to the Ni-NTA column before being loaded with HaCat cell lysate. As shown in Figure 22, the most evident band

on the SDS-PAGE was Lpl-his, followed by a few faint bands which were used for further analysis. Nano-HPLC-MS/MS identified the HaCat-specific proteins as human heat shock Hsp90 alpha (Hsp90 α) and beta (Hsp90 β) proteins.

Hsp90 proteins are about 90 kDa in size and are expressed extensively in various cell types, consisting of 1-2% of the total cellular proteins content (Whitesell & Lindquist, 2005). Both proteins are highly homologous, with 94% similarity and 86% identity. They function as molecular chaperones and are important players in protein homeostasis under stress conditions (Hoter *et al.*, 2018). In human, at least two isoforms are found; α and β which are inducible and constitutively-expressed forms respectively but the functional differences between them are poorly understood (Sreedhar *et al.*, 2004). However, Hsp90 α is well-documented to be involved in promoting cell motility which is important for both wound healing and cancer (Li *et al.*, 2012).

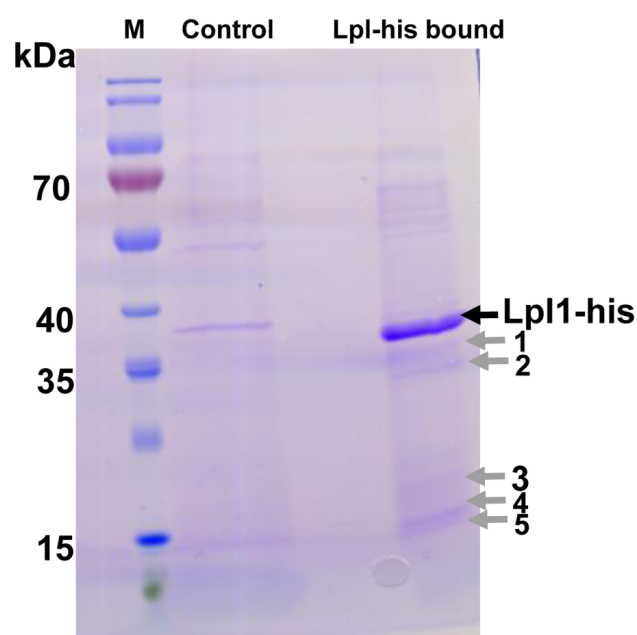


Figure 22: Human Hsp90 interacts with *S. aureus* Lpl-1 protein in pull-down experiments. Purified Lpl1-his was bound to NTA column and loaded with HaCat cells lysate. Elution fractions were ran on SDS-PAGE followed by Coomassie blue staining. M: prestained protein leader (Fermentas); Control: Control elution fraction without Lpl1-his; Lpl1-his: experimental elution fraction using Lpl1-his as bait and HaCaT cell lysate as source of human proteins; Lpl1 is indicated with a black arrow. Bands used for further analysis are indicated by grey arrows. Experiment was performed by Tribelli P.M. and figure adapted from (Tribelli *et al.*, 2019).

After identifying that Hsp90 on the host cell surface interacts with Lpl1 on the surface of *S. aureus* USA300, further experiments confirmed its role in triggering the host cell adherence and invasion. Polyclonal antibodies against Hsp90 (α -Hsp90 $\alpha\beta$) resulted in a seven-fold decrease in the invasion of USA300 in HaCat cells. For further validation, these antibodies were also tested using USA300 Δ lpl in which the entire lpl cluster was deleted and its complemented mutant USA300 Δ lpl (pTX-lpl1) (Nguyen *et al.*, 2015). The polyclonal α -Hsp90 $\alpha\beta$ antibodies did not have any effect on the invasion of USA300 Δ lpl, but showed a decrease in invasion again in the complemented mutant. Similar observation could be seen with both the monoclonal antibodies specific against Hsp90 α (α -Hsp90 α) and Hsp90 β (α -Hsp90 β), causing a four to five-fold decrease in the invasion of USA300, indicating that both isoforms can trigger invasion.

Despite this observation, it is postulated that Hsp90 α play the major role in facilitating the Lpl-triggered invasion based to the finding that silencing the expression of Hsp90 α by siRNA significantly decreased the invasion while the silencing of Hsp90 β expression was unsuccessful. In agreement with this hypothesis, the interactions of Hsp90 α with other pathogens or defined compounds are also reported. For instance, Hsp90 α acts as a receptor for adhesin A of *Neisseria meningitidis* and dengue virus as well as implicated in the diphtheria toxin uptake in host cells (Bozza *et al.*, 2014, Reyes-Del Valle *et al.*, 2005, Schuster *et al.*, 2017).

In addition, the effect of geldanamycin, a widely known cell permeable anti-neoplastic compound which inhibits Hsp90 activity was also investigated (Gorska *et al.*, 2012). It was found that geldanamycin decreased the invasion of USA300 of about three-fold in a concentration-dependent manner. With regard to this observation, a geldanamycin analogue, 17AAG was also tested. This compound is a Hsp90 inhibitor, and its inhibition leads to a decrease in F-actin formation (Taiyab & Rao, 2011). Following the treatment of HaCat cells with Lpl1-his, a 20% increase in F-actin formation was observed. It is suggested that the interaction between Hsp90 and the extracellular domain of HER-2, a ligand-less kinase receptor on the membrane, triggers signaling and leads to actin polymerization (Sidera & Patsavoudi, 2008).

An interesting observation is that pre-incubation of HaCat cells at 39°C led to an almost two-fold increase compared to the control at 37°C, indicating that high temperature as in fever favors the host cell invasion by *S. aureus* via Hsp90 α

upregulation. It is believed that pathogens such as *S. aureus* would invade and hide in non-professional cells to escape the T-lymphocytes killing, because fever increases the migration of these lymphocytes.

Given the fact that high number of *lpl* genes are found in epidemic *S. aureus* strains, it is believed that this *lpl* gene cluster may be responsible for the increased disseminative activity of certain isolates of *S. aureus* (Nguyen *et al.*, 2015). In this regard, the pathogen is protected from immune defense and antibiotics by internalizing itself into host cells. In the case of *S. aureus*, since intracellular pathogens are better protected, it is speculated that Lpl have a role in the rapid spreading of these lineages.

In conclusion, a model for the HSp90 role in USA300 invasion is proposed based on the findings in this work (Figure 23). The Lpls bound on the membrane of *S. aureus* interacts with the Hsp90 localized on the host cell surface. As a result of this Lpl-Hsp90 interaction, F-actin formation is induced leading to an endocytosis-like engulfment of *S. aureus*. Such internalization is most likely based on the zipper mechanism, which occurs following interaction of host cell receptor with a bacterial protein (Colonne *et al.*, 2016). In this regard, intracellular signaling cascade is triggered via activation of adapter proteins and kinases, followed by F-actin formation resulting in endocytosis (Colonne *et al.*, 2016). On the basis of this interaction, a new host cell invasion principle is revealed.

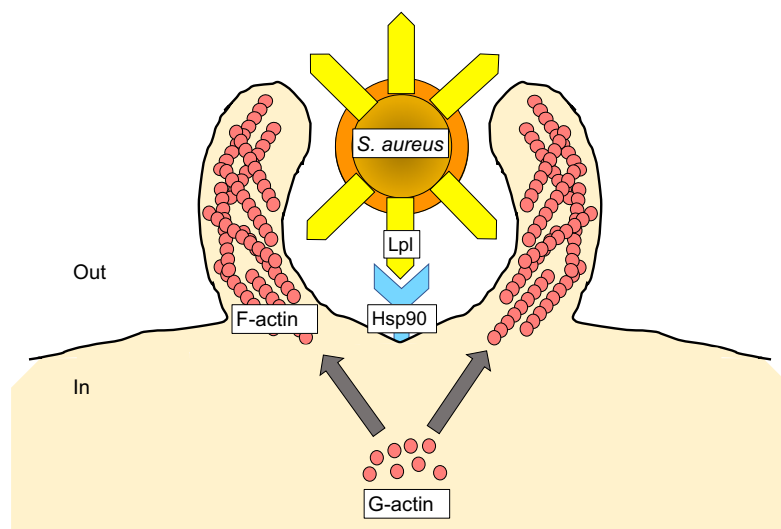


Figure 23: Proposed model for the role of Hsp90 in the invasion of *S. aureus* USA300. Lipoproteins (Lpls) on the surface of USA300 interact with HSp90 molecules on the host cell surface. The part of Lpl1 that showed interaction belong to the C-terminal sequences. Such interaction triggers F-actin formation, thus increasing the USA300 invasion. G-actin: monomer of actin protein; F-actin: filamentous actin. Figure adapted and edited from (Tribelli *et al.*, 2019).

References

- Adler, H., A. Widmer & R. Frei, (2003) Emergence of a teicoplanin-resistant small colony variant of *Staphylococcus epidermidis* during vancomycin therapy. *European journal of clinical microbiology & infectious diseases : official publication of the European Society of Clinical Microbiology* **22**: 746-748.
- Aguilera, J., J.P. Van Dijken, J.H. De Winde & J.T. Pronk, (2005) Carbonic anhydrase (Nce103p): an essential biosynthetic enzyme for growth of *Saccharomyces cerevisiae* at atmospheric carbon dioxide pressure. *Biochem J* **391**: 311-316.
- Almeida, R.A., K.R. Matthews, E. Cifrian, A.J. Guidry & S.P. Oliver, (1996) *Staphylococcus aureus* invasion of bovine mammary epithelial cells. *J Dairy Sci* **79**: 1021-1026.
- Baddour, L.M., L.P. Barker, G.D. Christensen, J.T. Parisi & W.A. Simpson, (1990) Phenotypic variation of *Staphylococcus epidermidis* in infection of transvenous endocardial pacemaker electrodes. *Journal of clinical microbiology* **28**: 676-679.
- Bates, D.M., C. von Eiff, P.J. McNamara, G. Peters, M.R. Yeaman, A.S. Bayer & R.A. Proctor, (2003) *Staphylococcus aureus* menD and hemB mutants are as infective as the parent strains, but the menadione biosynthetic mutant persists within the kidney. *J Infect Dis* **187**: 1654-1661.
- Baumert, N., C. von Eiff, F. Schaaff, G. Peters, R.A. Proctor & H.-G. Sahl, (2002) Physiology and antibiotic susceptibility of *Staphylococcus aureus* small colony variants. *Microbial drug resistance (Larchmont, N Y)* **8**: 253-260.
- Bayer, A.S., P. McNamara, M.R. Yeaman, N. Lucindo, T. Jones, A.L. Cheung, H.G. Sahl & R.A. Proctor, (2006) Transposon disruption of the complex I NADH oxidoreductase gene (*snoD*) in *Staphylococcus aureus* is associated with reduced susceptibility to the microbicidal activity of thrombin-induced platelet microbicidal protein 1. *J Bacteriol* **188**: 211-222.
- Berman, N. & L.F. Rettger, (1916) Bacterial Nutrition: a Brief Note on the Production of Erepsin by Bacteria. *J Bacteriol* **1**: 537-539.
- Berman, N. & L.F. Rettger, (1918) The Influence of Carbohydrate on the Nitrogen Metabolism of Bacteria. *J Bacteriol* **3**: 389-402.
- Besier, S., A. Ludwig, K. Ohlsen, V. Brade & T.A. Wichelhaus, (2007a) Molecular analysis of the thymidine-auxotrophic small colony variant phenotype of *Staphylococcus aureus*. *Int J Med Microbiol* **297**: 217-225.
- Besier, S., C. Smaczny, C. von Mallinckrodt, A. Krahl, H. Ackermann, V. Brade & T.A. Wichelhaus, (2007b) Prevalence and clinical significance of *Staphylococcus aureus* small-colony variants in cystic fibrosis lung disease. *J Clin Microbiol* **45**: 168-172.
- Bogut, A., J. Niedzwiadek, M. Koziol-Montewka, D. Strzelec-Nowak, J. Blacha, T. Mazurkiewicz, W. Marczynski & D. Plewik, (2014) Characterization of *Staphylococcus epidermidis* and *Staphylococcus warneri* small-colony variants associated with prosthetic-joint infections. *J Med Microbiol* **63**: 176-185.
- Borderon, E. & T. Horodniceanu, (1978) Metabolically deficient dwarf-colony mutants of *Escherichia coli*: deficiency and resistance to antibiotics of strains isolated from urine culture. *J Clin Microbiol* **8**: 629-634.
- Boron, W.F., L. Chen & M.D. Parker, (2009) Modular structure of sodium-coupled bicarbonate transporters. *J Exp Biol* **212**: 1697-1706.

- Bozza, G., M. Capitani, P. Montanari, B. Benucci, M. Biancucci, V. Nardi-Dei, E. Caproni, R. Barrile, B. Picciani, S. Savino, B. Arico, R. Rappuoli, M. Pizza, A. Luini, M. Sallesse & M. Merola, (2014) Role of ARF6, Rab11 and external Hsp90 in the trafficking and recycling of recombinant-soluble *Neisseria meningitidis* adhesin A (rNadA) in human epithelial cells. *PLoS One* **9**: e110047.
- Brückner, R. & F. Titgemeyer, (2002) Carbon catabolite repression in bacteria: choice of the carbon source and autoregulatory limitation of sugar utilization. *FEMS Microbiol Lett* **209**: 141-148.
- Bryan, L.E. & S. Kwan, (1983) Roles of Ribosomal Binding, Membrane Potential, and Electron Transport in Bacterial Uptake of Streptomycin and Gentamicin. *Antimicrob Agents Chemother* **23**: 835-845.
- Burghout, P., L.E. Cron, H. Gradstedt, B. Quintero, E. Simonetti, J.J. Bijlsma, H.J. Bootsma & P.W. Hermans, (2010) Carbonic anhydrase is essential for *Streptococcus pneumoniae* growth in environmental ambient air. *J Bacteriol* **192**: 4054-4062.
- Chambers, H.F. & F.R. Deleo, (2009) Waves of resistance: *Staphylococcus aureus* in the antibiotic era. *Nat Rev Microbiol* **7**: 629-641.
- Chatterjee, I., A. Kriegeskorte, A. Fischer, S. Deiwick, N. Theimann, R.A. Proctor, G. Peters, M. Herrmann & B.C. Kahl, (2008) In vivo mutations of thymidylate synthase (encoded by *thyA*) are responsible for thymidine dependency in clinical small-colony variants of *Staphylococcus aureus*. *J Bacteriol* **190**: 834-842.
- Chegwidden, W.R., S.J. Dodgson & I.M. Spencer, (2000) The roles of carbonic anhydrase in metabolism, cell growth and cancer in animals. In: *The Carbonic Anhydrases*. W.R. Chegwidden, N.D. Carter & Y.H. Edwards (eds). Basel: Birkhäuser, pp. 343-363.
- Cherniack, N.S. & G.S. Longobardo, (1970) Oxygen and carbon dioxide gas stores of the body. *Physiol Rev* **50**: 196-243.
- Chou, C.Y., L.P. Yu & L. Tong, (2009) Crystal structure of biotin carboxylase in complex with substrates and implications for its catalytic mechanism. *J Biol Chem* **284**: 11690-11697.
- Clements, M.O., S.P. Watson, R.K. Poole & S.J. Foster, (1999) CtaA of *Staphylococcus aureus* is required for starvation survival, recovery, and cytochrome biosynthesis. *J Bacteriol* **181**: 501-507.
- Collins, F.M. & J. Lascelles, (1962) The effect of growth conditions on oxidative and dehydrogenase activity in *Staphylococcus aureus*. *J Gen Microbiol* **29**: 531-535.
- Collins, M.D. & D. Jones, (1981) Distribution of isoprenoid quinone structural types in bacteria and their taxonomic implication. *Microbiol Rev* **45**: 316-354.
- Colonne, P.M., C.G. Winchell & D.E. Voth, (2016) Hijacking Host Cell Highways: Manipulation of the Host Actin Cytoskeleton by Obligate Intracellular Bacterial Pathogens. *Front Cell Infect Microbiol* **6**: 107.
- Colwell, C.A., (1946) Small Colony Variants of *Escherichia coli*. *Journal of bacteriology* **52**: 417-422.
- Coman, G., N. Mardare, B. Copacianu & M. Covic, (2008) [Persistent and recurrent skin infection with small-colony variant methicillin-resistant *Staphylococcus aureus*]. Infectie cutanata persistenta si recurenta cu *Staphylococcus aureus* metilino-rezistent, varianta cu colonii mici. *Revista medico-chirurgicala a Societatii de Medici si Naturalisti din Iasi* **112**: 104-107.

- Cotter, P.A., S.B. Melville, J.A. Albrecht & R.P. Gunsalus, (1997) Aerobic regulation of cytochrome d oxidase (*cydAB*) operon expression in *Escherichia coli*: roles of Fnr and ArcA in repression and activation. *Mol Microbiol* **25**: 605-615.
- Dickens, F., (1938) Oxidation of phosphohexonate and pentose phosphoric acids by yeast enzymes: Oxidation of phosphohexonate. II. Oxidation of pentose phosphoric acids. *Biochem J* **32**: 1626-1644.
- Diep, B.A., S.R. Gill, R.F. Chang, T.H. Phan, J.H. Chen, M.G. Davidson, F. Lin, J. Lin, H.A. Carleton, E.F. Mongodin, G.F. Sensabaugh & F. Perdreau-Remington, (2006) Complete genome sequence of USA300, an epidemic clone of community-acquired methicillin-resistant *Staphylococcus aureus*. *Lancet* **367**: 731-739.
- Efremov, R.G. & L.A. Sazanov, (2011) Structure of the membrane domain of respiratory complex I. *Nature* **476**: 414-420.
- Egeter, O. & R. Brückner, (1996) Catabolite repression mediated by the catabolite control protein CcpA in *Staphylococcus xylosus*. *Mol Microbiol* **21**: 739-749.
- Eisenberg, E.S., L.J. Mandel, H.R. Kaback & M.H. Miller, (1984) Quantitative association between electrical potential across the cytoplasmic membrane and early gentamicin uptake and killing in *Staphylococcus aureus*. *J Bacteriol* **157**: 863-867.
- El-Gebali, S., J. Mistry, A. Bateman, S.R. Eddy, A. Luciani, S.C. Potter, M. Qureshi, L.J. Richardson, G.A. Salazar, A. Smart, E.L.L. Sonnhammer, L. Hirsh, L. Paladin, D. Piovesan, S.C.E. Tosatto & R.D. Finn, (2019) The Pfam protein families database in 2019. *Nucleic Acids Res* **47**: D427-D432.
- Ellington, J.K., S.S. Reilly, W.K. Ramp, M.S. Smeltzer, J.F. Kellam & M.C. Hudson, (1999) Mechanisms of *Staphylococcus aureus* invasion of cultured osteoblasts. *Microb Pathog* **26**: 317-323.
- Faller, A. & K.H. Schleifer, (1981) Modified oxidase and benzidine tests for separation of staphylococci from micrococci. *J Clin Microbiol* **13**: 1031-1035.
- Faller, A.H., F. Götz & K.H. Schleifer, (1980) Cytochrome patterns of staphylococci and micrococci and their taxonomic implications. *Zentralbl bacteriol Hyg Abt. 1 Orig C* **1**: 26-39.
- Fan, S.-H., P. Ebner, S. Reichert, T. Hertlein, S. Zabel, A.K. Lankapalli, K. Nieselt, K. Ohlsen & F. Gotz, (2019) MpsAB is important for *Staphylococcus aureus* virulence and growth at atmospheric CO₂ levels. *Nat Commun* **10**: 3627.
- Felder, R.A., P.A. Jose, P. Xu & J.J. Gildea, (2016) The Renal Sodium Bicarbonate Cotransporter NBCe2: Is It a Major Contributor to Sodium and pH Homeostasis? *Curr Hypertens Rep* **18**: 71.
- Fillingame, R.H., (1997) Coupling H⁺ transport and ATP synthesis in F₁F₀-ATP synthases: glimpses of interacting parts in a dynamic molecular machine. *J Exp Biol* **200**: 217-224.
- Fowler, T., E.R. Wann, D. Joh, S. Johansson, T.J. Foster & M. Hook, (2000) Cellular invasion by *Staphylococcus aureus* involves a fibronectin bridge between the bacterial fibronectin-binding MSCRAMMs and host cell beta1 integrins. *European journal of cell biology* **79**: 672-679.
- Fraunholz, M. & B. Sinha, (2012) Intracellular *Staphylococcus aureus*: live-in and let die. *Frontiers in cellular and infection microbiology* **2**: 43.
- Fuchs, S., H. Mehlan, J. Bernhardt, A. Hennig, S. Michalik, K. Surmann, J. Panefarre, A. Giese, S. Weiss, L. Backert, A. Herbig, K. Nieselt, M. Hecker, U. Volker & U. Mäder, (2018) AureoWiki The repository of the *Staphylococcus aureus* research and annotation community. *Int J Med Microbiol* **308**: 558-568.

- Fujita, Y., H. Matsuoka & K. Hirooka, (2007) Regulation of fatty acid metabolism in bacteria. *Mol Microbiol* **66**: 829-839.
- Fuller, J.R., N.P. Vitko, E.F. Perkowski, E. Scott, D. Khatri, J.S. Spontak, L.R. Thurlow & A.R. Richardson, (2011) Identification of a lactate-quinone oxidoreductase in *Staphylococcus aureus* that is essential for virulence. *Front Cell Infect Microbiol* **1**: 19.
- Gardner, J.F. & J. Lascelles, (1962) The requirement for acetate of a streptomycin-resistant strain of *Staphylococcus aureus*. *J Gen Microbiol* **29**: 157-164.
- Gaupp, R., S. Schlag, M. Liebeke, M. Lalk & F. Götz, (2010) Advantage of upregulation of succinate dehydrogenase in *Staphylococcus aureus* biofilms. *J Bacteriol* **192**: 2385-2394.
- Goldenbaum, P.E. & D.C. White, (1974) Role of lipid in the formation and function of the respiratory system of *Staphylococcus aureus*. *Ann N Y Acad Sci* **236**: 115-123.
- Goldschmidt, M.C. & D.M. Powelson, (1953) Effect of the culture medium on the oxidation of acetate by *Micrococcus pyogenes var. aureus*. *Arch Biochem Biophys* **46**: 154-163.
- Gomez-Gonzalez, C., J. Acosta, J. Villa, L. Barrado, F. Sanz, M.A. Orellana, J.R. Otero & F. Chaves, (2010) Clinical and molecular characteristics of infections with CO₂-dependent small-colony variants of *Staphylococcus aureus*. *J Clin Microbiol* **48**: 2878-2884.
- Gordon, R.J. & F.D. Lowy, (2008) Pathogenesis of methicillin-resistant *Staphylococcus aureus* infection. *Clin Infect Dis* **46 Suppl 5**: S350-359.
- Gorska, M., U. Popowska, A. Sielicka-Dudzin, A. Kuban-Jankowska, W. Sawczuk, N. Knap, G. Cicero & F. Wozniak, (2012) Geldanamycin and its derivatives as Hsp90 inhibitors. *Front Biosci (Landmark Ed)* **17**: 2269-2277.
- Götz, F., T. Bannerman & K.H. Schleifer, (2006) The Genera *Staphylococcus* and *Micrococcus*. In: Prokaryotes. M. Dworkin (ed). New York: Springer, pp. 5-75.
- Götz, F. & S. Mayer, (2013) Both terminal oxidases contribute to fitness and virulence during organ-specific *Staphylococcus aureus* colonization. *MBio* **4**: e00976-00913.
- Goudie, J.G. & R.B. Goudie, (1955) Recurrent infections by a stable dwarf-colony variant of *Staphylococcus aureus*. *J Clin Pathol* **8**: 284-287.
- Grobner, S., J. Beck, M. Schaller, I.B. Autenrieth & B. Schulte, (2012) Characterization of an *Enterococcus faecium* small-colony variant isolated from blood culture. *International journal of medical microbiology : IJMM* **302**: 40-44.
- Grundmeier, M., M. Hussain, P. Becker, C. Heilmann, G. Peters & B. Sinha, (2004) Truncation of fibronectin-binding proteins in *Staphylococcus aureus* strain Newman leads to deficient adherence and host cell invasion due to loss of the cell wall anchor function. *Infection and immunity* **72**: 7155-7163.
- Hale, J.H., (1947) Studies on *Staphylococcus* mutation; characteristics of the G (gonidial) variant and factors concerned in its production. *Br J Exp Pathol* **28**: 202-210.
- Hale, J.H., (1951) Studies on *staphylococcus* mutation: a naturally occurring "G" gonidial variant and its carbon dioxide requirements. *British journal of experimental pathology* **32**: 307-313.
- Hall, W.H. & W.W. Spink, (1947) In vitro sensitivity of *Brucella* to streptomycin; development of resistance during streptomycin treatment. *Proc Soc Exp Biol Med* **64**: 403-406.

- Hammer, N.D., M.L. Reniere, J.E. Cassat, Y. Zhang, A.O. Hirsch, M. Indriati Hood & E.P. Skaar, (2013) Two heme-dependent terminal oxidases power *Staphylococcus aureus* organ-specific colonization of the vertebrate host. *MBio* **4**.
- Harper, L., D. Balasubramanian, E.A. Ohneck, W.E. Sause, J. Chapman, B. Mejia-Sosa, T. Lhaxhang, A. Heguy, A. Tsirigos, B. Ueberheide, J.M. Boyd, D.S. Lun & V.J. Torres, (2018) *Staphylococcus aureus* Responds to the Central Metabolite Pyruvate To Regulate Virulence. *MBio* **9**.
- Hauszler, S., C. Lehmann, C. Breselge, M. Rohde, M. Classen, B. Tummler, P. Vandamme & I. Steinmetz, (2003) Fatal outcome of lung transplantation in cystic fibrosis patients due to small-colony variants of the *Burkholderia cepacia* complex. *Eur J Clin Microbiol Infect Dis* **22**: 249-253.
- Hauszler, S., M. Rohde & I. Steinmetz, (1999a) Highly resistant *Burkholderia pseudomallei* small colony variants isolated in vitro and in experimental melioidosis. *Med Microbiol Immunol* **188**: 91-97.
- Hauszler, S., B. Tummler, H. Weissbrodt, M. Rohde & I. Steinmetz, (1999b) Small-colony variants of *Pseudomonas aeruginosa* in cystic fibrosis. *Clin Infect Dis* **29**: 621-625.
- Herbert, S., A.K. Ziebandt, K. Ohlsen, T. Schafer, M. Hecker, D. Albrecht, R. Novick & F. Götz, (2010) Repair of global regulators in *Staphylococcus aureus* 8325 and comparative analysis with other clinical isolates. *Infect Immun* **78**: 2877-2889.
- Hoter, A., M.E. El-Sabban & H.Y. Naim, (2018) The HSP90 Family: Structure, Regulation, Function, and Implications in Health and Disease. *Int J Mol Sci* **19**.
- Idelevich, E.A., C.A. Pogoda, B. Ballhausen, J. Wullenweber, L. Eckardt, H. Baumgartner, J. Waltenberger, G. Peters & K. Becker, (2013) Pacemaker lead infection and related bacteraemia caused by normal and small colony variant phenotypes of *Bacillus licheniformis*. *J Med Microbiol* **62**: 940-944.
- Jacobsen, K.A., (1910) Mitteilungen über einen variablen Typhusstamm (Bacterium typhi mutabile), sowie über eine eigentümliche hemmende Wirkung des gewöhnlichen agar, verursacht durch autoklavierung. *Zentralbl. Bakteriol. [Orig. A]* **56**: 208–216.
- Jankovic, I. & R. Brückner, (2002) Carbon catabolite repression by the catabolite control protein CcpA in *Staphylococcus xylosus*. *J Mol Microbiol Biotechnol* **4**: 309-314.
- Josse, J., F. Laurent & A. Diot, (2017) Staphylococcal Adhesion and Host Cell Invasion: Fibronectin-Binding and Other Mechanisms. *Frontiers in microbiology* **8**: 2433.
- Kahl, B.C., (2014) Small colony variants (SCVs) of *Staphylococcus aureus*--a bacterial survival strategy. *Infect Genet Evol* **21**: 515-522.
- Kahl, B.C., G. Belling, R. Reichelt, M. Herrmann, R.A. Proctor & G. Peters, (2003) Thymidine-dependent small-colony variants of *Staphylococcus aureus* exhibit gross morphological and ultrastructural changes consistent with impaired cell separation. *Journal of clinical microbiology* **41**: 410-413.
- Kaplan, M.L. & W. Dye, (1976) Growth requirements of some small-colony-forming variants of *Staphylococcus aureus*. *Journal of clinical microbiology* **4**: 343-348.
- Kendall A.I., Friedemann T.E & I. M., (1930) Quantitative Observations on the Chemical Activity of "Resting" *Staphylococcus aureus*: Studies in Bacterial Metabolism, XCIII. *J Infect Dis* **47**: 223-228.

- Kendall, A.I., A.A. Day & A.W. Walker, (1913) Observations on the Relative Constancy of Ammonia Production by Certain Bacteria: . *J. Infect. Dis* **13**: 425-428.
- Kluytmans, J., A. van Belkum & H. Verbrugh, (1997) Nasal carriage of *Staphylococcus aureus*: epidemiology, underlying mechanisms, and associated risks. *Clin Microbiol Rev* **10**: 505-520.
- Kohler, C., C. von Eiff, G. Peters, R.A. Proctor, M. Hecker & S. Engelmann, (2003) Physiological characterization of a heme-deficient mutant of *Staphylococcus aureus* by a proteomic approach. *J Bacteriol* **185**: 6928-6937.
- Kolle, W. & H. Hetsch, (1906) *Die experimentelle Bakteriologie und die Infektionskrankheiten mit besonderer Berücksichtigung der Immunitätslehre. Ein Lehrbuch für Studierende, Ärzte und Medizinalbeamte.* Urban & Schwarzenberg, Berlin, Germany.
- Koo, S.P., A.S. Bayer, H.G. Sahl, R.A. Proctor & M.R. Yeaman, (1996) Staphylocidal action of thrombin-induced platelet microbicidal protein is not solely dependent on transmembrane potential. *Infection and immunity* **64**: 1070-1074.
- Krebs, H.A., (1937) Dismutation of pyruvic acid in *Gonococcus* and *Staphylococcus*. *Biochem J* **31**: 661-671.
- Kriegeskorte, A., S. König, G. Sander, A. Pirkl, E. Mahabir, R.A. Proctor, C. von Eiff, G. Peters & K. Becker, (2011) Small colony variants of *Staphylococcus aureus* reveal distinct protein profiles. *Proteomics* **11**: 2476-2490.
- Kubota, N., K. Kuzumoto, E. Hidaka, K. Yoshizawa, K. Yumoto, K. Oana, Y. Ogiso, T. Nakamura & Y. Kawakami, (2013) First isolation of oleate-dependent *Enterococcus faecalis* small-colony variants from the umbilical exudate of a paediatric patient with omphalitis. *J Med Microbiol* **62**: 1883-1890.
- Langereis, J.D., A. Zomer, H.G. Stunnenberg, P. Burghout & P.W. Hermans, (2013) Nontypeable *Haemophilus influenzae* carbonic anhydrase is important for environmental and intracellular survival. *J Bacteriol* **195**: 2737-2746.
- Lee, M.H., C. Arrecubieta, F.J. Martin, A. Prince, A.C. Borczuk & F.D. Lowy, (2010) A postinfluenza model of *Staphylococcus aureus* pneumonia. *J Infect Dis* **201**: 508-515.
- Li, W., D. Sahu & F. Tsen, (2012) Secreted heat shock protein-90 (Hsp90) in wound healing and cancer. *Biochim Biophys Acta* **1823**: 730-741.
- Liang, F.Y., P. Lindberg & P. Lindblad, (2018) Engineering photoautotrophic carbon fixation for enhanced growth and productivity. *Sustain Energy Fuels* **2**: 2583-2600.
- Licitra, G., (2013) Etymologia: *Staphylococcus*. *Emerg Infect Dis*. **19**: 1553.
- Mangan, N.M., A. Flamholz, R.D. Hood, R. Milo & D.F. Savage, (2016) pH determines the energetic efficiency of the cyanobacterial CO₂ concentrating mechanism. *Proc Natl Acad Sci U S A* **113**: E5354-5362.
- Mangiapia, M., M. Usf, T.W. Brown, D. Chaput, E. Haller, T.L. Harmer, Z. Hashemy, R. Keeley, J. Leonard, P. Mancera, D. Nicholson, S. Stevens, P. Wanjugi, T. Zabinski, C. Pan & K.M. Scott, (2017) Proteomic and Mutant Analysis of the CO₂ Concentrating Mechanism of Hydrothermal Vent Chemolithoautotroph *Thiomicrospira crunogena*. *J Bacteriol* **199**.
- Marrakchi, H., K.H. Choi & C.O. Rock, (2002) A new mechanism for anaerobic unsaturated fatty acid formation in *Streptococcus pneumoniae*. *J Biol Chem* **277**: 44809-44816.

- Mates, S.M., E.S. Eisenberg, L.J. Mandel, L. Patel, H.R. Kaback & M.H. Miller, (1982) Membrane potential and gentamicin uptake in *Staphylococcus aureus*. *Proc Natl Acad Sci U S A* **79**: 6693-6697.
- Mates, S.M., L. Patel, H.R. Kaback & M.H. Miller, (1983) Membrane potential in anaerobically growing *Staphylococcus aureus* and its relationship to gentamicin uptake. *Antimicrob Agents Chemother* **23**: 526-530.
- Mayer, S., S. Junne, K. Ukkonen, J. Glazyrina, F. Glauche, P. Neubauer & A. Vasala, (2014) Lactose autoinduction with enzymatic glucose release: characterization of the cultivation system in bioreactor. *Protein Expr Purif* **94**: 67-72.
- Mayer, S., W. Steffen, J. Steuber & F. Götz, (2015) The *Staphylococcus aureus* NuoL-Like Protein MpsA Contributes to the Generation of Membrane Potential. *J Bacteriol* **197**: 794-806.
- McNamara, P.J. & R.A. Proctor, (2000) *Staphylococcus aureus* small colony variants, electron transport and persistent infections. *Int J Antimicrob Agents* **14**: 117-122.
- Melter, O. & B. Radojevic, (2010) Small colony variants of *Staphylococcus aureus*--review. *Folia microbiologica* **55**: 548-558.
- Merlin, C., M. Masters, S. McAteer & A. Coulson, (2003) Why is carbonic anhydrase essential to *Escherichia coli*? *J Bacteriol* **185**: 6415-6424.
- Mitchell, G., E. Brouillette, D.L. Seguin, A.-E. Asselin, C.L. Jacob & F. Malouin, (2010a) A role for sigma factor B in the emergence of *Staphylococcus aureus* small-colony variants and elevated biofilm production resulting from an exposure to aminoglycosides. *Microb Pathog* **48**: 18-27.
- Mitchell, G., C.-A. Lamontagne, E. Brouillette, G. Grondin, B.G. Talbot, M. Grandbois & F. Malouin, (2008) *Staphylococcus aureus* SigB activity promotes a strong fibronectin-bacterium interaction which may sustain host tissue colonization by small-colony variants isolated from cystic fibrosis patients. *Molecular microbiology* **70**: 1540-1555.
- Mitchell, G., D.L. Seguin, A.-E. Asselin, E. Deziel, A.M. Cantin, E.H. Frost, S. Michaud & F. Malouin, (2010b) *Staphylococcus aureus* sigma B-dependent emergence of small-colony variants and biofilm production following exposure to *Pseudomonas aeruginosa* 4-hydroxy-2-heptylquinoline-N-oxide. *BMC Microbiol* **10**: 33.
- Moisan, H., E. Brouillette, C.L. Jacob, P. Langlois-Begin, S. Michaud & F. Malouin, (2006) Transcription of virulence factors in *Staphylococcus aureus* small-colony variants isolated from cystic fibrosis patients is influenced by SigB. *J Bacteriol* **188**: 64-76.
- Morris, J.F., C.G. Barnes & T.F. Sellers, (1943) An Outbreak of Typhoid Fever Due to the Small Colony Variety of *Eberthella typhosa*. *American journal of public health and the nation's health* **33**: 246-248.
- Morton, H.E. & J. Shoemaker, (1945) The identification of *Neisseria gonorrhoeae* by means of bacterial variation and the detection of small colony forms in clinical material. *J Bacteriol* **50**: 585-587.
- Nguyen, M.T., M. Deplanche, M. Nega, Y. Le Loir, L. Peisl, F. Gotz & N. Berkova, (2016) *Staphylococcus aureus* Lpl Lipoproteins Delay G2/M Phase Transition in HeLa Cells. *Front Cell Infect Microbiol* **6**: 201.
- Nguyen, M.T., B. Kraft, W. Yu, D.D. Demircioglu, D.D. Demircioglu, T. Hertlein, M. Burian, M. Schmalzer, K. Boller, I. Bekeredjian-Ding, K. Ohlsen, B. Schitteck & F. Gotz, (2015) The nuSaalpha Specific Lipoprotein Like Cluster (lpl) of *S.*

- aureus* USA300 Contributes to Immune Stimulation and Invasion in Human Cells. *PLoS pathogens* **11**: e1004984.
- Niemann, V., M. Koch-Singenstreu, A. Neu, S. Nilkens, F. Gotz, G. Uden & T. Stehle, (2014) The NreA protein functions as a nitrate receptor in the staphylococcal nitrate regulation system. *J Mol Biol* **426**: 1539-1553.
- Ogston, A., (1880) Uber Abscesse. *Archiv fur Klinische Chirurgie* **25**: 588-600.
- Ogston, A., (1882) Micrococcus Poisoning. *J Anat Physiol* **16**: 526-567.
- Omata, T., G.D. Price, M.R. Badger, M. Okamura, S. Gohta & T. Ogawa, (1999) Identification of an ATP-binding cassette transporter involved in bicarbonate uptake in the cyanobacterium *Synechococcus* sp. strain PCC 7942. *Proc Natl Acad Sci U S A* **96**: 13571-13576.
- Peacock, S.J., T.J. Foster, B.J. Cameron & A.R. Berendt, (1999) Bacterial fibronectin-binding proteins and endothelial cell surface fibronectin mediate adherence of *Staphylococcus aureus* to resting human endothelial cells. *Microbiology* **145 (Pt 12)**: 3477-3486.
- Price, G.D., (2011) Inorganic carbon transporters of the cyanobacterial CO₂ concentrating mechanism. *Photosynth Res* **109**: 47-57.
- Price, G.D., F.J. Woodger, M.R. Badger, S.M. Howitt & L. Tucker, (2004) Identification of a SulP-type bicarbonate transporter in marine cyanobacteria. *Proc Natl Acad Sci U S A* **101**: 18228-18233.
- Proctor, R., (2019) Respiration and Small Colony Variants of *Staphylococcus aureus*. *Microbiol Spectr* **7**.
- Proctor, R.A., J.M. Balwit & O. Vesga, (1994) Variant subpopulations of *Staphylococcus aureus* as cause of persistent and recurrent infections. *Infectious agents and disease* **3**: 302-312.
- Proctor, R.A., A. Kriegeskorte, B.C. Kahl, K. Becker, B. Löffler & G. Peters, (2014) *Staphylococcus aureus* Small Colony Variants (SCVs): a road map for the metabolic pathways involved in persistent infections. *Front Cell Infect Microbiol* **4**: 99.
- Proctor, R.A., P. van Langevelde, M. Kristjansson, J.N. Maslow & R.D. Arbeit, (1995) Persistent and relapsing infections associated with small-colony variants of *Staphylococcus aureus*. *Clin Infect Dis* **20**: 95-102.
- Proctor, R.A., C. von Eiff, B.C. Kahl, K. Becker, P. McNamara, M. Herrmann & G. Peters, (2006) Small colony variants: a pathogenic form of bacteria that facilitates persistent and recurrent infections. *Nat Rev Microbiol* **4**: 295-305.
- Raven, J.A. & J. Beardall, (2016) The ins and outs of CO₂. *J Exp Bot* **67**: 1-13.
- Raven, J.A., J. Beardall & P. Sanchez-Baracaldo, (2017) The possible evolution and future of CO₂-concentrating mechanisms. *J Exp Bot* **68**: 3701-3716.
- Reyes-Del Valle, J., S. Chavez-Salinas, F. Medina & R.M. Del Angel, (2005) Heat shock protein 90 and heat shock protein 70 are components of dengue virus receptor complex in human cells. *J Virol* **79**: 4557-4567.
- Roggenkamp, A., A. Sing, M. Hornef, U. Brunner, I.B. Autenrieth & J. Heesemann, (1998) Chronic prosthetic hip infection caused by a small-colony variant of *Escherichia coli*. *J Clin Microbiol* **36**: 2530-2534.
- Romero, M.F., (2001) The electrogenic Na⁺/HCO₃⁻ cotransporter, NBC. *JOP* **2**: 182-191.
- Rosenbach, F.J., (1884) *Mikro-Organismen bei den Wund-Infektions-Krankheiten des Menschen*. Wiesbaden.

- Rucker R. B., Morris James & F.A. J., (2008) Chapter 23 Vitamins. In: Clinical Biochemistry of Domestic Animals (Sixth Edition). J.J. Kaneko, J.W. Harvey & M. Bruss (eds). Elsevier Inc, pp. 695-730.
- Savini, V., E. Carretto, E. Polilli, R. Marrollo, S. Santarone, P. Fazii, D. D'Antonio, A. Rossano & V. Perreten, (2014) Small colony variant of methicillin-resistant *Staphylococcus pseudintermedius* ST71 presenting as a sticky phenotype. *Journal of clinical microbiology* **52**: 1225-1227.
- Schuster, M., L. Schnell, P. Feigl, C. Birkhofer, K. Mohr, M. Roeder, S. Carle, S. Langer, F. Toppel, J. Buchner, G. Fischer, F. Hausch, M. Frick, C. Schwan, K. Aktories, C. Schiene-Fischer & H. Barth, (2017) The Hsp90 machinery facilitates the transport of diphtheria toxin into human cells. *Sci Rep* **7**: 613.
- Scott, K.M., J.M. Leonard, R. Boden, D. Chaput, C. Dennison, E. Haller, T.L. Harmer, A. Anderson, T. Arnold, S. Budenstein, R. Brown, J. Brand, J. Byers, J. Calarco, T. Campbell, E. Carter, M. Chase, M. Cole, D. Dwyer, J. Grasham, C. Hanni, A. Hazle, C. Johnson, R. Johnson, B. Kirby, K. Lewis, B. Neumann, T. Nguyen, J. Nino Charari, O. Morakinyo, B. Olsson, S. Roundtree, E. Skjerve, A. Ubaldini & R. Whittaker, (2019) Diversity in CO₂-Concentrating Mechanisms among Chemolithoautotrophs from the Genera *Hydrogenovibrio*, *Thiomicrothabodus*, and *Thiomicrospira*, Ubiquitous in Sulfidic Habitats Worldwide. *Appl Environ Microbiol* **85**.
- Seggewiss, J., K. Becker, O. Kotte, M. Eisenacher, M.R. Yazdi, A. Fischer, P. McNamara, N. Al Laham, R. Proctor, G. Peters, M. Heinemann & C. von Eiff, (2006) Reporter metabolite analysis of transcriptional profiles of a *Staphylococcus aureus* strain with normal phenotype and its isogenic hemB mutant displaying the small-colony-variant phenotype. *J Bacteriol* **188**: 7765-7777.
- Seifert, H., D. Oltmanns, K. Becker, H. Wisplinghoff & C. von Eiff, (2005) *Staphylococcus lugdunensis* pacemaker-related infection. *Emerging infectious diseases* **11**: 1283-1286.
- Sendi, P. & R.A. Proctor, (2009) *Staphylococcus aureus* as an intracellular pathogen: the role of small colony variants. *Trends in microbiology* **17**: 54-58.
- Shahmirzadi, S.V., M.-T. Nguyen & F. Gotz, (2016) Evaluation of *Staphylococcus aureus* Lipoproteins: Role in Nutritional Acquisition and Pathogenicity. *Frontiers in microbiology* **7**: 1404.
- Sherris, J.C., (1952) Two small colony variants of *Staphylococcus aureus* isolated in pure culture from closed infected lesions and their carbon dioxide requirements. *J Clin Pathol* **5**: 354-355.
- Shibata, M., H. Katoh, M. Sonoda, H. Ohkawa, M. Shimoyama, H. Fukuzawa, A. Kaplan & T. Ogawa, (2002) Genes essential to sodium-dependent bicarbonate transport in cyanobacteria: function and phylogenetic analysis. *J Biol Chem* **277**: 18658-18664.
- Shih, P.M., A. Occhialini, J.C. Cameron, P.J. Andralojc, M.A. Parry & C.A. Kerfeld, (2016) Biochemical characterization of predicted Precambrian RuBisCO. *Nat Commun* **7**: 10382.
- Sidera, K. & E. Patsavoudi, (2008) Extracellular HSP90: conquering the cell surface. *Cell Cycle* **7**: 1564-1568.
- Singh, R., P. Ray, A. Das & M. Sharma, (2009) Role of persisters and small-colony variants in antibiotic resistance of planktonic and biofilm-associated *Staphylococcus aureus*: an in vitro study. *J Med Microbiol* **58**: 1067-1073.

- Singh, R., P. Ray, A. Das & M. Sharma, (2010) Enhanced production of exopolysaccharide matrix and biofilm by a menadione-auxotrophic *Staphylococcus aureus* small-colony variant. *J Med Microbiol* **59**: 521-527.
- Sinha, B., P.P. Francois, O. Nusse, M. Foti, O.M. Hartford, P. Vaudaux, T.J. Foster, D.P. Lew, M. Herrmann & K.H. Krause, (1999) Fibronectin-binding protein acts as *Staphylococcus aureus* invasin via fibronectin bridging to integrin alpha5beta1. *Cellular microbiology* **1**: 101-117.
- Slifkin, M., L.P. Merkow, S.A. Kreuzberger, C. Engwall & M. Pardo, (1971) Characterization of CO₂ dependent microcolony variants of *Staphylococcus aureus*. *Am J Clin Pathol* **56**: 584-592.
- Smith, K.S. & J.G. Ferry, (2000) Prokaryotic carbonic anhydrases. *FEMS Microbiol Rev* **24**: 335-366.
- Somerville, G.A., (2016) *Staphylococcus aureus* Metabolism and Physiology. *Staphylococcus: Genetics and Physiology*: 107-118.
- Somerville, G.A., M.S. Chaussee, C.I. Morgan, J.R. Fitzgerald, D.W. Dorward, L.J. Reitzer & J.M. Musser, (2002) *Staphylococcus aureus* aconitase inactivation unexpectedly inhibits post-exponential-phase growth and enhances stationary-phase survival. *Infect Immun* **70**: 6373-6382.
- Somerville, G.A., A. Cockayne, M. Durr, A. Peschel, M. Otto & J.M. Musser, (2003a) Synthesis and deformylation of *Staphylococcus aureus* delta-toxin are linked to tricarboxylic acid cycle activity. *J Bacteriol* **185**: 6686-6694.
- Somerville, G.A. & R.A. Proctor, (2009) At the crossroads of bacterial metabolism and virulence factor synthesis in Staphylococci. *Microbiol Mol Biol Rev* **73**: 233-248.
- Somerville, G.A., B. Said-Salim, J.M. Wickman, S.J. Raffel, B.N. Kreiswirth & J.M. Musser, (2003b) Correlation of acetate catabolism and growth yield in *Staphylococcus aureus*: implications for host-pathogen interactions. *Infect Immun* **71**: 4724-4732.
- Sreedhar, A.S., E. Kalmar, P. Csermely & Y.F. Shen, (2004) Hsp90 isoforms: functions, expression and clinical importance. *FEBS Lett* **562**: 11-15.
- Stockland, A.E. & C.L. San Clemente, (1969) Multiple forms of lactate dehydrogenase in *Staphylococcus aureus*. *J Bacteriol* **100**: 347-353.
- Strasters, K.C. & K.C. Winkler, (1963) Carbohydrate metabolism of *Staphylococcus aureus*. *J Gen Microbiol* **33**: 213-229.
- Tabita, F.R., T.E. Hanson, S. Satagopan, B.H. Witte & N.E. Kreel, (2008) Phylogenetic and evolutionary relationships of RubisCO and the RubisCO-like proteins and the functional lessons provided by diverse molecular forms. *Philos Trans R Soc Lond B Biol Sci* **363**: 2629-2640.
- Taiyab, A. & C.M. Rao, (2011) HSP90 modulates actin dynamics: inhibition of HSP90 leads to decreased cell motility and impairs invasion. *Biochim Biophys Acta* **1813**: 213-221.
- Thomas, M.E., (1955) Studies on a CO₂-dependent *staphylococcus*. *J Clin Pathol* **8**: 288-291.
- Thöny-Meyer, L., (1997) Biogenesis of respiratory cytochromes in bacteria. *Microbiol Mol Biol Rev* **61**: 337-376.
- Tran Van Nhieu, G. & R.R. Isberg, (1993) Bacterial internalization mediated by beta 1 chain integrins is determined by ligand affinity and receptor density. *The EMBO journal* **12**: 1887-1895.
- Tribelli, P.M., A. Luqman, M.T. Nguyen, J. Madlung, S.H. Fan, B. Macek, P. Sass, K. Bitschar, B. Schitteck, D. Kretschmer & F. Gotz, (2019) *Staphylococcus aureus*

- Lpl protein triggers human host cell invasion via activation of Hsp90 receptor. *Cell Microbiol*: e13111.
- Usui, A., M. Murai, K. Seki, J. Sakurada & S. Masuda, (1992) Conspicuous ingestion of *Staphylococcus aureus* organisms by murine fibroblasts in vitro. *Microbiol Immunol* **36**: 545-550.
- Voggu, L., S. Schlag, R. Biswas, R. Rosenstein, C. Rausch & F. Götz, (2006) Microevolution of cytochrome *bd* oxidase in staphylococci and its implication in resistance to respiratory toxins released by *Pseudomonas*. *J Bacteriol* **188**: 8079-8086.
- von Eiff, C., C. Heilmann, R.A. Proctor, C. Woltz, G. Peters & F. Götz, (1997) A site-directed *Staphylococcus aureus hemB* mutant is a small-colony variant which persists intracellularly. *J Bacteriol* **179**: 4706-4712.
- von Eiff, C., P. McNamara, K. Becker, D. Bates, X.H. Lei, M. Ziman, B.R. Bochner, G. Peters & R.A. Proctor, (2006) Phenotype microarray profiling of *Staphylococcus aureus menD* and *hemB* mutants with the small-colony-variant phenotype. *J Bacteriol* **188**: 687-693.
- von Eiff, C., Peters, G. and Becker, K., (2006) The small colony variant (SCV) concept—the role of staphylococcal SCVs in persistent infections. *Injury* **37**: S26-S33.
- von Eiff, C., P. Vaudaux, B.C. Kahl, D. Lew, S. Emler, A. Schmidt, G. Peters & R.A. Proctor, (1999) Bloodstream infections caused by small-colony variants of coagulase-negative staphylococci following pacemaker implantation. *Clinical infectious diseases : an official publication of the Infectious Diseases Society of America* **29**: 932-934.
- Walker, J.E., (1992) The NADH:ubiquinone oxidoreductase (complex I) of respiratory chains. *Q Rev Biophys* **25**: 253-324.
- Warburg, O., W. Christian & A. Griese, (1935) Hydrogen-Transferring Coenzyme; Its Composition and Mode of Action. *Biochem. Ztschr.* **282**: 157-205.
- Whitesell, L. & S.L. Lindquist, (2005) HSP90 and the chaperoning of cancer. *Nat Rev Cancer* **5**: 761-772.
- Winstedt, L., K. Yoshida, Y. Fujita & C. von Wachenfeldt, (1998) Cytochrome *bd* biosynthesis in *Bacillus subtilis*: characterization of the *cydABCD* operon. *J Bacteriol* **180**: 6571-6580.
- Zapotoczna, M., Z. Jevnikar, H. Miajlovic, J. Kos & T.J. Foster, (2013) Iron-regulated surface determinant B (IsdB) promotes *Staphylococcus aureus* adherence to and internalization by non-phagocytic human cells. *Cellular microbiology* **15**: 1026-1041.
- Zbinden, A., C. Quiblier, D. Hernandez, K. Herzog, P. Bodler, M.M. Senn, Y. Gizard, J. Schrenzel & P. Francois, (2014) Characterization of *Streptococcus tigurinus* small-colony variants causing prosthetic joint infection by comparative whole-genome analyses. *J Clin Microbiol* **52**: 467-474.

Acknowledgements

First and foremost, I would like to thank Prof. Friedrich Götz for giving me the opportunity to do my PhD studies in his lab. I am grateful for his guidance and support all these years. I appreciate him for his patience and willingness to help whenever things did not work out. Thank you, Fritz for believing in me before I believed in myself.

Special thanks to Prof. Andreas Peschel for being my second supervisor. Also my sincere gratitude to Prof. Forchhammer for including me in the Research Training Group GRK1708 as an associate member and the travel support for attending various conferences. My deepest gratitude to DAAD for the PhD fellowship award.

My sincere thanks to Patrick and Sebastian for sharing their expertise in cloning and insightful discussions and ideas in this project. Thank you to all my collaborators for their contributions in this project.

I thank my all my past and present colleagues in Microbial Genetics for their help and support, also not forgetting the members from AG HBO and AG Peschel. Many thanks for the wonderful 'beer time' on Fridays and for all the fun we have had in the last four years. My heartfelt thanks to Paula for including me in her project.

I would like to express my gratitude to my close friends Anu, Iti, Carlos, Ash and Adi for making my life here in Tuebingen more enjoyable. Thank you for the friendship and the crazy but memorable time together.

Last but not least, I would like to thank my family for their continuous support and love. A big thank you to my sisters and brother for taking care of our parents so that I can focus on my research. Most importantly, I thank my mother for letting me to pursue my dream. Thank you all for believing in me because without you, I would not have the confidence to go halfway around the world and do my best to make you proud.

Appendix

Written permission for the use of Table 1 from ASM Press

American Society For Microbiology Copyright Limited License Agreement

Requestor ("Licensee"):

Invoice No.: P2019.22

Name: Ms Sook-Ha, Fan

Organization: University of Tübingen

Address:

PhD student

Microbial Genetics (AG Götz)

Interfaculty Institute of Microbiology and Infection

Medicine Auf der, Morgenstelle 28E

72076 Tübingen

GERMANY

Email:

This agreement pertains to: Table 1 (the "Work") in the ASM Press publication,

<https://www.asmscience.org/content/journal/microbiolspec/10.1128/microbiolspec.GPP3-0069-2019> for the purpose of: PhD thesis (the "Use").

In exchange for good and valuable consideration being given and acknowledged, ASM Press, the book publishing division of the American Society for Microbiology ("ASM") hereby provides Licensee with this license, contingent upon Licensee's adherence to the following terms and conditions:

License: ASM Press grants Licensee a nonexclusive, nontransferable, non-sublicensable, revocable limited license to Use the Work, subject to the restrictions contained in this agreement.

Term of Use: one-time perpetual other (specify): print and digital use

Termination: ASM Press reserves the right to terminate this agreement and license for cause at any time effective immediately upon written notice to Licensee in the event that Licensee has violated the terms of this agreement.

License Fee: \$ Fee Waived

If fee is required, this license shall not commence until ASM Press receives payment. Payment shall be made to ASM Press, 1752 N Street, NW, Washington, DC 20036.

**American Society For Microbiology
Copyright Limited License Agreement**

Ownership of Intellectual Property: At all times ASM or its licensors will retain all right, title and interest in and to the Work, including without limitation, copyrights, trademarks and any other rights and interests. This license does not convey to Licensee any right, title or interest in the Work, nor in any portion of the Work, but only constitutes a limited license to Use the Work as specified herein.

Restrictions: Licensee should not remove or alter any copyright or trademark notices referenced in the Work. Licensee may not adapt, reproduce, distribute, publicly display, or create derivative works of the Work in any other manner or formats or for any other purpose, other than as expressly licensed herein.

Copyright Acknowledgment. The following statement must be used conspicuously on or near the Work: "©2019 American Society for Microbiology. Used with permission. No further reproduction or distribution is permitted without the prior written permission of American Society for Microbiology."

Representation and Warranty: By signing below, each person represents and warrants that he/she is authorized to sign this agreement and bind their respective company or, if this agreement is granted directly to an individual, bind them personally to this agreement's terms.

Agreed and accepted by:

Sook-Ha, FAN
Licensee (signature)
Sook-Ha, FAN
Licensee (printed name)
10 Sept 2019
Date

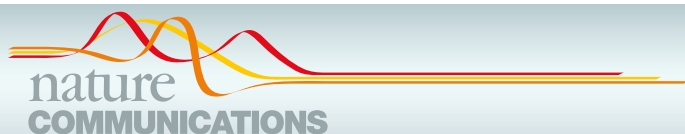
Lindsay Williams
ASM Press (signature)
Lindsay Williams
ASM Press (printed name)
Editorial Rights Coordinator
ASM Press title
9/10/19
Date

Accepted Publication 1

MpsAB is important for *Staphylococcus aureus* virulence and growth at atmospheric CO₂ levels,

Fan SH, Ebner P, Reichert S, Hertlein T, Zabel S, Lankapalli AK, Nieselt K, Ohlsen K, Götz F

Nat Commun. 2019 Aug 9;10(1):3627. doi: 0.1038/s41467-019-11547-5.




ARTICLE

<https://doi.org/10.1038/s41467-019-11547-5>

OPEN

MpsAB is important for *Staphylococcus aureus* virulence and growth at atmospheric CO₂ levels

Sook-Ha Fan^{1,5}, Patrick Ebner^{1,5}, Sebastian Reichert¹, Tobias Hertlein², Susanne Zabel³, Aditya Kumar Lankapalli⁴, Kay Nieselt ³, Knut Ohlsen² & Friedrich Götz¹

The mechanisms behind carbon dioxide (CO₂) dependency in non-autotrophic bacterial isolates are unclear. Here we show that the *Staphylococcus aureus* *mpsAB* operon, known to play a role in membrane potential generation, is crucial for growth at atmospheric CO₂ levels. The genes *mpsAB* can complement an *Escherichia coli* carbonic anhydrase (CA) mutant, and CA from *E. coli* can complement the *S. aureus* delta-*mpsABC* mutant. In comparison with the wild type, *S. aureus* *mps* mutants produce less hemolytic toxin and are less virulent in animal models of infection. Homologs of *mpsA* and *mpsB* are widespread among bacteria and are often found adjacent to each other on the genome. We propose that MpsAB represents a dissolved inorganic carbon transporter, or bicarbonate concentrating system, possibly acting as a sodium bicarbonate cotransporter.

¹Microbial Genetics, Interfaculty Institute of Microbiology and Infection Medicine Tübingen (IMIT), University of Tübingen, Auf der Morgenstelle 28, D-72076 Tübingen, Germany. ²Institute for Molecular Infection Biology (IMIB), University of Würzburg, Josef-Schneider-Strasse 2, D-97080 Würzburg, Germany. ³Center for Bioinformatics Tübingen, University of Tübingen, Sand 14, D-72076 Tübingen, Germany. ⁴Department of Archaeogenetics, Max Planck Institute for the Science of Human History, Kahlaische Strasse 10, D-07745 Jena, Germany. ⁵These authors contributed equally: Sook-Ha Fan, Patrick Ebner. Correspondence and requests for materials should be addressed to F.G. (email: friedrich.goetz@uni-tuebingen.de)

Early concepts of the function of CO₂ in bacterial growth can be traced back to as early as a century ago. However, convincing experimental evidence only surfaced in 1935 when Gladstone reported that CO₂ is an essential factor in the growth of bacteria¹. The growth-promoting effect of CO₂ was observed in various bacteria, including *Staphylococcus aureus*, particularly when glucose was substituted by another carbon source. Many years later, CO₂-dependent *S. aureus* was isolated from abscesses and osteomyelitis^{2,3}. These strains, though very rare, were well documented as dwarf or gonidial (G) strains and usually produced tiny colonies in the absence of additional CO₂⁴. Although G strains can be isolated from lesions, their virulence is low in a mouse infection model³. Since the early 1970's, the CO₂ dependence of staphylococci has been largely overlooked due in part to the routine cultivation of clinical isolates in CO₂ incubators.

Renewed interest in these so-called dwarf colonies, now referred to as small colony variants (SCVs), was initiated in large part because they were frequently associated with persistent and relapsing infections such as airway infections and osteomyelitis⁵⁻⁷. In most cases, SCVs consist of mutants that are frequently affected in respiration comprising thymidine, hemin, or menadione auxotrophs⁸⁻¹⁰. However, unlike the earlier dwarf mutants described by Slifkin³ the respiratory mutants cannot be complemented by elevated CO₂. There are several reports where CO₂-dependent SCVs of *S. aureus* have been isolated from patients with catheter-related bacteremia, endocarditis, wound infections, respiratory infections, or nasal colonization¹¹. This shows that CO₂-dependent SCVs play a role in certain infections and further studies are necessary to unravel the genetic and biochemical basis of this type of auxotrophy.

We previously investigated whether *S. aureus* possesses a type I electrogenic NADH:quinone oxidoreductase (Ndh1), a proton pump that translocates cations, such as H⁺ or Na⁺¹². It turned out that such an Ndh1 is not present in staphylococci; however, we found *S. aureus* has a homolog of the *Escherichia coli* specific NuoL protein, one of the core components of the proton pumping mechanism in *E. coli*¹³. We named the gene *mpsA* (membrane potential-generating system), because an *mpsA* mutant was severely defected in membrane potential generation and also grew like an SCV¹². This connection and in light of the recent attention on SCVs, we sought to determine the function of the *mps* operon.

In *S. aureus*, *mpsA* is cotranscribed with the *mpsB* gene, and is separated by a weak transcription terminator from the downstream *mpsC*. It was unknown at that time whether *mpsC* contributes to the MpsAB function. MpsA, like the NuoL homolog is a membrane protein with predicted 14 transmembrane domains, while MpsB is a cytoplasmic protein with a predicted metal binding site. While MpsABC lacks NADH oxidation activity, it participates in Na⁺ transport as *mpsABC* complemented an Na⁺/H⁺ antiporter-deficient *E. coli* strain, suggesting that MpsABC constitutes a cation-translocating system¹².

Here, we extend our previous observations by analyzing the function of MpsABC in greater detail. In principle, this study builds on the work of the 1970s, in which dwarf colonies were found to be complemented by CO₂. We show that MpsAB increase the uptake of bicarbonate and represents a new class of dissolved inorganic carbon (DIC) transporter. DIC transporters are responsible for creating an elevated concentration of intracellular bicarbonate and supplying it to carboxysomes and Rubisco. Such transporters are most well studied in cyanobacteria¹⁴, but are not fully described in other autotrophic bacteria. In *S. aureus*, SCV-like *mpsAB* mutants cannot supply and store sufficient bicarbonate from atmospheric air to feed the important carboxylase reactions in central metabolism. The severe growth defect can only be compensated by increased CO₂/bicarbonate supplementation. Importantly, MpsAB homologs are

widespread in bacteria and were recently found in autotrophic bacteria functioning as DIC transporters to supply carboxysomes and RubisCO with bicarbonate/CO₂^{15,16}.

Results

Growth defect of $\Delta mpsABC$ is rescued by elevated CO₂/NaHCO₃. As previously reported, deletion of the *mpsABC* operon in *S. aureus* strain SA113 resulted in a severe growth defect, with the typical SCV-like phenotype¹². To further characterize this operon, we constructed single deletion mutants of $\Delta mpsA$, $\Delta mpsB$, and $\Delta mpsC$, as well as a deletion of the entire operon, $\Delta mpsABC$, in the *agr*-positive *S. aureus* strain HG001¹⁷. The mutants were analyzed for growth in liquid culture under atmospheric growth conditions. As shown in Fig. 1a, the mutants $\Delta mpsA$, $\Delta mpsB$, and $\Delta mpsABC$ grew slowly and did not achieve the final OD of the wild type (WT) strain HG001, even after 72 h. The growth delay was most pronounced in the first 24 h. In contrast to $\Delta mpsA$ and $\Delta mpsB$, the growth of $\Delta mpsC$ was not affected, indicating that *mpsC* does not contribute to the *mpsAB* activity.

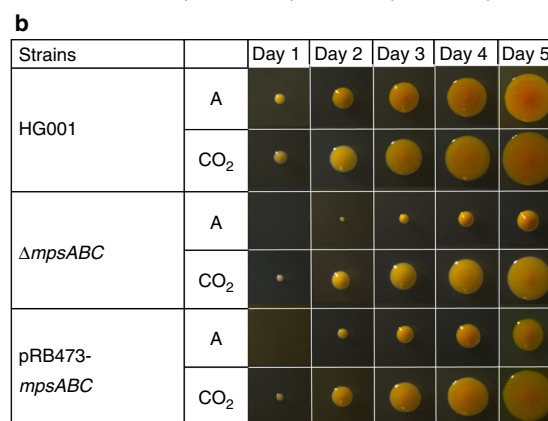
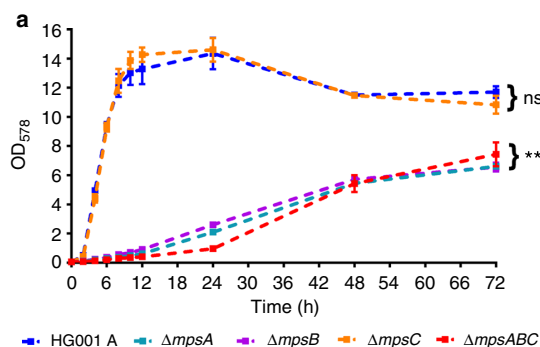


Fig. 1 Growth of HG001 $\Delta mpsABC$. **a** Growth of wild type HG001, $\Delta mpsA$, $\Delta mpsB$, $\Delta mpsC$, and $\Delta mpsABC$ in atmospheric (A) conditions. The growth of all mutants except $\Delta mpsC$ was significantly lower compared to HG001, $**p < 0.01$ by unpaired two-sided *t*-test. $\Delta mpsC$ showed no significant difference (ns) in growth compared to HG001. Each point shown in the graph represents the mean value \pm standard error mean (SEM) from three independent experiments. Source data are provided as a Source Data file. **b** Colony appearances of wild type HG001, $\Delta mpsABC$, and its complemented mutant (plasmid pRB473-*mpsABC*) during 5 days of incubation in atmospheric (A) conditions and 5% CO₂. White bar represents a scale of 1 mm

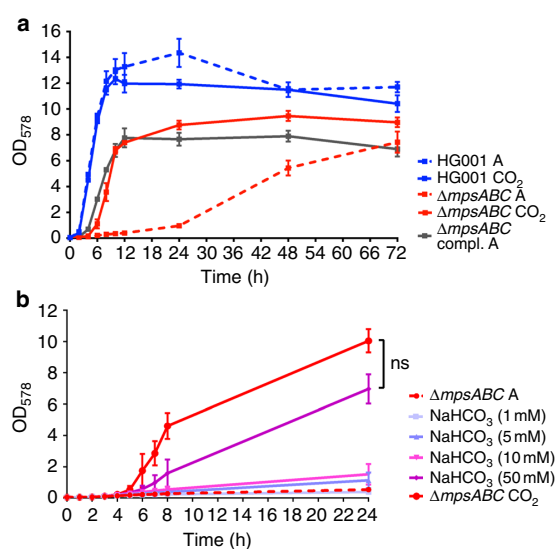


Fig. 2 Growth of HG001 $\Delta mpsABC$ can be complemented with 5% CO₂ and NaHCO₃. **a** Growth of HG001, $\Delta mpsABC$ in atmospheric (A) conditions and 5% CO₂. The growth of the mutant can also be complemented by plasmid pRB473 carrying *mpsABC* (compl.). Each point shown in the graph represents the mean value \pm standard error mean (SEM) from three independent experiments. **b** Growth of $\Delta mpsABC$ in atmospheric (A) and with additions of NaHCO₃ ranging from concentrations of 1 to 50 mM, and 5% CO₂. The growth of $\Delta mpsABC$ with addition of 50 mM NaHCO₃ was similar to that under 5% CO₂, as there was no significance difference (ns) between the two conditions ($p > 0.05$) by unpaired two-sided *t*-test. Each point shown in the graph represents the mean value \pm standard error mean (SEM) from two independent experiments. Source data are provided as a Source Data file

Interestingly, growth of all mutants could be restored to near WT levels under elevated (5%) CO₂ concentrations. During the course of 5 days incubation in 5% CO₂, the colonies of all mutants were significantly larger than those grown in atmospheric air. Growth of the WT strain was largely uninfluenced by CO₂, although the colony size was slightly increased (Fig. 1b and Supplementary Fig. 1). The growth-promoting effect of CO₂ was also seen in liquid medium (Fig. 2a and Supplementary Fig. 2). Comparison of the growth in tryptic soy broth (TSB) in the absence or presence of 5% CO₂ revealed that growth of the $\Delta mpsABC$ mutant was significantly improved in the presence of CO₂ (Fig. 2a). This growth tendency is similar in the complemented mutant $\Delta mpsABC$ (pRB473-*mpsABC*) under atmospheric conditions. Given that CO₂ and bicarbonate are interconvertible in aqueous solution, we also attempted to complement $\Delta mpsABC$ with sodium bicarbonate (NaHCO₃). NaHCO₃ at concentration ranging from 1 to 50 mM were added to the growth medium and growth of $\Delta mpsABC$ was followed for 24 h. At low concentrations (1 mM NaHCO₃) no difference in the growth of $\Delta mpsABC$ was observed (Fig. 2b). However, with increasing concentrations of up to 50 mM NaHCO₃, its growth increased steadily before reaching final OD values comparable with those of 5% CO₂. Similar observation was also seen with $\Delta mpsB$ (Supplementary Fig. 3a and 3b). The pH of the medium (TSB) increased with the addition of NaHCO₃, however the effect of pH of the medium did not play a crucial role on the growth of $\Delta mpsABC$ (see Supplementary Note 1, Supplementary Table 3 and Supplementary Fig. 8). The results indicate that the growth

deficiency of $\Delta mpsABC$ can be largely compensated by the addition of 5% CO₂ and high concentrations of NaHCO₃.

MpsABC increase the uptake of bicarbonate. The diminished ability of the $\Delta mpsABC$ mutant to grow under atmospheric conditions as well as the rescue of this defect by CO₂ and bicarbonate led us to the suggestion that MpsAB may play a role in CO₂ and bicarbonate transport. As the determination of the CO₂ transport is very difficult, we compared the bicarbonate uptake activity in the WT strain HG001 and the $\Delta mpsABC$ mutant with radiolabeled NaH¹⁴CO₃. Both strains were grown aerobically in TSB until reaching its respective exponential growth phase before being washed to remove the growth media and resuspended to the same OD₅₇₈ in Tris buffer. Prior to the addition of NaH¹⁴CO₃, the cell suspensions were incubated with fluorocitrate and glucose. Fluorocitrate, an aconitase inhibitor, was added to block the TCA cycle so that NaH¹⁴CO₃ accumulated intracellularly and is not immediately expired by the decarboxylation reactions of the TCA cycle. Glucose was added as energy source because the cells were resuspended in only Tris buffer. After addition of NaH¹⁴CO₃, samples were rapidly harvested at several time points and the ¹⁴C uptake was measured by liquid scintillation counting. The immediate uptake occurred within 120 s until a steady state level was reached (Fig. 3a). Compared with the WT strain HG001, $\Delta mpsABC$ showed significantly decreased ¹⁴C uptake in the first 120 s. After 15 min, $\Delta mpsABC$ showed a 6.6-fold lower radioactivity than the WT strain indicating that the bicarbonate uptake was impaired in the mutant.

***mpsAB* complements an *E. coli* CA mutant and vice versa.**

Previously we described that MpsB contains a metal binding motif (His607, Cys622, and Cys625), which is reminiscent of a carbonic anhydrase (CA) motif¹². Therefore, we tried to detect CA activity with purified MpsB alone and cell extracts expressing MpsABC. However, we were unable to detect any CA activity with various methods. In the absence of any detectable enzymatic data, we asked if *mpsAB* could complement a CO₂-dependent *E. coli* mutant, EDCM636¹⁸. EDCM636 is an *E. coli* K-12 mutant in which the CA gene, *can*, was deleted. As a result, this strain is unable to grow under atmospheric air, but can grow in the presence of high CO₂. This phenotype of EDCM636 is similar to that of HG001 $\Delta mpsABC$; hence, we investigated whether *mpsAB* can restore growth of EDCM636 under atmospheric conditions. To do this, we inserted the *S. aureus mpsA*, *mpsB*, *mpsAB*, and *mpsABC* genes into *E. coli* strain EDCM636. The vector alone, pRB473, served as control. Interestingly, neither *mpsA* nor *mpsB* alone could restore growth of EDCM636. Plasmids containing *mpsAB* and *mpsABC* were able to restore the growth equally well (Fig. 4a), indicating that *mpsC* was dispensable. As expected, all six strains were able to grow under 5% CO₂ conditions (Fig. 4a).

Since *mpsAB* restored the growth of EDCM636, we asked if the CA gene (*can*) from *E. coli* could complement the *S. aureus* $\Delta mpsABC$. To address this question, *can* from *E. coli* K-12 was expressed in $\Delta mpsABC$ (pTX30-*can*) under a xylose inducible promoter. As shown in Fig. 4b, without xylose $\Delta mpsABC$ (pTX30-*can*) could not grow under atmospheric air. However, when *can* expression was induced by xylose, growth was restored. All clones grew in the presence of 5% CO₂ (Fig. 4b), suggesting that both the bicarbonate transporter and CA enable growth under atmospheric CO₂ level and both are interchangeable. Although the activities of bicarbonate transporters and CA are different, they represent a CO₂/bicarbonate concentrating system that can functionally replace each other.

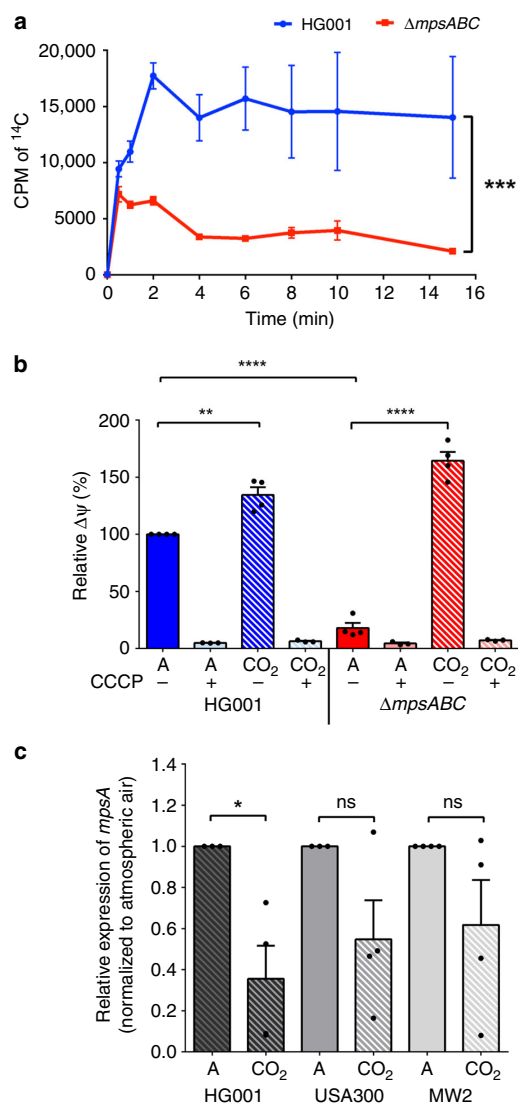


Fig. 3 Uptake of $\text{NaH}^{14}\text{CO}_3$ by HG001 and $\Delta mpsABC$, membrane potential determination and *mpsA* expression. **a** Cells were preincubated with fluorocitrate for 30 mins prior to the addition of $\text{NaH}^{14}\text{CO}_3$ (50 μCi). $\text{NaH}^{14}\text{CO}_3$ was added at time 0 and 1 ml of cell samples collected at times indicated. The H^{14}CO_3 uptake was determined by ^{14}C accumulation in cells measured by liquid scintillation counting. The $\text{NaH}^{14}\text{CO}_3$ uptake in $\Delta mpsABC$ was significantly lower than WT HG001; $***p < 0.001$ by paired two-sided *t*-test. Each point shown in the graph represents the mean value \pm standard error mean (SEM) from three independent experiments. (CPM = counts per minute). **b** $\Delta mpsABC$ grown in 5% CO_2 showed increased membrane potential compared with those grown in atmospheric conditions. Membrane potential was determined by fluorescence intensity measurements using BacLight bacterial membrane potential kit. The values for WT HG001 in atmospheric were set equal to 100%. Cells were grown to exponential growth phase in atmospheric (A) and 5% CO_2 (CO_2). As a negative control, the H^+ ionophore CCCP caused a collapse of the membrane potential in all strains tested both in atmospheric CO_2 and in the presence of 5% CO_2 . When grown under 5% CO_2 conditions, HG001 and $\Delta mpsABC$ showed significantly higher relative membrane potential ($**p < 0.01$ and $****p < 0.0001$, respectively, as determined by unpaired two-sided *t*-test) compared with their corresponding strains in atmospheric conditions. Each bar shown in the graph represents the mean value \pm standard error mean (SEM) from four independent experiments (three independent experiments for CCCP), each with three technical replicates. **c** *mpsA* expression in three wild-type *Staphylococcus aureus* strains HG001, USA300, and MW2 under atmospheric and 5% CO_2 conditions. The relative expression of *mpsA* under 5% CO_2 conditions, normalized to its corresponding strains grown in atmospheric (A) conditions. Only *mpsA* expression in HG001 is significantly lower in 5% CO_2 compared with atmospheric conditions; $*p < 0.05$ by unpaired two-sided *t*-test. (ns = not significant). Each bar shown in the graph represents the mean value \pm standard error mean (SEM) from four independent experiments, each with three technical replicates. Source data are provided as a Source Data file

Impaired membrane potential in $\Delta mpsABC$ is rescued by 5% CO_2 . Previously, it was reported that MpsABC represents a membrane potential-generating and cation-translocating system, and that membrane potential was severely affected in the $\Delta mpsABC$ mutant¹². Because elevated CO_2 restores the growth of $\Delta mpsABC$, we wondered whether 5% CO_2 also restores the membrane potential in this mutant. The membrane potential of the WT strain, HG001, grown under atmospheric air was set equal to 100% and was used as a comparator for other strains (Fig. 3b). In the $\Delta mpsABC$ mutant, the membrane potential was decreased to only 18% of HG001. In contrast, the presence of 5% CO_2 increased the membrane potential of the $\Delta mpsABC$ mutant and the WT strain up to 164% and 134%, respectively. As a negative control, the H^+ ionophore CCCP caused a collapse of the membrane potential in all strains tested both in atmospheric CO_2 and in the presence of 5% CO_2 . Based on these findings, elevated CO_2 not only restores growth but also the membrane potential generation in the $\Delta mpsABC$.

***mpsA* expression was downregulated under 5% CO_2 conditions.** Since the *mps* deletion mutants, except $\Delta mpsC$, are responsive to 5% CO_2 , we postulated that the expression of *mpsAB* could be affected by CO_2 . To investigate whether high CO_2 levels influence *mps* transcription, Quantitative Reverse Transcriptase-PCR (qRT-PCR) was performed to determine the transcription of *mpsA* in atmospheric and 5% CO_2 conditions. To exclude strain specific effects, three different WT *S. aureus* strains were used, namely HG001, USA300 LAC, and MW2 (USA400). RNA was isolated during the exponential growth phase and the mRNA of *mpsA* from the three strains grown in atmospheric air and in 5% CO_2 were compared. Transcript abundance for each strain cultivated in 5% CO_2 was normalized to its corresponding strain grown in atmospheric conditions. Relative to the growth in atmospheric air, *mpsA* in HG001 grown in CO_2 was downregulated the most, namely 2.5-fold, in USA300 2-fold, and in MW2 1.7-fold (Fig. 3c). In short, *mpsA* expression was lower in 5% CO_2 compared with atmospheric conditions in all three strains tested; however, only *mpsA* downregulation in HG001 reached statistical significance ($p < 0.05$). A downregulation of *mpsA* (SAOUHSC_00412) by CO_2 was also observed under cell culture conditions, as reported in Aureowiki¹⁹.

***ΔmpsA* produces fewer hemolytic toxins and is less pathogenic.** Because the CO_2 /bicarbonate transporter MpsAB is important for growth and membrane potential generation, we predicted that the mutant would have less toxin production and be less virulent. To examine this question, the hemolytic activity of $\Delta mpsA$ and HG001 grown in atmospheric and 5% CO_2 was tested on sheep blood agar

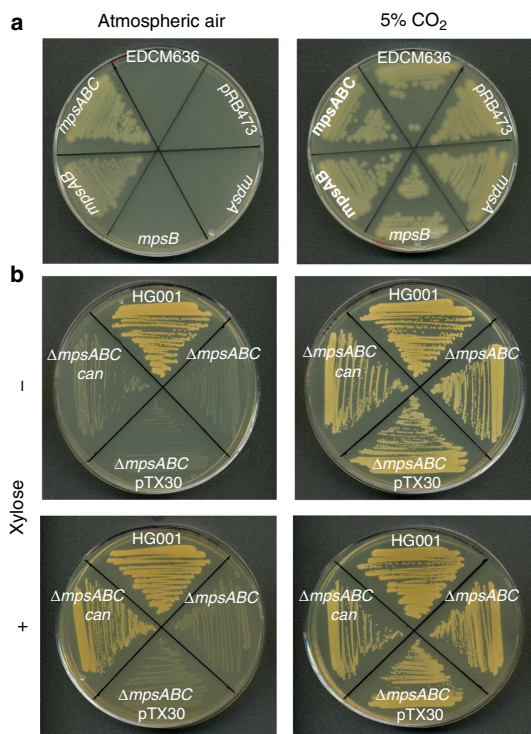


Fig. 4 *mpsAB(C)* complements an *E. coli* carbonic anhydrase mutant and vice versa. **a** *E. coli* carbonic anhydrase mutant (EDCM636) can be complemented with *mpsAB* and *mpsABC* using plasmid pRB473 under the control of its native promoter in atmospheric (left) and 5% CO₂ (right). Clockwise from the top; EDCM636, EDCM636 pRB473 (empty plasmid), EDCM636 pRB473 *mpsA*, EDCM636 pRB473 *mpsB*, EDCM636 pRB473 *mpsAB*, and EDCM636 pRB473 *mpsABC*. **b** Δ *mpsABC* can be complemented with carbonic anhydrase, *can* from *E. coli* MG1655 using pTX30, a xylose-inducible promoter plasmid. Clockwise from the top; wild-type HG001, Δ *mpsABC*, Δ *mpsABC* pTX30 (empty plasmid), and Δ *mpsABC* pTX30 *can*. Plates were supplemented with xylose (+) or without xylose (–)

followed by cold shock treatment. Consistent with our hypothesis, no visible hemolytic zone was seen in Δ *mpsA* when cultivated in atmospheric air, while the presence of 5% CO₂ restored toxin production as indicated by a clear halo on blood agar (Fig. 5a). The same result was also observed for the Δ *mpsB* and Δ *mpsABC* mutants (Supplementary Fig. 4). The WT strain HG001 formed a hemolysis zone independent of the presence of 5% CO₂.

Following the finding of decreased toxin production from Δ *mpsA*, we were interested to find out if this effect is relevant in vivo. To characterize the role of *mps* on virulence, *Galleria mellonella* larvae were used as an invertebrate infection model. The survival rate of larvae injected with WT HG001, Δ *mpsA*, and PBS as control were observed over the course of 5-day period (Fig. 5b). In the PBS control group, 95% of the larvae were alive at the end of the 5-day period. In contrast, larvae infected with HG001 showed a survival rate of only 13% after the 5-day period, while 53% of the larvae survived when infected with Δ *mpsA*. These results indicate that deletion of *mpsA* rendered *S. aureus* less virulent in an invertebrate infection model.

To assess the contributions of *mpsAB* to *S. aureus* pathogenesis using an intranasal mouse infection model (pneumonia model), female Balb/c mice were intranasally infected with HG001 and

Δ *mpsA*. After 48 h, mice were sacrificed and the lungs, kidneys, and livers were recovered to determine the bacterial burden. Although the Δ *mpsA* generally exhibited a lower bacterial burden in all three organs, only the bacterial load in the lung was significantly lower compared with its WT strain HG001 (Fig. 5c). These results indicate that the Δ *mpsA* is attenuated in pathogenicity compared with its WT strain in this mouse infection model. Taken together, these findings suggest that a functional bicarbonate transport system (*mps*) is required for fitness and pathogenicity in vivo.

Phylogenetic distribution of *mpsAB* homologs. Considering the significant effect of *mpsAB* in *S. aureus*, we examined the phylogenetic distribution of both genes. Searching the RefSeq database revealed genes homologous to *mpsA* and *mpsB* were found in a number of species that span the Firmicutes phylum (Fig. 6). These included bacteria from the genus *Staphylococcus*, *Bacillus* and a few from *Alicyclobacillus*, *Geobacillus*, *Parageobacillus*, *Sulfobacillus*, and *Thermaerobacter* (Fig. 6 and Supplementary Fig. 6). Furthermore, homologs of *mpsAB* were also widespread in genomes from multiple phyla of prokaryotes (Supplementary Fig. 7). Among those which were well depicted in the phylogenetic tree are from the phyla Proteobacteria, Actinobacteria, and Bacteroidetes. *MpsAB* are highly conserved in the genus *Staphylococcus* and to a lesser extent in *Bacillus* and other Firmicutes (Supplementary Fig. 5). Apart from few exceptions in Actinobacteria and Proteobacteria, in most genomes *mpsA* and *mpsB* homologs are always adjacent. In *Acidimicrobium ferrooxidans*, a ferrous-iron-oxidizing bacterium, *mpsA* and *mpsB* homologs exist as a single fused gene (Supplementary Fig. 5).

Apart from *S. aureus*, *mpsAB* homologs were found in a few human pathogens such as *Bacillus anthracis*, *Legionella pneumophila*, and *Vibrio cholerae* (Table 1). Interestingly, all these three pathogens also carry genes encoding protein with CA domain in addition to *mpsAB* homologs. In the family of *Staphylococcaceae*, only *Macrococcus caseolyticus* JCS5402, *Staphylococcus carnosus* TM300, and *Staphylococcus pseudintermedius* ED99 do not have *mpsAB* homologs. Instead, they carry genes with CA homologs. This surprising observation also extend to a number of human pathogens; *Listeria monocytogenes*, *Streptococcus pyogenes*, *Enterococcus faecalis*, *Enterococcus faecium*, *Mycobacterium tuberculosis*, *Helicobacter pylori*, *Escherichia coli*, and *Pseudomonas aeruginosa* (Table 1). All these important pathogens have CA homologs instead of *mpsAB* homologs, emphasizing the importance of bicarbonate/CO₂ supply to the microorganisms.

Discussion

Despite an almost 50-year-old observation of CO₂-dependent *S. aureus* growth, little is known about the genetic basis of *S. aureus* regarding its response to changes in CO₂ availability. In the present work, we demonstrate that the growth defect of the Δ *mpsABC* mutant under atmospheric CO₂ levels could be largely rescued by 5% CO₂ (Fig. 2a) or by ≥ 50 mM bicarbonate (Fig. 2b). Uptake studies with radiolabeled NaH¹⁴CO₃ indicates that *MpsABC* contributed to a significant accumulation of H¹⁴CO₃[–] in the cytoplasm of the WT strain (Fig. 3a). The bicarbonate uptake experiment is tricky because we had to prevent CO₂ evaporation as much as possible. This is most likely the reason why we observed increased variations after 5 min. However, one should consider that for substrate uptake, the first 2 min are crucial. During this time range, the standard error mean (SEM) values were really small. We assume that the addition of fluorocitrate was probably not inhibiting the TCA cycle completely; we do not dare to increase the concentration any higher because of the side effects it may cause (we used 10 mM fluorocitrate and the normal concentration used for aconitase enzyme assay is 100 μ M).

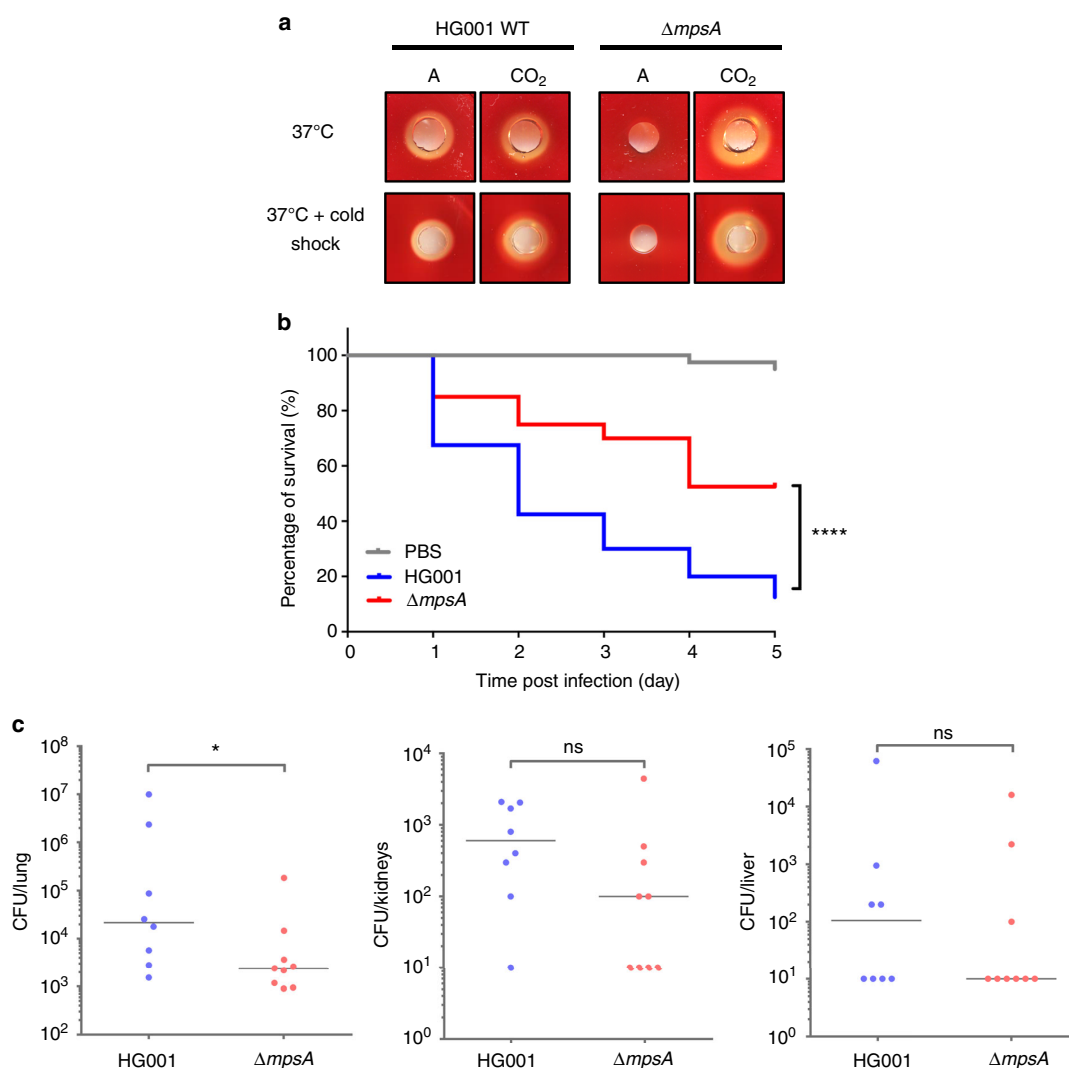


Fig. 5 Δ mpsA produces less hemolytic toxin in atmospheric conditions and is less virulent in animal infection models. **a** Hemolytic toxin production in HG001 and Δ mpsA grown in atmospheric (left) and 5% CO₂ (right) at 37 °C after overnight incubation (above) and after cold shock treatment (below). **b** Kaplan–Meier plot of the survival of *Galleria mellonella* larvae infected with HG001 and Δ mpsA. Larvae injected with PBS were used as control. Larvae infected with Δ mpsA showed significantly better survival rate compared with the larvae infected with wild-type HG001; **** p < 0.0001 as determined by Log-rank (Mantel–Cox) test. Results are representative of four independent experiments. **c** Comparison of wild-type HG001 and Δ mpsA in a 48 h intranasal mouse infection model (pneumonia model) in the lung, kidneys, and liver. The bacterial burden of Δ mpsA in the lung was significantly lower (* p = 0.036) compared with HG001. There was no significant difference (ns) in bacterial burden in the kidney and liver between the two strains. The number of bacteria per organ based on determination of CFU in n = 8 (WT HG001) and n = 9 mice (Δ mpsA) is shown. The vertical line indicates the median. The detection limit was 10 CFU per organ. Data were analyzed using two-tailed Mann–Whitney test. Source data are provided as a Source Data file

Deletion of the *mpsC* gene showed no phenotypic alterations or growth defect, suggesting it is not a functional part of the *mpsAB* operon. Furthermore, the *E. coli* CA mutant could be complemented with only *mpsAB*, and the gene synteny revealed that *mpsC* is not collocated with *mpsAB* homologs in other bacteria than staphylococci. Taken together, these observations speak in favor of MpsAB representing a bicarbonate or DIC transporter with the ability to accumulate intracellular DIC.

CAs are Zn²⁺ metalloenzymes, which catalyze the reversible hydration of CO₂ (CO₂ + H₂O ↔ HCO₃⁻ + H⁺). For this reason, we hypothesized that a CA mutant in *E. coli* (EDCM636)

could be complemented by *mpsAB*. The *E. coli can* gene encodes a β -class CA, which is essential under atmospheric but not at 5% CO₂¹⁸. As expected, the *E. coli can* mutant could be complemented by *mpsAB* and vice versa; the *S. aureus mpsABC* mutant could be complemented by *E. coli* specific *can* (Fig. 4). Due to the mutual complementation, we thought that MpsB, MpsAB, or MpsABC might have CA activity. Unfortunately, we were unable to detect CA activity using purified proteins or with whole cell extracts. The absence of CA activity in MpsAB suggests that MpsAB and CA have different enzymatic mechanisms, yet they serve the same function; namely, preventing evaporation of

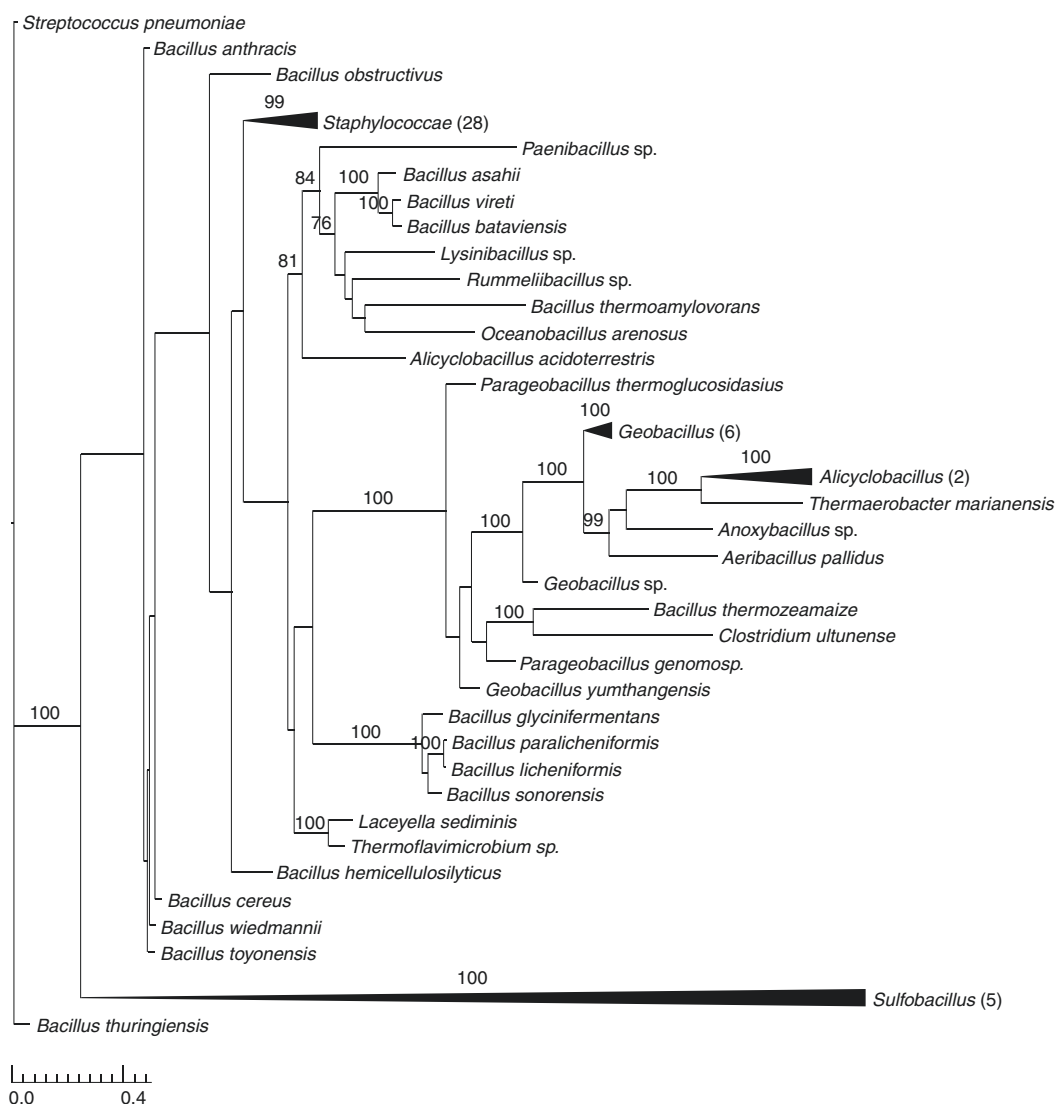


Fig. 6 *mpsAB* homologs are widespread in the *Firmicutes* phylum. Maximum likelihood phylogenetic analysis of concatenated alignments of *mpsA* and *mpsB* homologs amongst the phylum *Firmicutes*. Node support is indicated by bootstrap values from 100 resamplings of the alignment when they exceeded 70%. Collapsed clades are labeled by the genus of associated taxa. The number of taxa belonging to the respective clade is indicated in brackets. Source data are provided as a Source Data file

CO₂ by trapping it as bicarbonate for anaerobic metabolism. Although a considerable amount of CO₂ is produced by a functional TCA cycle, this CO₂ will be lost in the cytoplasm due to an insufficient concentration for anaerobic reactions. To prevent this from happening, CA catalyzed the formation of bicarbonate from CO₂, which significantly delays the release of intracellular CO₂ and providing bicarbonate required for carboxylation reactions²⁰.

The observation that EDCM636 could only be complemented by both *MpsAB* suggests they function together as a transporter. This is also supported by the collocation of *mpsAB* homologs in many microorganisms across multiple phyla (Fig. 6, Supplementary Figs. 5 and 7). Furthermore, *MpsA* belongs to PFam00361²¹, which consists of a diverse family of proton-conducting membrane transporters,

including NADH:quinone oxidoreductase subunits (complex I)²². In this regard, we demonstrated that *MpsABC* constitutes a cation-translocating system, capable of Na⁺ transport similar to the observation regarding *NuoL*¹². *MpsB* on the other hand belongs to PFam10070, a family of conserved proteins in bacteria of unknown function. Based on these observations, we propose a model that *MpsAB* is a sodium bicarbonate cotransporter (NBC) as illustrated in Fig. 7. Such NBC transporters are prevalent in mammals²³, having important functions in maintaining intracellular and whole-body pH, as well as contributing to the transepithelial transport processes. The bicarbonate cotransporters are composed of 13 transmembrane domains²⁴, similar to *MpsA* which has 14. It is unknown whether mammals also require an *MpsB* homolog; although the NBC stoichiometry in *Xenopus* oocytes is 1 Na⁺: 2 HCO₃⁻, indicating a

Table 1 Distribution of MpsAB and carbonic anhydrase (CA) homologs in various species

Species	MpsAB homolog	CA homolog
<i>Staphylococcus aureus aureus</i> NCTC 8325	+	—
<i>Staphylococcus carnosus carnosus</i> TM300	—	+(a)
<i>Staphylococcus pseudintermedius</i> ED99	—	+(a)
<i>Macrococcus caseolyticus</i> JCS5402	—	+(a)
<i>Bacillus anthracis</i> delta Sterne	+	+(a)
<i>Bacillus subtilis subtilis</i> 168	+	+(a)
<i>Listeria monocytogenes</i> R479a	+	+(b)
<i>Streptococcus pneumoniae</i> R6	—	+(a)
<i>Streptococcus pyogenes</i> A20	—	+(a)
<i>Enterococcus faecalis</i> V583	—	+(b)
<i>Enterococcus faecium</i> DO	—	+(b)
<i>Mycobacterium tuberculosis</i> H37Rv	—	+++ (a)+
<i>Helicobacter pylori</i> J99	—	+(a) +(b)
<i>Escherichia coli</i> O157:H7 Sakai (EHEC)	—	+(a)
<i>Legionella pneumophila pneumophila</i> Philadelphia-1	+	+++ (a)+
<i>Pseudomonas aeruginosa</i> PAO1	—	+++ (a)
<i>Vibrio cholerae</i> sv. O1 bv. El Tor N16961	+	+(a) +(b)

Homologies were inferred based on Pfam domains search from finished bacterial genomes in Integrated Microbial Genomes & Microbiomes (IGM/G) database. MpsA, MpsB, prokaryotic type-CA, and eukaryotic-type CA belongs to Pfam00361, Pfam10070, Pfam00484, and Pfam00194, respectively. The symbol +/- indicates the presence or absence of homolog, while (a) and (b) indicates prokaryotic and eukaryotic-CA, respectively. Asterisk indicates that one of the three CAs is a gene fusion and has a probable transmembrane domain in which the N-terminal part has Pfam00916 (sulfate transporter family) and Pfam00484 in the C-terminal part

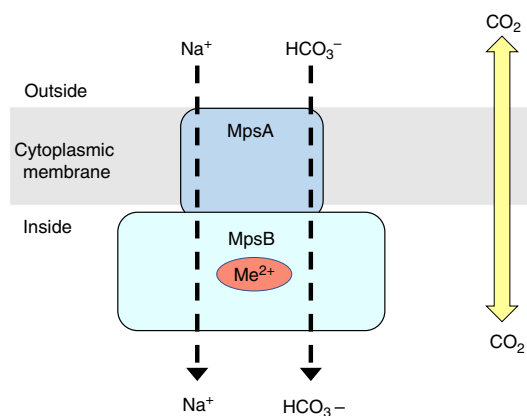


Fig. 7 Proposed function for MpsAB. We proposed that MpsAB represents a sodium bicarbonate cotransporter (NBC). These transporters are prevalent in mammals and are expressed throughout the body. Unlike CO_2 which can diffuse passively in and out of the cells, bicarbonate (HCO_3^-) needs to be transferred into the cells via a transporter. In *S. aureus*, MpsAB most likely function together as cotransporter to transport Na^+ and HCO_3^- . Me^{2+} indicates a metal binding site in MpsB

possible accessory protein interaction²⁵. As CO_2 is volatile, transporting bicarbonate or DIC helps to “trap” it in the cytoplasm for the carboxylation reactions of anaplerotic metabolism. In *Firmicutes*, these include pyruvate carboxylase fuelling the TCA cycle, acetyl-CoA-carboxylase as the first enzyme of fatty acid synthesis, or phosphoribosylaminoimidazole carboxylase involved in purine biosynthesis.

Phylogenetic analysis revealed that *mpsAB* are widespread, not only among *Firmicutes*, but also across multiple phyla (Fig. 6 and Supplementary Fig. 7). Bacteria that possess homologs of MpsAB

have diverse lifestyles; for example hyperthermophilic (e.g., *Aquifex aeolicus*), thermophilic and acidophilic (e.g., *Acidimicrobium ferrooxidans* and *Acidithiobacillus caldus*), CO_2 fixing bacteria (e.g., *Chloroflexus aurantiacus*), and nitrogen-fixing bacteria (e.g., *Bradyrhizobium oligotrophicum* and *Frankia sp.*). In addition, MpsAB homologs were also described in the gammaproteobacterial chemolithoautotroph *Thiomicrospira crunogena*¹⁵. Similar to *S. aureus*, the *T. crunogena* genes *Tcr_0853* (*mpsA* homolog) and *Tcr_0854* (*mpsB* homolog) were cotranscribed, constitute a probable DIC transporter, and its mutants required elevated DIC for growth¹⁵. Although *T. crunogena* has CO_2 concentrating mechanisms (CCMs), its DIC uptake process is unclear due to the lack of cyanobacterial transporter homologs. That being said, it is assumed that in autotrophic bacteria, a DIC concentrating system is necessary to ensure that Rubisco is saturated with CO_2 , so that carboxylation proceeds at its maximum rate.

Another problem with the “ancient” Rubisco is that it also reacts with oxygen²⁶. In this respect, the atmospheric CO_2 content in ancient times was high, while that of O_2 was low. In a CO_2 -rich environment, the CO_2 -fixing enzymes in autotrophic bacteria, such as Rubisco could work properly despite its low affinity and limited discrimination between CO_2 and O_2 . However, due to oxygenic photosynthesis in the subsequent 2.5 billion years, the atmosphere became O_2 rich and CO_2 poor²⁷. As a consequence, the cytoplasmic CO_2 levels became too low for proper CO_2 fixation and assimilation^{28,29}. Therefore, it is assumed that autotrophic bacteria that grow in atmosphere appear to uniformly have CCMs²⁷. Bacterial CCM involves two main functions: (a) active transport of inorganic carbon species (HCO_3^- and CO_2) to concentrate HCO_3^- within the cell, and (b) the pool of HCO_3^- is then utilized to provide elevated CO_2 concentrations around primary CO_2 fixing enzyme, Rubisco, encapsulated in carboxysomes which also contain CA¹⁴. Recently, DIC transporters from four evolutionary distinct families were described in several genera of sulfur-oxidizing chemolithoautotrophs¹⁶. Two of these DIC transporters demonstrate DIC uptake even though they share low protein identity with the well-characterized cyanobacterial transporters, SbtA- and SuIP-family bicarbonate transporters. SbtA is an inducible, high-affinity Na^+ -dependent HCO_3^- transporter³⁰, while BicA, a member of the SuIP family, is a low-affinity, high-flux Na^+ -dependent HCO_3^- transporter³¹. Heterologously expressed chromate ion transporter from *Hydrogenovibrio thermophilus* JR2 is also capable of DIC uptake¹⁶. The fourth type of transporter is a two component DIC transporter encoded by the genes *Tcr_0853* and *Tcr_0854* in *Hydrogenovibrio crunogenus* (previously known as *T. crunogena*) as discussed previously^{15,16}. Another well-characterized DIC transporter expressed in cyanobacteria is BCTI, encoded by the *cmpABCD* operon is an inducible, high-affinity HCO_3^- transporter belonging to the ATP binding cassette transporter family³². It is thought that these transporters differ in their affinities and mechanisms for transport (as cation symporter or anion antiporter), which provide advantages under specific growth conditions¹⁶. Out of all these distinct transporters families, MpsAB belongs to the same type as encoded by *Tcr_0853* and *Tcr_0854* from *H. crunogenus* in terms of function and homology; MpsAB is 29–30% identical to *Tcr_0853* and *Tcr_0854*. Such transporters and their function were so far not described in *Firmicutes*.

Staphylococci, like most other *Firmicutes*, are neither autotrophic nor do they possess typical carboxysome structures or Rubisco. The question is, therefore, why do they need MpsAB as a DIC concentrating system. The most rational answer would be that enzymes involved in substrate carboxylation are not sufficiently supplied with HCO_3^- under atmospheric CO_2 , thus

require a higher HCO_3^- concentration for proper activity. For example, the biotin-dependent pyruvate carboxylase has a central function in fueling the TCA cycle with oxaloacetate. If this reaction is impaired, not only the TCA cycle but also respiration and the membrane potential would be impaired. This is exactly the observed phenotype of the *mpsABC* mutant, which exhibited the typical features of SCV in atmospheric CO_2 and similar to the *S. aureus hemB* mutant^{10,12}. It is also tempting to speculate that MpsAB serve to prevent the depletion of cellular DIC, a role which is conventionally played by CA or other known cyanobacterial bicarbonate transporter. *S. aureus* has neither of them, however since CO_2 or HCO_3^- is crucial for many cellular processes, a DIC concentrating mechanism is likely to be important for its growth and survival. As a major pathogen *S. aureus* needs to adapt to different niches; as commensal inhabitant on environmentally exposed skin and mucosal surfaces to colonization and infection inside the mammalian host. Variations of CO_2 levels are one of the evident conditions it would encounter in this process, and having a DIC concentrating mechanism would ensure its sufficient supply intracellularly. Collectively, these hypotheses could explain the role of MpsAB beyond the known carbon-fixing bacteria.

Due to the interchangeable role of MpsAB and CA, we sought to compare the occurrence of both the genes in *Firmicutes*. In this phyla, there is tendency that either one of them is present; in some cases both genes are present in one strain/species, for example in *B. anthracis* and *B. subtilis* (Table 1). This same observation appears to hold true for selected species of Gram-positive and Gram-negative pathogens (Table 1). Interestingly, highly pathogenic species for example *Legionella pneumophila* and *Vibrio cholera* have MpsAB homologs as well as at least two CA homologs, while *Mycobacterium tuberculosis*, *Helicobacter pylori*, *E. coli* O157:H7, and *Pseudomonas aeruginosa* have two or even three CAs. The importance of the distribution of MpsAB and CA in the respective strains or species is not yet clear. Nevertheless, the occurrence of two and even three CA genes, and/or MpsAB suggests that DIC concentrating mechanism play an important role in fitness and pathogenicity. We assume that the decreased virulence of the *mpsA* mutant is due to the very low intracellular bicarbonate levels. Bicarbonate is the substrate for biotin carboxylase that produces carboxybiotin, the substrate for other carboxylases, such as PEP-, or pyruvate carboxylase that feed the TCA cycle. For example, the K_m value for bicarbonate of the *E. coli* biotin carboxylase is comparatively high at 16 mM³³, indicating that the enzyme has a very low affinity for bicarbonate. This suggests that a high level of intracellular bicarbonate is needed to fuel the TCA cycle, respiration, fatty acid biosynthesis, and membrane potential. ATP and membrane potential are important for toxin secretion.

The virulence attenuation of the $\Delta mpsA$ was also seen in vivo. In the *Galleria mellonella* larvae survival model, the killing rate by the mutant was significantly decreased (Fig. 5b). In the intranasal *S. aureus* mouse infection model (pneumonia model), the CFU/lung was also significantly decreased with $\Delta mpsA$ (Fig. 5c). We have chosen a lung infection model because the CO_2 content in the lung is higher and we expect that the *mpsA* mutant might have a better chance to grow. CO_2 is produced during respiration and is carried by the blood through the venous system to the lungs, where it is exhaled with a concentration of ~3.8% in the tidal air or 450 l of CO_2 per day³⁴. There was no statistically significant difference in bacterial burden in the kidney and liver between HG001 and the *mpsA* mutant. This can be explained that the lung was the primary organ that was infected with *S. aureus*. From there, *S. aureus* spreads to other organs during the course of infection. Spreading is a complex process as the bacteria have several barriers to pass: first the lung epithelium and endothelium

of blood vessels, and then again the endothelium of blood vessels to establish infections in other organs. Thus, infection burden in kidneys and liver was lower than in the lung, as it has also been observed by Lee et al.³⁵.

In conclusion, we propose that MpsAB constitutes a DIC transporter that is important for growth of *S. aureus* under low, atmospheric CO_2 conditions. This transporter system underlies the importance of CO_2 /bicarbonate in the fitness and pathogenicity of *S. aureus* and may help shed some light on earlier observations about CO_2 -dependent variants. Furthermore, *mpsAB* homologs are widespread in diverse groups of microorganisms that adopt different lifestyles and occupy a wide range of niches. In contrast to the dogma of DIC transporters, MpsAB plays an important function even in non-autotrophic bacteria by concentrating bicarbonate for anaplerotic pathways that are relevant across most microorganisms. An interesting finding in our study was that MpsAB and CA could functionally replace one another in our mutual complementation experiments, further supporting the essentiality of bicarbonate. Within this context, a number of the pathogenic species have either MpsAB or CA, whereas both are present in some of these species, suggesting their roles in growth and virulence.

Methods

Bacterial strains and growth conditions. The strains used in this study are listed in Supplementary Table 1. For cloning procedures, all staphylococcal and *E. coli* strains were cultivated at 37 °C with shaking at 150 rpm in basic medium (BM) (1% soy peptone, 0.5% yeast extract, 0.5% NaCl, 0.1% glucose, and 0.1% K_2HPO_4 , pH 7.2), unless specified otherwise. All cultures were grown in 10 ml medium using baffled 100 ml shake flasks (flask-to-medium ratio 10:1) as recommended³⁶, with the exception of growth studies, which were grown in 15 ml medium (flask-to-medium ratio 7:1). The medium was supplemented with the following antibiotics, where applicable at the indicated final concentrations: chloramphenicol at 10 $\mu\text{g ml}^{-1}$, tetracycline at 25 $\mu\text{g ml}^{-1}$, for staphylococcal strains and 100 $\mu\text{g ml}^{-1}$ ampicillin and 30 $\mu\text{g ml}^{-1}$ kanamycin for *E. coli* strains.

Growth studies of staphylococcal strains. TSB (Sigma-Aldrich) and TSA plates (Sigma-Aldrich) were used for growth studies involving *S. aureus*. For growth characterization on solid medium, *S. aureus* strains were precultured for 24 h at 37 °C under continuous shaking starting from a single colony. Cultures were then diluted to 10^{-5} – 10^{-7} and an aliquot of 100 μl was plated on TSA plates. The plates were incubated for 5 days at 37 °C under atmospheric and 5% CO_2 conditions. The 5% CO_2 level was achieved in a CO_2 incubator (Heraeus Instruments). The colony size and appearance on TSA was observed every 24 h for 5 days and documented with a Leica M125 stereomicroscope. For growth characterization in liquid medium, *S. aureus* cells were precultured in TSB as described above. *S. aureus* strains involved were WT HG001, $\Delta mpsA$, $\Delta mpsB$, $\Delta mpsC$, and $\Delta mpsABC$ that were transformed with pRB473-*mpsA*, pRB473-*mpsB*, pRB473-*mpsC*, and pRB473-*mpsABC*, respectively. Main cultures were inoculated to $\text{OD}_{578} = 0.05$ and grown under atmospheric and 5% CO_2 conditions at 37 °C under continuous shaking. Aliquots were taken at 2, 4, 6, 8, 10, 12, 24, 48, and 72 h for OD_{578} measurements.

Growth studies of $\Delta mpsABC$ with bicarbonate supplemented media. Media were supplemented with NaHCO_3 . Precultures were grown as described above. Main cultures were cultivated as described above as well, but with the addition of the supplements at final concentrations of 1, 5, 10, and 50 mM and grown under atmospheric conditions. $\Delta mpsABC$ grown under atmospheric and 5% CO_2 conditions were used as controls.

Complementation experiments of $\Delta mpsABC$ and EDCM636. With regards to *S. aureus* $\Delta mpsABC$ complemented with *can* from *E. coli*, the cultures were inoculated and were adjusted to $\text{OD}_{578} = 5$, then the strains were streaked on agar plates containing no xylose or 0.5% xylose (filter sterilized). Complementation of EDCM636 with pRB473-*mpsA*, pRB473-*mpsB*, pRB473-*mpsAB*, and pRB473-*mpsABC*, were also performed as described above, with the exception that BM and BMA were used instead of TSB and TSA.

Construction of the *S. aureus* deletion mutants. All oligonucleotides used in this study are listed in Supplementary Table 2. Nucleotide and amino acid sequences were obtained from the Kyoto Encyclopedia of Genes and Genomes (KEGG). The deletion mutants *S. aureus* HG001 $\Delta mpsB$ (KEGG accession no. SAOUHSC_00413) and $\Delta mpsC$ (SAOUHSC_00414) were constructed as markerless deletions using allelic replacements as described by Bae and Schneewind³⁷.

ARTICLE

NATURE COMMUNICATIONS | <https://doi.org/10.1038/s41467-019-11547-5>

Briefly, 1 kb upstream and 1 kb downstream of *mpsB* and *mpsC*, respectively were amplified from the chromosomal DNA of *S. aureus* HG001. The fragments were assembled with linearized (BglIII restriction enzyme) plasmid pBASE6³⁸ by Gibson assembly³⁹ using Hi-Fi DNA Assembly Master Mix (New England Biolabs). The resulting plasmids were first introduced into *E. coli* DC10B⁴⁰ and then into *S. aureus* RN4220 via electroporation before transformation of *S. aureus* HG001. Deletion of the genes were confirmed by PCR and sequence analysis. For *S. aureus* HG001 Δ *mpsA* and Δ *mpsABC*, pKOR1³⁷ carrying up- and downstream flanking regions of ~2 kb each for both deletions¹² were used.

Construction of complementation vectors. Complementation of Δ *mpsB* was carried out with plasmid pCtufamp⁴¹ and Δ *mpsC* with plasmid pRB473⁴². For construction of complementation vector for *mpsB*, *mpsB* was amplified and then assembled into linearized pCtufamp plasmid (HindIII and PacI restriction enzyme) by Gibson assembly. As for construction of complementation vector for *mpsC*, the putative native promoter sequence for *mpsABC* as well as *mpsC* were amplified and then inserted into linearized pRB473 (EcoRI restriction enzyme). The putative promoter regions were determined by DNA sequence analysis. The constructed plasmids were first introduced into *E. coli* DC10B then into *S. aureus* RN4220 before being transformed into *S. aureus* HG001 Δ *mpsB* and Δ *mpsC*, respectively. For complementation of Δ *mpsA* and Δ *mpsABC*, recombinant vector plasmids pRB473-*mpsA* and pRB473-*mpsABC* from previous study¹² were isolated and the corresponding deletion mutants were transformed as described above. In addition, all constructed pRB473 derivatives were transformed into EDCM636, an *E. coli* MG1655 derivative harboring a kanamycin resistance marker replacing a deletion of the *CA* encoding gene *can*. It was purchased from *E. coli* Genetic Stock Center, Yale University. Additional complementation vectors pRB473-*mpsB* and pRB473-*mpsAB* were constructed and transformed into EDCM636, including the empty vector.

Construction of pTX30-*can*. The xylose inducible plasmid pTX30⁴³ was used for expression of *can* (KEGG accession no. b0126). Therefore, *can* was amplified from the chromosomal DNA of *E. coli* MG1655. The insert was inserted into the linearized pTX30 (BamHI and EcoRI restriction enzymes) using T4 DNA ligase (Thermo Scientific). The resulting plasmids was transformed into *S. aureus* RN4220 via electroporation before being transformed into Δ *mpsABC*.

Quantitative RT-PCR. qRT-PCR was carried out to determine the gene expression of *mpsA* in three WT *S. aureus* strains, namely HG001, USA300⁴⁴, and MW2⁴⁵ under atmospheric and 5% CO₂ conditions. All bacteria precultures were pre-cultivated in atmospheric and 5% CO₂ conditions, respectively, for 24 h. Main cultures were inoculated at an OD₅₇₈ = 0.1 for each strain and grown in its respective growth conditions for 3 hrs. Subsequently an aliquots of OD₅₇₈ = 2.0 were harvested. RNA isolation was carried out using a RNeasy Mini kit (Qiagen) according to manufacturer's instructions. The resulting RNA was treated with RQ1 RNase-Free DNase (Promega). Subsequently, the RNA was analyzed for DNA contamination using ReproFast DNA Polymerase (Genaxxon Bioscience) with no-RT control PCR. Power SYBR[®] Green RNA-to-CT[™] 1-Step Kit (Applied Biosystems) was used in AviaMx Real-Time PCR System (Agilent Technologies) with primers directed to *mpsA* using 50 ng of RNA as template in each reaction. DNA gyrase subunit B (*gyrB*) was used as housekeeping gene control. The RNA used in qRT-PCR was isolated from four independent experiments. The relative expression of *mpsA* under 5% CO₂ was normalized to its corresponding strains grown in atmospheric conditions.

Bicarbonate uptake analysis. Main cultures were inoculated to an OD₅₇₈ = 0.1 and grown until exponential growth phase for 3 h (*S. aureus* HG001) and 18 h (Δ *mpsABC*). Cells were then centrifuged and washed with 10 mM Tris buffer at pH 7. Cells were resuspended in Tris buffer and adjusted to OD₅₇₈ of 1 in a final volume of 10 ml. Fluorocitrate and glucose at a final concentration of 10 mM and 5 mM, respectively, were added to both cell suspensions before incubated at room temperature with magnetic stirring for 30 min. After that, 50 μ Ci of NaH¹⁴CO₃ (specific activity 58 mCi mmol⁻¹, Hartmann Analytic) was added. One milliliter of samples was collected at time 0 (before the addition of NaH¹⁴CO₃), 0.5, 1, 2, 4, 6, 8, 10, and 15 min. After each sample was collected, cells were immediately filtered by vacuum filtration onto membrane filters (Whatman[™] ME 25 mixed cellulose ester membrane filters 0.45 μ m) and washed with 10 ml of Tris NaCl buffer (10 mM Tris with 100 mM NaCl). The membrane filters were then placed in a vial containing 10 ml of liquid scintillation cocktail (Ultima Gold, PerkinElmer). Radioactivity retained on the membrane filters was taken as H¹⁴CO₃ uptake which was determined by ¹⁴C accumulation in cells, measured by liquid scintillation counting (LKB Wallac 1209 RackBeta liquid scintillation counter). Results were recorded as counts per minute (CPM).

Hemolysis assay. To analyze hemolytic toxin production, overnight cultures of HG001 Δ *mpsA*, Δ *mpsB*, and Δ *mpsABC* grown in 5% CO₂ were used. Each bacterial strain was adjusted to an OD₅₇₈ of 2 and streaked onto blood agar (Oxoid). In addition, to better visualize the hemolysin halo zones, cultures were grown in atmospheric (16 h for HG001 and 48 h for Δ *mpsA*) and in 5% CO₂ conditions (16 h

for both HG001 and Δ *mpsA*). An aliquot of same OD₅₇₈ was collected for each strain before being centrifuged to remove the cell pellets. The remaining supernatant was filtered and concentrated with SpeedVac. The concentrated supernatant was then dropped into blood agar. All plates were incubated at 37 °C under atmospheric and 5% CO₂ conditions respectively for 24 h before subjected to cold shock treatment for 72 h.

Galleria mellonella larvae infection model. Final-stage instar larvae of *G. mellonella* were purchased from Reptilienkosmos.de, Germany. Ten larvae weighing between 300 and 600 mg were infected with *S. aureus* HG001 and Δ *mpsA*, respectively. Bacteria were grown in TSB at 37 °C with shaking for 24 h (HG001) and 48 h (Δ *mpsA*). Cells were washed twice and resuspended in Dulbecco's Phosphate-Buffered Saline (DPBS) (Gibco[™]) before being adjusted to an OD₅₇₈, which corresponds to 5 × 10⁸ colony-forming unit (CFU) for each strain. Each larva was injected with 5 × 10⁶ cells. Larvae injected with DPBS served as control group. The larvae were incubated at 37 °C for 5 days after infection and surviving larvae were counted every day starting from 24 h after infection. The experiments were replicated four times. Data collected from each independent experiment were pooled for statistical analysis, resulting in *n* = 40 for every strain.

Membrane potential measurement. Main cultures were grown to exponential growth phase for HG001 (3 h in atmospheric and 5% CO₂, respectively) and also for Δ *mpsABC* (18 h in atmospheric and 3 h in 5% CO₂ conditions). Cells were washed once in phosphate-buffered saline (PBS) before adjusted to an OD₅₇₈ of 0.4. Membrane potential was determined using BacLight bacterial membrane potential kit (Invitrogen) according to the manufacturer's protocol. Briefly, 10 μ l of the dye 3,3'-diethyloxycarbocyanine iodide (DiOC2[3]) was added to the bacterial suspension samples and incubated for 30 min. Then, 200 μ l of the stained or unstained sample was applied to a black, flat-bottomed 96-well plate to determine the red and green fluorescence intensity using a microplate reader (Tecan Infinite M200). Excitation and emission wavelengths were chosen as recommended by the kit's protocol. The fluorescence intensities of wild-type HG001 grown in atmospheric was set equal to 100%.

Mouse infection experiments. Overnight cultures of HG001 and Δ *mpsA* in Brain Heart Infusion Broth (BHI) medium were diluted to a final OD₆₀₀ of 0.05 in 50 ml fresh BHI medium and grown until exponential growth phase (3.5 h for HG001 and 6 h for Δ *mpsA*) at 37 °C with 5% CO₂. After centrifugation, the cell pellet was resuspended in BHI with 20% glycerol, aliquoted and stored at -80 °C. For the generation of in vivo infection, aliquots were thawed and washed twice with PBS. The infectious dose used for infection was very similar for both strains (2.1 × 10⁸ CFU/HG001 and 1.7 × 10⁸ CFU/ Δ *mpsA* in 20 μ l). A sample of the infection inoculum was plated on TSB agar plates in order to control the infection dose. For the intranasal *S. aureus* infection model (pneumonia model) we used female Balb/c mice (8 or 9 per group, 6 weeks, Janvier Labs, Le Genest-Saint-Isle, France). They were intranasally infected with 2.1 × 10⁸ CFU of HG001 and with 1.7 × 10⁸ CFU of Δ *mpsA*. During infection, mice were scored twice a day and the severity of infection was determined accordingly to recognize if humane endpoint was reached. After 48 h of infection, mice were sacrificed, the lungs, kidneys, and livers recovered, homogenized and plated in serial dilutions on TSB agar plates incubated overnight at 37 °C with 5% CO₂ in order to determine the bacterial burden. Significant difference in the CFU counts in the organs between the two groups was determined with Mann-Whitney test.

Ethics statement. All of the animal studies were approved by the local government of Lower Franconia, Germany (approval number 55.2-2532-2-155) and performed in strict accordance with the guidelines for animal care and experimentation of German Animal Protection Law and the DIRECTIVE 2010/63/EU of the EU. The mice were housed in individually ventilated cages under normal diet in groups of four to five throughout the experiment with ad libitum access to food and water.

Phylogenetic analysis of *mpsA* and *mpsB* homologs. Homologs of *mpsA* (YP_498998.1) and *mpsB* (YP_498999.1) from *S. aureus* were identified from the RefSeq database⁴⁶ using Microbial Protein BLAST. All searches were either conducted within the whole Bacteria domain, or restricted to the bacterial phylum Firmicutes or the bacterial genus Staphylococcus. Since several species have more than one putative homologs of *mpsA* and *mpsB*, we restricted the hits only to those protein pairs of *mpsA* and *mpsB*, whose coding sequences, extracted from the respective GenBank files, are in immediate proximity in the genome. The protein sequences of *mpsA* and *mpsB* homologs were aligned separately using Clustal Omega (version 1.2.1)⁴⁷. The multiple sequence alignments (MSAs) were subsequently concatenated into one single MSA comprising 350 taxa (Bacteria), 83 taxa (Firmicutes), and 29 (*Staphylococcus*), respectively. Phylogenetic trees were constructed using maximum likelihood (ML) analysis provided by the program RAxML (version 8.2.9)⁴⁸. The GAMMA Model of rate heterogeneity was used and all model parameters were estimated by RAxML. LG (Bacteria, *Staphylococcus*) and JTT (Firmicutes) with empirical base frequencies were determined to be the best-scoring (likelihood score) protein substitution model. Results were assessed using

100 bootstrap replicates. The best tree was visualized using TreeGraph2 (version 2.14.0–771 beta)⁴⁹.

Occurrence of MpsAB and CA homologs based on Pfam domains. The occurrence of MpsAB and CA homologs were inferred based on Pfam domains²¹ search from finished bacterial genomes in Integrated Microbial Genomes & Microbiomes (IGM/G) database⁵⁰. MpsA, MpsB, prokaryotic type-CA, and eukaryotic-type CA belongs to Pfam00361, Pfam10070, Pfam00484, and Pfam00194, respectively. Results were presented as the presence (if yes, the frequency it was found in a particular species) or absence of the respective Pfam domains.

CA assays. CA assay was performed using purified N-terminal strep-tagged MpsB protein. Two methods were used to detect CA activity, electrometric and colorimetric methods. The electrometric method refers to enzymatic assay of CA for Wilbur-Anderson Units (EC 4.2.1.1), as listed in the website of Sigma-Aldrich (document CR BIOT-MAJ-1013), based on cited references^{51–53}. One Wilbur-Anderson unit will cause the pH of a 20 mM Trizma buffer to drop from 8.3 to 6.3 per minute at 0 °C. The assay is briefly described here and the full protocol can be found on Sigma-Aldrich's website⁵⁴. Assay buffer was prepared at 20 mM using Trizma Base and purified water (Milli-Q) and the pH was adjusted to 8.3 with 2 N Sulfuric Acid. CO₂ saturated solution was used as substrate and was prepared by placing a small piece of dry ice into cold Milli-Q water for at least 30 min prior to the experiment. CA enzyme standard solution was used as control. It was prepared fresh prior to the experiment by dissolving 2 mg of CA from bovine erythrocytes lyophilized powder, ≥2000 W-A units mg⁻¹ protein (Sigma-Aldrich, Germany). Then the concentrated standard solution was diluted to 60–90 U ml⁻¹. This concentration corresponds to a reaction time between 10 and 20 s. The buffer reference standards (pH 4.7, and 10) and pH electrode to equilibrate to <3 °C before calibrating the pH meter with each of the reference buffer. All solutions and dram vials were kept cold on ice prior to use. To perform the blank reaction, 3 ml of ice cold assay buffer and 0.05 ml of ice cold purified water were pipetted into a dram vial with a micro stir bar. The temperature of the reaction mixture was checked with thermometer and proceed to the next step if the temperature was <3 °C, by placing the pH electrode in the solution, with stirring. After the pH had reached >8.5, 2 ml of ice cold CO₂ saturated solution was added. The time required for the pH to change from 8.3 to 6.3 was recorded. This step was repeated a few times and once the blank time of 65 s was reached, the experiment proceeded immediately with CA control. For control, 3 ml of ice cold assay buffer was added to the dram vial and if the temperature was <3 °C and subsequently when the pH > 8.5, 2 ml of ice cold CO₂ saturated solution was added to the reaction mixture. When the pH reached 8.4–8.5, 0.05 ml of CA standard solution was added. The time required for the pH to change from 8.3 to 6.3 was recorded. If the time is not in the 10–20 s range, a more concentrated enzyme standard must be prepared. If the blank average time (from a minimum of five blank values) was in the range of 70–100 s, the experiment could proceed with purified MpsB protein. The steps for MpsB protein were the same as control, in which 0.05 ml of MpsB was used instead of CA standard solution. The CA U ml⁻¹ is determined as:

$$\text{Units ml}^{-1} \text{ enzyme} = \frac{(T_{\text{blank average}} - T_{\text{sample average}}) / \text{df}}{(T_{\text{sample average}}) (0.05)}$$

where df = Dilution factor

T = Time (in seconds) required for the pH to change from 8.3 to 6.3 as per the Unit Definition

0.05 = Volume (in milliliter) of enzyme used

We found that this method is unreliable because of the difficulty in maintaining the temperature at <3 °C. Therefore, inconsistencies in the pH readings and subsequently the deviations in the time for the pH change from 8.3 to 6.3 resulted in inaccurate and non-reproducible readings. Therefore, we attempted another assay using colorimetric method. The colorimetric method to detect CA activity was performed according to previous studies^{20,55} with slight modifications. The assay was based on changing-pH/dye indicator method using a Tecan Infinite M200 injector system. Briefly, two reaction buffers were prepared: (a) a buffer using phenol red as indicator (200 mM), 50 mM HEPES, and 200 mM Na₂SO₄ at pH 6.5, 7, and 7.5, (b) a buffer using m-cresol purple as indicator (200 mM), 50 mM TAPS, and 200 mM Na₂SO₄ at pH 7.5 and 8.4. CO₂ saturated water was prepared by placing a small piece of dry ice in Milli-Q water for at least 30 mins prior to the experiment. Purified MpsB protein was diluted in buffers and the reaction was initiated by adding an equivalent amount of CO₂ saturated water with the Tecan injector system. The subsequent color changes of the pH-sensitive dye indicators were monitored by Tecan microplate reader every 0.2 s for 1 min at 558 nm (pH 6.5–7.5) or 578 nm (pH 7.5–8.4). All reactions were performed at room temperature (~25 °C) and in a final volume of 1 ml. The CA activities (if any) of MpsB protein and positive control CA from bovine erythrocytes lyophilized powder (Sigma-Aldrich, Germany) were measured at final concentrations of 100 and 0.1 μg ml⁻¹, respectively. A total of 50 mM Tris-HCl at corresponding pH of the buffers was used as nonenzymatic controls. Due to the nondetectable CA activity, we repeated the assay with whole cell lysate of wild-type HG001, ΔmpsB, and ΔmpsABC with and without

addition of NADH and finally with resting cell suspensions of the three strains. However, no detectable CA activity was observed.

Statistical analyses. Data are presented as mean values and SEM from at least three independent biological replicates unless specified otherwise. Data from the mouse experiment are presented as median values. Normal distributions were analyzed by Student's *t*-test. The larvae infection model was analyzed using Log-rank (Mantel-Cox) test. For the mouse infection experiments, two-tailed Mann-Whitney-test was employed to compare the difference of CFU counts in the organs between the mutant clones with the WT HG001. All statistical analyses were performed using GraphPad Prism 6.0 software. A *p* value of <0.05 was considered to be statistically significant, with *n* represents independent biological replicates.

Reporting summary. Further information on research design is available in the Nature Research Reporting Summary linked to this article.

Data availability

The source data underlying Figs. 1a, 2, 3, 5b & c, 6 and Supplementary Figs. 2, 3, 6, and 7 are provided as a Source Data file. Other data supporting the findings of this work are available within the paper and its Supplementary Information files, or from the corresponding author upon request.

Received: 9 March 2019 Accepted: 16 July 2019

Published online: 09 August 2019

References

- Gladstone, G. P., Fildes, P. & Richardson, G. M. Carbon dioxide as an essential factor in the growth of bacteria. *Br. J. Exp. Pathol.* **16**, 335–348 (1935).
- Gill, P. & Lobban, D. Carbon dioxide-dependent *Staphylococcus aureus*. *Br. Med. J.* **2**, 706 (1977).
- Slifkin, M., Merkow, L. P., Kreuzberger, S. A., Engwall, C. & Pardo, M. Characterization of CO₂ dependent microcolony variants of *Staphylococcus aureus*. *Am. J. Clin. Pathol.* **56**, 584–592 (1971).
- Wise, R. I. & Spink, W. W. The influence of antibiotics on the origin of small colonies (G variants) of *Micrococcus pyogenes* var. *aureus*. *J. Clin. Investig.* **33**, 1611–1622 (1954).
- Proctor, R. A., van Langevelde, P., Kristjansson, M., Maslow, J. N. & Arbeit, R. D. Persistent and relapsing infections associated with small-colony variants of *Staphylococcus aureus*. *Clin. Infect. Dis.* **20**, 95–102 (1995).
- Proctor, R. A. et al. Small colony variants: a pathogenic form of bacteria that facilitates persistent and recurrent infections. *Nat. Rev. Microbiol.* **4**, 295–305 (2006).
- Kahl, B. C., Becker, K. & Löffler, B. Clinical Significance and Pathogenesis of *Staphylococcal* Small Colony Variants in Persistent Infections. *Clin. Microbiol. Rev.* **29**, 401–427 (2016).
- García, L. G. et al. Intracellular forms of menadione-dependent small-colony variants of methicillin-resistant *Staphylococcus aureus* are hypersusceptible to beta-lactams in a THP-1 cell model due to cooperation between vacuolar acidic pH and oxidant species. *J. Antimicrob. Chemother.* **67**, 2873–2881 (2012).
- Kriegeskorte, A. et al. Thymidine-dependent *Staphylococcus aureus* small-colony variants Are Induced by trimethoprim-sulfamethoxazole (SXT) and have increased fitness during SXT challenge. *Antimicrob. Agents Chemother.* **59**, 7265–7272 (2015).
- von Eiff, C. et al. A site-directed *Staphylococcus aureus* *hemB* mutant is a small-colony variant which persists intracellularly. *J. Bacteriol.* **179**, 4706–4712 (1997).
- Gomez-Gonzalez, C. et al. Clinical and molecular characteristics of infections with CO₂-dependent small-colony variants of *Staphylococcus aureus*. *J. Clin. Microbiol.* **48**, 2878–2884 (2010).
- Mayer, S., Steffen, W., Steuber, J. & Götz, F. The *Staphylococcus aureus* nuoL-like protein MpsA contributes to the generation of membrane potential. *J. Bacteriol.* **197**, 794–806 (2015).
- Mathiesen, C. & Hagerhall, C. Transmembrane topology of the NuoL, M and N subunits of NADH:quinone oxidoreductase and their homologues among membrane-bound hydrogenases and bona fide antiporters. *Biochim. Biophys. Acta* **1556**, 121–132 (2002).
- Price, G. D. Inorganic carbon transporters of the cyanobacterial CO₂ concentrating mechanism. *Photosynth. Res.* **109**, 47–57 (2011).
- Mangiapià, M. et al. Proteomic and mutant analysis of the CO₂ concentrating mechanism of hydrothermal vent chemolithoautotroph *Thiomicrospira crunogena*. *J. Bacteriol.* **199**, e00871-16 (2017).
- Scott, K. M. et al. Diversity in CO₂-concentrating mechanisms among chemolithoautotrophs from the genera *Hydrogenovibrio*, *Thiomicrobacterium*,

- and *Thiomicrospira*, ubiquitous in sulfidic habitats worldwide. *Appl. Environ. Microbiol.* **85**, e02096-18 (2019).
17. Herbert, S. et al. Repair of global regulators in *Staphylococcus aureus* 8325 and comparative analysis with other clinical isolates. *Infect. Immun.* **78**, 2877–2889 (2010).
 18. Merlin, C., Masters, M., McAteer, S. & Coulson, A. Why is carbonic anhydrase essential to *Escherichia coli*? *J. Bacteriol.* **185**, 6415–6424 (2003).
 19. Fuchs, S. et al. AureoWiki The repository of the *Staphylococcus aureus* research and annotation community. *Int. J. Med. Microbiol.* **308**, 558–568 (2018).
 20. Burghout, P. et al. Carbonic anhydrase is essential for *Streptococcus pneumoniae* growth in environmental ambient air. *J. Bacteriol.* **192**, 4054–4062 (2010).
 21. El-Gebali, S. et al. The Pfam protein families database in 2019. *Nucleic Acids Res.* **47**, D427–D432 (2019).
 22. Walker, J. E. The NADH:ubiquinone oxidoreductase (complex I) of respiratory chains. *Q. Rev. Biophys.* **25**, 253–324 (1992).
 23. Boron, W. F., Chen, L. & Parker, M. D. Modular structure of sodium-coupled bicarbonate transporters. *J. Exp. Biol.* **212**, 1697–1706 (2009).
 24. Felder, R. A., Jose, P. A., Xu, P. & Gildea, J. J. The renal sodium bicarbonate cotransporter NBCe2: is it a major contributor to sodium and pH homeostasis? *Curr. Hypertens. Rep.* **18**, 71 (2016).
 25. Romero, M. F. The electrogenic Na⁺/HCO₃⁻ cotransporter, NBC. *JOP* **2**, 182–191 (2001).
 26. Raven, J. A. & Beardall, J. The ins and outs of CO₂. *J. Exp. Bot.* **67**, 1–13 (2016).
 27. Raven, J. A., Beardall, J. & Sanchez-Baracaldo, P. The possible evolution and future of CO₂-concentrating mechanisms. *J. Exp. Bot.* **68**, 3701–3716 (2017).
 28. Shih, P. M. et al. Biochemical characterization of predicted Precambrian RubisCO. *Nat. Commun.* **7**, 10382 (2016).
 29. Tabita, F. R., Hanson, T. E., Satagopan, S., Witte, B. H. & Kree, N. E. Phylogenetic and evolutionary relationships of RubisCO and the RubisCO-like proteins and the functional lessons provided by diverse molecular forms. *Philos. Trans. R. Soc. Lond. B Biol. Sci.* **363**, 2629–2640 (2008).
 30. Shibata, M. et al. Genes essential to sodium-dependent bicarbonate transport in cyanobacteria: function and phylogenetic analysis. *J. Biol. Chem.* **277**, 18658–18664 (2002).
 31. Price, G. D., Woodger, F. J., Badger, M. R., Howitt, S. M. & Tucker, L. Identification of a SulP-type bicarbonate transporter in marine cyanobacteria. *Proc. Natl. Acad. Sci. USA* **101**, 18228–18233 (2004).
 32. Omata, T. et al. Identification of an ATP-binding cassette transporter involved in bicarbonate uptake in the cyanobacterium *Synechococcus* sp. strain PCC 7942. *Proc. Natl. Acad. Sci. USA* **96**, 13571–13576 (1999).
 33. Chou, C. Y., Yu, L. P. & Tong, L. Crystal structure of biotin carboxylase in complex with substrates and implications for its catalytic mechanism. *J. Biol. Chem.* **284**, 11690–11697 (2009).
 34. Cherniack, N. S. & Longobardo, G. S. Oxygen and carbon dioxide gas stores of the body. *Physiol. Rev.* **50**, 196–243 (1970).
 35. Lee, M. H. et al. A postinfluenza model of *Staphylococcus aureus* pneumonia. *J. Infect. Dis.* **201**, 508–515 (2010).
 36. Somerville, G. A. & Proctor, R. A. Cultivation conditions and the diffusion of oxygen into culture media: the rationale for the flask-to-medium ratio in microbiology. *BMC Microbiol.* **13**, 9 (2013).
 37. Bae, T. & Schneewind, O. Allelic replacement in *Staphylococcus aureus* with inducible counter-selection. *Plasmid* **55**, 58–63 (2005).
 38. Geiger, T. et al. The stringent response of *Staphylococcus aureus* and its impact on survival after phagocytosis through the induction of intracellular PSMs expression. *PLoS Pathog.* **8**, e1003016 (2012).
 39. Gibson, D. G. et al. Enzymatic assembly of DNA molecules up to several hundred kilobases. *Nat. Methods* **6**, 343–345 (2009).
 40. Monk I. R., Shah I. M., Xu M., Tan M. W., Foster T. J. Transforming the untransformable: application of direct transformation to manipulate genetically *Staphylococcus aureus* and *Staphylococcus epidermidis*. *MBio* **3**, e00277-11 (2012).
 41. Ebner, P. et al. Excretion of cytoplasmic proteins (ECP) in *Staphylococcus aureus*. *Mol. Microbiol.* **97**, 775–789 (2015).
 42. Brückner, R. A series of shuttle vectors for *Bacillus subtilis* and *Escherichia coli*. *Gene* **122**, 187–192 (1992).
 43. Strauss, A., Thumm, G. & Götz, F. Influence of Lif, the lysostaphin immunity factor, on acceptors of surface proteins and cell wall sorting efficiency in *Staphylococcus carnosus*. *J. Bacteriol.* **180**, 4960–4962 (1998).
 44. Diep, B. A. et al. Complete genome sequence of USA300, an epidemic clone of community-acquired methicillin-resistant *Staphylococcus aureus*. *Lancet* **367**, 731–739 (2006).
 45. Baba, T. et al. Genome and virulence determinants of high virulence community-acquired MRSA. *Lancet* **359**, 1819–1827 (2002).
 46. O’Leary, N. A. et al. Reference sequence (RefSeq) database at NCBI: current status, taxonomic expansion, and functional annotation. *Nucleic Acids Res.* **44**, D733–D745 (2016).
 47. Sievers, F. et al. Fast, scalable generation of high-quality protein multiple sequence alignments using Clustal Omega. *Mol. Syst. Biol.* **7**, 539 (2011).
 48. Stamatakis, A. RAxML version 8: a tool for phylogenetic analysis and post-analysis of large phylogenies. *Bioinformatics* **30**, 1312–1313 (2014).
 49. Stover, B. C. & Muller, K. F. TreeGraph 2: combining and visualizing evidence from different phylogenetic analyses. *BMC Bioinforma.* **11**, 7 (2010).
 50. Chen, I. A. et al. IMG/M v.5.0: an integrated data management and comparative analysis system for microbial genomes and microbiomes. *Nucleic Acids Res.* **47**, D666–D677 (2019).
 51. Tripp, B. C., Smith, K. & Ferry, J. G. Carbonic anhydrase: new insights for an ancient enzyme. *J. Biol. Chem.* **276**, 48615–48618 (2001).
 52. Wilbur, K. M. & Anderson, N. G. Electrometric and colorimetric determination of carbonic anhydrase. *J. Biol. Chem.* **176**, 147–154 (1948).
 53. Worthington, C. C. (ed.) *Worthington Enzyme Manual*. pp 57–59, (Worthington Biochemical Corporation, Freehold, NJ, 1988).
 54. Sigma Aldrich. *Enzymatic Assay of Carbonic Anhydrase for Wilbur-Anderson units (EC 4.2.1.1)*. Sigma Aldrich. <https://www.sigmaaldrich.com/technical-documents/protocols/biology/enzymatic-assay-of-carbonic-anhydrase.html>
 55. Khalifah, R. G. The carbon dioxide hydration activity of carbonic anhydrase. I. Stop-flow kinetic studies on the native human isoenzymes B and C. *J. Biol. Chem.* **246**, 2561–2573 (1971).

Acknowledgements

This work was supported by grants from the Deutsche Forschungsgemeinschaft (DFG: SFB766, TRR34). S.H.F. received a PhD fellowship from the German Academic Exchange Service (DAAD) and Graduiertenkolleg (GRK) 1708. We thank Thomas Haug for his assistance with ¹⁴C measurement. We would like to dedicate this article to the memory of Prof. Dr. Georg Peters and Prof. Dr. Olaf Schneewind, who passed away in August 2018 and May 2019, respectively. Both were wonderful colleagues whose passion and commitment to research greatly contributed to the field of microbiology, especially *S. aureus* biology.

Author contributions

F.G., P.E. and S.H.F. designed the study. S.R., P.E. and S.H.F. performed the cloning. T.H. and K.O. performed the mouse infection experiments. A.K.L., S.Z. and K.N. performed the phylogenetic and bioinformatics analyses. S.H.F. performed the rest of the experiments. F.G., S.H.F. and P.E. analyzed the data and wrote the paper.

Additional information

Supplementary Information accompanies this paper at <https://doi.org/10.1038/s41467-019-11547-5>.

Competing interests: The authors declare no competing interests.

Reprints and permission information is available online at <http://npg.nature.com/reprintsandpermissions/>

Peer review information: *Nature Communications* thanks Stephen Kidd, Greg Somerville and other anonymous reviewer(s) for their contribution to the peer review of this work.

Publisher’s note: Springer Nature remains neutral with regard to jurisdictional claims in published maps and institutional affiliations.



Open Access This article is licensed under a Creative Commons Attribution 4.0 International License, which permits use, sharing, adaptation, distribution and reproduction in any medium or format, as long as you give appropriate credit to the original author(s) and the source, provide a link to the Creative Commons license, and indicate if changes were made. The images or other third party material in this article are included in the article’s Creative Commons license, unless indicated otherwise in a credit line to the material. If material is not included in the article’s Creative Commons license and your intended use is not permitted by statutory regulation or exceeds the permitted use, you will need to obtain permission directly from the copyright holder. To view a copy of this license, visit <http://creativecommons.org/licenses/by/4.0/>.

© The Author(s) 2019

Accepted Publication 2

***Staphylococcus aureus* Lpl protein triggers human host cell invasion via activation of Hsp90 receptor.**

Tribelli PM, Luqman A, Nguyen MT, Madlung J, **Fan SH**, Macek B, Sass P, Bitschar K, Schittek B, Kretschmer D and Götz F.

Cellular Microbiology, 2019;e131111. <https://doi.org/10.1111/cmi.13111>



Received: 11 June 2019 | Revised: 2 August 2019 | Accepted: 26 August 2019

DOI: 10.1111/cmi.13111

RESEARCH ARTICLE

WILEY

Staphylococcus aureus Lpl protein triggers human host cell invasion via activation of Hsp90 receptor

Paula M. Tribelli^{1,2,3}  | Arif Luqman^{1,4} | Minh-Thu Nguyen^{1,5} | Johannes Madlung⁶ | Sook-Ha Fan¹ | Boris Macek⁶ | Peter Sass⁷ | Katharina Bitschar⁸ | Birgit Schitteck⁸ | Dorothee Kretschmer⁹ | Friedrich Götz¹ ¹ Microbial Genetics, Interfaculty Institute of Microbiology and Infection Medicine Tübingen (IMIT), University of Tübingen, Tübingen, Germany² Departamento de Química Biológica, FCEyN-UBA, Buenos Aires, Argentina³ IQUIBICEN-CONICET, Buenos Aires, Argentina⁴ Institut Teknologi Sepuluh Nopember, Biology Department, Surabaya, Indonesia⁵ Division of Microbiology, Paul-Ehrlich Institute, Langen, Germany⁶ Proteome Center Tübingen, University of Tübingen, Tübingen, Germany⁷ Microbial Bioactive Compounds, Interfaculty Institute of Microbiology and Infection Medicine Tübingen (IMIT), University of Tübingen, Tübingen, Germany⁸ Department of Dermatology, University of Tübingen, Tübingen, Germany⁹ Department of Infection Biology, Interfaculty Institute for Microbiology and Infection Medicine Tübingen (IMIT), University of Tübingen, Tübingen, Germany**Correspondence**

Friedrich Götz, Department of Microbial Genetics, University of Tübingen, Auf der Morgenstelle 28.72076 Tübingen, Germany. Email: friedrich.goetz@uni-tuebingen.de

Funding information

Alexander von Humboldt-Stiftung, Grant/Award Number: Alexander von Humboldt postdoctoral fellowship for; Consejo Nacional de Investigaciones Científicas y Técnicas, Grant/Award Number: Paula M. Tribelli Researcher from CONICET; GRK1708, Grant/Award Number: Sook-ha Fan GRK1708; German Academic Exchange Service (DAAD), Grant/Award Number: GRK1708; Deutsche Forschungsgemeinschaft, Grant/Award Numbers: SFB766 and TR156

Abstract

Staphylococcus aureus is a facultative intracellular pathogen. Recently, it has been shown that the protein part of the lipoprotein-like lipoproteins (Lpls), encoded by the *lpl* cluster comprising of 10 *lpls* paralogue genes, increases pathogenicity, delays the G2/M phase transition, and also triggers host cell invasion. Here, we show that a recombinant Lpl1 protein without the lipid moiety binds directly to the isoforms of the human heat shock proteins Hsp90 α and Hsp90 β . Synthetic peptides covering the Lpl1 sequence caused a twofold to fivefold increase of *S. aureus* invasion in HaCaT cells. Antibodies against Hsp90 decrease *S. aureus* invasion in HaCaT cells and in primary human keratinocytes. Additionally, inhibition of ATPase function of Hsp90 or silencing Hsp90 α expression by siRNA also decreased the *S. aureus* invasion in HaCaT cells. Although the Hsp90 β is constitutively expressed, the Hsp90 α isoform is heat-inducible and appears to play a major role in Lpl1 interaction. Pre-incubation of HaCaT cells at 39°C increased both the Hsp90 α expression and *S. aureus* invasion. Lpl1-Hsp90 interaction induces F-actin formation, thus, triggering an endocytosis-like internalisation. Here, we uncovered a new host cell invasion principle on the basis of Lpl-Hsp90 interaction.

Abbreviations: α -Hsp90 α , primary mouse antibody to Hsp90 α ; α -Hsp90 β , primary mouse antibody to Hsp90 β ; α -Hsp90 $\alpha\beta$, primary rabbit antibody to Hsp90 $\alpha\beta$; BSA, Bovine serum albumin; CFU, colony-forming unit; DPBS, Phosphate Buffer Saline without calcium or magnesium; F-actin, filamentous actin; Lpl, lipoprotein like protein from *Staphylococcus aureus*; MOI, multiplicity of infection; Nano-HPLC-MS/MS, Nanoscale liquid chromatography coupled to tandem mass spectrometry; Ni-NTA, nickel - nitrilotriacetic acid agarose; NPPCs, non-professional phagocytic cells; OD, optical density; USA300, *Staphylococcus aureus* USA300;

This is an open access article under the terms of the Creative Commons Attribution License, which permits use, distribution and reproduction in any medium, provided the original work is properly cited.

© 2019 The Authors. Cellular Microbiology published by John Wiley & Sons Ltd

Cellular Microbiology. 2019;e13111.
<https://doi.org/10.1111/cmi.13111>

wileyonlinelibrary.com/journal/cmi | 1 of 14

KEYWORDS

F-actin, Hsp90 receptor, invasion, Lpl, *Staphylococcus aureus*

1 | INTRODUCTION

Many bacterial pathogens trigger internalisation into non-professional phagocytes, which is crucial to virulence because this shields the pathogen from certain immune defenses, antibiotics and enables the proliferation in relatively protected niches. Although previously considered an exclusively extracellular pathogen, *Staphylococcus aureus* is now regarded as a facultative intracellular pathogen that triggers internalisation by non-professional phagocytic cells (NPPCs) such as endothelial, epithelial, and mammary cells as well as fibroblasts or osteoclasts and can persist intracellularly for various periods of time (Bayles et al., 1998; Lowy, 1998; Sinha et al., 1999). Clinical studies also indicate a possible role for an intracellular staphylococcal reservoir in recurring diseases, such as rhinosinusitis or osteomyelitis (Clement et al., 2005; Kalinka et al., 2014; Mohamed et al., 2014). *Staphylococcus aureus* can also survive for long periods inside professional phagocytes, such as macrophages (Kubica et al., 2008) and polymorphonuclear neutrophils (PMN; Voyich et al., 2005). Additionally, infected PMNs can transmit the infection to naive mice (Gresham et al., 2000). Indeed, there is evidence that phagocytes could facilitate *S. aureus* infection because bacterial cells can survive after phagosomal escape (Kozziel et al., 2009; O'Keefe et al., 2015).

Staphylococcus aureus post-invasion events in non-professional phagocytes are only partially understood. It has been shown that they are able to escape the phagosome, which is associated with the induction of cell death (Bayles et al., 1998; Esen et al., 2001; Menzies & Kourteva, 1998; Wesson et al., 1998) and intracellular persistence (Garzoni & Kelley, 2009). The phagosomal escape is triggered by phenol-soluble modulins (PSMs) (Grosz et al., 2014) and a cyclic dipeptide, phevalin, produced by a non-ribosomal peptide synthetase (NRPS) (Blättner et al., 2016; Zimmermann & Fischbach, 2010).

A prerequisite for any internalisation into NPPCs is host cell adhesion. This step mainly involves fibronectin (Fn), forming a bridge between $\alpha 5 \beta 1$ integrin on the cellular side and Fn-binding proteins on the bacteria (Fowler et al., 2000; Grundmeier et al., 2004; Sinha et al., 1999; Tran Van Nhieu & Isberg, 1993). The FnBP-Fn- $\alpha 5 \beta 1$ integrin pathway is widely acknowledged to be the main internalisation process. However, there are various so-called secondary mechanisms. These mechanisms mainly involve bacterial serine aspartate repeat-containing protein D (SdrD), clumping factor A (ClfA), serine-rich adhesin for platelets, and the major autolysin, Atl (Josse, Laurent, & Diot, 2017; Zapotoczna, Jevnikar, Miajlovic, Kos, & Foster, 2013). These proteins are microbial surface components recognising adhesive matrix molecules (MSCRAMMs) and (except for Atl) have a cell-wall anchoring sequence located in their C-terminal portion (Josse et al., 2017). For example, SdrD binds, for example, directly to Desmoglein 1 in keratinocytes, promoting adhesion (Askarian et al., 2016; Corrigan, Miajlovic, & Foster, 2009). Additionally, ClfA can

interact through fibrinogen bridges to the $\alpha V \beta 3$ integrin ($\alpha V \beta 3$) or complex bridge involving von Willebrand factor, the secreted von Willebrand factor binding protein and the $\alpha V \beta 3$ integrin that promotes adhesion in vascular endothelial cells (Claes et al., 2017; McDonnell et al., 2016). On the other hand, SraP adheres to gp340, a salivary scavenger protein, in A549 cell line (Yang et al., 2014). The major autolysin, Atl, mediates *S. aureus* internalisation via direct interactions with Hsc70 (Hirschhausen et al., 2010). It has been speculated that the various internalisation mechanisms allow the bacteria to expand their internalisation to changing environmental conditions; for example, in the absence or scarcity of Fn, they can make use of alternative binding partners to trigger invasion (Josse et al., 2017).

Recently, a certain class of lipoproteins, the so-called "lipoprotein-like lipoproteins" (Lpls) were found to induce host cell internalisation (Nguyen et al., 2015). The *lpl*-genes are clustered on a pathogenicity island called vSaa island (non-phage and non-staphylococcal cassette chromosome genomic island), which is present in all *S. aureus* strains tested so far (Diep et al., 2006; Shahmirzadi, Nguyen, & Götz, 2016). The *lpl* cluster comprises 10 *lpl* paralogous genes that encode 10 Lpl proteins with high sequence similarity and two accessory genes (Nguyen et al., 2015). When the entire *lpl* gene cluster is deleted in *S. aureus* USA300, the mutant showed a marked decrease in invasion of *S. aureus* into human primary keratinocytes and mouse skin and also showed a decreased pathogenicity in a mouse sepsis model (Nguyen et al., 2015). The Lpl lipoproteins not only trigger host cell invasion, but also delay the G2/M phase transition in HeLa cells (Nguyen et al., 2016). As the number of *lpl* genes is particularly high in epidemic *S. aureus* strains, it is assumed that the *lpl* gene cluster might contribute to increased dissemination and epidemic spreading by shielding the pathogen from the immune defence and antibiotic treatment (Nguyen et al., 2015). However, the mechanism of how Lpl proteins trigger the host cell internalisation was unknown.

Here, we identified the human heat shock protein Hsp90 as the host receptor for Lpl-induced *S. aureus* USA300 invasion of human keratinocytes using Lpl1 as a model of Lpls for in vitro experiments. The Hsp90-Lpl interaction triggers a cascade of reactions including ATPase activity and F-actin formation, indicating that the bacterial internalisation underlies an endocytosis-like process.

2 | RESULTS

2.1 | Human Hsp90 interacts with *S. aureus* Lpl1 protein in pull-down experiments

Previously, it has been shown that Lpl lipoproteins from *S. aureus* USA300 increase the internalisation into HaCaT cells, a human keratinocyte cell line and also in human primary cells (Nguyen et al.,

2015; Nguyen, Peisl, Barletta, Luqman, & Götz, 2018). As the lipid moiety is anchored in the cytoplasmic membrane, we expect that the protein part interacts with the potential host cell receptor. To capture the host cell receptor, we used Ni-NTA (nikel-nitrilotriacetic acid agarose)-bound Lpl1-his as a bait. Lpl1 from USA300 was used as our model Lpl protein. It was expressed without the lipo signal peptide and with a C-terminal His-tag in *S. aureus* SA113 (pTX30::lpl1-his) and purified by Ni-NTA affinity chromatography. Purified Lpl1-his was bound to Ni-NTA and loaded with HaCaT cell lysate. After extensive washing, the HaCaT proteins bound to Lpl1-his were eluted with 250 mM imidazole and 500 mM NaCl.

The elution fraction containing the proteins that interacted with the Lpl1-his and the control fraction (in which the cell lysate passed through Ni-NTA without bound Lpl1-his) were separated by SDS-PAGE followed by Coomassie blue staining (Figure S1a).

The most prominent band on the SDS-PAGE was Lpl1-his. There were five lower-sized protein bands that were not present in the control lane and were used for further analysis by Nano-HPLC-MS/MS. The identified HaCaT-specific proteins are listed in Table 1. We only considered HaCaT proteins that were present in the Lpl1-bound Ni-NTA but not in the control column. The most abundant proteins with the highest coverage and posterior error probability (PEP) of 0.01 or lower were the human heat shock Hsp90 alpha (Hsp90 α) and beta (Hsp90 β) proteins. Both proteins are highly homologous, sharing 94% similarity and 86% identity. Hsp90 proteins are approximately 90 kDa; however, the Lpl1-interacting proteins were about 15 kDa. This indicates that the detected Hsp90 proteins were truncated, most likely due to proteolytic degradation, although a protease inhibitor cocktail was used during the preparation of HaCaT cell lysate.

2.2 | Hsp90 α and Hsp90 β are localised to the cell surface in HaCaT cells

It has been described that both the Hsp90 α and Hsp90 β isoforms were found on the cellular surface in different cell lines and tissues (Bozza et al., 2014; Eustace et al., 2004; Suzuki & Kulkarni, 2010). Here, we confirmed that both the Hsp90 proteins were localised to

the cell surface of HaCaT cells and co-localised with FM 5-95 stained membrane via immunofluorescence analysis (Figure 1).

2.3 | Hsp90 antibodies block USA300 adherence and invasion

To further confirm the contribution of Hsp90 in Lpl-triggered invasion into HaCaT cells, we blocked Hsp90 proteins with specific antibodies in invasion assays in the presence of fetal serum to mimic *in vivo* conditions where soluble fibronectin is present. We used monoclonal antibodies specific against Hsp90 α (α -Hsp90 α) and Hsp90 β (α -Hsp90 β) and a polyclonal antibody that recognises both Hsp90 α and Hsp90 β (α -Hsp90 $\alpha\beta$). Pre-incubation of the HaCaT cells with polyclonal α -Hsp90 $\alpha\beta$ antibodies caused a decrease in the invasion of USA300 from 145.3 ± 40 CFU to 19.1 ± 8.8 CFU per 1×10^5 HaCaT cells, indicating that the antibodies caused a sevenfold decrease in invasion (Figure 2a). To further validate our results, we investigated the impact of the polyclonal α -Hsp90 $\alpha\beta$ antibodies on the internalisation of USA300 Δ lpl and its complemented mutant USA300 Δ lpl (pTX-lpl1). In USA300 Δ lpl, the entire lpl cluster was deleted (Nguyen et al., 2015). In this strain, the polyclonal α -Hsp90 $\alpha\beta$ antibodies showed no effect on invasion; however, in the lpl-complemented mutant, the invasion was decreased again (Figure 2a). As fibronectin binding protein (FnBPs)-fibronectin- α 5 β 1 integrin pathway is a key mechanism for *S. aureus* adherence and invasion into the host cells, we verified that the FnBPs expression was similar in the wild type USA300 and the Δ lpl mutant (Figure S1b).

We also investigate whether *S. aureus* adherence was affected by α -Hsp90 α monoclonal antibodies. When HaCaT cells were pre-blocked with α -Hsp90 α , *S. aureus* adherence was almost threefold decreased, from $21,960 \pm 3,721$ to $7,969 \pm 1,951$ CFU per 1×10^5 HaCaT cells ($p < 0.05$, one-way ANOVA).

The invasion frequency was normalised to the unblocked HaCaT cells, which was set at 1.0 and was used as a comparator for further experiments. Pre-incubation with monoclonal α -Hsp90 α caused a decrease in invasion from 1.0 to 0.20 ± 0.05 , whereas pre-incubation with monoclonal α -Hsp90 β caused a decrease in invasion from 1.0 to

TABLE 1 Proteins identified by Nano-HPLC-MS/MS analysis from pull-down experiments

Protein name	Gene name
Heat shock protein HSP 90-beta	HSP90AB1
Heat shock protein HSP 90-alpha	HSP90AA1
Eukaryotic initiation factor 4A-I;Eukaryotic initiation factor 4A-II	EIF4A1;EIF4A2
Tubulin beta-4B chain;Tubulin beta-4A chain	TUBB4B;TUBB4A
Tubulin alpha-1B chain;Tubulin alpha-1A chain;Tubulin alpha-3C/D chain;Tubulin alpha-3E chain	TUBA1B;TUBA1A;TUBA3C;TUBA3E;TUBA4A
Pre-mRNA-processing factor 19	PRPF19
Aldose reductase	AKR1B1
Not identified 1	
Not identified 2	
Isocitrate dehydrogenase [NADP] cytoplasmic	IDH1

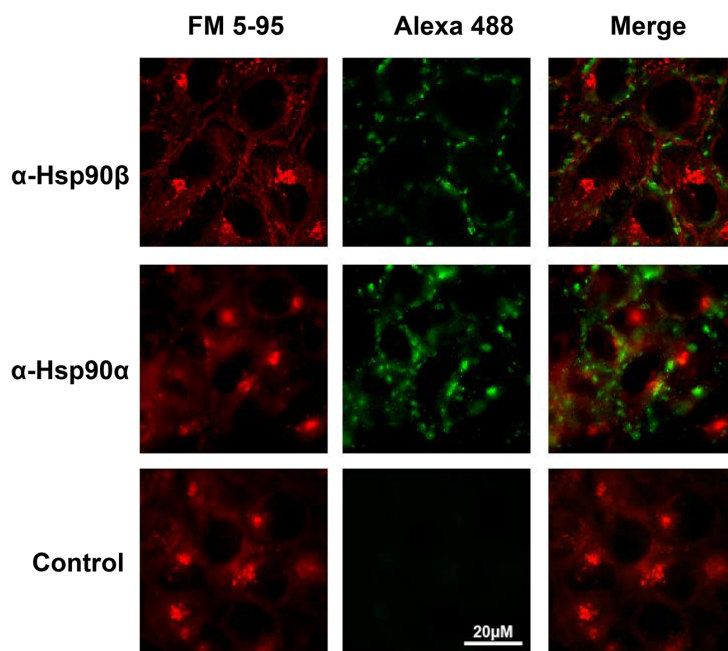


FIGURE 1 Hsp90 α and Hsp90 β are localised to the cell surface in HaCaT cells. Seeded and fixed with 4% paraformaldehyde were 1×10^5 HaCaT cells. Immunofluorescence was performed using α -Hsp90 α or α -Hsp90 β as primary antibody and α -mouse IgG-Alexafluor488 as secondary antibody. Control samples were treated the same as experimental samples but without primary antibody. FM5-95 was used as membrane stain. α -Hsp90 α : primary mouse antibody to Hsp90 α ; α -Hsp90 β : primary mouse antibody to Hsp90 β .

0.27 ± 0.08 ; in both cases, the invasion was decreased to fivefold and fourfold, respectively. As a control, we used human IgG that has no effect on internalisation (Figure 2b).

We also investigated the influence of Hsp90 proteins in human embryonic kidney 293 cell line which is untransfected by TLR2 (HEK-0). The result was similar to our earlier observation; α -Hsp90 α decreased the internalisation by fivefold (Figure S2).

Additionally, we investigated the role of Hsp90 α in USA300 invasion on primary keratinocytes by using α -Hsp90 α to block Hsp90 α . Pre-incubation with α -Hsp90 α decreased the USA300 invasion by twofold (Figure 2c).

2.4 | Geldanamycin blocks *S. aureus* invasion in HaCat cells

Geldanamycin is a well-known cell permeable anti-neoplastic compound that competes with ATP binding in Hsp90, thus inhibiting Hsp90 activity (Gorska et al., 2012). Here, we investigated whether this compound affects USA300 internalisation. Indeed, the addition of geldanamycin at a concentration of 5 μ M decreased the USA300 invasion in a dose-dependent manner by approximately threefold (Figure 2d). These results further confirm the role of Hsp90 in USA300 invasion. It should be mentioned that geldanamycin had no growth-inhibiting effect on *S. aureus* at all used concentrations.

2.5 | Silencing of Hsp90 α expression by siRNA causes a decrease of USA300 invasion

We have shown that the blocking of both Hsp90 α and Hsp90 β by antibodies caused a fourfold to fivefold decrease in invasion of *S. aureus*

cells. However, for reasons of simplicity, we focus mainly on Hsp90 α in the following experiments. Hsp90 α is a protein that is inducible by oxidative and heat stress (Prodromou, 2016; Profumo et al., 2018), and is reported to interact with envelope proteins of certain viruses and lipopolysaccharide of Gram-negative bacteria (Reyes-Del Valle, Chavez-Salinas, Medina, & Del Angel, 2005; Triantafilou, Triantafilou, & Dedrick, 2001). Silencing the Hsp90 α mRNA expression by an anti-sense RNA (siRNA) caused a decrease in invasion by approximately twofold (Figure 3a). As a control, random siRNA was used and no effect on invasion was seen (Figure 3a). The silencing of Hsp90 expression was also confirmed by Western blot analysis (Figure S3a).

2.6 | High temperature-induced expression of Hsp90 α causes an increase of USA300 invasion

Hsp90 α is an inducible heat shock protein. Its expression increases when the temperature increases, whereas the Hsp90 β isoform is constitutively expressed (Prodromou, 2016). An increased body temperature (fever) is frequent during bacterial infection. Therefore, we investigated if an increased temperature upregulates Hsp90 α expression, thus leading to an increased USA300 invasion. In order to study this, HaCaT cells were pre-incubated for 2 hr at 39°C prior to the invasion assay. The higher temperature used resulted in an almost twofold (1.86 ± 0.24) increase in invasion relative to the control at 37°C (Figure 3b). To confirm that the increased invasion was indeed due to the increased Hsp90 α expression, we blocked it with α -Hsp90 α ; as expected, it caused a decrease in invasion at 39°C (Figure 3b). The increased Hsp90 α expression at 39°C was also confirmed by Western blot analysis (Figure S3b).

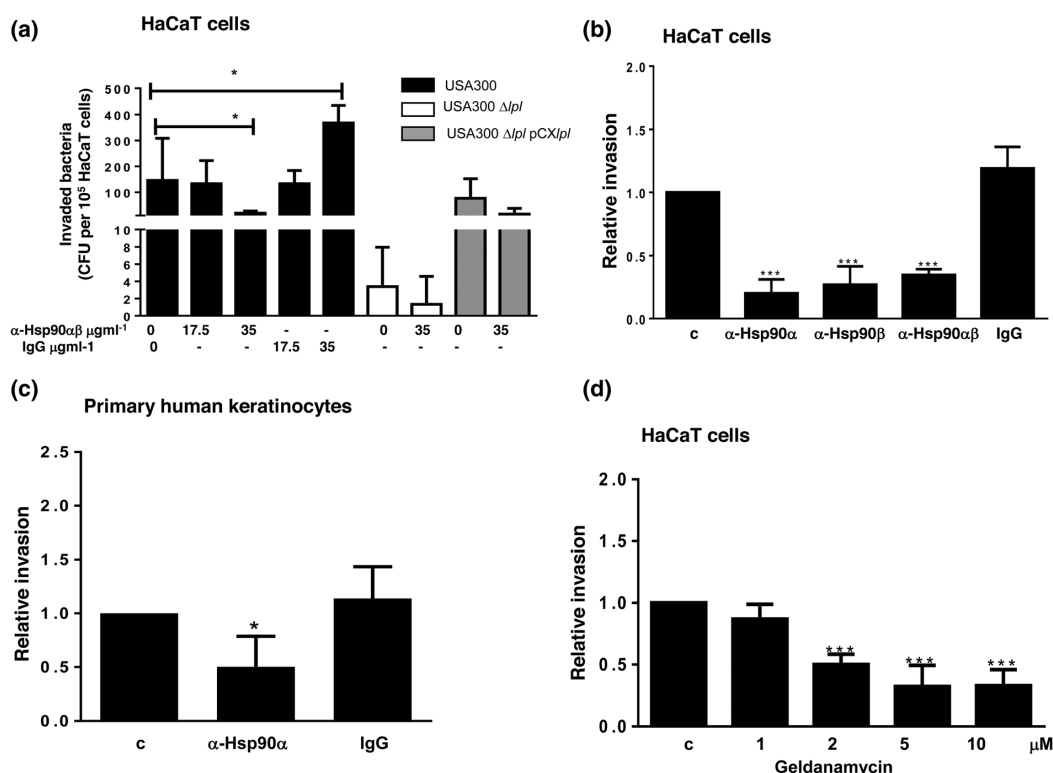


FIGURE 2 Hsp90 antibodies or inhibitors block USA300 invasion. (a) 1×10^6 HaCaT cells with or without pre-incubation during 1 hr with α -Hsp90 $\alpha\beta$ or control human IgG (IgG). Cells were further infected with *Staphylococcus aureus* USA300 strain, USA300 Δ lpl mutant strain, or USA300 Δ lpl + pTXlpl with a MOI of 30 in DMEM medium, supplemented with 10% FBS. Host cells were infected for 1.5 hr followed by lysostaphin treatment for 1.5 hr. Cells were lysed and USA300 CFU was determined by plating on TSA agar plates. The experiments were performed in at least three independent biological replicates. Error bars indicate standard deviation. The statistical was calculated by using Student *t* test; $**p < .01$; $*p < 0.05$, comparing with the control for each strain. (b) Invasion assays using *S. aureus* USA300 wild type were performed as described above but specific isoform antibodies (35 μ g ml⁻¹) were used: α -Hsp90 α , α -Hsp90 β , and human IgG (IgG) as an extra control. Relative invasion was calculated by normalising USA300 invasion in treated HaCaT cells to USA300 invasion in untreated control cells (C). The experiments were performed at least in three independent biological replicates with at least three technical replicates. Error bars indicate standard deviation. The statistical was calculated by using One-way Anova with multiple comparison to invasion in the control (C) sample, $**p < 0.01$, $*p < 0.05$. (c) Primary human keratinocytes were cultured in collagen-coated tissue flasks in epidermal keratinocyte medium. Keratinocytes were differentiated with 1.7 mM CaCl₂ in epidermal keratinocyte base medium 24 hr prior to experiments. Incubated with or without α -Hsp90 α or a control human IgG prior to USA300 invasion using a MOI of 30 were 2.5×10^5 differentiated keratinocytes. Relative invasion was calculated by normalising USA300 invasion in treated cells to USA300 invasion in cells without treatment (C). The experiments were performed using cells from three independent donors with at least three technical replicates. Error bars indicate standard deviation. The statistical was calculated using one-way ANOVA with multiple comparison with the control (C) sample, $*p < 0.05$. (d) Pretreated with different concentrations of geldanamycin during 1 hr were 1×10^6 cells. Relative invasion was calculated by normalising to invasion in control (C) cells. The experiments were performed in at least three independent biological replicates. Error bars indicate standard deviation. The statistical was calculated by using one-way ANOVA with multiple comparison with the control (C) sample, $*p < 0.05$, $**p < 0.01$, $***p < 0.001$. USA300, *S. aureus* USA300. MOI, multiplicity of infection; CFU, colony-forming unit; α -Hsp90 α , primary mouse antibody to Hsp90 α ; α -Hsp90 β , primary mouse antibody to Hsp90 β ; α -Hsp90 $\alpha\beta$, primary rabbit antibody to Hsp90 $\alpha\beta$

3 | USA300 DOES NOT ALTER Hsp90 EXPRESSION OR LOCALISATION IN HaCaT CELLS

We investigated if USA300 or Lpl1-his affected Hsp90 α expression by using Western blot analysis. Neither USA300 nor purified Lpl1-

his affected Hsp90 α expression within a period of 6 hr after the addition of USA300 (Figure S4a). In addition, we also tested whether USA300 affects Hsp90 α localisation by using flow cytometry analysis in non-permeabilized HaCaT cells. The amount of Hsp90 on HaCaT surface was similar after 1.5 hr exposure of the cells to USA300 (Figure S4b).

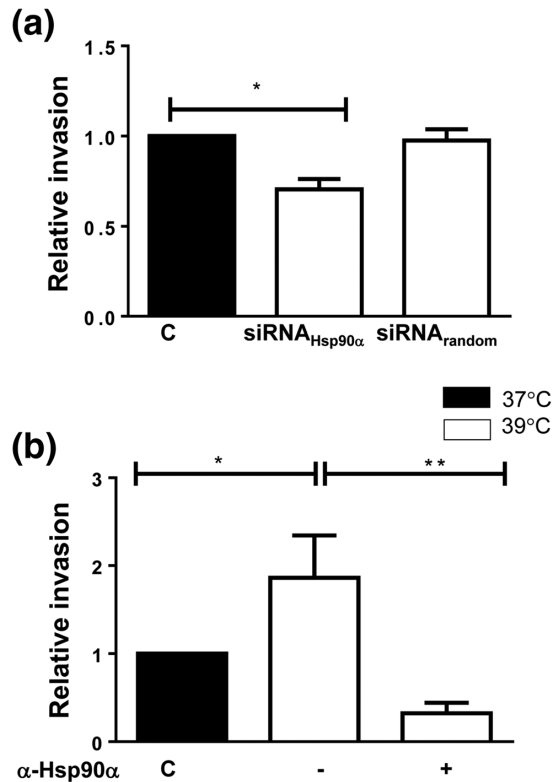


FIGURE 3 Changes in Hsp90 expression lead to modified USA300 invasion in HaCaT cells. (a) Transfected with a commercial siRNA against Hsp90α (siRNA_{Hsp90α}) were 5×10^5 HaCaT cells, a random siRNA (siRNA_{random}) with or without RNA but with lipofectamin as a control (C) sample. The cells were incubated 24 hr prior to the invasion assay. Relative invasion was calculated by normalising USA300 invasion in treated cells to the control (C) sample. (b) Pre-incubated at 39°C during 2 hr and afterwards incubated with or without α-Hsp90α ($35 \mu\text{g ml}^{-1}$) for 1 hr at 37°C before the invasion assay were 1×10^6 HaCaT cells. Control cells were incubated at only 37°C (control: C). Relative invasion was calculated by normalising USA300 invasion in temperature-treated HaCaT cells to USA300 invasion in control (C) cells. All experiments were performed at in least three independent experiments with at least three technical replicates. Error bars indicate standard deviation. The statistical was calculated using one-way ANOVA with multiple comparison with the control (C) sample, * $p < 0.05$; ** $p < 0.01$; *** $p < 0.001$. USA300, *Staphylococcus aureus* USA300; α-Hsp90α, primary mouse antibody to Hsp90α

3.1 | Lpl1-Hsp90α/β interaction boosts F-actin formation

It has been reported that the geldanamycin analogue, 17AAG, an Hsp90 Inhibitor, decreased F-actin formation upon Hsp90 inhibition (Taiyab & Rao Ch, 2011). Therefore, we investigated if actin polymerisation could be enhanced by Lpl1-his in an Hsp90-dependent manner. Indeed, F-actin formation could be enhanced by >20%, following treatment of HaCaT cells with Lpl1-his (Figure 4a). This was confirmed by the addition of α-Hsp90α, which caused a decrease of F-actin

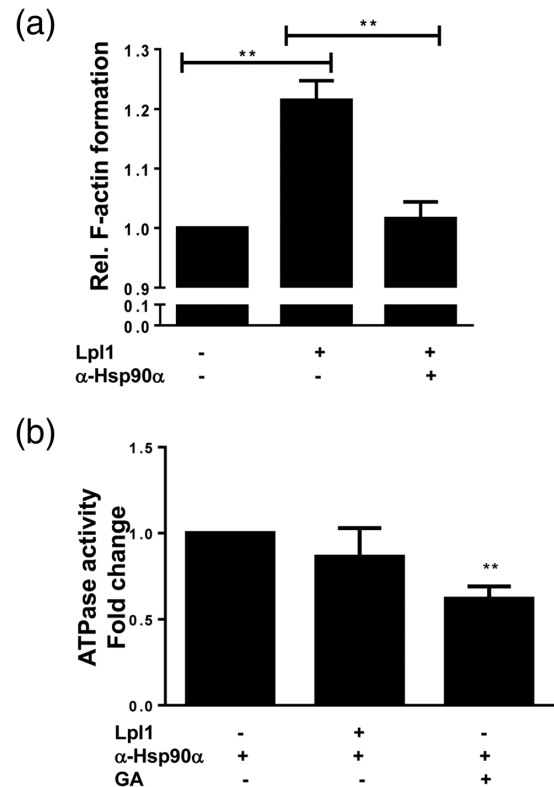


FIGURE 4 Lpl1 interaction with Hsp90α triggers F-actin formation but did not affect ATPase activity. (a) HaCaT cells were seeded into 96-well black microtiter plate for 48 hr. Cells were pre-incubated with or without α-Hsp90α antibodies for 1 hr. Afterwards, $35 \mu\text{g ml}^{-1}$ of Lpl1-his protein was added and cells were incubated during 1.5 hr. F-actin was stained with ActinGreen™ 488 ReadyProbes® (Thermo Fischer). The amount of F-actin formation in treated cells were determined by the measurement at 495 nm for the excitation and 518 nm for the emission, normalised to the untreated control. Relative F-actin formation was calculated to HaCaT cells without treatment (C). (b) ATPase activity was determined in vitro as pmol of phosphate per μg Hsp90α per minute and the ATPase activity was normalised to the control (Hsp90α assay). The experiments were performed in three independent experiments with three technical replicates. Statistical significance was calculated by using one-way ANOVA, * $p < 0.05$; ** $p < 0.01$; *** $p < 0.001$. F-actin, filamentous actin; α-Hsp90α, primary mouse antibody to Hsp90α; GA, geldanamycin

formation to the control level (Figure 4a). These results showed that Lpl1 triggers F-actin formation in an Hsp90-dependent manner.

3.2 | Lpl1-Hsp90α/β interaction has no effect on Hsp90 ATPase activity

Next, we investigated if Lpl1 would directly affect Hsp90α ATPase activity. The addition of Lpl1 to a functional Hsp90α did not significantly affect the ATPase activity, whereas the specific inhibitor

geldanamycin inhibited the ATPase activity by 46% (Figure 4b). These results showed that Lpl1 did not directly affect the ATPase activity of Hsp90.

3.3 | Lpl1-his interacts directly with purified Hsp90 α and Hsp90 β

By using far-western blot assay, we could detect interactions between Lpl1-his and purified Hsp90 α and Hsp90 β , whereas no interaction was seen when bovine serum albumin (BSA) as a control (Figure S5). In order to find out which protein domains of Lpl1 are interacting with the Hsp90 proteins, peptides covering the Lpl1 sequences were synthesised and assayed for invasion and F-actin formation (Table S1). The synthesised peptides covered almost entirely the length of Lpl1 protein. Lpl1 has a conserved “core” region near the N-terminus that shows high similarity with the other Lpl proteins (Nguyen et al., 2015). Because of this similarity, we thought that peptides from the core region might have an effect. However, it turned out that only some C-terminal localised non-core peptides affected internalisation and F-actin formation (Table S1). The peptides P2, P10, and P11 enhanced internalisation and significantly increased F-actin formation (Figure 5a-c). As a control, we showed that α -Hsp90 α blocked the stimulating effect of P10 and P11 on invasion (Figure 5a).

We also tested the interaction of Hsp90 α with the mentioned peptides that increased *S. aureus* invasion and F-actin formation using far-western blot assay. P10 and P11 were found to interact with Hsp90 α , as well as with Hsp90 β . No interaction with P2 was seen, presumably due to weak binding (Figure S4). All the other peptides that showed no effect on invasion also exhibited no detectable binding to Hsp90 α .

4 | DISCUSSION

Almost all pathogenic bacteria have developed the ability to directly invade or to trigger invasion into non-phagocytic host cells. Triggering the internalisation of pathogenic bacteria into the host cells is a survival strategy because the human body is constantly patrolled by immune cells and contains antibodies and other molecules that can target and kill the bacteria. Therefore, the environment inside the host cells provides a safe place to avoid detection by the immune system. Internalised staphylococci may induce apoptosis, autophagy, or exist freely within the cytoplasm (Mauthe et al., 2012; Menzies & Kourteva, 1998).

There are several reports describing *S. aureus* surface proteins that interact with specific receptors of the host cell. For example, fibronectin-binding proteins bind via fibronectin to α 5 β 1 integrin (Sinha et al., 2000) or human Hsp60 (Dziewanowska et al., 2000), and Atl binds to the heat shock cognate protein Hsc70 (Hirschhausen et al., 2010). However, the host cell receptor for Lpl lipoproteins was still unclear (Nguyen et al., 2015).

Here, we show that Lpl1, which served as a model Lpl-lipoprotein, interacts with the human heat shock protein Hsp90 to trigger host cell invasion in HaCaT cells and primary keratinocytes. Hsp90 (90 kDa)

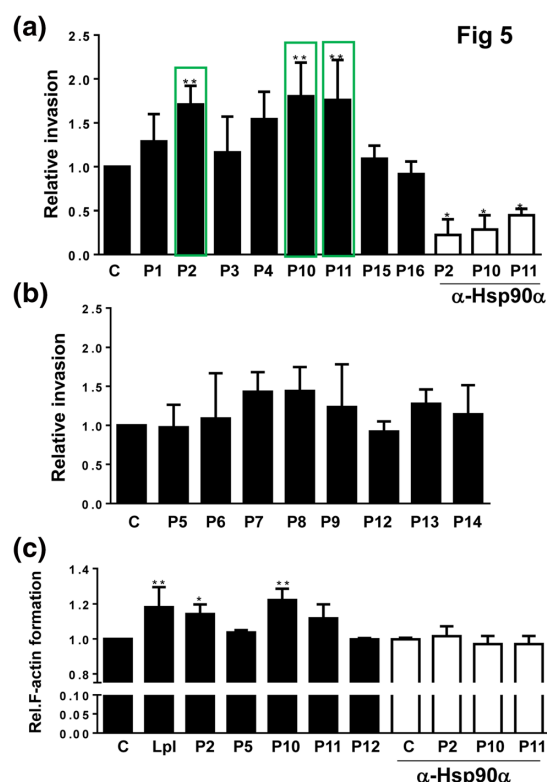


FIGURE 5 Impact of Lpl1-derived synthetic peptides on USA300 invasion and F-actin formation. (a) Pre-incubated with different peptides of 64 or 38 amino acids length ($35 \mu\text{ ml}^{-1}$, sequences in Table S1) during 1 hr prior to invasion assay using USA300 were 1×10^6 HaCaT cells. In some experiments, α -Hsp90 α was added and pre-incubated during 1 hr prior to the peptide incubation. Relative invasion was calculated by normalising USA300 invasion in HaCaT-treated cells to USA300 invasion in untreated cells (C). (b) Pre-incubated with different peptides of 15 amino acids length ($35 \mu\text{ ml}^{-1}$, sequences in Table S1) during 1 hr prior to invasion assay using USA300 were 1×10^6 HaCaT cells. Relative invasion was calculated by normalising USA300 invasion in treated HaCaT cells to USA300 invasion in untreated cells (C). (c) F-actin formation. HaCaT were pre-incubated with or without α -Hsp90 α antibodies for 1 hr. Afterwards, $35 \mu\text{ g ml}^{-1}$ of each peptide was added and cells were incubated for 1.5 hr. F-actin was stained with ActinGreenTM 488 ReadyProbes® (Thermo Fischer). The amount of F-actin formation in treated cells were determined and normalised to the untreated control (C). All the experiments were performed in at least triplicates and in three independent replications. Error bars indicate standard deviation. Statistical significance was calculated by using one-way ANOVA with multiple comparisons with the control (C). * $p < 0.05$; ** $p < 0.01$; *** $p < 0.001$. USA300, *Staphylococcus aureus* USA300; F-actin, filamentous actin; α -Hsp90 α , primary mouse antibody to Hsp90 α

proteins are expressed abundantly in a variety of cell types amounting to 2–3% of total proteins. They represent molecular chaperones and have a central role in protein homeostasis under stress conditions (Albrecht, Raue, Rosenstein, Nieselt, & Götz, 2012). At least two isoforms can be found in humans, the inducibly expressed Hsp90 α and

the constitutively expressed Hsp90 β (Zuehlke, Beebe, Neckers, & Prince, 2015).

The activities of Hsp90 proteins are diverse and not completely analysed. They are found to be membrane-bound, intracellularly, and are also as secreted form. Hsp90 α for example, is membrane-bound but can be secreted in response to tissue injury. A well-characterised function of secreted Hsp90 α is to promote cell motility, a crucial event for both wound healing and cancer (Li, Sahu, & Tsen, 2012). The anchoring of Hsp90 α and Hsp90 β to the plasma membrane involves co-localisation with heparan sulfate proteoglycans (HSPGs) on the cell surface (Snigireva, Vrublevskaia, Afanasyev, & Morenkov, 2015). Hsp90 α secretion is proposed to occur through the exosome pathway (Snigireva, Vrublevskaia, Skarga, & Morenkov, 2016). The presence of extracellular Hsp90 protein was found in normal tissues like dermal, epidermal, endothelial cells and in the nervous system development (Cheng et al., 2008; Cheng et al., 2011; Miyakoshi et al., 2017; Profumo et al., 2018; Sidera, Samiotaki, Yfanti, Panayotou, & Patsavoudi, 2004), and also during pathological processes like cancer or autoimmune diseases (Albrecht et al., 2012; Eustace et al., 2004; Tsutsumi & Neckers, 2007; Weidle, Maisel, Klostermann, Schiller, & Weiss, 2011).

Using specific antibodies against both α and β forms, we could block the invasion of *S. aureus*, suggesting that both forms can trigger invasion. However, we speculate that Hsp90 α primarily functions to facilitate Lpl-triggered invasion for the following reasons: (a) We tried to silence Hsp90 α and Hsp90 β expression by siRNA. This worked perfectly with Hsp90 α , whereas silencing of Hsp90 β expression was unsuccessful, which is in agreement with other reports (Didelot et al., 2008; Lee, Jang, & Chung, 2010). Silencing of Hsp90 α caused a significant decrease in Lpl-triggered invasion. (b) In particular, the Hsp90 α protein has been reported to interact with pathogens or defined compounds. For example, Hsp90 α serves as a receptor for dengue virus (Reyes-Del Valle et al., 2005), adhesin A of *Neisseria meningitidis* (Bozza et al., 2014), and is involved in the uptake of diphtheria toxin in host cells (Schuster et al., 2017).

Expression of Hsp90 α is inducible by oxidative stress and increased temperature. Therefore, we investigated whether increased temperature such as 39°C affects invasion. Interestingly, pretreatment of HaCaT cells at 39°C prior to the invasion assay led to an almost twofold increase in invasion relative to the control at 37°C. This suggests that fever favours *S. aureus* host cell invasion by upregulating Hsp90 α (Figure S2c). Fever is an evolutionarily conserved response that promotes T-lymphocyte trafficking through Hsp90-induced α 4 integrin activation and signalling in T cells, thus enhancing immune surveillance during infection (Lin et al., 2019). However, fever induces many factors, among them is the pyrogenic cytokine interleukin-6 (IL-6) which is involved in the mobilisation of lymphocytes to the lymphoid organs that are the staging ground for immune defence (Evans, Repasky, & Fisher, 2015). Although fever increases the migration of T-lymphocytes, some pathogens like *S. aureus* try to escape the lymphocyte killing by hiding in nonprofessional cells.

At present, we do not know which partners are involved in the Lpl-Hsp90-triggered signalling cascade. Proteins and complexes described

as potential clients of Hsp90 are growing constantly and include kinases and receptors (Miyata, Nakamoto, & Neckers, 2013). For example, it is assumed that Hsp90 interacts with the extracellular domain of the Her-2 receptor in the membrane and this interaction triggers signalling in which the cytoplasmic Hsp90 also participates in actin polymerisation (Sidera & Patsavoudi, 2008; Taiyab & Rao Ch, 2011). The Lpl-Hsp90-induced internalisation of *S. aureus* is probably on the basis of a zipper mechanism in which an intracellular signalling cascade involving the activation of adapter proteins and kinases and the formation of F-actin leading to endocytosis (Colonne, Winchell, & Voth, 2016). Thus, rapid actin polymerisation causes internalisation of the pathogen into non-phagocytic cells.

In addition, we attempted to identify the Lpl1 epitopes that trigger *S. aureus* internalisation, increased F-actin formation and displayed direct interaction with Hsp90 α . We found two overlapping peptides, which consist of 64 and 38 amino acids and both are located at the C-terminal part of Lpl1 (Figure S5). This finding is reasonable, as this part is the tip of the Lpl proteins and most likely protrudes out of the cell wall. The similarity of the two epitopes to other Lpl-proteins is around 65%.

The *lpl* gene cluster is localised on a pathogenicity island, termed vSaa. This island is predominant in *S. aureus* clonal complexes that are spreading worldwide. The key for any additional invasion mechanism lies in the increased ability of a pathogen to hide (and multiply) intracellularly in a safe environment. The internalised cells are protected not only from the host's own innate and adaptive immune response, but also from antibiotics. Interestingly, the number of tandem *lpls*' is particularly high in *S. aureus* clones that are known to spread worldwide. For example, the USA300 lineage is spreading rapidly and this lineage is distinguished by a high number of tandem *lpl* repeats (Carrel, Perencevich, & David, 2015; Tickler et al., 2017). We posit that the Lpls play a role in the rapid spreading of such lineages, as intracellular pathogens are better protected. With the identification of Hsp90 as a receptor for Lpls, we laid the basis for the development of drugs that block Hsp90 mediated invasion.

In conclusion, we propose a model (Figure 6) in which the membrane-bound *S. aureus* Lpls interact with the cell surface localised Hsp90. This interaction triggers a cascade of reactions involving ATPase in an indirect manner, given that geldanamycin blocked *S. aureus* invasion and the ATPase activity and F-actin formation are not affected by Lpl1, resulting in an endocytosis-like engulfment of bacteria.

5 | EXPERIMENTAL PROCEDURES

5.1 | Bacterial strains, antibodies, and cell lines

Bacterial strains used in this study are listed in Table S2. Bacteria were grown aerobically at 37°C in either basic medium, BM (1% soy peptone, 0.5% yeast extract, 0.5% NaCl, 0.1% glucose and 0.1% K₂HPO₄, pH 7.4) or tryptic soy broth (TSB, Sigma). When appropriate, the media was supplemented with tetracycline (25 μ g/ml, Carl Roth,

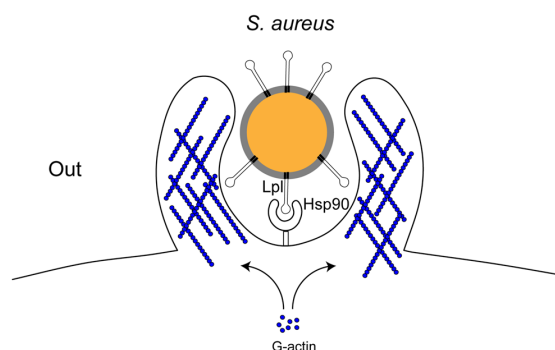


FIGURE 6 Proposed model for Hsp90 role in USA300 invasion. Lipoproteins (Lpl) in *Staphylococcus aureus* USA300 surface interact with Hsp90 molecules on the host cell surface. The portion of Lpl1 that showed interaction belongs to the C-terminal sequences. The interaction triggers F-actin formation, thus increasing USA300 invasion. G-actin, monomer of actin protein; F-actin, filamentous actin

Karlsruhe, Germany). HaCaT, a keratinocyte human cell line, was obtained from the Department of Dermatology at the University of Tübingen and cultured in Dulbecco's Modified Eagle Medium (DMEM) (Thermo Fisher, Waltham, MA, USA) supplemented with 10% fetal bovine serum (FBS) (BiochromAG, Berlin, Germany) and 1% penicillin-streptomycin (Thermo Fisher, Waltham, MA, USA). Cells were cultured at 37°C under 5% CO₂. Antibodies used are listed in Table S2.

5.2 | Purification of Lpl1-his

Lpl1-his (-sp) named Lpl1-his is an Lpl-1 version that lacks the lipid signal (-sp) and has a his tag at the C-terminal and was isolated from the cytoplasmic fraction of *S.aureus* SA113 (pTX30::lpl1-his (-sp)), as described previously (Nguyen et al., 2015). Briefly, clones carrying pTX30 were first cultivated in the absence of xylose until OD_{578nm} of approximately 0.5 was reached. Xylose (0.5%) was added to induce Lpl1-his expression and cultured for 4 hr. Bacterial cells were harvested and the pellet was washed with Tris buffer (20 mM Tris, 100 mM HCl, pH 8.0). Bacterial cells lysis were performed using Tris buffer containing protease inhibitor tablet (Merck, Darmstadt, Germany) and lysostaphin (30 µg/ml, Sigma-Aldrich, Germany) and incubating it at 37°C for 2 hr to disrupt the cell wall. Cytoplasmic fraction was obtained after ultracentrifugation at 235,000 × g for 45 min at 4°C. The supernatant was incubated with Ni-NTA super flow beads (Qiagen, Germany). After overnight incubation, the NTA beads were intensively washed and eluted with buffer containing 400 mM imidazole. Lpl1 was concentrated via centrifugal ultra-filter unit with a molecular mass cut-off of 10 kDa (Sartorius AG, Göttingen, Germany). The obtained protein was dialysed using D-Tube Dialyzer Maxi MWCO 6-8 kDa. (Novagen Cod) with DPBS (phosphate buffer saline without calcium or magnesium, Gibco). Finally, the Lpl1-his purification was verified by SDS-PAGE and the total protein amount was determined using a Bradford assay kit.

5.3 | Synthesis of Lpl1 derivative peptides

Lpl1 derivative peptides were designed on the basis of the sequence (Nguyen et al., 2015) and structural analysis performed with Phyre2 (Kelley, Mezulis, Yates, Wass, & Sternberg, 2015) and listed in Table S1. The peptides were synthesised by Apeptide (Shanghai, China) with a purity of >95%. The peptides solution at 1 mg/ml was prepared in water and stored at -20°C.

5.4 | Pull-down experiments

Pull-down experiments were performed as described before (Hirschhausen et al., 2010). Briefly, confluent HaCaT cells from one cell culture flask (75 cm², Greiner Bio-One) were detached, washed twice with DPBS, and then resuspended in lysis buffer (containing 30 mM Hepes, 1 mM EDTA, 14 mM NaCl, 2 mM MgCl₂, 1% Triton X-100, 1 mM DTT, and protease inhibitors). The complete cell lysis was assured by additional mechanical disruption using a 21-G needle (BD Bioscience). Next, the cell lysate was centrifuged. A 10 ml disposable column (Pierce) containing 500 µl of the Ni-NTA agarose (Qiagen) equilibrated with washing buffer (30 mM Hepes, 10 mM imidazole, 500 mM NaCl, 10 mM b-mercaptoethanol) was used. Then, 25–50 µg of Lpl1-his protein was bound to the Ni-NTA column and washed three times with three-column volumes with washing buffer. Next, 500 µl of the HaCaT cell lysate was added and the column was intensively washed with washing buffer (five washes with three-column volumes). Bound proteins were eluted with elution buffer (30 mM Hepes, 250 mM imidazole, 500 mM NaCl, 10 mM b-mercaptoethanol). The elution fraction was precipitated with Strata Clean Resin and consequently analysed by SDS-PAGE. To ensure that proteins from cell lysates do not directly interact with Ni-NTA agarose, a control was performed using the same procedure but without the addition of Lpl1-his. Next, an SDS-page gel was run and stained with Coomassie Blue reagent, and bands present in experimental samples (with Lpl1-his) and in the control (without Lpl1-his) were analysed Nano-HPLC-MS/MS analysis.

5.5 | Nano-HPLC-MS/MS analysis

Nano-HPLC-MS/MS was used to analyse the protein bands from the Lpl1-HaCat cells pull-down experiment. Excised protein bands were digested in-gel using trypsin. Nano-HPLC-MS/MS analysis was done on an LC-MS/MS analysis on a Proxeon Easy-nLC 1200, coupled to a LTQ Orbitrap Elite mass spectrometer with a setting of 60 min gradient and Top15 CIDMS. Data was processed using MaxQuant software suite v.1.5.2. 8 (Cox and Mann, 2008). Employing the Andromeda search engine (Cox et al., 2011), the spectra were searched against *Homo sapiens* and *S. aureus* and a database comprising the sequence of Lpl1-his. False discovery rate (FDR) was set to 1% at both the protein and peptide level and posterior error probability (PEP) was set to 0.01, or smaller, for each peptide to consider a valid identification. The most abundant proteins with high coverage and

low FDR and PEP below 0.01 were Hsp90 alpha (Hsp90 α) and beta (Hsp90 β) proteins. Both of the isoforms of Hsp90 were found in the analysed samples: alpha Hsp90 (Accession No: P_005339) and beta Hsp90 (Accession No: P_001258899) encoded by *HSP90AA1* and *HSP90AB1*, respectively.

5.6 | Invasion and adherence assays of HaCaT cells

Invasion assay was performed as described previously (Nguyen, Peisl, et al., 2018). For bacterial infection, 2.5×10^5 HaCaT cells were seeded into 24-well plates and incubated at 37°C under 5% CO₂ for 48 hr. After 48 hr, cells were washed two times with DPBS and then 1 ml DMEM supplemented with 10% FBS, but without the addition of antibiotics. Afterwards, the cells, in the presence of DMEM supplemented with 10% FBS, were incubated with different antibodies or peptides (Table S1 and Table S2) for 1 hr prior to the addition of bacteria. Before stimulation, the strains were cultured for 16 hr in TSB and washed two times with DPBS. Bacterial pellets were resuspended in DMEM/F-12 without any supplements and incubated with host cells for 1.5 hr. For detection of invaded bacteria, cells were treated with 2.5 $\mu\text{g ml}^{-1}$ lysostaphin (Sigma-Aldrich, Germany) for an additional 1.5 hr to remove extracellular bacteria. Keratinocytes were lysed with 0.1% Triton X-100, 0.5% Trypsin, and 0.3 mg ml^{-1} DNase in DPBS. Serial dilutions were performed and 10 μl of several dilutions were seeded on agar plates. Internalised bacteria were determined on the basis of the calculation of bacterial colonies grown on the agar plates. In some experiments, cells were pre-incubated for 1 hr with α -Hsp90 α , α -Hsp90 β , or α -Hsp90 $\alpha\beta$ or human IgG as a control (Table S2) in different concentrations (17.5 or 35 $\mu\text{g ml}^{-1}$).

Adherence experiments were performed in the presence of 10% FBS similar to the invasion assays but without the addition of lysostaphin. HaCaT cells were lysed and serial dilutions of the lysates were performed. Ten microliters of the dilutions were seeded on agar plates. Internalised bacteria were not considered because their contribution to adherence is very low. Adhered bacteria were determined as CFU per 10^6 HaCaT cells.

5.7 | Hsp90 α induction and siRNA experiments

For siRNA-mediated gene silencing, predesigned RNA oligonucleotide targeted against human Hsp90 α (siRNA_{Hsp90 α}) or a random siRNA negative control (Silencer™ Negative Control No. 1 siRNA, Thermo Scientific) were used. HaCaT cells of 2.5×10^6 were seeded in 24-well plates and after 24 hr, cells were transfected with 6 μl of 10 μM dsRNA oligonucleotide or without dsRNA using Lipofectamin RNAiMAX reagent according to the manufacturer's instructions (Invitrogen, Carlsbad, CA). After 24 hr, invasion assay was performed as described above. For heat shock Hsp90 α induction, 24-wells plate with 1×10^6 HaCaT cells per well was pre-incubated for 2 hr at 39°C prior to the invasion assay.

5.8 | Primary human keratinocytes invasion

Primary human keratinocytes were isolated from human foreskin after routine circumcision from the Loretto Clinic in Tübingen as previously described (Nguyen et al., 2018). Primary human keratinocytes were cultured in collagen-coated tissue flasks (Corning, BioCoat™) in epidermal keratinocyte medium (CELLnTEC) at 37°C under 5% CO₂. At 24 hr prior to experiments, keratinocytes were differentiated with 1.7 mM CaCl₂ in epidermal keratinocyte base medium (CELLnTEC). Confluent cells, approximately 2.5×10^5 cells per well, were used for USA300 invasion experiments with an MOI of 30. For blocking, cells were incubated with α -Hsp90 α or human IgG (17.5 $\mu\text{g ml}^{-1}$) for 1 hr prior to the invasion assay.

5.9 | F-Actin measurement

Seeded into black cell culture microplate (Greiner, Germany) were 2.5×10^4 HaCaT cells in 200 μl for 48 hr prior to incubation with 35 $\mu\text{g ml}^{-1}$ of Lpl1 or the derivative peptides for 1 hr. In some cases, HaCaT cells were pre-incubated with 35 $\mu\text{g ml}^{-1}$ of α -Hsp90 α antibody for 1 hr prior to the addition of Lpl1 or peptide. F-actin levels were measured as described before (Nguyen, Peisl, et al., 2018), using ActinGreen™ 488 ReadyProbes® (Thermo Fischer). The treated cells were washed with DPBS, permeabilized with 0.25% (v/v) Triton X-100, stained with the dye for 30 min and washed again with DPBS. Then, the fluorescence was measured at 495 nm for the excitation and 518 nm for the emission using Tecan Reader.

5.10 | Immunofluorescence of surface Hsp90

To detect Hsp90 α on the cellular surface, an immunofluorescence assay was carried out. Briefly, 2.5×10^5 of HaCaT cells were seeded in CellView glass bottom culture dish (Greiner, Germany) for 36 hr. Afterwards, the cells were washed three times with DPBS and fixed with paraformaldehyde 4% in DPBS at pH 7 before incubating it for 10 min at room temperature. The cells were washed again three times with DPBS and blocked with 3% of BSA (Sigma) in DPBS for 30 min at room temperature. The cells were washed and incubated overnight at 4°C with the corresponding antibodies. α -Hsp90 α or α -Hsp90 β mouse monoclonal antibodies (Table S2) used were diluted at 1:50. Cells were intensely washed and incubated with the secondary antibody donkey α -mouse IgG H&L pre-absorbed Alexa Fluor® 488 (Abcam) in a 1:450 dilution for 1 hr at room temperature. Cell membranes were stained with FM5-95 in a 1:1000 dilution for 5 min. Controls with incubation of the cells with only the secondary antibody was also performed. Cells were imaged using the Zeiss Axio Observer Z1 fluorescence microscope equipped with a C Plan-Apo 63x/1.4 Oil DIC objective (Zeiss) and an ORCA-Flash 4.0 LT camera (Hamamatsu). Images were acquired and analysed via ZEN 2.6 imaging software package (Zeiss) and Fiji software (Schindelin et al., 2012).

5.11 | Far-western blot experiments

The study of Hsp90 α or Hsp90 β binding with Lpl1-his proteins was performed by far-western blot assay according to previous study (Nguyen, Peisl, et al., 2018). Briefly, 10 μ g of Lpl1-his or BSA (as a negative control) was loaded in a polyacrylamide gel in native conditions. Proteins were transferred to a PDV nitrocellulose membrane (Bio-Rad, USA) and was blocked with 3% BSA for 1 hr. The blocked membrane was incubated with 20 μ g of recombinant Hsp90 α or Hsp90 β recombinant protein (Abcam) overnight at 4°C. For immunoblotting, monoclonal specific α -Hsp90 α or α -Hsp90 β antibodies (Abcam) were used as first antibody and goat- α -mouse IgG (Sigma, Germany) as secondary antibody. The detection of the reaction was performed with BCIP®/NBT solution (Sigma, Germany) according to the manufacturer's instructions. In the case of synthetic peptides, 2 μ g of each peptide was blotted directly to the PDV nitrocellulose membrane following the same steps described above but with 6 μ g of recombinant Hsp90 α .

For fibronectin binding proteins (FnBPs) detection, we followed the protocol described previously with modifications (Mongodin et al., 2002). Briefly, cells from *S. aureus* USA300 wild type and Δ lpl strain were lysed with lysostaphin and treated with DNase. Protein concentration was determinate using Bradford assay and 10 μ g of proteins were loaded into a polyacrylamide gel in native conditions. For immunoblotting, the steps described above were followed but the membrane was incubated with 30 μ g of fibronectin (Sigma Aldrich, Germany) overnight at 4°C. After extensive washes, the membrane was incubated with monoclonal primary antibody to human fibronectin (clone FN3, eBioscience) overnight at 4°C and with GapA polyclonal primary antibody as a loading control (Nega et al., 2015). Goat- α -mouse IgG (Sigma, Germany) as secondary antibody. The detection of the reaction was performed with BCIP®/NBT solution (Sigma, Germany) according to the manufacturer's instructions.

5.12 | Western blot experiments

Western blot experiments were performed using standard techniques. Briefly, protein concentration in the samples was determined by Bradford assay. Proteins were ran on an SDS-page and then transferred to a PDV nitrocellulose membrane and blocked with 3% BSA. The blocked membrane was incubated with α -Hsp90 α (Thermo Fisher, Table S2) or α -GDPH (Thermo Fisher, Table S2) as a loading control (Thermo Fisher) and goat- α -rabbit IgG or goat- α -mouse IgG was used as secondary antibody. Pre-stained protein ladder (Fermentas) was used as molecular weight marker.

5.13 | Flow cytometry assay (FACs)

In a MOI of 30 as described previously, 1×10^6 HaCaT cells were exposed to USA300. Cells were washed with DPBS and further incubated for 1 hr with DMEM/F-12, supplemented with lysostaphin and

2 mM of EDTA. Cells were desegregated, centrifuged, and incubated for 30 min with α -Hsp90 α in PBS and 1% fetal calf serum (FCS) in 1:100 dilution or with an isotype control (Sigma) or the secondary antibody alone as control. The cells were washed in PBS and 1% FCS and further incubated for 30 min with donkey α -mouse IgG H&L pre-absorbed Alexa Fluor® 488 (Abcam) in 1:1000 dilution. Cells were resuspended in 100 μ l of PBS, and 4% paraformaldehyde was added to a final volume of 300 μ l. Fluorescence intensity was determined with a BD FACSCalibur. We analysed 10 000 events and the data analysis was performed with FlowJo 10.

5.14 | Ethic statements

Keratinocyte isolation from human foreskin was approved by the ethics committee of the medical faculty of the University Tübingen (654/2014BO2) and performed according to the principles of the Declaration of Helsinki.

5.15 | Statistical analysis

Student's *t* tests or one-way analysis of variance (ANOVA) were employed whenever appropriate to compare the difference of means. Statistical analysis was performed by GraphPad Prism. The significance level was set as follows: *p* value > 0.05 was considered not significant (ns). In figures, significant differences are depicted as follows: **p* < 0.05; ***p* < 0.01; ****p* < 0.001; and *****p* < 0.0001.

ACKNOWLEDGEMENT

We would like thank to Mulugueta Nega for provide the Lpl1 non-related peptide. This work was supported by grants from the Deutsche Forschungsgemeinschaft (DFG: SFB766 and TR156). PMT is supported by a postdoctoral Alexander von Humboldt fellowship and by CONICET, Argentina. SHF is supported by a PhD fellowship from the German Academic Exchange Service (DAAD) and by the Graduate College GRK1708 (DFG). The funders had no role in study design, data collection and analysis or decision to publish.

COMPETING INTERESTS

The authors declare no competing financial, personal, or professional interests.

ORCID

Paula M. Tribelli  <https://orcid.org/0000-0001-9558-6275>

Friedrich Götz  <https://orcid.org/0000-0002-2042-0518>

REFERENCES

- Albrecht, T., Raue, S., Rosenstein, R., Nieselt, K., & Götz, F. (2012). Phylogeny of the staphylococcal major autolysin and its use in genus and species typing. *Journal of Bacteriology*, 194(10), 2630–2636. <https://doi.org/10.1128/JB.06609-11>
- Askarian, F., Ajayi, C., Hanssen, A. M., van Sorge, N. M., Pettersen, I., Diep, D. B., ... Johannessen, M. (2016). The interaction between

- Staphylococcus aureus* SdrD and desmoglein 1 is important for adhesion to host cells. *Scientific Reports*, 6, 22134. <https://doi.org/10.1038/srep22134>
- Bayles, K. W., Wesson, C. A., Liou, L. E., Fox, L. K., Bohach, G. A., & Trumble, W. R. (1998). Intracellular *Staphylococcus aureus* escapes the endosome and induces apoptosis in epithelial cells. *Infection and Immunity*, 66(1), 336–342.
- Blättner, S., Das, S., Paprotka, K., Eilers, U., Kruschke, M., Kretschmer, D., ... Fraunholz, M. J. (2016). *Staphylococcus aureus* exploits a non-ribosomal cyclic dipeptide to modulate survival within epithelial cells and phagocytes. *PLoS Pathogens*, 12(9), e1005857. <https://doi.org/10.1371/journal.ppat.1005857>
- Bozza, G., Capitani, M., Montanari, P., Benucci, B., Biancucci, M., Nardi-Dei, V., ... Merola, M. (2014). Role of ARF6, Rab11 and external Hsp90 in the trafficking and recycling of recombinant-soluble *Neisseria meningitidis* adhesin A (rNadA) in human epithelial cells. *PLoS ONE*, 9(10), e110047. <https://doi.org/10.1371/journal.pone.0110047>
- Carrel, M., Perencevich, E. N., & David, M. Z. (2015). USA300 Methicillin-resistant *Staphylococcus aureus*, United States, 2000–2013. *Emerging Infectious Diseases*, 21(11), 1973–1980. <https://doi.org/10.3201/eid2111.150452>
- Cheng, C. F., Fan, J., Fedesco, M., Guan, S., Li, Y., Bandyopadhyay, B., ... Li, W. (2008). Transforming growth factor alpha (TGFalpha)-stimulated secretion of HSP90alpha: using the receptor LRP-1/CD91 to promote human skin cell migration against a TGFbeta-rich environment during wound healing. *Molecular and Cellular Biology*, 28(10), 3344–3358. <https://doi.org/10.1128/MCB.01287-07>
- Cheng, C. F., Sahu, D., Tsen, F., Zhao, Z. W., Fan, J. H., Kim, R., ... Li, W. (2011). A fragment of secreted Hsp90 alpha carries properties that enable it to accelerate effectively both acute and diabetic wound healing in mice. *Journal of Clinical Investigation*, 121(11), 4348–4361. <https://doi.org/10.1172/Jci46475>
- Claes, J., Liesenborghs, L., Peetermans, M., Veloso, T. R., Missiakas, D., Schneewind, O., ... Vanassche, T. (2017). Clumping factor A, von Willebrand factor-binding protein and von Willebrand factor anchor *Staphylococcus aureus* to the vessel wall. *Journal of Thrombosis and Haemostasis*, 15(5), 1009–1019. <https://doi.org/10.1111/jth.13653>
- Clement, S., Vaudaux, P., Francois, P., Schrenzel, J., Huggler, E., Kampf, S., ... Lacroix, J. S. (2005). Evidence of an intracellular reservoir in the nasal mucosa of patients with recurrent *Staphylococcus aureus* rhinosinusitis. *The Journal of Infectious Diseases*, 192(6), 1023–1028. <https://doi.org/10.1086/432735>
- Colonne, P. M., Winchell, C. G., & Voth, D. E. (2016). Hijacking host cell highways: manipulation of the host actin cytoskeleton by obligate intracellular bacterial pathogens. *Frontiers in Cellular and Infection Microbiology*, 6, 107. <https://doi.org/10.3389/fcimb.2016.00107>
- Corrigan, R. M., Miajlovic, H., & Foster, T. J. (2009). Surface proteins that promote adherence of *Staphylococcus aureus* to human desquamated nasal epithelial cells. *BMC Microbiology*, 9, 22. <https://doi.org/10.1186/1471-2180-9-22>
- Didelot, C., Lanneau, D., Brunet, M., Bouchot, A., Cartier, J., Jacquel, A., ... Garrido, C. (2008). Interaction of heat-shock protein 90 beta isoform (HSP90 beta) with cellular inhibitor of apoptosis 1 (c-IAP1) is required for cell differentiation. *Cell Death and Differentiation*, 15(5), 859–866. <https://doi.org/10.1038/cdd.2008.5>
- Diep, B. A., Gill, S. R., Chang, R. F., Phan, T. H., Chen, J. H., Davidson, M. G., ... Perdreau-Remington, F. (2006). Complete genome sequence of USA300, an epidemic clone of community-acquired methicillin-resistant *Staphylococcus aureus*. *Lancet*, 367(9512), 731–739. [https://doi.org/10.1016/S0140-6736\(06\)68231-7](https://doi.org/10.1016/S0140-6736(06)68231-7)
- Dziewanowska, K., Carson, A. R., Patti, J. M., Deobald, C. F., Bayles, K. W., & Bohach, G. A. (2000). Staphylococcal fibronectin binding protein interacts with heat shock protein 60 and integrins: role in internalisation by epithelial cells. *Infection and Immunity*, 68(11), 6321–6328. <https://doi.org/10.1128/IAI.68.11.6321-6328.2000>
- Esen, M., Schreiner, B., Jendrossek, V., Lang, F., Fassbender, K., Grassme, H., & Gulbins, E. (2001). Mechanisms of *Staphylococcus aureus* induced apoptosis of human endothelial cells. *Apoptosis*, 6(6), 431–439. <https://doi.org/10.1023/A:1012445925628>
- Eustace, B. K., Sakurai, T., Stewart, J. K., Yimlamai, D., Unger, C., Zehetmeier, C., ... Jay, D. G. (2004). Functional proteomic screens reveal an essential extracellular role for hsp90 alpha in cancer cell invasiveness. *Nature Cell Biology*, 6(6), 507–514. <https://doi.org/10.1038/ncb1131>
- Evans, S. S., Repasky, E. A., & Fisher, D. T. (2015). Fever and the thermal regulation of immunity: The immune system feels the heat. *Nature Reviews Immunology*, 15(6), 335–349. <https://doi.org/10.1038/nri3843>
- Fowler, T., Wann, E. R., Joh, D., Johansson, S., Foster, T. J., & Hook, M. (2000). Cellular invasion by *Staphylococcus aureus* involves a fibronectin bridge between the bacterial fibronectin-binding MSCRAMMs and host cell beta1 integrins. *European Journal of Cell Biology*, 79(10), 672–679. <https://doi.org/10.1078/0171-9335-00104>
- Garzoni, C., & Kelley, W. L. (2009). *Staphylococcus aureus*: new evidence for intracellular persistence. *Trends in Microbiology*, 17(2), 59–65. <https://doi.org/10.1016/j.tim.2008.11.005>
- Gorska, M., Popowska, U., Sielicka-Dudzina, A., Kuban-Jankowska, A., Sawczuk, W., Knap, N., ... Wozniak, F. (2012). Geldanamycin and its derivatives as Hsp90 inhibitors. *Front Biosci (Landmark Ed)*, 17, 2269–2277. <https://doi.org/10.2741/4050>
- Gresham, H. D., Lowrance, J. H., Caver, T. E., Wilson, B. S., Cheung, A. L., & Lindberg, F. P. (2000). Survival of *Staphylococcus aureus* inside neutrophils contributes to infection. *Journal of Immunology*, 164(7), 3713–3722. <https://doi.org/10.4049/jimmunol.164.7.3713>
- Grosz, M., Kolter, J., Paprotka, K., Winkler, A. C., Schafer, D., Chatterjee, S. S., ... Fraunholz, M. (2014). Cytoplasmic replication of *Staphylococcus aureus* upon phagosomal escape triggered by phenol-soluble modulins. *Cellular Microbiology*, 16(4), 451–465. <https://doi.org/10.1111/cmi.12233>
- Grundmeier, M., Hussain, M., Becker, P., Heilmann, C., Peters, G., & Sinha, B. (2004). Truncation of fibronectin-binding proteins in *Staphylococcus aureus* strain Newman leads to deficient adherence and host cell invasion due to loss of the cell wall anchor function. *Infection and Immunity*, 72(12), 7155–7163. <https://doi.org/10.1128/IAI.72.12.7155-7163.2004>
- Hirschhausen, N., Schlesier, T., Schmidt, M. A., Götz, F., Peters, G., & Heilmann, C. (2010). A novel staphylococcal internalization mechanism involves the major autolysin Atl and heat shock cognate protein Hsc70 as host cell receptor. *Cellular Microbiology*, 12(12), 1746–1764. <https://doi.org/10.1111/j.1462-5822.2010.01506.x>
- Josse, J., Laurent, F., & Diot, A. (2017). Staphylococcal adhesion and host cell invasion: Fibronectin-binding and other mechanisms. *Frontiers in Microbiology*, 8, 2433. <https://doi.org/10.3389/fmicb.2017.02433>
- Kalinka, J., Hachmeister, M., Geraci, J., Sordelli, D., Hansen, U., Niemann, S., ... Tuchscherer, L. (2014). *Staphylococcus aureus* isolates from chronic osteomyelitis are characterized by high host cell invasion and intracellular adaptation, but still induce inflammation. *International Journal of Medical Microbiology*, 304(8), 1038–1049. <https://doi.org/10.1016/j.ijmm.2014.07.013>
- Kelley, L. A., Mezulis, S., Yates, C. M., Wass, M. N., & Sternberg, M. J. (2015). The Phyre2 web portal for protein modeling, prediction and

- analysis. *Nature Protocols*, 10(6), 845–858. <https://doi.org/10.1038/nprot.2015.053>
- Koziel, J., Maciag-Gudowska, A., Mikolajczyk, T., Bzowska, M., Sturdevant, D. E., Whitney, A. R., ... Potempa, J. (2009). Phagocytosis of *Staphylococcus aureus* by macrophages exerts cytoprotective effects manifested by the upregulation of antiapoptotic factors. *PLoS ONE*, 4(4), e5210. <https://doi.org/10.1371/journal.pone.0005210>
- Kubica, M., Guzik, K., Koziel, J., Zarebski, M., Richter, W., Gajkowska, B., ... Potempa, J. (2008). A potential new pathway for *Staphylococcus aureus* dissemination: The silent survival of *S. aureus* phagocytosed by human monocyte-derived macrophages. *PLoS ONE*, 3(1), e1409. <https://doi.org/10.1371/journal.pone.0001409>
- Lee, K. H., Jang, Y., & Chung, J. H. (2010). Heat shock protein 90 regulates I κ B kinase complex and NF- κ B activation in angiotensin II-induced cardiac cell hypertrophy. *Experimental & Molecular Medicine*, 42(10), 703–711. <https://doi.org/10.3858/em.2010.42.10.069>
- Li, W., Sahu, D., & Tsen, F. (2012). Secreted heat shock protein-90 (Hsp90) in wound healing and cancer. *Biochimica et Biophysica Acta*, 1823(3), 730–741. <https://doi.org/10.1016/j.bbamcr.2011.09.009>
- Lin, C., Zhang, Y., Zhang, K., Zheng, Y., Lu, L., Chang, H., ... Chen, J. (2019). Fever promotes T lymphocyte trafficking via a thermal sensory pathway involving heat shock protein 90 and alpha4 integrins. *Immunity*, 50(1), 137–151. <https://doi.org/10.1016/j.immuni.2018.11.013>
- Lowy, F. D. (1998). *Staphylococcus aureus* infections. *The New England Journal of Medicine*, 339(8), 520–532. <https://doi.org/10.1056/NEJM199808203390806>
- Mauthe, M., Yu, W., Krut, O., Kronke, M., Götz, F., Robenek, H., & Proikas-Cezanne, T. (2012). WIPI-1 positive autophagosome-like vesicles entrap pathogenic *Staphylococcus aureus* for lysosomal degradation. *Int J Cell Biol*, 2012, 179207–179213. <https://doi.org/10.1155/2012/179207>
- McDonnell, C. J., Garciarena, C. D., Watkin, R. L., McHale, T. M., McLoughlin, A., Claes, J., ... Kerrigan, S. W. (2016). Inhibition of major integrin alphaV beta3 reduces *Staphylococcus aureus* attachment to sheared human endothelial cells. *Journal of Thrombosis and Haemostasis*, 14(12), 2536–2547. <https://doi.org/10.1111/jth.13501>
- Menzies, B. E., & Kourteva, I. (1998). Internalization of *Staphylococcus aureus* by endothelial cells induces apoptosis. *Infection and Immunity*, 66(12), 5994–5998.
- Miyakoshi, L. M., Marques-Coelho, D., De Souza, L. E. R., Lima, F. R. S., Martins, V. R., Zanata, S. M., & Hedin-Pereira, C. (2017). Evidence of a cell surface role for Hsp90 complex proteins mediating neuroblast migration in the subventricular zone. *Frontiers in Cellular Neuroscience*, 11, 138. <https://doi.org/10.3389/fncel.2017.00138>
- Miyata, Y., Nakamoto, H., & Neckers, L. (2013). The therapeutic target Hsp90 and cancer hallmarks. *Current Pharmaceutical Design*, 19(3), 347–365. <https://doi.org/10.2174/138161213804143725>
- Mohamed, W., Sommer, U., Sethi, S., Domann, E., Thormann, U., Schutz, I., ... Alt, V. (2014). Intracellular proliferation of *S. aureus* in osteoblasts and effects of rifampicin and gentamicin on *S. aureus* intracellular proliferation and survival. *European Cells & Materials*, 28, 258–268. <https://doi.org/10.22203/eCM.v028a18>
- Mongodin, E., Bajolet, O., Cutrona, J., Bonnet, N., Dupuit, F., Puchelle, E., & de Bentzmann, S. (2002). Fibronectin-binding proteins of *Staphylococcus aureus* are involved in adherence to human airway epithelium. *Infection and Immunity*, 70(2), 620–630.
- Nega, M., Dube, L., Kull, M., Ziebandt, A. K., Ebner, P., Albrecht, D., ... Gotz, F. (2015). Secretome analysis revealed adaptive and non-adaptive responses of the *Staphylococcus carnosus* *femB* mutant. *Proteomics*, 15(7), 1268–1279. <https://doi.org/10.1002/pmic.201400343>
- Nguyen, M. T., Deplanche, M., Nega, M., Le Loir, Y., Peisl, L., Götz, F., & Berkova, N. (2016). *Staphylococcus aureus* Lpl lipoproteins delay G2/M phase transition in HeLa cells. *Frontiers in Cellular and Infection Microbiology*, 6, 201. <https://doi.org/10.3389/fcimb.2016.00201>
- Nguyen, M. T., Kraft, B., Yu, W., Demircioglu, D. D., Hertlein, T., Burian, M., ... Götz, F. (2015). The nuSaalpha specific lipoprotein like cluster (lpl) of *S. aureus* USA300 contributes to immune stimulation and invasion in human cells. *PLoS Pathogens*, 11(6), e1004984. <https://doi.org/10.1371/journal.ppat.1004984>
- Nguyen, M. T., Luqman, A., Bitschar, K., Hertlein, T., Dick, J., Ohlsen, K., ... Götz, F. (2018). Staphylococcal (phospho)lipases promote biofilm formation and host cell invasion. *International Journal of Medical Microbiology*, 308(6), 653–663. <https://doi.org/10.1016/j.ijmm.2017.11.013>
- Nguyen, M. T., Peisl, L., Barletta, F., Luqman, A., & Götz, F. (2018). Toll-like receptor 2 and lipoprotein-like lipoproteins enhance *Staphylococcus aureus* invasion in epithelial cells. *Infection and Immunity*, 86(8). <https://doi.org/10.1128/IAI.00343-18>
- O'Keeffe, K. M., Wilk, M. M., Leech, J. M., Murphy, A. G., Laabei, M., Monk, I. R., ... McLoughlin, R. M. (2015). Manipulation of autophagy in phagocytes facilitates *Staphylococcus aureus* bloodstream infection. *Infection and Immunity*, 83(9), 3445–3457. <https://doi.org/10.1128/IAI.00358-15>
- Prodromou, C. (2016). Mechanisms of Hsp90 regulation. *The Biochemical Journal*, 473(16), 2439–2452. <https://doi.org/10.1042/BCJ20160005>
- Profumo, E., Buttari, B., Tinaburri, L., D'Arcangelo, D., Sorice, M., Capozzi, A., ... Rigano, R. (2018). Oxidative stress induces HSP90 upregulation on the surface of primary human endothelial cells: Role of the antioxidant 7,8-Dihydroxy-4-methylcoumarin in preventing HSP90 exposure to the immune system. *Oxidative Medicine and Cellular Longevity*, 2018, 2373167–9. <https://doi.org/10.1155/2018/2373167>
- Reyes-Del Valle, J., Chavez-Salinas, S., Medina, F., & Del Angel, R. M. (2005). Heat shock protein 90 and heat shock protein 70 are components of dengue virus receptor complex in human cells. *Journal of Virology*, 79(8), 4557–4567. <https://doi.org/10.1128/JVI.79.8.4557-4567.2005>
- Schindelin, J., Arganda-Carreras, I., Frise, E., Kaynig, V., Longair, M., Pietzsch, T., ... Cardona, A. (2012). Fiji: An open-source platform for biological-image analysis. *Nature Methods*, 9(7), 676–682. <https://doi.org/10.1038/nmeth.2019>
- Schuster, M., Schnell, L., Feigl, P., Birkhofer, C., Mohr, K., Roeder, M., ... Barth, H. (2017). The Hsp90 machinery facilitates the transport of diphtheria toxin into human cells. *Scientific Reports*, 7(1), 613. <https://doi.org/10.1038/s41598-017-00780-x>
- Shahmirzadi, S. V., Nguyen, M. T., & Götz, F. (2016). Evaluation of *Staphylococcus aureus* lipoproteins: Role in nutritional acquisition and pathogenicity. *Frontiers in Microbiology*, 7, 1404. <https://doi.org/10.3389/fmicb.2016.01404>
- Sidera, K., & Patsavoudi, E. (2008). Extracellular HSP90: Conquering the cell surface. *Cell Cycle*, 7(11), 1564–1568. <https://doi.org/10.4161/cc.7.11.6054>
- Sidera, K., Samiotaki, M., Yfanti, E., Panayotou, G., & Patsavoudi, E. (2004). Involvement of cell surface HSP90 in cell migration reveals a novel role in the developing nervous system. *The Journal of Biological Chemistry*, 279(44), 45379–45388. <https://doi.org/10.1074/jbc.M405486200>
- Sinha, B., Francois, P., Que, Y. A., Hussain, M., Heilmann, C., Moreillon, P., ... Herrmann, M. (2000). Heterologously expressed *Staphylococcus aureus* fibronectin-binding proteins are sufficient for invasion of host cells. *Infection and Immunity*, 68(12), 6871–6878. <https://doi.org/10.1128/IAI.68.12.6871-6878.2000>

- Sinha, B., Francois, P. P., Nusse, O., Foti, M., Hartford, O. M., Vaudaux, P., ... Krause, K. H. (1999). Fibronectin-binding protein acts as *Staphylococcus aureus* invasin via fibronectin bridging to integrin alpha5beta1. *Cellular Microbiology*, 1(2), 101–117. <https://doi.org/10.1046/j.1462-5822.1999.00011.x>
- Snigireva, A. V., Vrublevskaia, V. V., Afanasyev, V. N., & Morenkov, O. S. (2015). Cell surface heparan sulfate proteoglycans are involved in the binding of Hsp90alpha and Hsp90beta to the cell plasma membrane. *Cell Adhesion & Migration*, 9(6), 460–468. <https://doi.org/10.1080/19336918.2015.1103421>
- Snigireva, A. V., Vrublevskaia, V. V., Skarga, Y. Y., & Morenkov, O. S. (2016). The role of membrane-bound heat shock proteins Hsp90 in migration of tumor cells in vitro and involvement of cell surface heparan sulfate proteoglycans in protein binding to plasma membrane. *Biofizika*, 61(2), 328–336.
- Suzuki, S., & Kulkarni, A. B. (2010). Extracellular heat shock protein HSP90beta secreted by MG63 osteosarcoma cells inhibits activation of latent TGF-beta1. *Biochemical and Biophysical Research Communications*, 398(3), 525–531. <https://doi.org/10.1016/j.bbrc.2010.06.112>
- Taiyab, A., & Rao Ch, M. (2011). HSP90 modulates actin dynamics: Inhibition of HSP90 leads to decreased cell motility and impairs invasion. *Biochimica et Biophysica Acta*, 1813(1), 213–221. <https://doi.org/10.1016/j.bbamcr.2010.09.012>
- Tickler, I. A., Goering, R. V., Mediavilla, J. R., Kreiswirth, B. N., Tenover, F. C., & Consortium, H. A. I (2017). Continued expansion of USA300-like methicillin-resistant *Staphylococcus aureus* (MRSA) among hospitalized patients in the United States. *Diagnostic Microbiology and Infectious Disease*, 88(4), 342–347. <https://doi.org/10.1016/j.diagmicrobio.2017.04.016>
- Tran Van Nhieu, G., & Isberg, R. R. (1993). Bacterial internalization mediated by beta 1 chain integrins is determined by ligand affinity and receptor density. *The EMBO Journal*, 12(5), 1887–1895. <https://doi.org/10.1002/j.1460-2075.1993.tb05837.x>
- Triantafyllou, K., Triantafyllou, M., & Dedrick, R. L. (2001). A CD14-independent LPS receptor cluster. *Nature Immunology*, 2(4), 338–345. <https://doi.org/10.1038/86342>
- Tsutsumi, S., & Neckers, L. (2007). Extracellular heat shock protein 90: A role for a molecular chaperone in cell motility and cancer metastasis. *Cancer Science*, 98(10), 1536–1539. <https://doi.org/10.1111/j.1349-7006.2007.00561.x>
- Voyich, J. M., Braughton, K. R., Sturdevant, D. E., Whitney, A. R., Said-Salim, B., Porcella, S. F., ... DeLeo, F. R. (2005). Insights into mechanisms used by *Staphylococcus aureus* to avoid destruction by human neutrophils. *Journal of Immunology*, 175(6), 3907–3919. <https://doi.org/10.4049/jimmunol.175.6.3907>
- Weidle, U. H., Maisel, D., Klostermann, S., Schiller, C., & Weiss, E. H. (2011). Intracellular proteins displayed on the surface of tumor cells as targets for therapeutic intervention with antibody-related agents. *Cancer Genomics Proteomics*, 8(2), 49–63.
- Wesson, C. A., Liou, L. E., Todd, K. M., Bohach, G. A., Trumble, W. R., & Bayles, K. W. (1998). *Staphylococcus aureus* Agr and Sar global regulators influence internalization and induction of apoptosis. *Infection and Immunity*, 66(11), 5238–5243.
- Yang, Y. H., Jiang, Y. L., Zhang, J., Wang, L., Bai, X. H., Zhang, S. J., ... Zhou, C. Z. (2014). Structural insights into SraP-mediated *Staphylococcus aureus* adhesion to host cells. *PLoS Pathogens*, 10(6), e1004169. <https://doi.org/10.1371/journal.ppat.1004169>
- Zapotoczna, M., Jevnikar, Z., Miajlovic, H., Kos, J., & Foster, T. J. (2013). Iron-regulated surface determinant B (IsdB) promotes *Staphylococcus aureus* adherence to and internalization by non-phagocytic human cells. *Cellular Microbiology*, 15(6), 1026–1041. <https://doi.org/10.1111/cmi.12097>
- Zimmermann, M., & Fischbach, M. A. (2010). A family of pyrazinone natural products from a conserved nonribosomal peptide synthetase in *Staphylococcus aureus*. *Chemistry & Biology*, 17(9), 925–930. <https://doi.org/10.1016/j.chembiol.2010.08.006>
- Zuehlke, A. D., Beebe, K., Neckers, L., & Prince, T. (2015). Regulation and function of the human HSP90AA1 gene. *Gene*, 570(1), 8–16. <https://doi.org/10.1016/j.gene.2015.06.018>

SUPPORTING INFORMATION

Additional supporting information may be found online in the Supporting Information section at the end of the article.

How to cite this article: Tribelli PM, Luqman A, Nguyen M-T, et al. *Staphylococcus aureus* Lpl protein triggers human host cell invasion via activation of Hsp90 receptor. *Cellular Microbiology*. 2019;e13111. <https://doi.org/10.1111/cmi.13111>

Publication in preparation

Stefan Raue, **Sook-Ha Fan**, Ralf Rosenstein, Susanne Zabel, Arif Luqman, Kay Nieselt & Friedrich Götz.

The genome of *Staphylococcus epidermidis* O47. In preparation.

The genome of *Staphylococcus epidermidis* O47

Stefan Raue¹, Sook-Ha Fan¹, Ralf Rosenstein², Susanne Zabel³, Arif Luqman¹ Kay Nieselt³, and Friedrich Götz^{1*}

¹Microbial Genetics, Interfaculty Institute of Microbiology and Infection Medicine Tübingen (IMIT), University of Tübingen, Auf der Morgenstelle 28, D-72076 Tübingen, Germany;

²Department of Infection Biology, Interfaculty Institute for Microbiology and Infection Medicine Tübingen (IMIT), University of Tübingen, Auf der Morgenstelle 28, 72076 Tübingen, Germany;

³Center for Bioinformatics Tübingen, University of Tübingen, Sand 14, D-72076 Tübingen, Germany

* Corresponding author

Running title: Genome of O47

Key words: *Staphylococcus epidermidis*, O47, genome, virulence factors,

Abbreviations: Aap: accumulation associated protein; ABC transporter: ATP-binding cassette transporter; AMP: antimicrobial peptides; ATP: Adenosine Triphosphate; CRISPR: clustered regularly interspaced short palindromic repeats, DNA: Deoxyribonucleic acid, KAAS: KEGG Automatic Annotation Server; KEGG: Kyoto Encyclopedia of Genes and Genomes, PIA: polysaccharide intercellular adhesin; PSM: phenol soluble modulin, RBH: reciprocal best hit; RNA: Ribonucleic acid; SCC: Staphylococcal Cassette Chromosome; STAR: *S. aureus* repeats.

Correspondence:

Prof. Dr. Friedrich Götz
Microbial Genetics
Interfaculty Institute of Microbiology and Infection Medicine (IMIT)
University of Tübingen
Auf der Morgenstelle 28
72076 Tübingen, Germany
Phone: +49 7071 29-74128
Fax: +49 7071 29-5065
E-mail: friedrich.goetz@uni-tuebingen.de

Abstract

The skin colonizing coagulase negative *Staphylococcus epidermidis* causes nosocomial infections and is an important opportunistic and highly adaptable pathogen. To gain more insight into this species, we sequenced the genome of the biofilm positive, methicillin resistance negative *S. epidermidis* O47 strain (hereafter O47). This strain belongs to the most frequently isolated sequence type 2. In comparison to the RP62A strain, O47 can be transformed, which makes it a preferred strain for molecular studies. *S. epidermidis* O47's genome has a single chromosome of about 2.5 million base pairs and no plasmids. Its *oriC* sequence has the same directionality as *S. epidermidis* RP62A, *S. carnosus*, *S. haemolyticus*, *S. saprophyticus* and is inverted in comparison to *Staphylococcus aureus* and *S. epidermidis* ATCC 12228. A phylogenetic analysis based on 1200 orthologous genes of all *S. epidermidis* genomes currently available at GenBank revealed the strain M23864:W2(grey) as the closest relative to O47. The genome of O47 contains genes for the typical global regulatory systems known in staphylococci. In addition, it contains most of the genes encoding for the typical virulence factors for *S. epidermidis* but not for *S. aureus* with the exception of a putative hemolysin III. O47 has the typical *S. epidermidis* genetic islands and several mobile genetic elements, which include staphylococcal cassette chromosome (SCC) of about 54 kb length and two prophages ϕ O47A and ϕ O47B. However, its genome has no transposons and the smallest number of IS elements compared to the other known *S. epidermidis* genomes. By sequencing and analyzing the genome of O47, we provide the basis for its utilization in genetic and molecular studies of biofilm formation.

Introduction

Staphylococcus epidermidis is a ubiquitous inhabitant of human skin and mucous membranes. Originally, this species was thought to rarely cause infections in normal host (Pulverer *et al.*, 1987). In the meantime, however, the number of infections by *S. epidermidis* has been steadily increasing with the growing number of immunocompromised patients in hospitals and the widespread medical use of prosthetic and indwelling devices (Christensen *et al.*, 1982b, Christensen *et al.*, 1982a, Christensen *et al.*, 1994). In the past years, it was found that the major cause of persistent infections is mainly due to the ability to form a biofilm on implant material and tissues. It was therefore not surprising that staphylococci biofilm associated factors have been first investigated in *S. epidermidis*.

Already in the early 1980s, electron microscopic studies of polymer devices infected by *S. epidermidis* have shown that multilayered cell clusters of staphylococci are embedded in a thick matrix of a slime substance (Locci *et al.*, 1981, Peters *et al.*, 1982). In the strain RP62A, a mitomycin-induced mutant has been isolated which was slime-negative (Schumacher-Perdreau *et al.*, 1994). Later, it was revealed that the slimy material is mainly composed of polysaccharide intercellular adhesin (PIA), a linear β -1,6-linked glucosaminoglycan (Mack *et al.*, 1996). Almost simultaneously, in the same year, the PIA biosynthesis proteins are found to be encoded by the *ica* operon in the *S. epidermidis* strain O47 (hereafter, O47) (Heilmann *et al.*, 1996b). Since then, the function of the PIA biosynthesis proteins have been extensively unraveled. The IcaA and IcaD (the latter as a helper protein) have N-acetylglucosaminyltransferase activity (Gerke *et al.*, 1998), and IcaB is a surface-attached protein that is responsible for deacetylation of the poly-N-acetylglucosamine molecule (Vuong *et al.*, 2004). Besides this poly-glucosaminoglycan, there are also proteins involved in intercellular aggregation such as the accumulation-associated protein, Aap (Hussain *et al.*, 1997); however, Aap acts as an intercellular adhesin only when it is proteolytically processed (Rohde *et al.*, 2005).

Molecular analysis of the genes involved in biofilm formation revealed that biofilm formation involves two major steps. The first step is the adherence of bacterial cells to a surface. Once adhered, it can proceed to the second step which is cell aggregation (accumulation phase) (Götz, 2002). A number of adherence factors have been identified that contribute in varying extents to the adherence to various surfaces. Again, one of the first adherence factors, the major autolysin (AtlE), has been described in the strain O47 (Heilmann *et al.*, 1996a, Heilmann *et al.*, 1997). Anoxic conditions (Cramton *et al.*, 2001) or pure fermentative growth as in small colony variants of O47 (Al Laham *et al.*, 2007) increased *ica* expression and consequently biofilm formation. Biofilm formation in *S. epidermidis* appears to be influenced by many factors. Iron limitation enhanced slime production (Deighton & Borland, 1993) and *ica* expression in O47 is increased and controlled by glucose (Gerke *et al.*, 1998). Besides, a novel mechanism of phase variation of the *ica* operon based on alternating insertion and excision of the insertion sequence element IS256 has been described (Ziebuhr *et al.*, 1999). Furthermore, *ica* expression is influenced by NaCl and ethanol and is also *sigB* dependent in *S. epidermidis* 1457 (Knobloch *et al.*, 2001). There are several evidences that *ica* plays a crucial role in the infection by *S. epidermidis*. Ica-positive *S. epidermidis* strains are prevalent in blood culture strains and mucosal isolates (Ziebuhr *et al.*, 1997), and the pathogenesis of

intravascular catheter-associated infection in a rat model was increased compared to its corresponding mutants (Fey *et al.*, 1999, Rupp *et al.*, 2001). With the discovery of the *ica* genes in *Staphylococcus aureus* (Cramton *et al.*, 1999), the focus of biofilm studies was shifted to *S. aureus* where the same as well as additional adherence factors have been identified.

The first genome-based analysis of virulence genes was carried out in *S. epidermidis* ATCC 12228 (hereafter, ATCC 12228), a non-biofilm-forming, non-infection associated strain used for the detection of residual antibiotics in food products (Zhang *et al.*, 2003), followed by *S. epidermidis* RP62A (ATCC 35984) (hereafter, RP62A), a methicillin-resistant biofilm isolate (Gill *et al.*, 2005). RP62A is a slime-producing strain isolated between 1979 and 1980 during the outbreak of intravascular catheter-associated sepsis in Memphis, Tennessee (Christensen *et al.*, 1982b). As such, the first molecular-based biofilm studies have been carried out in RP62A (Schumacher-Perdreau *et al.*, 1994).

However, we previously discovered that RP62A has a disadvantage in the studies of molecular basis of biofilm formation and infection as it is resistant to DNA transformation and its plasmid (pEpi62) encodes resistance to erythromycin, kanamycin, streptomycin, and penicillin (Schumacher-Perdreau *et al.*, 1994). Furthermore, we were unsuccessful in curing the 29-kb pEpi62. Therefore, for molecular analysis, we used O47 which was quite similar to RP62A, only that in the latter strain biofilm-forming capacity was more pronounced (Heilmann *et al.*, 1996a). O47 could be transformed, sensitive to antibiotics, carries no plasmid and is therefore appropriate for transposon mutagenesis. For these reasons, O47 was chosen for further genetic analyses of biofilm formation and virulence studies. O47 is functionally *agr*-negative, hardly produces delta-toxin and other phenol-soluble modulins (PSMs) which are *agr*-controlled (Cheung *et al.*, 2010, Vuong *et al.*, 2003). Because of the pioneering studies on biofilm formation and virulence in O47, its genome was analyzed and compared with other known staphylococcal genomes. Here, we highlight a few of the outcomes.

Results

General features of the genome. The assembly of the reads resulted in one contig. *S. epidermidis* O47 contains this whole chromosome and no plasmids. The genome of O47 (Figure 1, Table 1) has 2,518,182 bp. With 2,337 predicted protein coding genes, it has less proteins than *S. epidermidis* ATCC 12228 and RP62A. The coding density of 83.3% is similar to ATCC 12228. The GC content of the coding regions of O47 is 32.9%, which is comparable with the other *S. epidermidis* strains. The GC skew of the O47 genome is asymmetrical, which was also observed for ATCC 12228, RP62A, and other coagulase-negative species. The *oriC* of O47 is inverted compared to *S. aureus* and *S. epidermidis* ATCC 12228. Thus, the highly conserved genes flanking the *oriC* are in the same order as in *S. carnosus*, *S. haemolyticus*, *S. saprophyticus*, and *S. epidermidis* RP62A with *rpmH* as start gene instead of *dnaA* (Figure 2).

***S. epidermidis* phylogenetic analysis.** For the computation of the phylogenetic tree of the seven (also partly) sequenced *S. epidermidis* strains, we used 1,198

genes which have orthologous representatives in each of the genomes. The corresponding alignment of the concatenated nucleotide sequences comprises 1,081,233 nucleotide rows. According to the resulting phylogram (Figure 3), *S. epidermidis* O47 is closest related to M23864:W2(grey) and closer to ATCC 12228 than to RP62A. *S. epidermidis* W23144 is most distantly related to all other six *S. epidermidis* strains.

Noncoding RNAs. We searched for bacterial ncRNAs (noncoding RNAs) in the *S. epidermidis* strains O47, RP62A, and ATCC 12228 from the Rfam 10.1 database (Table 2). We found 39 ncRNA families conserved in the three *S. epidermidis* strains. In nine of these families, we could observe a small difference in the number of detected ncRNAs while the remaining 30 families showed the same number of ncRNAs. In all strains, we found tmRNA, ctRNA, RNAlII, RsaA, RsaD, RsaE, RsaH, and RsaOG.

Repetitive elements. Clustered regularly interspaced short palindromic repeats (CRISPRs) contribute to prevent conjugation and plasmid transformation (Marraffini & Sontheimer, 2008). We used the CRISPRfinder tool (Grissa *et al.*, 2007b) to find CRISPR elements in *S. epidermidis* O47. We found four candidates for O47 (Table 3) and *S. epidermidis* 1457. According to CRISPRdb (Grissa *et al.*, 2007a), ATCC 12228 contains one candidate, RP62A contains one CRISPR element and one candidate. Like ATCC 12228, the genome of *S. epidermidis* O47 lacks CRISPR-associated genes (*cas1*, *cas2*, and *cas6*) and *cas* subtype *M. tuberculosis* genes (*csm1* - *csm6*) which are present in RP62A (Marraffini & Sontheimer, 2008). The signature sequence for another kind of repeats, the *S. aureus* repeat (STAR) element (Cramton *et al.*, 2000), is present in ten loci of the O47 genome (Table 4). The same magnitude of occurrences can be observed for the strains ATCC 12228 and RP62A with nine and eight times, respectively.

Truncated and fragmented genes. We identified ten genes whose coding sequence is split into two ORFs and seven truncated genes (Table 5). These fragmented genes are two hypothetical proteins, the fibrinogen binding protein gene *sdrG*, the glucose-6-phosphate 1-dehydrogenase *zwf*, the plasmid recombination enzyme gene *pre*, a manganese transport protein gene, the accessory gene regulator C *agrC*, the lipase *gehC*, and a two-component sensor histidine kinase. The eight truncated genes of O47 in comparison to the RefSeq annotations of ATCC 12228 and RP62A are five hypothetical proteins, the arsenate reductase *arsC*, and the metallothiol transferase *fosB*. We verified the fragmentation or truncation of the genes *sdrG*, *zwf*, *agrC*, *gehC* and *fosB* by Sanger-Resequencing.

***S. epidermidis* O47 specific genes.** We found 187 genes for which O47 is specific in comparison to RefSeq annotations of ATCC 12228 and RP62A. These genes include the 61 genes of the staphylococcal cassette chromosome (SCC) and the genes of the putative prophages ϕ O47A (48 genes) and ϕ O47B (47 genes). The remaining genes are 15 transposases and 16 hypothetical genes.

***S. epidermidis* species specific genes.** Next, we analyzed which genes are specific for the *S. epidermidis* species. For this reason, we searched for genes found only in *S. epidermidis* O47, ATCC 12228, and RP62A and not found in *S. aureus* N315, USA300 and NCTC 8325, *S. haemolyticus* JCSC1435, *S. saprophyticus*

ATCC 15305, *S. carnosus* TM300, *S. lugdunensis* HKU09-01, *S. pseudintermedius* HKU10-03 or in the draft annotations of *S. warneri* L37603, *S. capitis* SK14, *S. hominis* SK119 and *S. lugdunensis* M23590. We identified 46 genes where 16 of these are not hypothetical genes such as cell wall located protein genes, *ebh*, *epbS* and *gldA* (Table 6).

Mobile genetic elements. Like other staphylococci, *S. epidermidis* contains several mobile genetic elements (Table 7). Besides the housekeeping recombinases (*recA*, *recD*, *recF*, *recG*, *recJ*, *recN*, *recO*, *recQ*, *recR*, *recU*, *recX*, *xerC*, *xerD*) for DNA replication and repair, the O47 genome contains some site-specific recombinases which can participate in mobile genetic elements. The contained cassette chromosome recombinase *ccrC* is part of the SCC and the Sin recombinase (FHQ17_09405) regulates strand exchange in *S. aureus* (Rowland *et al.*, 2002). The latter is also present in ATCC 12228 but currently is not annotated in RP62A. Furthermore, a truncated plasmid recombination enzyme containing a stop codon leading to the frame +2 ORFs *pre'* (SEO_579) and *pre''* (SEO_580). Besides, we found nine integrase and 44 transposase genes where 16 of these are IS1272 transposase or truncated IS1272 transposase genes although the genome is absent of the IS1272 element.

The genome of O47 contains two putative prophages which were named ϕ O47A (FHQ17_08005-FHQ17_07785) and ϕ O47B (FHQ17_04820-FHQ17_05045) (Figures 1 and 2). They are 33kb and 37kb in size, respectively, and thus belong to the *Staphylococcus* class II phages according to (Kwan *et al.*, 2005). Both sites contain integrase, lambda repressor like, sigma-like factor, phage terminase, phage portal protein, tail protein, and holin genes.

We used megablast (Zhang *et al.*, 2000) on a database of IS elements of Staphylococci provided by (Siguier *et al.*, 2006) and identified 15 IS elements in O47 (Table 8). The IS6-family IS431mec-like elements are all located in the SCC (Figure 1 and 4). Like ATCC 12228, the genome of O47 lacks transposons in contrast to RP62A which contains the transposons Tn554 and Tn4001.

Several genomic islands were identified for *S. epidermidis* (Table 9). vSe1 is found only in RP62A except for the universal stress protein family gene SERP2220 which has an ortholog in ATCC 12228. The genome of RP62A, on the other hand, lacks the island vSe2. The islands vSe3, vSe5 and vSe6 can be found in all three of these genomes. Except for the lipoprotein-related protein gene FHQ17_07780, vSe4 is absent in O47. However, ϕ O47A can be found near this locus. An integrase gene is absent in the islands vSe1 and vSe3. The integrase for vSe6 is fragmented in O47 and ATCC 12228. None of the RP62A islands contain an integrase gene.

The mauve alignment (Figure 2) shows another region named vSe7 which is contained in O47 (Bases 24,528 - 36,133) and ATCC 12228 (Bases 2,464,131 - 2,485,736) but not in RP62A. FHQ17_12320 is the *sdrF* gene and the other genes are a glucosyltransferase gene (FHQ17_12310), an acetyltransferase gene (SEO_27), and an ABC transporter gene (FHQ17_12285). The other four genes are hypothetical.

Staphylococcal Cassette Chromosome (SCC). The genome of O47 contains a 54kb allotype-5 SCC non-mec element (Figure 4). The SCC is flanked by the classical SCC-specific terminal repeats and contains a cassette chromosome recombinase C7 (*ccrC* at locus SEO_2286) with an identity of 100% to the *S. epidermidis* *ccrC7* gene (accession ABP68833). We found four IS elements in the SCC: two IS431mec-like elements flank the mercury resistance cluster (Laddaga *et al.*, 1987) while two IS431mec-like elements are located between *ccrC* and *orfX* flanking a conserved hypothetical protein and a probable manganese transport protein (*mntH*). Besides these, the SCC element also contains the arsenical resistance cluster, a multicopper oxidase (*mco*), a copper transporting ATPase (*copB*), the restriction modification system (*hsd*) and the DNA repair protein gene *radC*.

Metabolic pathways of O47 in comparison to other *S. epidermidis* strains. The KEGG Automatic Annotation Server (KAAS) was used to identify the functional properties and biological roles of the O47, ATCC 12228, and RP62A genes (Moriya *et al.*, 2007) and the differences between these strains were examined. Regarding the metabolic KEGG pathways, O47 and ATCC 12228 contain genes which are missing or nonfunctional in RP62A. One of these is a glutamate synthase (large chain) gene *gltB* (K00265) whose product is involved in the nitrogen (ko00910) and the alanine, aspartate and glutamate metabolism (ko00250). In RP62A, *gltB* (SERP0108) is a pseudogene since it contains a frame shift. Another frame shift can be observed for the RP62A pseudogene *pabB* (SERP0375). The *pabB* product and the product of the gene *pabC*, which is missing in RP62A in contrast to the other two strains, participate in the folate biosynthesis (ko00790). We found that the genes *pbp4* (K07258) and a hypothetical *vanY* (K07260), which are involved in peptidoglycan biosynthesis (ko00550), are specific for ATCC 12228 and thus are missing in O47 and RP62A.

On the other hand, RP62A contains genes which are absent in the other two strains. Besides the methicillin resistance genes *mecR1* (K02547), *mecI* (K02546), and *mecA* (K02545), RP62A contains a DNA (cytosine-5-)-methyltransferase gene (K00558) participating in the cysteine and methionine metabolism (ko00270). In addition, RP62A is specific for a gene (K00680) whose product is involved in the tyrosine metabolism (ko00350), benzoate degradation (ko00362), naphthalene degradation (ko00626), aminobenzoate degradation (ko00627), ethylbenzene degradation (ko00642), and limonene and pinene degradation (ko00903).

Recently, O47 has been reported to be able to produce trace amines from aromatic amino acids. We then characterized a *sadA* gene, which first described in *S. pseudintermedius* ED99 and encodes an aromatic amino acid decarboxylase (Luqman *et al.*, 2018), in O47 (FHQ17_00300). It has 52% identity with *sadA* gene in *S. pseudintermedius* ED99 and 99% identity with a gene encoding pyridoxal-dependent decarboxylase located in locus SE0112 in ATCC 12228 genome. We proved the function of the gene by cloning it in an expression plasmid (pCtufamp) and analyzed the overnight supernatant using HPLC (Figure 5).

Non-metabolic pathways of O47 in comparison to other *S. epidermidis* strains. Considering the non-metabolic KEGG pathways, we found *uhpT* (K07784), which is involved in the glucose-6-P uptake and assigned to the two-component system

pathway (ko02020), present in O47 and ATCC 12228 but not in RP62A. According to the KAAS, none of these *S. epidermidis* strains contain the other glucose-6-P uptake genes *uhpA* (K07686), *uhpB* (K07675), or *uhpC* (K07783).

Although all of the three *S. epidermidis* strains contain two ATP-binding protein genes (K09687) of the antibiotic transport system in the ABC transporters pathway (ko2010), only ATCC 12228 has the permease protein gene (K09686). For RP62A, the *kdp* operon, a two component system (ko02020) and in *E. coli* an inducible high-affinity K⁺ transporter (Altendorf *et al.*, 1994), is specific. The *kdpF* gene (K01545) of this operon, however, is not present in RP62A. Apart from that, RP62A contains an ATP dependent DNA ligase (K01971) which is involved in base excision repair (ko03410), nucleotide excision repair (ko03420), mismatch repair (ko03430), and non-homologous end-joining (ko03450).

Global regulatory systems. The typical global regulatory systems known in staphylococci are involved in cell wall biosynthesis, adhesion, biofilm formation, autolysis, secretion and regulation of exoproteins, and virulence factor expression. Except for *sarS*, *sarT* and *mepRABC*, orthologs for these systems exist in O47 with a high similarity ($\geq 98\%$ identity in all cases) to other *S. epidermidis* strains (Table 10). This includes the *aps* system which is equivalent to the *graRS* system of *S. aureus* and belongs to a resistance mechanism to antimicrobial peptides (Li *et al.*, 2007). In O47, the *agr* system likely is nonfunctional since a stop codon in the coding sequence of *agrC* leads to the ORFs *agrC'* (frame +2) and *agrC''* (frame +3). A similar observation for *agrC* was made in *S. carnosus* TM300 (Rosenstein *et al.*, 2009).

***S. epidermidis* virulence factors in *S. epidermidis* O47.** *S. epidermidis* genes are involved in biofilm formation, lysozyme and antimicrobial protein (AMP) resistance, toxin production and iron uptake. In O47, most genes for the typical *S. epidermidis* virulence factors according to an overview by (Otto, 2009) are present (Table 11). All these genes have a query coverage $>99\%$ except for *sdrH* which is a consequence of a decreased number of Asp-Ser repeats in the SdrH amino acid sequence. For all genes, the identity is $\geq 98\%$. The genes for the staphyloferrin A biosynthesis proteins were annotated using the primer sequence provided in (Cotton *et al.*, 2009). While the peptide sequence of the annotated phenol soluble modulins (PSM) genes corresponds exactly to those observed by (Yao *et al.*, 2005), we did not annotate related sequences.

As with ATCC 12228 and RP62A, the capsule biosynthesis gene *capD* is missing in O47. Furthermore, the O47 strain lacks the biofilm associated protein gene *bap* which is also absent in ATCC 12228. The *S. epidermidis* virulence factor genes for the accumulation associated protein Aap, the lipase GehC and the fibrinogen binding protein SdrG are fragmented in *S. epidermidis* O47 and might be nonfunctional. To examine some of these phenotypes, we performed agar diffusion assay to check for protease and lipase activity and also biofilm assay. In agreement with the genomic findings, no protease and lipase activity was observed in O47 compared to the other *S. epidermidis* strains (Figure 6). The biofilm formation in O47 was moderate in comparison to ATCC 12228 which showed no biofilm formation and RP62A which showed more pronounced biofilm formation (Figure 6).

The *tarIJK* and *tagAHGBXD* clusters which are involved in the teichoic acid biosynthesis (recently reviewed for *S. aureus* by (Swoboda *et al.*, 2010), are also present in *S. epidermidis* O47. On the other hand, O47 lacks the genes *tarI'J'L* which are homologous to *tarIJK*, were suggested to have the same enzymatic function and observed in *S. aureus*.

Resistances in *S. epidermidis* O47. The genome of O47 contains several antibiotic resistance related genes with high identity ($\geq 98\%$) to other *S. epidermidis* strains (Table 12). We determined the minimum inhibitory concentration MIC values for penicillin and methicillin in O47 and other strains and found that O47 was resistant to penicillin (MIC $> 128 \mu\text{l/ml}$) (Table 13), in agreement with the penicillin binding proteins genes found in its genome. The MIC of O47 for methicillin was intermediate ($2 \mu\text{l/ml}$).

The beta-lactam resistance gene and its regulators (*blaIRZ*) are in the genomic sequence next to two hypothetical genes and the Tn554-related transposase genes CBA. The same neighborhood can be observed for ATCC 12228 and RP62A. The genome of O47 contains several resistances (Table 14) such as an arsenical, a mercuric or an azaleucine resistance.

***S. aureus* virulence factors in *S. epidermidis* O47.** We searched the O47 genome for the typical *S. aureus* virulence factors and found a putative hemolysin III (FHQ17_03540) with high similarity in other *S. epidermidis* strains (identity 100%). However, O47 showed no hemolysis on blood agr (Figure 6). On the other hand, *S. epidermidis* O47 lacks the typical *S. aureus* adhesins, toxins, and invasins (Table 15).

Material and methods

Isolation of high molecular weight genomic DNA from bacterial cells. Cells from 10 ml overnight culture were lysed by treatment with lysostaphin in 2 ml lysis buffer (P1 buffer (Qiagen, Hilden) supplemented with $25 \mu\text{g}$ lysostaphin) for 30 min at 37°C . Preparation of chromosomal DNA from the cell lysate was performed according to the procedure by Marmur (Marmur, 1961).

Sequencing. The genome of O47 was de novo sequenced in a pyrosequencing approach by the Göttingen Genomics Laboratory (Institute of Microbiology and Genetics, Georg-August University Göttingen). The Genome Sequencer FLX Instrument and Titanium chemistry (Roche Applied Science) was used for DNA nebulization, single-stranded template DNA library preparation and sequencing according to the General FLX Library Protocol of the manufacturer. An assembly of the 261,085 reads (Q40 coverage of 99.93%) with the Roche Newbler Assembler 2.0.1 (454 Life Sciences) obtained 56 contigs. The GAP4 software of the Staden package (Staden *et al.*, 2003) was used for editing of the sequences. Sequencing with ABI 3730xl (Applied Biosystems) of standard PCR and combinatorial multiplex PCR products were used to close remaining sequence gaps. The O47 genome sequence can be accessed in the GenBank database with the accession number CP040883.

Gene and function prediction. The GenDB annotation system (Meyer *et al.*, 2003) was used to predict the ORFs, tRNAs, rRNAs, and to perform a functional ORF annotation. The noncoding RNAs were predicted with nocoRNAC (Herbig & Nieselt, 2011) which uses cmsearch (Nawrocki *et al.*, 2009) and the Rfam 10.1 database (Gardner *et al.*, 2009). The stricter TC (trusted cutoff) thresholds for bacterial Rfam seeds were used for this computation. To identify the functional properties and biological roles of the O47, ATCC 12228 and RP62A genes, we used the KEGG Automatic Annotation Server (KAAS) (Moriya *et al.*, 2007).

Comparative genomics. To compare the protein contents, we used Blastp (Altschul *et al.*, 1990) and the reciprocal best hit (RBH) method (Bork *et al.*, 1998, Tatusov *et al.*, 1997). For the computation, we used an E-value cut-off of 1e-8 and a coverage threshold of 75%. The coverage threshold was not used for the computation of truncated genes. Genes were considered as truncated if they are in their 3'-end ten or more nucleotides shorter than their orthologous gene in one of the RefSeq annotations of ATCC 12228 or RP62A.

For comparative genomic analysis, we used the strains ATCC 12228 (NC_004461, (Zhang *et al.*, 2003)), RP62A (NC_002976, (Gill *et al.*, 2005)), and the draft *S. epidermidis* sequences of strain W23144 (NZ_ACJC00000000), M23864:W2(grey) (NZ_ADMU00000000), BCM-HMP0060 (NZ_ACHE00000000), and SK135 (NZ_ADEY00000000). Additionally, we used the *S. aureus* strains N315 (NC_002745, (Kuroda *et al.*, 2001)), USA300_FPR3757 (NC_007793, (Diep *et al.*, 2006)), NCTC 8325 (NC_007795, (Gillaspy *et al.*, 2006)), and the strains *S. haemolyticus* JCSC1435 (NC_007168, (Takeuchi *et al.*, 2005)), *S. saprophyticus* ATCC 15305 (NC_007350, (Kuroda *et al.*, 2005)), *S. carnosus* TM300 (NC_012121, (Rosenstein *et al.*, 2009)), *S. lugdunensis* HKU09-01 (NC_013893, (Tse *et al.*, 2010)), and *S. pseudintermedius* HKU10-03 (NC_014925, (Tse *et al.*, 2011)). Furthermore, we used the draft sequences of the strains *S. warneri* L37603 (NZ_ACPZ00000000), *S. capitis* SK14 (NZ_ACFR00000000), *S. hominis* SK119 (NZ_ACLP00000000), and *S. lugdunensis* M23590 (NZ_AEQA00000000).

Transposons. To identify transposons in the O47 genome, we used Blastn (Zhang *et al.*, 2000) and the sequences of transposons Tn551 (accession number Y13600), Tn552 (X52734), Tn554 (X03216), Tn558 (58577493), Tn559 (302064329), Tn4001 (13383306), Tn4003 (13383306), Tn5404 (L43098.1), Tn5406 (AF186237.2), Tn5801 (289166909), Tn6072 (GU235985.1), and the *S. epidermidis* composite transposon (13383306) as query.

Phylogenetic analysis. The phylogenetic analysis of the *S. epidermidis* strains was based on the method published by (Rokas *et al.*, 2003). First, a multiple sequence alignment of the protein sequence of those genes which have orthologs in each *S. epidermidis* strain is performed by ClustalW (Larkin *et al.*, 2007). For the identification of the orthologous genes, we used Blastp (Altschul *et al.*, 1990) with an E-value cutoff of 1e-10 and the coverage constraint of 100%. The latter was chosen in order to avoid an evolutionary distance originating from differentially predicted translational start sites. Subsequently, the alignments are concatenated and the sequences are back translated to the corresponding nucleotide sequence. Finally, the neighbor joining method implemented in SplitsTree4 (Huson & Bryant, 2006) was used to construct a phylogenetic tree.

Repeats. The CRISPR finder tool (Grissa *et al.*, 2007b) was used to find CRISPRs in the O47 genome. Blastn with a word size of 14 was used for the identification of the STAR element signature sequence (Cramton *et al.*, 2000).

Plasmid construction. Plasmid construction was carried out by ligating the amplified *sadA* from *S. epidermidis* O47 using designed primers (**Table S1**) into linearized pCtufamp plasmid (Ebner *et al.*, 2015), cut by HindIII and PaeI, using Hi-Fi DNA Assembly Master Mix (New England Biolabs). The constructed plasmid was transformed into *E. coli* C2987 (New England Biolabs) and then into *E. coli* DC10B. Plasmid harboring colonies were picked and verified by DNA sequencing. The correct plasmid was then transformed into *S. aureus* RN4220.

HPLC analysis. The staphylococcal strains were inoculated into TSB supplemented with the corresponding antibiotic (chloramphenicol 10 µg/ml for pCtuf-harboring strain) and incubated at 37°C for 24 h with shaking at 150 rpm. The supernatant was collected and analyzed using reversed-phase preparative HPLC (RP-HPLC) on an Eclipse XDB-C18 column (Agilent) with a 15-min linear gradient of 0.1% phosphoric acid to acetonitrile at a flow rate of 1.5 mL/min.

Protease activity test by agar diffusion assay. Overnight cultures of staphylococcal strains were adjusted to OD₅₇₈ of 1 and were streaked on the skim milk agar (skim milk powder 2.8%, tryptone 0.5%, yeast extract 0.25%, glucose 0.1%, and agar 1.5% at pH 7). The plates were incubated overnight at 37°C and subsequently stored at 4°C for an additional 24 h. Protease activity was observed as visible halo due to the casein degradation.

Lipase activity test by agar diffusion assay. The tryptic soy agar (TSA) plates containing 1% Tween 20 were used to monitor lipase activity of different staphylococcal strains. Overnight cultures of staphylococcal strains were adjusted to OD₅₇₈ of 0.1 and 10 µl was dropped on the Tween 20 containing TSA. The plates were incubated overnight at 37°C and subsequently stored at 4°C for an additional 24 h. Lipase activity was observed as a visible halo due to the precipitation of liberated fatty acids.

Hemolysis assay. Overnight cultures of staphylococcal strains were adjusted to OD₅₇₈ of 0.1 and 10 µl was dropped on the Columbia sheep blood agar plates (Thermo Scientific). The plates were incubated overnight at 37°C and subsequently stored at 4°C for an additional 24 h. Hemolysis activity was indicated by the presence of a visible halo was observed due to the erythrocytes lysis

Biofilm assay. The biofilm assay was performed according to (Saising *et al.*, 2012) with modifications. Overnight cultures of staphylococcal strains grown in TSB with additional 0.25% glucose were adjusted to OD₅₇₈ of 0.1. 20 µl of the bacterial suspension was added to 180 µl of TSB in wells of a 96 well flat bottom microtiter plate (Greiner Bio-One), resulting in a final OD₅₇₈ of 0.01 which corresponds to approximately 10⁶ CFU/ml. The microtiter plate was incubated at 37°C without agitation for 24 h. After 24 h, the culture supernatant was discarded and the wells were rinsed twice with 200 µl of PBS before being air dried for 30 min. Then, the wells were stain with 200 µl of 0.1% crystal violet for 30 min and subsequently rinsed

with purified water (MilliQ). The plate was air dried again for 30 min and image of the wells was taken with an image scanner (Epson).

MIC determinations. The MIC values were determined by the microdilution method. Antibiotics used (penicillin and methicillin) were serially diluted (128 µg/ml to 0.25 µg/ml) with Muller Hinton Broth (MHB) (with 2% NaCl) in 96 well microtiter plates. Equal volumes of bacterial inoculum from overnight cultures adjusted to the final OD₅₇₈ of 0.05 were added. The microtiter plates were incubated at 37°C with continuous shaking for 18 h. The MIC was determined as the lowest concentration that completely inhibited visible growth of the bacteria.

Acknowledgments

We would like to thank Daniel Lehle and Alexander Herbig for their help. This work was supported by funding from BNBF and Deutsche Forschungsgemeinschaft (DFG: SFB766, TRR34). S.H.F. received a PhD fellowship from the German Academic Exchange Service (DAAD) and also supported by Graduiertenkolleg (GRK) 1708.

References

- Al Laham, N., H. Rohde, G. Sander, A. Fischer, M. Hussain, C. Heilmann, D. Mack, R. Proctor, G. Peters, K. Becker & C. von Eiff, (2007) Augmented expression of polysaccharide intercellular adhesin in a defined *Staphylococcus epidermidis* mutant with the small-colony-variant phenotype. *J Bacteriol* **189**: 4494-4501.
- Altendorf, K., P. Voelkner & W. Puppe, (1994) The sensor kinase KdpD and the response regulator KdpE control expression of the kdpFABC operon in *Escherichia coli*. *Res Microbiol* **145**: 374-381.
- Altschul, S.F., W. Gish, W. Miller, E.W. Myers & D.J. Lipman, (1990) Basic local alignment search tool. *J Mol Biol* **215**: 403-410.
- Arrecubieta, C., M.H. Lee, A. Macey, T.J. Foster & F.D. Lowy, (2007) SdrF, a *Staphylococcus epidermidis* surface protein, binds type I collagen. *J Biol Chem* **282**: 18767-18776.
- Bera, A., R. Biswas, S. Herbert & F. Götz, (2006) The presence of peptidoglycan O-acetyltransferase in various staphylococcal species correlates with lysozyme resistance and pathogenicity. *Infect Immun* **74**: 4598-4604.
- Bork, P., T. Dandekar, Y. Diaz-Lazcoz, F. Eisenhaber, M. Huynen & Y. Yuan, (1998) Predicting function: from genes to genomes and back. *J Mol Biol* **283**: 707-725.
- Brandenberger, M., M. Tschierske, P. Giachino, A. Wada & B. Berger-Bachi, (2000) Inactivation of a novel three-cistronic operon tcaR-tcaA-tcaB increases teicoplanin resistance in *Staphylococcus aureus*. *Biochim Biophys Acta* **1523**: 135-139.
- Brown, S., Y.H. Zhang & S. Walker, (2008) A revised pathway proposed for *Staphylococcus aureus* wall teichoic acid biosynthesis based on in vitro reconstitution of the intracellular steps. *Chem Biol* **15**: 12-21.
- Brunskill, E.W. & K.W. Bayles, (1996) Identification and molecular characterization of a putative regulatory locus that affects autolysis in *Staphylococcus aureus*. *J Bacteriol* **178**: 611-618.

- Cheung, A.L., J.M. Koomey, C.A. Butler, S.J. Projan & V.A. Fischetti, (1992) Regulation of exoprotein expression in *Staphylococcus aureus* by a locus (*sar*) distinct from *agr*. *Proc Natl Acad Sci U S A* **89**: 6462-6466.
- Cheung, G.Y., K. Rigby, R. Wang, S.Y. Queck, K.R. Braughton, A.R. Whitney, M. Teintze, F.R. DeLeo & M. Otto, (2010) *Staphylococcus epidermidis* strategies to avoid killing by human neutrophils. *PLoS Pathog* **6**: e1001133.
- Christensen, G.D., L. Baldassarri & W.A. Simpson, (1994) Colonization of medical devices by coagulase-negative staphylococci. In: Infections associated with indwelling medical devices. A.L. Bisno & F.A. Waldvogel (eds). Washington, D.C.: ASM Press, pp. 45-78.
- Christensen, G.D., A.L. Bisno, J.T. Parisi, M.G. Mc Laughlin, G.M. Hester & R.W. Luther, (1982a) Nosocomial septicemia due to multiple-resistant *Staphylococcus epidermidis*. *Ann Int Med* **96**: 1-10.
- Christensen, G.D., W.A. Simpson, A.L. Bisno & E.H. Beachey, (1982b) Adherence of slime-producing strains of *Staphylococcus epidermidis* to smooth surfaces. *Infect Immun* **37**: 318-326.
- Cockayne, A., P.J. Hill, N.B. Powell, K. Bishop, C. Sims & P. Williams, (1998) Molecular cloning of a 32-kilodalton lipoprotein component of a novel iron-regulated *Staphylococcus epidermidis* ABC transporter. *Infect Immun* **66**: 3767-3774.
- Cotton, J.L., J. Tao & C.J. Balibar, (2009) Identification and characterization of the *Staphylococcus aureus* gene cluster coding for staphyloferrin A. *Biochemistry* **48**: 1025-1035.
- Cramton, S.E., C. Gerke, N.F. Schnell, W.W. Nichols & F. Götz, (1999) The intercellular adhesion (*ica*) locus is present in *Staphylococcus aureus* and is required for biofilm formation. *Infect Immun* **67**: 5427-5433.
- Cramton, S.E., N.F. Schnell, F. Götz & R. Brückner, (2000) Identification of a new repetitive element in *Staphylococcus aureus*. *Infect Immun* **68**: 2344-2348.
- Cramton, S.E., M. Ulrich, F. Götz & G. Döring, (2001) Anaerobic conditions induce expression of polysaccharide intercellular adhesin in *Staphylococcus aureus* and *Staphylococcus epidermidis*. *Infect Immun* **69**: 4079-4085.
- Darling, A.E., B. Mau & N.T. Perna, (2010) progressiveMauve: multiple genome alignment with gene gain, loss and rearrangement. *PLoS One* **5**: e11147.
- Deighton, M. & R. Borland, (1993) Regulation of slime production in *Staphylococcus epidermidis* by iron limitation. *Infect Immun* **61**: 4473-4479.
- Diep, B.A., S.R. Gill, R.F. Chang, T.H. Phan, J.H. Chen, M.G. Davidson, F. Lin, J. Lin, H.A. Carleton, E.F. Mongodin, G.F. Sensabaugh & F. Perdreau-Remington, (2006) Complete genome sequence of USA300, an epidemic clone of community-acquired methicillin-resistant *Staphylococcus aureus*. *Lancet* **367**: 731-739.
- Dubin, G., D. Chmiel, P. Mak, M. Rakwalska, M. Rzychon & A. Dubin, (2001) Molecular cloning and biochemical characterisation of proteases from *Staphylococcus epidermidis*. *Biol Chem* **382**: 1575-1582.
- Ebner, P., M. Prax, M. Nega, I. Koch, L. Dube, W. Yu, J. Rinker, P. Popella, M. Flötenmeyer & F. Götz, (2015) Excretion of cytoplasmic proteins (ECP) in *Staphylococcus aureus*. *Mol Microbiol* **97**: 775-789.
- Fey, P.D., J.S. Ulphani, F. Götz, C. Heilmann, D. Mack & M.E. Rupp, (1999) Characterization of the relationship between polysaccharide intercellular adhesin and hemagglutination in *Staphylococcus epidermidis*. *J Infect Dis* **179**: 1561-1564.

- Fitzgerald, S.N. & T.J. Foster, (2000) Molecular analysis of the tagF gene, encoding CDP-Glycerol:Poly(glycerophosphate) glycerophosphotransferase of *Staphylococcus epidermidis* ATCC 14990. *J Bacteriol* **182**: 1046-1052.
- Fournier, B. & D.C. Hooper, (2000) A new two-component regulatory system involved in adhesion, autolysis, and extracellular proteolytic activity of *Staphylococcus aureus*. *J Bacteriol* **182**: 3955-3964.
- Gardner, P.P., J. Daub, J.G. Tate, E.P. Nawrocki, D.L. Kolbe, S. Lindgreen, A.C. Wilkinson, R.D. Finn, S. Griffiths-Jones, S.R. Eddy & A. Bateman, (2009) Rfam: updates to the RNA families database. *Nucleic Acids Res* **37**: D136-140.
- Gerke, C., A. Kraft, R. Süssmuth, O. Schweitzer & F. Götz, (1998) Characterization of the N-acetylglucosaminyltransferase activity involved in the biosynthesis of the *Staphylococcus epidermidis* polysaccharide intercellular adhesin. *J Biol Chem* **273**: 18586-18593.
- Gill, S.R., D.E. Fouts, G.L. Archer, E.F. Mongodin, R.T. Deboy, J. Ravel, I.T. Paulsen, J.F. Kolonay, L. Brinkac, M. Beanan, R.J. Dodson, S.C. Daugherty, R. Madupu, S.V. Angiuoli, A.S. Durkin, D.H. Haft, J. Vamathevan, H. Khouri, T. Utterback, C. Lee, G. Dimitrov, L. Jiang, H. Qin, J. Weidman, K. Tran, K. Kang, I.R. Hance, K.E. Nelson & C.M. Fraser, (2005) Insights on evolution of virulence and resistance from the complete genome analysis of an early methicillin-resistant *Staphylococcus aureus* strain and a biofilm-producing methicillin-resistant *Staphylococcus epidermidis* strain. *J Bacteriol* **187**: 2426-2438.
- Gillaspy, A.F., V. Worrell, J. Orvis, B.A. Roe, D.W. Dyer & J.J. Iandolo, (2006) *Staphylococcus aureus* NCTC8325 genome. ASM Press, Washington, DC.
- Götz, F., (2002) *Staphylococcus* and biofilms. *Mol Microbiol* **43**: 1367-1378.
- Grissa, I., G. Vergnaud & C. Pourcel, (2007a) The CRISPRdb database and tools to display CRISPRs and to generate dictionaries of spacers and repeats. *BMC Bioinformatics* **8**: 172.
- Grissa, I., G. Vergnaud & C. Pourcel, (2007b) CRISPRFinder: a web tool to identify clustered regularly interspaced short palindromic repeats. *Nucleic Acids Res* **35**: W52-57.
- Heilmann, C., C. Gerke, F. Perdreau-Remington & F. Götz, (1996a) Characterization of Tn917 insertion mutants of *Staphylococcus epidermidis* affected in biofilm formation. *Infect Immun* **64**: 277-282.
- Heilmann, C., M. Hussain, G. Peters & F. Götz, (1997) Evidence for autolysin-mediated primary attachment of *Staphylococcus epidermidis* to a polystyrene surface. *Mol Microbiol* **24**: 1013-1024.
- Heilmann, C., O. Schweitzer, C. Gerke, N. Vanittanakom, D. Mack & F. Götz, (1996b) Molecular basis of intercellular adhesion in the biofilm-forming *Staphylococcus epidermidis*. *Mol Microbiol* **20**: 1083-1091.
- Herbig, A. & K. Nieselt, (2011) nocoRNAC: characterization of non-coding RNAs in prokaryotes. *BMC Bioinformatics* **12**: 40.
- Holland, L.M., B. Conlon & J.P. O'Gara, (2011) Mutation of tagO reveals an essential role for wall teichoic acids in *Staphylococcus epidermidis* biofilm development. *Microbiology* **157**: 408-418.
- Huson, D.H. & D. Bryant, (2006) Application of phylogenetic networks in evolutionary studies. *Mol Biol Evol* **23**: 254-267.

- Hussain, M., M. Herrmann, C. von Eiff, F. Perdreau-Remington & G. Peters, (1997) A 140-kilodalton extracellular protein is essential for the accumulation of *Staphylococcus epidermidis* strains on surfaces. *Infect Immun* **65**: 519-524.
- Ingavale, S., W. van Wamel, T.T. Luong, C.Y. Lee & A.L. Cheung, (2005) Rat/MgrA, a regulator of autolysis, is a regulator of virulence genes in *Staphylococcus aureus*. *Infect Immun* **73**: 1423-1431.
- Knobloch, J.K., K. Bartscht, A. Sabottke, H. Rohde, H.H. Feucht & D. Mack, (2001) Biofilm formation by *Staphylococcus epidermidis* depends on functional RsbU, an activator of the *sigB* operon: differential activation mechanisms due to ethanol and salt stress. *J Bacteriol* **183**: 2624-2633.
- Kocianova, S., C. Vuong, Y. Yao, J.M. Voyich, E.R. Fischer, F.R. DeLeo & M. Otto, (2005) Key role of poly-gamma-DL-glutamic acid in immune evasion and virulence of *Staphylococcus epidermidis*. *J Clin Invest* **115**: 688-694.
- Kuroda, M., H. Kuroda, T. Oshima, F. Takeuchi, H. Mori & K. Hiramatsu, (2003) Two-component system *VraSR* positively modulates the regulation of cell-wall biosynthesis pathway in *Staphylococcus aureus*. *Mol Microbiol* **49**: 807-821.
- Kuroda, M., T. Ohta, I. Uchiyama, T. Baba, H. Yuzawa, I. Kobayashi, L. Cui, A. Oguchi, K. Aoki, Y. Nagai, J. Lian, T. Ito, M. Kanamori, H. Matsumaru, A. Maruyama, H. Murakami, A. Hosoyama, Y. Mizutani-Ui, N.K. Takahashi, T. Sawano, R. Inoue, C. Kaito, K. Sekimizu, H. Hirakawa, S. Kuhara, S. Goto, J. Yabuzaki, M. Kanehisa, A. Yamashita, K. Oshima, K. Furuya, C. Yoshino, T. Shiba, M. Hattori, N. Ogasawara, H. Hayashi & K. Hiramatsu, (2001) Whole genome sequencing of methicillin-resistant *Staphylococcus aureus*. *Lancet* **357**: 1225-1240.
- Kuroda, M., A. Yamashita, H. Hirakawa, M. Kumano, K. Morikawa, M. Higashide, A. Maruyama, Y. Inose, K. Matoba, H. Toh, S. Kuhara, M. Hattori & T. Ohta, (2005) Whole genome sequence of *Staphylococcus saprophyticus* reveals the pathogenesis of uncomplicated urinary tract infection. *Proc Natl Acad Sci U S A* **102**: 13272-13277.
- Kwan, T., J. Liu, M. DuBow, P. Gros & J. Pelletier, (2005) The complete genomes and proteomes of 27 *Staphylococcus aureus* bacteriophages. *Proc Natl Acad Sci U S A* **102**: 5174-5179.
- Laddaga, R.A., L. Chu, T.K. Misra & S. Silver, (1987) Nucleotide sequence and expression of the mercurial-resistance operon from *Staphylococcus aureus* plasmid p1258. *Proc Natl Acad Sci U S A* **84**: 5106-5110.
- Larkin, M.A., G. Blackshields, N.P. Brown, R. Chenna, P.A. McGettigan, H. McWilliam, F. Valentin, I.M. Wallace, A. Wilm, R. Lopez, J.D. Thompson, T.J. Gibson & D.G. Higgins, (2007) Clustal W and Clustal X version 2.0. *Bioinformatics* **23**: 2947-2948.
- Li, M., Y. Lai, A.E. Villaruz, D.J. Cha, D.E. Sturdevant & M. Otto, (2007) Gram-positive three-component antimicrobial peptide-sensing system. *Proc Natl Acad Sci U S A* **104**: 9469-9474.
- Lindsay, J.A., T.V. Riley & B.J. Mee, (1994) Production of siderophore by coagulase-negative staphylococci and its relation to virulence. *Eur J Clin Microbiol Infect Dis* **13**: 1063-1066.
- Locci, R., G. Peters & G. Pulverer, (1981) Microbial colonization of prosthetic devices. IV. Scanning electron microscopy of intravenous catheters invaded by yeasts. *Zentralbl Bakteriol Mikrobiol Hyg [B]* **173**: 419-424.
- Longshaw, C.M., A.M. Farrell, J.D. Wright & K.T. Holland, (2000) Identification of a second lipase gene, *gehD*, in *Staphylococcus epidermidis*: comparison of

- sequence with those of other staphylococcal lipases. *Microbiology* **146 (Pt 6)**: 1419-1427.
- Luqman, A., M. Nega, M.T. Nguyen, P. Ebner & F. Götz, (2018) SadA-Expressing Staphylococci in the Human Gut Show Increased Cell Adherence and Internalization. *Cell Rep* **22**: 535-545.
- Mack, D., W. Fischer, A. Krokotsch, K. Leopold, R. Hartmann, H. Egge & R. Laufs, (1996) The intercellular adhesin involved in biofilm accumulation of *Staphylococcus epidermidis* is a linear beta-1,6-linked glucosaminoglycan: purification and structural analysis. *J Bacteriol* **178**: 175-183.
- Marmur, J., (1961) A procedure for isolation of deoxyribonucleic acid from microorganisms. *J. Mol. Biol.* **3**: 208-218.
- Marraffini, L.A. & E.J. Sontheimer, (2008) CRISPR interference limits horizontal gene transfer in staphylococci by targeting DNA. *Science* **322**: 1843-1845.
- McCrea, K.W., O. Hartford, S. Davis, D.N. Eidhin, G. Lina, P. Speziale, T.J. Foster & M. Hook, (2000) The serine-aspartate repeat (Sdr) protein family in *Staphylococcus epidermidis*. *Microbiology* **146 (Pt 7)**: 1535-1546.
- McNamara, P.J., K.C. Milligan-Monroe, S. Khalili & R.A. Proctor, (2000) Identification, cloning, and initial characterization of rot, a locus encoding a regulator of virulence factor expression in *Staphylococcus aureus*. *J Bacteriol* **182**: 3197-3203.
- Meyer, F., A. Goesmann, A.C. McHardy, D. Bartels, T. Bekel, J. Clausen, J. Kalinowski, B. Linke, O. Rupp, R. Giegerich & A. Puhler, (2003) GenDB--an open source genome annotation system for prokaryote genomes. *Nucleic Acids Res* **31**: 2187-2195.
- Moriya, Y., M. Itoh, S. Okuda, A.C. Yoshizawa & M. Kanehisa, (2007) KAAS: an automatic genome annotation and pathway reconstruction server. *Nucleic Acids Res* **35**: W182-185.
- Nawrocki, E.P., D.L. Kolbe & S.R. Eddy, (2009) Infernal 1.0: inference of RNA alignments. *Bioinformatics* **25**: 1335-1337.
- Otto, M., (2009) *Staphylococcus epidermidis*--the 'accidental' pathogen. *Nat Rev Microbiol* **7**: 555-567.
- Pamp, S.J., D. Frees, S. Engelmann, M. Hecker & H. Ingmer, (2006) Spx is a global effector impacting stress tolerance and biofilm formation in *Staphylococcus aureus*. *J Bacteriol* **188**: 4861-4870.
- Park, P.W., J. Rosenbloom, W.R. Abrams, J. Rosenbloom & R.P. Mecham, (1996) Molecular cloning and expression of the gene for elastin-binding protein (ebpS) in *Staphylococcus aureus*. *J Biol Chem* **271**: 15803-15809.
- Peng, H.L., R.P. Novick, B. Kreiswirth, J. Kornblum & P. Schlievert, (1988) Cloning, characterization, and sequencing of an accessory gene regulator (agr) in *Staphylococcus aureus*. *J Bacteriol* **170**: 4365-4372.
- Peschel, A., R.W. Jack, M. Otto, L.V. Collins, P. Staubitz, G. Nicholson, H. Kalbacher, W.F. Nieuwenhuizen, G. Jung, A. Tarkowski, K.P. van Kessel & J.A. van Strijp, (2001) *Staphylococcus aureus* resistance to human defensins and evasion of neutrophil killing via the novel virulence factor MprF is based on modification of membrane lipids with l-lysine. *J Exp Med* **193**: 1067-1076.
- Peschel, A., M. Otto, R.W. Jack, H. Kalbacher, G. Jung & F. Götz, (1999) Inactivation of the *dlt* operon in *Staphylococcus aureus* confers sensitivity to defensins, protegrins, and other antimicrobial peptides. *J Biol Chem* **274**: 8405-8410.

- Peters, G., R. Locci & G. Pulverer, (1982) Adherence and growth of coagulase-negative staphylococci on surfaces of intravenous catheters. *J Infect Dis* **146**: 479-482.
- Pulverer, G., G. Peters & F. Schumacher-Perdreau, (1987) Coagulase-negative staphylococci. *Zbl. Bact. Hyg. A* **264**: 1-28.
- Qian, Z., Y. Yin, Y. Zhang, L. Lu, Y. Li & Y. Jiang, (2006) Genomic characterization of ribitol teichoic acid synthesis in *Staphylococcus aureus*: genes, genomic organization and gene duplication. *BMC Genomics* **7**: 74.
- Rennermalm, A., M. Nilsson & J.I. Flock, (2004) The fibrinogen binding protein of *Staphylococcus epidermidis* is a target for opsonic antibodies. *Infect Immun* **72**: 3081-3083.
- Rohde, H., C. Burdelski, K. Bartscht, M. Hussain, F. Buck, M.A. Horstkotte, J.K. Knobloch, C. Heilmann, M. Herrmann & D. Mack, (2005) Induction of *Staphylococcus epidermidis* biofilm formation via proteolytic processing of the accumulation-associated protein by staphylococcal and host proteases. *Mol Microbiol* **55**: 1883-1895.
- Rokas, A., B.L. Williams, N. King & S.B. Carroll, (2003) Genome-scale approaches to resolving incongruence in molecular phylogenies. *Nature* **425**: 798-804.
- Rosenstein, R., C. Nerz, L. Biswas, A. Resch, G. Raddatz, S.C. Schuster & F. Götz, (2009) Genome analysis of the meat starter culture bacterium *Staphylococcus carnosus* TM300. *Appl Environ Microbiol* **75**: 811-822.
- Rowland, S.J., W.M. Stark & M.R. Boocock, (2002) Sin recombinase from *Staphylococcus aureus*: synaptic complex architecture and transposon targeting. *Mol Microbiol* **44**: 607-619.
- Rupp, M.E., P.D. Fey, C. Heilmann & F. Götz, (2001) Characterization of the Importance of *Staphylococcus epidermidis* Autolysin and Polysaccharide Intercellular Adhesin in the pathogenesis of intravascular catheter-associated infection in a rat model. *J Infect Dis* **183**: 1038-1042.
- Saising, J., L. Dube, A.K. Ziebandt, S.P. Voravuthikunchai, M. Nega & F. Gotz, (2012) Activity of gallidermin on *Staphylococcus aureus* and *Staphylococcus epidermidis* biofilms. *Antimicrob Agents Chemother* **56**: 5804-5810.
- Schumacher-Perdreau, F., C. Heilmann, G. Peters, F. Götz & G. Pulverer, (1994) Comparative analysis of a biofilm-forming *Staphylococcus epidermidis* strain and its adhesion-positive, accumulation-negative mutant M7. *FEMS Microbiol Lett* **117**: 71-78.
- Siguier, P., J. Perochon, L. Lestrade, J. Mahillon & M. Chandler, (2006) ISfinder: the reference centre for bacterial insertion sequences. *Nucleic Acids Res* **34**: D32-36.
- Staden, R., D.P. Judge & J.K. Bonfield, (2003) *Managing Sequencing Projects in the GAP4 Environment. Introduction to Bioinformatics. A Theoretical and Practical Approach*. Human Press Inc., Totawa, NJ 07512.
- Stothard, P. & D.S. Wishart, (2005) Circular genome visualization and exploration using CGView. *Bioinformatics* **21**: 537-539.
- Swoboda, J.G., J. Campbell, T.C. Meredith & S. Walker, (2010) Wall teichoic acid function, biosynthesis, and inhibition. *ChemBiochem* **11**: 35-45.
- Takeuchi, F., S. Watanabe, T. Baba, H. Yuzawa, T. Ito, Y. Morimoto, M. Kuroda, L. Cui, M. Takahashi, A. Ankai, S. Baba, S. Fukui, J.C. Lee & K. Hiramatsu, (2005) Whole-genome sequencing of *staphylococcus haemolyticus* uncovers the extreme plasticity of its genome and the evolution of human-colonizing staphylococcal species. *J Bacteriol* **187**: 7292-7308.

- Tatusov, R.L., E.V. Koonin & D.J. Lipman, (1997) A genomic perspective on protein families. *Science* **278**: 631-637.
- Teufel, P. & F. Götz, (1993) Characterization of an extracellular metalloprotease with elastase activity from *Staphylococcus epidermidis*. *J Bacteriol* **175**: 4218-4224.
- Tse, H., H.W. Tsoi, S.P. Leung, S.K. Lau, P.C. Woo & K.Y. Yuen, (2010) Complete genome sequence of *Staphylococcus lugdunensis* strain HKU09-01. *J Bacteriol* **192**: 1471-1472.
- Tse, H., H.W. Tsoi, S.P. Leung, I.J. Urquhart, S.K. Lau, P.C. Woo & K.Y. Yuen, (2011) Complete genome sequence of the veterinary pathogen *Staphylococcus pseudintermedius* strain HKU10-03, isolated in a case of canine pyoderma. *J Bacteriol* **193**: 1783-1784.
- Vuong, C., C. Gerke, G.A. Somerville, E.R. Fischer & M. Otto, (2003) Quorum-sensing control of biofilm factors in *Staphylococcus epidermidis*. *J Infect Dis* **188**: 706-718.
- Vuong, C., S. Kocianova, J.M. Voyich, Y. Yao, E.R. Fischer, F.R. DeLeo & M. Otto, (2004) A crucial role for exopolysaccharide modification in bacterial biofilm formation, immune evasion, and virulence. *J Biol Chem* **279**: 54881-54886.
- Weidenmaier, C., J.F. Kokai-Kun, S.A. Kristian, T. Chanturiya, H. Kalbacher, M. Gross, G. Nicholson, B. Neumeister, J.J. Mond & A. Peschel, (2004) Role of teichoic acids in *Staphylococcus aureus* nasal colonization, a major risk factor in nosocomial infections. *Nat Med* **10**: 243-245.
- Wu, S., H. de Lencastre & A. Tomasz, (1996) Sigma-B, a putative operon encoding alternate sigma factor of *Staphylococcus aureus* RNA polymerase: molecular cloning and DNA sequencing. *J Bacteriol* **178**: 6036-6042.
- Xu, L., H. Li, C. Vuong, V. Vadyvaloo, J. Wang, Y. Yao, M. Otto & Q. Gao, (2006) Role of the luxS quorum-sensing system in biofilm formation and virulence of *Staphylococcus epidermidis*. *Infect Immun* **74**: 488-496.
- Yao, Y., D.E. Sturdevant & M. Otto, (2005) Genomewide analysis of gene expression in *Staphylococcus epidermidis* biofilms: insights into the pathophysiology of *S. epidermidis* biofilms and the role of phenol-soluble modulins in formation of biofilms. *J Infect Dis* **191**: 289-298.
- Yarwood, J.M., J.K. McCormick & P.M. Schlievert, (2001) Identification of a novel two-component regulatory system that acts in global regulation of virulence factors of *Staphylococcus aureus*. *J Bacteriol* **183**: 1113-1123.
- Zhang, Y.Q., S.X. Ren, H.L. Li, Y.X. Wang, G. Fu, J. Yang, Z.Q. Qin, Y.G. Miao, W.Y. Wang, R.S. Chen, Y. Shen, Z. Chen, Z.H. Yuan, G.P. Zhao, D. Qu, A. Danchin & Y.M. Wen, (2003) Genome-based analysis of virulence genes in a non-biofilm-forming *Staphylococcus epidermidis* strain (ATCC 12228). *Mol Microbiol* **49**: 1577-1593.
- Zhang, Z., S. Schwartz, L. Wagner & W. Miller, (2000) A greedy algorithm for aligning DNA sequences. *J Comput Biol* **7**: 203-214.
- Ziebuhr, W., C. Heilmann, F. Götz, P. Meyer, K. Wilms, E. Straube & J. Hacker, (1997) Detection of the intercellular adhesion gene cluster (*ica*) and phase variation in *Staphylococcus epidermidis* blood culture strains and mucosal isolates. *Infect Immun* **65**: 890-896.
- Ziebuhr, W., V. Krimmer, S. Rachid, I. Lößner, F. Götz & J. Hacker, (1999) A novel mechanism of phase variation of virulence in *Staphylococcus epidermidis*: evidence for control of the polysaccharide intercellular adhesin synthesis by alternating insertion and excision of the insertion sequence element IS256. *Mol Microbiol* **32**: 345-356.

Tables

Table 1: General genomic features of the *S. epidermidis* O47 genome in comparison to other staphylococci

Strain	Size[bp]	No. CDS	Coding density [%]	GC content [%]		No. tRNA genes	No. rRNA	
				Total	Coding		Genes	Operons
<i>S. epidermidis</i>								
O47	2,518,182	2,337	83.3	32.1	32.9	61	19	5
RP62A	2,616,530	2,493	82.6	32.2	32.9	61	19	5
ATCC 12228	2,499,279	2,416	83.5	32.1	32.9	60	16	5
<i>S. aureus</i>								
N315	2,814,816	2,583	83.5	32.8	33.6	62	16	5
USA300	2,872,769	2,560	82,1	32.8	33.5	53	16	5
NCTC 8325	2,821,361	2,891	85,1	32.9	33.5	61	16	5
<i>S. haemolyticus</i>								
JCSC1435	2,685,015	2,676	86.0	32.8	33.4	59	16	5
<i>S. saprophyticus</i>								
ATCC 15305	2,516,575	2,446	83.7	33.2	34.0	61	20	5
<i>S. carnosus</i>								
TM300	2,566,424	2,461	85.8	34.6	35.3	60	16	5

Table 2: sRNA content in *S. epidermidis*

Rfam Seed	Description	No. present in		
		O47	RP62A	ATCC 12228
RF00010	Bacterial RNase P class A	1	1	1
RF00011	Bacterial RNase P class B	1	1	1
RF00013	6S / SsrS RNA	1	1	1
RF00023	transfer-messenger RNA	1	1	1
RF00050	FMN riboswitch (RFN element)	2	2	2
RF00059	TPP riboswitch (THI element)	5	5	5
RF00080	yybP-ykoY leader	1	1	1
RF00162	SAM riboswitch (S box leader)	4	4	4
RF00167	Purine riboswitch	1	1	1
RF00168	Lysine riboswitch	2	2	2
RF00177	Bacterial small subunit ribosomal RNA	6	6	5
RF00230	T-box leader	14	14	14
RF00234	glmS glucosamine-6-phosphate activated ribozyme	1	1	1
RF00238	ctRNA	2	1	3
RF00503	RNAIII	1	1	1
RF00504	Glycine riboswitch	1	1	1
RF00515	PyrR binding site	2	2	2
RF00522	PreQ1 riboswitch	1	1	1
RF00555	Ribosomal protein L13 leader	1	1	1
RF00556	Ribosomal protein L19 leader	1	1	1

RF00557	Ribosomal protein L10 leader	1	1	1
RF00558	Ribosomal protein L20 leader	1	1	1
RF00559	Ribosomal protein L21 leader	1	1	1
RF01118	Pseudoknot of the domain G(G12) of 23S ribosomal RNA	6	6	5
RF01405	STnc490k Hfq binding RNA	2	2	3
RF01458	<i>Listeria</i> sRNA rli23	1	2	2
RF01691	Bacillus-plasmid RNA	1	1	1
RF01694	Bacteroides-1 RNA	1	1	1
RF01725	SAM-I/IV variant riboswitch	1	1	1
RF01751	potC RNA	1	1	1
RF01764	yjdF RNA	1	3	1
RF01775	RNA <i>S.aureus</i> Orsay G	1	1	1
RF01797	Fst antitoxin sRNA	4	6	4
RF01816	RNA Staph. aureus A	1	1	1
RF01819	RNA Staph. aureus D	1	1	1
RF01820	RNA Staph. aureus E	1	1	1
RF01821	RNA Staph. aureus H	1	1	1
RF01854	Bacterial large signal recognition particle RNA	1	1	1
<hr/> Σ		76	80	77

Table 3: *S. epidermidis* CRISPR elements

Start	End	Length	Direct Repeat		Spacers		
			Consensus	Length	No.	Length	
<i>S. epidermidis</i> O47 CRISPR candidates (CRISPRfinder)							
332,374	332,464	90	CAACATAGAGAATTTACCGAGAAATTCAACA	32	1	26	
795,622	795,723	101	TCATGTATAAGAAACACTAAATACCTATGTATTAAGTG	38	1	25	
803,654	803,749	95	CATGCATAACCAAAAGTACGATTTACTTCGTAAA	34	1	27	
2,071,669	2,071,752	83	CAACTTGCCTTGTCCGTGGAATTC	25	1	33	
<i>S. epidermidis</i> ATCC 12228 CRISPR candidate (CRISPRdb)							
587,189	587,284	96	CATAAGTGACACAAGCAATTA AAAATTGCAGTG	33	1	30	
<i>S. epidermidis</i> RP62A							
CRIPSR candidate (CRISPRdb)							
1,993,515	1,993,597	83	ATCATAGATAGTTTTGCTTCTGTTT	25	1	33	
CRIPSR element (CRISPRdb)							
2,517,620	2,517,868	249	GTTCTCGTCCCCTTTTCTTCGGGGTGGGTATCGATCC	37	3	33	
<i>S. epidermidis</i> 1457 CRISPR candidates (CRISPRfinder)							
446,430	446,513	83	GAAATTCTACGGACAAGGCAAGTTG	25	1	34	
1,722,487	1,722,551	92	TTATACATGAACCTCAAGCTCATGTGTTT	29	1	35	
2,034,010	2,034,073	33	CACTGCAATTTTTAATTGCTTGTGTCACTTATG	33	1	30	
2,185,718	2,185,777	32	TGTTGAATTTCCCGGTGAAATTCTCTATGTTG	32	1	27	

Table 4: *S. epidermidis* STAR elements

Strain	No. STAR elements		Start	End	Sequence
	Total	Sequence			
<i>S. epidermidis</i>					
O47	10		276,312	276,299	
		3	1,928,864	1,928,851	TGTGTTGGGGCCCC
			2,100,125	2,100,138	
			57,083	57,070	
			57,141	57,128	
		6	357,412	357,399	TTTGTTGGGGCCCC
		1,293,199	1,293,212		
		1,293,258	1,293,271		
		2,071,708	2,071,721		
ATCC 12228	9	1	57,198	57,185	TTTGTTGGGGCCCA
		3			TGTGTTGGGGCCCC
		5			TTTGTTGGGGCCCC
		1			TTTGTTGGGGCCCA
RP62A	8	1			TGTGTTGGGGCCCC
		6			TTTGTTGGGGCCCC
		1			TTTGTTGGGGCCCA
<i>S. aureus</i>					
N315	58	36			TGTGTTGGGGCCCC
		9			TGTGTTGGGGCCCA

		3	TATGTTGGGGCCCA
		6	TTTGTGGGGCCCC
		4	TTTGTGGGGCCCA
		21	TGTGTTGGGGCCCC
		5	TGTGTTGGGGCCCA
USA300	42	3	TATGTTGGGGCCCA
		1	TATGTTGTGGCCCC
		6	TTTGTGGGGCCCC
		6	TTTGTGGGGCCCA
		22	TGTGTTGGGGCCCC
		5	TGTGTTGGGGCCCA
NCTC 8325	42	3	TATGTTGGGGCCCA
		1	TATGTTGTGGCCCC
		7	TTTGTGGGGCCCC
		4	TTTGTGGGGCCCA
<i>S. carnosus</i>			
TM300	0		

Table 5: Truncated and fragmented genes in *S. epidermidis* O47

Gene	Product	Locus
	fragmented hypothetical	SEO_381
		SEO_382
	fragmented hypothetical	SEO_1180
		SEO_1181
<i>sdrG'</i>	fragmented fibrinogen binding protein	SEO_199
<i>sdrG''</i>		SEO_200
<i>zwf'</i>	fragmented glucose-6-phosphate 1-dehydrogenase	FHQ17_09435
<i>zwf''</i>		SEO_555
<i>pre'</i>	fragmented plasmid recombination enzyme	SEO_579
<i>pre''</i>		SEO_580
	fragmented manganese transport protein	SEO_651
		SEO_650
	fragmented manganese transport protein	SEO_2300
		SEO_2299
<i>agrC'</i>	fragmented accessory gene regulator C	SEO_1541
<i>agrC''</i>		SEO_1542
<i>gehC'</i>	fragmented lipase	SEO_2129
<i>gehC''</i>		SEO_2128
	fragmented putative lipoprotein	SEO_2212
		SEO_2213
	fragmented two-component sensor histidine kinase	SEO_2227
		SEO_2228
		SEO_27
		SEO_32
	truncated hypothetical	FHQ17_11070
		FHQ17_05450
		SEO_2233
<i>arsC'</i>	truncated arsenate reductase	SEO_202
<i>fosB'</i>	truncated metallothiol transferase	SEO_2176

Table 6: *S. epidermidis* species genes

Gene	Product	Locus
		FHQ17_10710
	putative lipoprotein	FHQ17_10095
		FHQ17_00490
		FHQ17_08795
	cell wall surface anchor family protein	FHQ17_05655
		FHQ17_04260
		FHQ17_07780
	surface lipoprotein-related protein	FHQ17_05475
		SEO_78
	putative transposase	FHQ17_09440
<i>psmβ3</i>	phenol soluble modulins beta 3	SEO_692
<i>ebh</i>	extracellular matrix binding protein	SEO_1008
<i>epbS</i>	elastin binding protein	SEO_1045
	transposase	SEO_1735
<i>gldA</i>	glycerol dehydrogenase	FHQ17_00820
	tributyryl esterase	FHQ17_00780
	K05846 osmoprotectant transport system permeaseprotein	FHQ17_00765
<i>mgo2</i>	malate:quinone oxidoreductase	FHQ17_00510

Table 7: Mobile elements of *S. epidermidis* in comparison to other staphylococci

Strain	IS elements	Transposons	Prophages	SCC	Genomic island
<i>S. epidermidis</i>					
O47	15	-	2	1	6
RP62A	17	4	1	1	6
ATCC 12228	18	-	-	2	7
<i>S. aureus</i>					
N315	11	5	1	1	3
USA300	6	2	2	1	3
NCTC 8325	2	-	3	-	2
<i>S. haemolyticus</i>					
JCSC1435	82	2	2	1	5
<i>S. saprophyticus</i>					
ATCC 15305	2	-	-	2	1
<i>S. carnosus</i>					
TM300	-	-	1	-	1

Table 8: Family characterisation of the 15 IS elements in *S. epidermidis* O47

IS element	Family	Length (Ref)	Start	Stop	Strand	
			176,242	177,805	+	
			382,194	383,757	-	
			549,603	551,166	+	
ISSep2	IS110	1564 (1564)	570,617	572,182	-	
			1,423,352	1,424,915	+	
			1,839,954	1,841,517	-	
			1,893,463	1,895,026	+	
			2,079,660	2,081,223	-	
ISSep3	IS200/IS605	741 (741)	1,241,794	1,242,534	-	
			2,217,989	2,218,729	-	
			2,442,798	2,443,587	+	
IS431mec-like	IS6	790 (790)	2,451,288	2,452,077	+	
			791 (790)	2,478,083	2,478,873	-
			789 (790)	2,481,200	2,481,988	-
ISSau4	IS3	1249 (1261)	2,416,939	2,418,187	+	

Table 9: Genomic islands in *S. epidermidis*

Island	Start	End	Integrase	No. genes	Reference
vSe1					(Gill <i>et al.</i> , 2005)
O47	-	-	-	-	
ATCC 12228	SE0110	-	-	1	
RP62A	SERP2213	SERP2237	-	25	
vSe2/φSe1					(Gill <i>et al.</i> , 2005, Takeuchi <i>et al.</i> , 2005)
O47	FHQ17_05445	SEO_1369	SEO_1369	36	
ATCC 12228	SE1472	SE1509	SE1509	38	
RP62A	-	-	-	-	
vSeγ					(Gill <i>et al.</i> , 2005)
O47	FHQ17_08705	FHQ17_08680	-	5	
ATCC 12228	SE0845	SE0850	-	5	
RP62A	SERP0735	SERP0740	-	5	
vSe3					(Takeuchi <i>et al.</i> , 2005)
O47	SEO_427	FHQ17_09985	SEO_427	20	
ATCC 12228	SE0568	SE0588	SE0568	21	
RP62A	SERP0455	SERP0477	-	23	
vSe4					(Takeuchi <i>et al.</i> , 2005)
O47	-	FHQ17_07780	-	1	
ATCC 12228	SE0988	SE0994	SE0988	7	
RP62A	SERP0878	SERP0882	-	5	

vSe5					(Takeuchi <i>et al.</i> , 2005)
O47	FHQ17_05495	FHQ17_05445	FHQ17_05445	8	
ATCC 12228	SE1463	SE1473	SE1472	11	
RP62A	SERP1357	SERP1362	-	6	
vSe6					(Takeuchi <i>et al.</i> , 2005)
O47	FHQ17_12035	FHQ17_12065	Fragments: SEO_72 - SEO_70	7	
ATCC 12228	SE2339	SE2346	Fragments: SE2343 - SE2345	8	
RP62A	SERP0075	SERP0071	-	5	
vSe7					
O47	,FHQ17_12320	SEO_32	-	9	
ATCC 12228	SE2395	SE2388	-	8	
RP62A	-	-	-	-	

Table 10: Global regulatory systems of *S. epidermidis* O47 and their homologs

Gene	Locus	Best hit (strain/accession)	Function	Reference
<i>agrB</i>	FHQ17_04225	BCM-HMP0060/ZP_04824327		
<i>agrD</i>	HQ17_04220	ATCC 12228/NP_765191		
<i>agrC'</i>	SEO_1541	BCM-HMP0060/ZP_04824325	required for a series of secreted exoproteins	(Peng <i>et al.</i> , 1988)
<i>agrC''</i>	SEO_1542	BCM-HMP0060/ZP_04824325		
<i>agrA</i>	FHQ17_04210	ATCC 12228NP_765193		
<i>arlR</i>	FHQ17_07265	ATCC 12228/NP_764654	involved in Adhesion, Autolysis, and Extracellular Proteolytic Activity	(Fournier & Hooper, 2000)
<i>arlS</i>	FHQ17_07270	ATCC 12228/NP_764655		
<i>apsX</i>	FHQ17_10815	ATCC 12228/NP_763981		
<i>apsR</i>	FHQ17_10810	ATCC 12228/NP_763982	controlling resistance mechanisms to antimicrobial peptides	(Li <i>et al.</i> , 2007)
<i>apsS</i>	FHQ17_10805	ATCC 12228/NP_763983		
<i>lytR</i>	FHQ17_02300	RP62A/YP_189581	control the rate of autolysis	(Brunskill & Bayles, 1996)
<i>lytS</i>	HQ17_02305	BCM-HMP0060/ZP_04826339		
<i>mgrA</i>	FHQ17_10660	ATCC 12228/NP_764012	regulator of Autolysis	(Ingavale <i>et al.</i> , 2005)
<i>saeR</i>	FHQ17_10550	ATCC 12228/NP_764033		
<i>saeS</i>	FHQ17_10555	ATCC 12228/NP_764034		
<i>rot</i>	FHQ17_05625	RP62A/YP_188894	regulator of Virulence Factor Expression	(McNamara <i>et al.</i> , 2000)
<i>sarA</i>	FHQ17_11000	ATCC 12228/NP_763945		
<i>sarR</i>	FHQ17_03000	ATCC 12228/NP_765423		
<i>sarV</i>	FHQ17_03140	ATCC 12228/NP_765395		
<i>sarX</i>	FHQ17_10765	BMC-HMP0060/ZP_04824566	involved in the global regulation of exoproteins	(Cheung <i>et al.</i> , 1992)
<i>sarY</i>	FHQ17_02990	ATCC 12228/NP_765425		
<i>sarZ</i>	FHQ17_02505	ATCC 12228/NP_765522		
<i>sigB</i>	FHQ17_04040	ATCC 12228/NP_765223	alternate sigma factor	(Wu <i>et al.</i> , 1996)

<i>ssrA</i>	FHQ17_06900	RP62A/YP_188631		
<i>ssrB</i>	FHQ17_06905	ATCC 12228/NP_764731	regulation of Virulence Factors	(Yarwood <i>et al.</i> , 2001)
<i>spxA</i>	FHQ17_09530	ATCC 12228/NP_764241	impacting Stress Tolerance and Biofilm Formation	(Pamp <i>et al.</i> , 2006)
<i>tcaR</i>	FHQ17_02655	ATCC 12228/NP_765492		
<i>tcaA</i>	FHQ17_02660	ATCC 12228/NP_765491	involved in cell wall synthesis	(Brandenberger <i>et al.</i> , 2000)
<i>tcaB</i>	FHQ17_02665	ATCC 12228/NP_765490		
<i>vraR</i>	FHQ17_04555	ATCC 12228/NP_765124		
<i>vraS</i>	FHQ17_04550	ATCC 12228/NP_765125	regulator of cell wall peptidoglycan synthesis	(Kuroda <i>et al.</i> , 2003)
<i>yycF</i>	FHQ17_00110	ATCC 12228/NP_763573		
<i>yycG</i>	SEO_2312	ATCC 12228/NP_763574		
<i>yycH</i>	FHQ17_00120	W23144/ZP_04797681		
<i>yycI</i>	FHQ17_00125	ATCC 12228/NP_763576		
<i>yycJ</i>	FHQ17_00130	ATCC 12228/NP_763577		
<i>luxS</i>	FHQ17_03720	ATCC 12228/NP_765287	repressed biofilm formation through a cell-cell signaling mechanism	(Xu <i>et al.</i> , 2006)

Table 11: *S. epidermidis* virulence factors in *S. epidermidis* O47

Gene	Locus	Best hit (strain/accession)	Product	Reference
<i>aae</i>	FHQ17_11920	ATCC 12228/NP_765874	bifunctional autolysin and adhesin	(Heilmann <i>et al.</i> , 1997)
<i>aap</i>	SEO_2222	RP62A/YP_189945	accumulation associated protein	(Rohde <i>et al.</i> , 2005)
<i>atlE</i>	FHQ17_09190	RP62A/YP_188221	bifunctional autolysin and adhesin	(Heilmann <i>et al.</i> , 1997)
<i>capB</i>	FHQ17_01885	RP62A/YP_189663		
<i>capC</i>	FHQ17_01890	ATCC 12228/NP_765647	capsule biosynthesis protein	(Kocianova <i>et al.</i> , 2005)
<i>capA</i>	FHQ17_01895	RP62A/YP_189661		
<i>dltA</i>	FHQ17_09805	ATCC 12228/NP_764179		
<i>dltB</i>	FHQ17_09800	ATCC 12228/NP_764180	dlt protein	(Peschel <i>et al.</i> , 1999)
<i>dltC</i>	FHQ17_09795	ATCC 12228/NP_764181		
<i>dltD</i>	FHQ17_09790	ATCC 12228/NP_764182		
<i>ebp</i>	SEO_1045	BCM-HMP0060/ZP_04825375	elastin binding protein	(Park <i>et al.</i> , 1996)
<i>gehC'</i>	SEO_2129	RP62A/YP_189847		
<i>gehC''</i>	SEO_2128	RP62A/YP_189847	lipase	(Longshaw <i>et al.</i> , 2000)
<i>gehD</i>	SEO_2214	RP62A/YP_189935		
<i>icaA</i>	FHQ17_01070	sp—Q8GLC5.1—ICAA_STAEP		
<i>icaD</i>	FHQ17_01065	RP62A/YP_189844	intercellular adhesion protein	(Heilmann <i>et al.</i> , 1996b)
<i>icaB</i>	FHQ17_01060	RP62A/YP_189845		
<i>icaC</i>	FHQ17_01055	RP62A/YP_189846		
<i>mprF</i>	FHQ17_07565	RP62A/YP_188509	multiple peptide resistance factor	(Peschel <i>et al.</i> , 2001)
<i>oatA</i>	FHQ17_01730	RP62A/YP_189693	O-acetyltransferase A	(Bera <i>et al.</i> , 2006)
<i>psma</i>	FHQ17_12005	RP62A/AAW55287	phenol soluble modulín	(Yao <i>et al.</i> , 2005)

<i>psmβ1</i>	FHQ17_08685	ATCC 12228/NP_764403		
<i>psmβ2</i>	FHQ17_08690	ATCC 12228/NP_764402		
<i>psmβ3</i>	SEO_692	RP62A/YP_188319		
<i>hld</i>	SEO_1538A	ATCC 12228/NP_765189		
<i>psmδ</i>	FHQ17_12000			
<i>psmε</i>	FHQ17_10045			
<i>sepA</i>	FHQ17_01275	ATCC 12228/NP_765774	extracellular elastase	(Teufel & Götz, 1993)
<i>sdrF</i>	FHQ17_12320	ATCC 12228/NP_765950	collagen-binding protein	(Arrecubieta <i>et al.</i> , 2007)
<i>sdrG'</i>	SEO_199	ATCC 12228/NP_763886		
<i>sdrG''</i>	SEO_200	sp—Q9KI13.1—SDRG_STAEP	fibrinogen binding protein	(Rennermalm <i>et al.</i> , 2004)
<i>sdrH</i>	SEO_1537	BCM-HMP0060/ZP_04824329	fibrinogen binding protein	(McCrea <i>et al.</i> , 2000)
<i>sitA</i>	FHQ17_10915	W23144/ZP_04796443		
<i>sitB</i>	FHQ17_10920	ATCC 12228/NP_76961	iron ABC transporter protein	(Cockayne <i>et al.</i> , 1998)
<i>sitC</i>	FHQ17_10925	ATCC 12228/NP_76960		
<i>sfnaD</i>	FHQ17_03480	RP62A/YP_189345		
<i>sfnaA</i>	FHQ17_03485	ATCC 12228/NP_765326		
<i>sfnaB</i>	FHQ17_03490	RP62A/YP_189343	staphyloferrin A biosynthesis protein	(Lindsay <i>et al.</i> , 1994, Cotton <i>et al.</i> , 2009)
<i>sfnaC</i>	FHQ17_03495	ATCC 12228/NP_765324		
<i>sspA</i>	FHQ17_05050	ATCC 12228/NP_765098	serine protease	
<i>sspB</i>	FHQ17_00605	ATCC 12228/NP_763739	cysteine protease	(Dubin <i>et al.</i> , 2001)
<i>tarI</i>	FHQ17_11345	ATCC 12228/NP_763874		
<i>tarJ</i>	FHQ17_11340	ATCC 12228/NP_763875		
<i>tarL</i>	FHQ17_11335	BCM-HMP0060/ZP_04824448	teichoic acid biosynthesis protein	(Brown <i>et al.</i> , 2008, Fitzgerald & Foster, 2000, Holland <i>et al.</i> , 2011, Qian <i>et al.</i> , 2006, Swoboda <i>et al.</i> , 2010,
<i>tagA</i>	SEO_277	ATCC 12228/NP_763965		
<i>tagH</i>	FHQ17_10895	BCM-HMP0060/ZP_04824541		

<i>tagG</i>	FHQ17_10890	ATCC 12228/NP_763867		Weidenmaier <i>et al.</i> , 2004)
<i>tagB</i>	FHQ17_10885	ATCC 12228/NP_763868		
<i>tagX</i>	FHQ17_10880	ATCC 12228/NP_763869		
<i>tagD</i>	FHQ17_10875	ATCC 12228/NP_763870		
<i>tagO</i>	FHQ17_10310	BCM-HMP0060/ZP_04824654		
<i>tagF</i>	FHQ17_02600	M23864:W2(grey)/ZP_06613749		
<i>tagE</i>	FHQ17_02150	ATCC 12228/NP_765596		
<i>vraG</i>	SEO_295	ATCC 12228/NP_763984		
<i>vraF</i>	FHQ17_10800	ATCC 12228/NP_763985	ABC transporter	(Li <i>et al.</i> , 2007)

Table 12: Penicillin binding proteins in *S. epidermidis*

Gene	Product	Locus		
		O47	RP62A	ATCC 12228
<i>pbp1</i>	penicillin binding protein 1	FHQ17_08650	SERP0746	SE0856
<i>pbp2</i>	penicillin binding protein 2	FHQ17_07075	SERP1020	SE1138
<i>pbp3</i>	penicillin binding protein 3	FHQ17_06590	SERP1117	SE1238
<i>pbp4</i>	penicillin binding protein 4	-	-	SE0035

Table 13: MIC values for *S. epidermidis* O47, ATCC 12228 and RP62A and *S. carnosus* TM300 and *S. aureus* USA300.

Strains	MIC (μ l/ml)	
	Penicillin	Methicillin
<i>Staphylococcus carnosus</i> TM300	Sensitive (< 0.5)	4
<i>Staphylococcus epidermidis</i> O47	>128	2
<i>Staphylococcus epidermidis</i> 12228	>128	4
<i>Staphylococcus epidermidis</i> RP62A	>128	>128
<i>Staphylococcus aureus</i> USA300	64	>128

Table 14: Resistances in *S. epidermidis* O47

Gene	Locus	Product
	FHQ17_12065	COG: Abortive infection bacteriophage resistance protein
<i>uppP</i>	FHQ17_10675	COG: Uncharacterized bacitracin resistance protein
<i>norA</i>	FHQ17_10615	quinolone resistance protein
	FHQ17_10050	cobalt-zinc-cadmium resistance protein
	FHQ17_09350	COG: Membrane protein TerC, possibly involved in tellurium resistance
	FHQ17_08020	COG: Cystathionine beta-lyase family protein involved in aluminum resistance
	FHQ17_07320	COG: Uncharacterized protein involved in tellurite resistance
<i>cadD</i>	FHQ17_05180	cadmium resistance transporter CadD
<i>vraR</i>	FHQ17_04555	K07694 two-component system, NarL family, vancomycin resistance associated response regulator VraR
<i>vraS</i>	FHQ17_04550	K07681 two-component system, NarL family, vancomycin resistance sensor histidine kinase VraS
	FHQ17_03555	EmrB/QacA family drug resistance transporter
<i>fmhB</i>	FHQ17_03175	COG: Uncharacterized protein involved in methicillin resistance
<i>ykkC</i>	SEO_1772	K11741 quaternary ammonium compound-resistance protein SugE
	FHQ17_02950	K11741 quaternary ammonium compound-resistance protein SugE
	FHQ17_02675	COG: Multidrug resistance efflux pump
<i>tcaB</i>	FHQ17_02665	
<i>tcaA</i>	FHQ17_02660	teicoplanin-associated operon
<i>tcaR</i>	FHQ17_02665	
	SEO_1847	COG: Uncharacterized protein, homolog of Cure resistance protein CopC
<i>fmhA</i>	HQ17_02405	COG: Uncharacterized protein involved in methicillin resistance
<i>bcr</i>	FHQ17_02350	bicyclomycin resistance protein
	FHQ17_02310	K08170 MFS transporter, DHA2 family, multidrug resistance protein
<i>ohr</i>	FHQ17_01205	organic hydroperoxide resistance protein
	FHQ17_00650	K08170 MFS transporter, DHA2 family, multidrug resistance protein

<i>arsR</i>	FHQ17_00425	
<i>arsD</i>	SEO_2251	
<i>arsA</i>	FHQ17_00415	arsenical resistance operon
<i>arsR</i>	SEO_2253	
<i>arsB</i>	FHQ17_00405	
<i>arsC</i>	FHQ17_00400	
<i>merB</i>	SEO_2262	
<i>merA</i>	FHQ17_00350	mercuric resistance operon
<i>merT</i>	SEO_2263A	
<i>merR</i>	SEO_2265A	
<i>azlC</i>	FHQ17_00055	azaleucine resistance
<i>azlD</i>	FHQ17_00060	

Table 15: *S. aureus* virulence factors not found in *S. epidermidis* O47

Genes	Product
<i>clfA</i>	clumping factors
<i>clfB</i>	
<i>sdrC</i>	
<i>sdrD</i>	adhesins
<i>sdrE</i>	
<i>fnbA</i>	
<i>fnbB</i>	fibronectin binding protein
<i>cna</i>	
<i>spa</i>	immunoglobulin G-binding protein A
<i>fbpA</i>	fibrinogen binding protein gene
<i>ebp</i>	extracellular adherence protein
<i>map</i>	major histocompatibility complex class II analog protein
<i>vWbp</i>	Von Willebrand factor
<i>efb</i>	extracellular fibrinogen-binding protein
<i>coa</i>	coagulase
<i>sbi</i>	immunoglobulin binding protein
<i>tst</i>	toxic shock syndrome toxin
<i>set1-26</i>	exotoxins
<i>entA-B</i>	enterotoxins
<i>entC1-3</i>	
<i>entD-H</i>	
<i>spIA-F</i>	
<i>lukE</i>	leukotoxins
<i>lukF</i>	
<i>hla</i>	α -hemolysin
<i>hlgA-C</i>	γ -hemolysin
<i>sak</i>	staphylokinase
<i>eta</i>	exfoliative toxins
<i>etb</i>	
<i>nuc</i>	thermonuclease

Table S1: Primers used for cloning of pCtuf-sadA O47

Primer	Sequence (5'-3')
pCtuf-sadA O47 F	AGAGTTCGAGGAGGTTTAATATGGAAATGGAATTCAATGAG
pCtuf-sadA O47 R	TTAAGTACTTCAGCTAATTATTAAGCATCTTTCATATCGTAATC

Figures

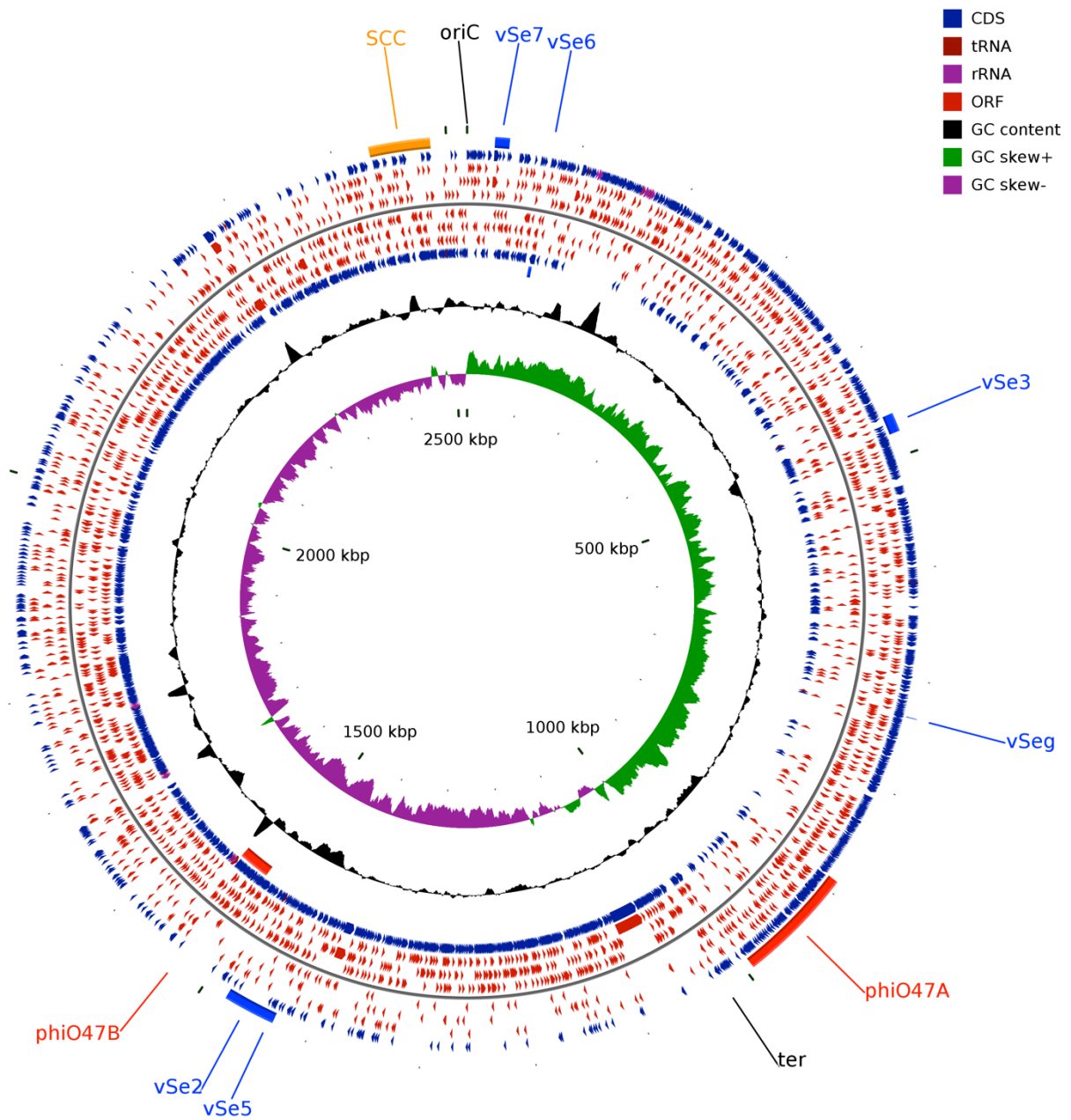


Figure 1: Circular genome plot of *S. epidermidis* O47. From outer to inner circle: ORFs of the forward strand, ORFs in the 3 different reading frames of the forward strand, ORFs of the reverse strand, ORFs in the 3 different reading frames of the reverse strand, G+C content, G+C skew. The regions containing the Staphylococcal Cassette Chromosome (SCC, orange), the putative prophages ϕ O47A, ϕ O47B (red), and the genomic islands vSe2, vSe3, vSe5, vSe6, and vSe7 (blue) are highlighted. The plot was generated using CGView (Stothard & Wishart, 2005).

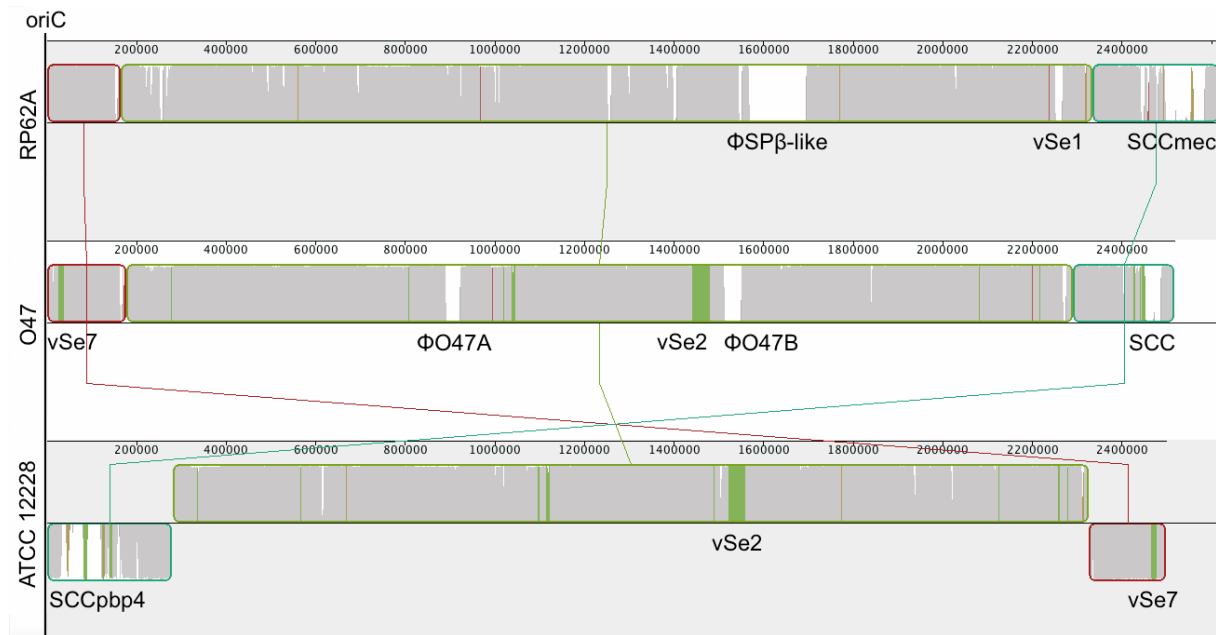


Figure 2: Mauve (Darling *et al.*, 2010) alignment of *S. epidermidis* RP62A (top), O47 (middle) and ATCC 12228 (bottom). The blocks are genomic regions which are aligned to a part of another genome. They are free from genomic rearrangement and lie above the center line if the region is in forward orientation relative to the reference sequence (RP62A at topmost) or down the center line for reverse complement orientation. The similarity profile is displayed in the blocks. White areas are regions not aligned to other genomes and colored areas are conserved among two genomes. The Staphylococcal Cassette Chromosomes (SCC), ϕ SP β , the putative prophages ϕ O47A and ϕ O47B and the genomic islands vSe1, vSe2, and vSe7 are highlighted.

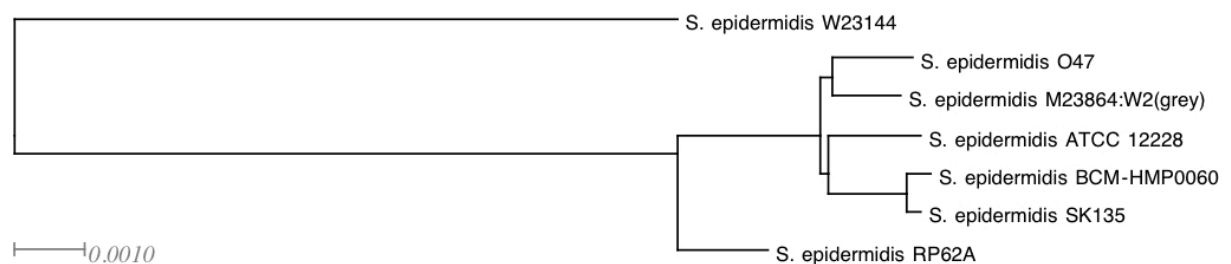


Figure 3: Phylogenetic tree of sequenced *S. epidermidis*. Strains O47, ATCC 12228, RP62A and the draft sequences of W23144, M23864:W2(grey), BCM-HMP0060, and SK135 displayed as phylogram. The sequence divergence of 0.0010% corresponds to 1081 nucleotides. *S. epidermidis* O47 is closest related to M23864:W2(grey) and W23144 is most distantly related to the other strains.

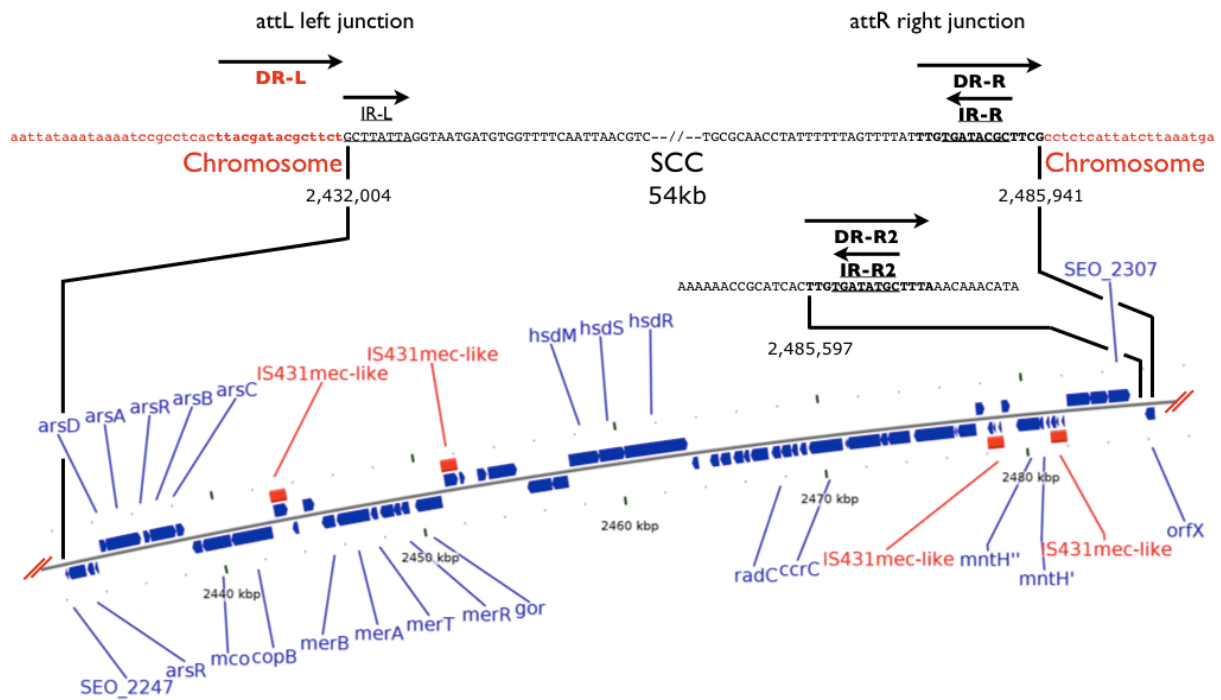


Figure 4: The junction sites and the region of the *S. epidermidis* O47 genome showing the Staphylococcal Cassette Chromosome (SCC). The SCC contains four IS431mec-like elements. They flank the mercury resistance cluster and a fragmented manganese transport protein (*mntH'* and *mntH''*), respectively. Additionally, an arsenical resistance cluster, a multicopper oxidase (*mco*), a copper transporting ATPase (*copB*), a glutathione reductase (*gor*), the restriction modification system (*hsd*), and the DNA repair protein gene *radC* is located in the SCC. Lower case red letters: part of the *S. epidermidis* O47 Chromosome; capital black letters: part of the SCC; bold letters: direct repeat (DR); underlined letters: inverted repeat (IR). The plot was generated using CGview (Stothard & Wishart, 2005).

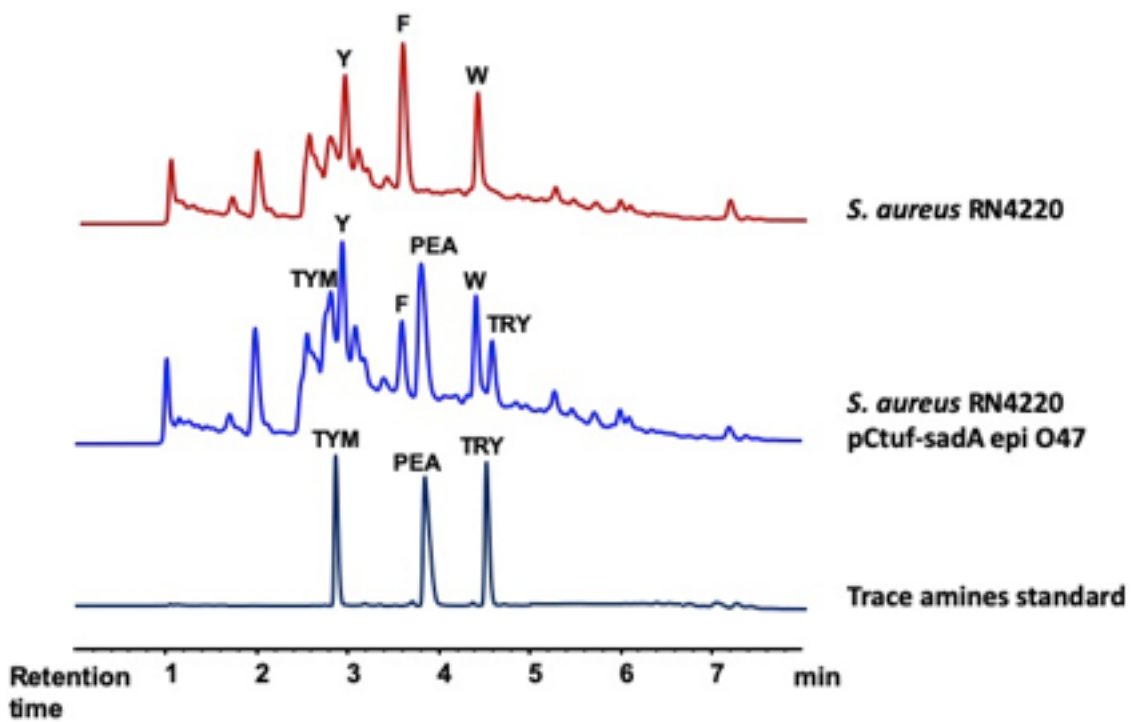


Figure 5: HPLC chromatograms of *sadA* of *S. epidermidis* O47 expression. *sadA* gene of *S. epidermidis* O47 was cloned into pCtufamp plasmid (Ebner *et al.*, 2015) and expressed in *S. aureus* RN4220. The overnight culture of *S. aureus* RN4220 harboring pCtuf-sadA epi O47 with 10 $\mu\text{g/ml}$ of chloramphenicol containing (basic medium) BM medium was collected and analyzed using HPLC. *S. aureus* RN4220 harboring pCtuf-sadA epi O47 was shown to be able to produce trace amines (TYM-tyramine; PEA-pehenthylamine; TRY-tryptamine) from aromatic amino acids (Y-tyrosine; F-phenylalanine; W-tryptophan).

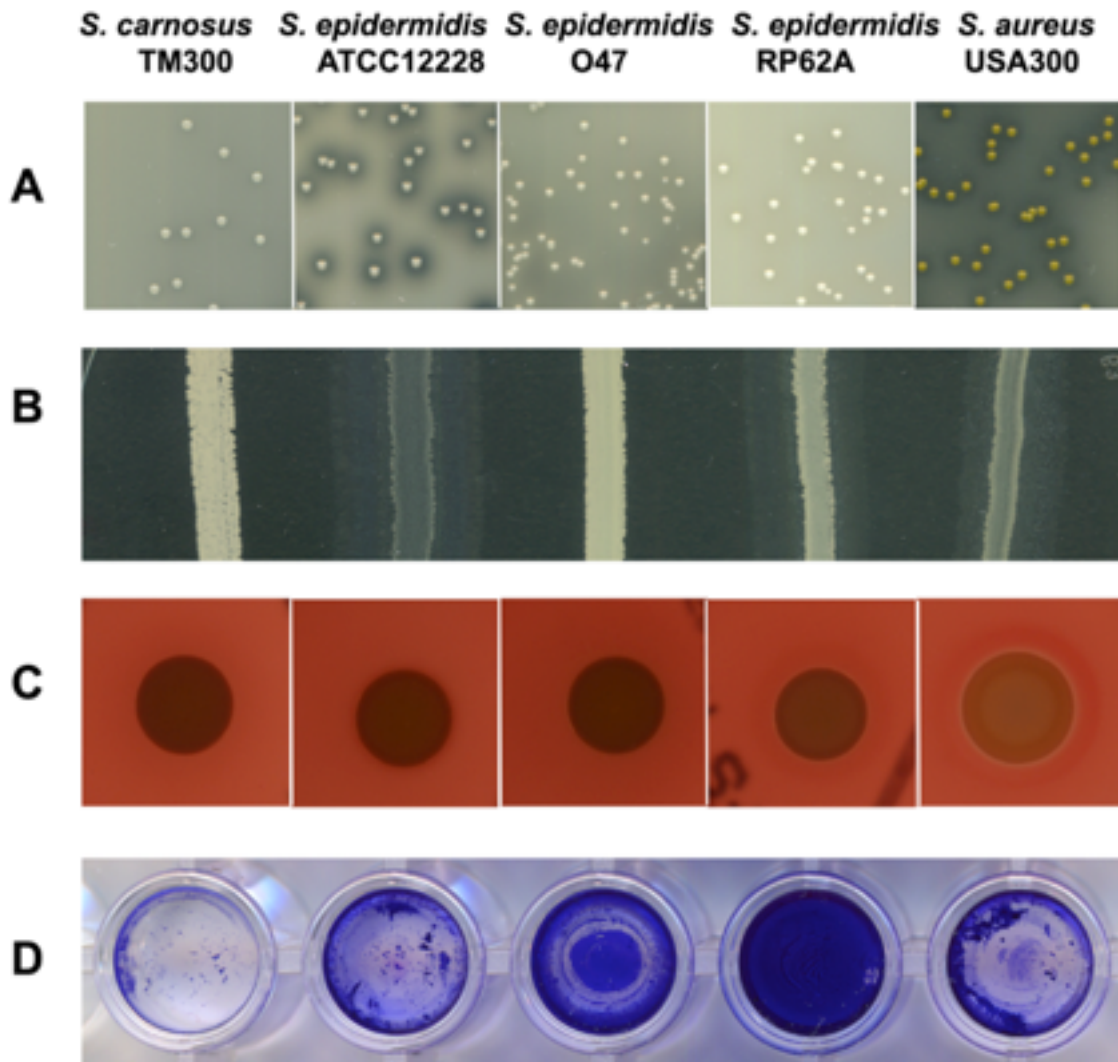


Figure 6: Comparison of characteristics associated with pathogenicity and/or virulence factors among selected *S. epidermidis* strains. From left: *S. carnosus* TM300, *S. epidermidis* ATCC 12228, *S. epidermidis* O47, *S. epidermidis* RP62A and *S. aureus* USA300. The general virulence factors (in brackets) caused the following characteristics: (A) proteolysis (protease) (B) lipolysis (lipase) (C) hemolysis (hemolysin) (D) biofilm formation (accumulation associated protein Aap). *S. epidermidis* O47 showed no protease, lipase and hemolysin activity and moderate biofilm formation. Detailed information on the generation of these results are described in the Methods section.